INFORMATION TO USERS

This manuscript has been reproduced from the microfilm master. UMI films the text directly from the original or copy submitted. Thus, some thesis and dissertation copies are in typewriter face, while others may be from any type of computer printer.

The quality of this reproduction is dependent upon the quality of the copy submitted. Broken or indistinct print, colored or poor quality illustrations and photographs, print bleedthrough, substandard margins, and improper alignment can adversely affect reproduction.

In the unlikely event that the author did not send UMI a complete manuscript and there are missing pages, these will be noted. Also, if unauthorized copyright material had to be removed, a note will indicate the deletion.

Oversize materials (e.g., maps, drawings, charts) are reproduced by sectioning the original, beginning at the upper left-hand corner and continuing from left to right in equal sections with small overlaps. Each original is also photographed in one exposure and is included in reduced form at the back of the book.

Photographs included in the original manuscript have been reproduced xerographically in this copy. Higher quality 6" x 9" black and white photographic prints are available for any photographs or illustrations appearing in this copy for an additional charge. Contact UMI directly to order.

UMI®

Bell & Howell Information and Learning
300 North Zeeb Road, Ann Arbor, MI 48106-1346 USA
800-521-0600

STERIC AND ELECTROSTERIC STABILIZATION OF COLLOIDS IN AQUEOUS SALT SOLUTIONS

by

Victoria Susan Stenkamp

A dissertation submitted in partial fulfillment

of the requirements for the degree of

Doctor of Philosophy

University of Washington

1999

Program Authorized to Offer Degree: Department of Chemical Engineering

UMI Number: 9952906

UMI Microform9952906

Bell & Howell Information and Learning Company
300 North Zeeb Road
P.O. Box 1346
Ann Arbor, MI 48106-1346

In presenting this thesis in partial fulfillment of the requirements for the Doctoral degree at the University of Washington, I agree that the Library shall make its copies freely available for inspection. I further agree that extensive copying of the dissertation is allowable only for scholarly purposes, consistent with "fair use" as prescribed in the U.S. Copyright Law. Requests for copying or reproduction of this dissertation may be referred to University Microfilms, 300 North Zeeb Road, Ann Arbor, MI 48106-1346, to whom the author has granted "the right to reproduce and sell (a) copies of the manuscript in microform and/or (b) printed copies of the manuscript made from microform."

Signature Victoria S. Stuckamp

Date 11-19-99

This is to certify that I have examined this copy of a doctoral dissertation by

Victoria Susan Stenkamp

and have found that it is complete and satisfactory in all respects,
and that any and all revisions required by the final
examining committee have been made.

Chair of Supervisory Committee:

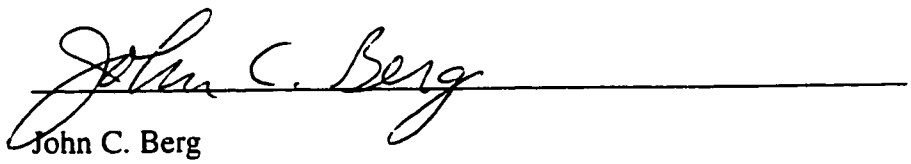

John C. Berg

Reading Committee:

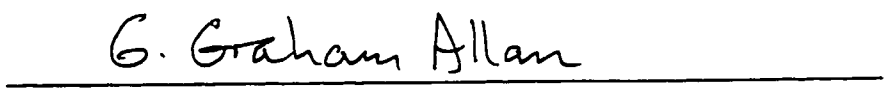

Graham G. Allan

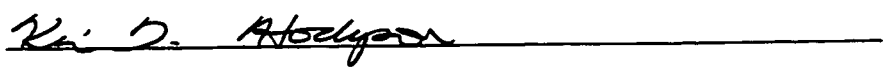

Kevin T. Hodgson

Date: 11-19-99

University of Washington

Abstract

STERIC AND ELECTROSTERIC STABILIZATION OF COLLOIDS IN AQUEOUS SALT SOLUTIONS

Victoria Susan Stenkamp

Chairperson of the Supervisory Committee:

Professor John C. Berg

Department of Chemical Engineering

Steric stabilization of colloidal particles occurs through the presence of a layer of adsorbed polymer, and can be important in a number of activities such as paint formulation, treatment of waste water, and drug delivery. Conventional wisdom dictates that the polymer must be attached well, have good solvency, and be of high molecular weight in order for good stability to be achieved. Although much progress has been made, there are still many unresolved issues concerning stability, especially in the case of aqueous salt solutions. The purpose of this study is to explore two such issues.

The first issue concerns the details of the attached polymer's conformation, which is often ignored. In this study, it is shown that only a few long attached "tails" of polymer in the presence of a low molecular weight adlayer can impart stability, despite the dictates of conventional wisdom.

The second issue centers around the fact that steric stability should decrease with decreasing polymer solvency. In the case of a thin polymer adlayer overlying charged colloidal particles, the stability should decrease upon the addition of salt due to this decrease in solvency, as well as a decrease in electrostatic repulsion. Surprisingly, it has been observed that certain latices stabilized with low molecular weight, triblock copolymers

exhibit an increase in stability upon an increase in salt concentration. This unexpected increase has been defined as restabilization. The purpose of the second part of the study is to systematically characterize when restabilization occurs and its possible causes. It was observed that the phenomena is a strong function of the type of salt, the molecular weight of the polymer and its concentration in solution. It appears that large increases in the adsorbed amount of and ion binding by the polymer are not responsible for the phenomena. One plausible cause is the presence of micelles, which are formed from the unadsorbed triblock copolymer.

TABLE OF CONTENTS

LIST OF FIGURES

PAGE

LIST OF TABLES

PAGE

ACKNOWLEDGMENTS

I would like to acknowledge the financial and technical support of Battelle Pacific Northwest National Laboratories and Professor John Berg. In particular, I would like to thank Dr. Jud Virden, Dr. Bruce Bunker, and Dr. Joel Tingey for their efforts to ensure continual funding during my entire stay. I must also thank Joel for his participation on my committee, when it is much more difficult to do so from a long distance.

I would also like to thank the people who made the time during my Ph.D. worthwhile, either through their friendship or through technical support that was above the call of duty. For the latter, I am most indebted to Dr. Patty McGuiggan, who ran the SFA measurements out of the sheer goodness of her heart, and to Dr. Lou Balmer, for recommending Patty. I am also equally indebted to Dr. Chuck Windisch, for running the Raman spectroscopy and salvaging me from a rather unproductive time. I also greatly appreciate Jud's recommendation of Chuck. I thank Dr. Bjorn Hrutfiord and Dr. Francois Baneyx for lending me high pressure liquid chromatography equipment, and I am extremely grateful for Bob Lewis's efforts in putting it all together and showing me how to run it. I thank Dr. Mark Benjamin and Dr. Gregory Korschin for generously allowing me use of their ICP-AES and atomic absorption equipment, and I thank Mark Jensen and Pierre Kwan for training me.

I would be at a loss technically and emotionally without the company of my wonderful group members, many of whom I hope to call friends for life. In particular, I must thank Dr. Jill Seebergh for taking several days to teach me how to run light scattering experiments (and how to have impeccable planning). I thoroughly enjoyed the many discussions, technical and otherwise, with all my group members; however, I must note that my own work benefited greatly from technical discussions with Bret Snyder and Andy Kim. Thanks to Dale Schmidt and Andy (again!), my computer troubles were much easier

to overcome. I would also like to thank Ron Sinicki, Lily Woo, Lynne Dickson, Eric Aston, and Direak Tan for daring to support me at my most difficult time. Thanks to the above, all my other group members (Mark, Heather, Phil...), and all my other wonderful friends (Chris, Kelly, Maren, Dawn, Jeff, Stephanie, Kip, Phen, Matt...) who made it worthwhile.

I also must thank members of my family, especially Kathy and Sharon, who rearranged their schedules so that I could both graduate and help participate in my father's recovery from heart surgery. I am very indebted to Devota Madrano for her efforts in scheduling my defense while I was gone, as well as her administrative help, wise counseling and positive outlook on life.

Finally, I must thank my husband Jim above and beyond all others. I love you more with each passing day and cannot tell you how much you mean to me.

DEDICATION

This thesis is dedicated to:

My mother, who showed great character and strength in her living and in her death

My father, who taught me to be curious and to love nature

and

My husband, who has been and always will be my biggest inspiration

CHAPTER 1: INTRODUCTION

During World War II and the Cold War, 55 million gallons of radioactive waste were created and stored at the Hanford Site in Washington[1](p.11). The wastes were created primarily from the irradiation of uranium and subsequent purification of plutonium, which was used for defense purposes. The wastes are high in salt content, extremely alkaline, and contain particulates, organics, and inorganics, some of which are radioactive[2]. Up to 90% by number of the particles are less than 2 μm in size[3], suggesting the importance of colloidal behavior. During attempts at remediation, these colloids have been known to form networks which have clogged transfer lines, while in other processes, the smallest particles remain dispersed, threatening to contaminant ion exchange or filtration systems[4].

Despite what is observed in the tank wastes, theory has traditionally predicted that aggregation will occur at these conditions. If a colloid is stabilized by electrostatic repulsion, then continuum theories suggest that aggregation will occur at a rate that is limited primarily by the diffusion rate of the particles at less than molar concentrations of salt[5]. The colloid can be stabilized through the presence of dissolved polymer at somewhat higher salt concentrations; however, as the concentration is increased further, the polymer usually phase separates, causing aggregation[6].

Throughout the study of colloidal behavior it has been apparent that other mechanisms are important, sometimes dominating the forces between the colloidal particles and causing unexpected stability. Within the last few decades, it has been accepted that forces can arise due to the structure of the solvent and its interactions with colloidal surfaces[5]. These are called solvation forces, and can result in the stabilization of colloids at extremely high salt concentrations. Unfortunately, a full understanding of them has not

been obtained, and they typically cannot explain stability in the presence of polymer adlayers since the mechanisms are believed to be important for hard smooth surfaces. Therefore, it is the purpose of this study to explore unusual mechanisms of stability in concentrated aqueous salt solutions in the presence of polymers. The findings will hopefully result in a greater understanding of the wastes and the ability to exert greater control of the remediation processes. The focus has been on two particular cases.

The first case was partially prompted by the fact that the majority of organics in the tank wastes are low molecular weight and are relatively low in concentration. Common knowledge suggests that colloidal stability can be obtained through adsorption of a full sheath of polymer, even when its concentration is in the range of a few hundred parts per million. The mechanism described is called steric stabilization. At first glance, it seems that this mechanism should not be applicable since the polymer must form a thick sheath through virtue of its high molecular weight in order for stability to occur[6]. However, a few key studies in the past suggest that only a few outward, most extending polymer tails are responsible for the majority of repulsion[7-11]. The primary purpose of this study was to experimentally quantify the number of tails required for stability in a model case. The results suggest that the adlayer composition requires only 0.5% by weight of long tails in order for significant stability to be imparted. To obtain an idea of how astoundingly low this concentration is, imagine that the amount of polymer coating a surface is scaled to equal the size of a small human, say 100 pounds. Of this quantity, 8 ounces or one cup of material would be sufficient to impact the stability.

A second purpose of the study was to determine if hydrodynamic measurements of the adlayer thickness adequately reflect the state of stability. These measurements are convenient and easy to make, but full consensus on their applicability to steric stability has not been obtained[11-16]. This study shows that the adlayer thickness, as measured by

hydrodynamic measurements, correlates with the stability qualitatively over the entire range of tail density and linearly when the tail density is low. Details are given in Chapter 3.

The second study was prompted by the fact that increasing the salt concentration for certain charged colloidal particles with thin neutral adlayers resulted in an increase in stability. The increase in stability or restabilization was most unexpected, since the salt concentration was so high that electrostatic repulsion should be negligible and the solubility of the stabilizing polymer was decreasing. One plausible explanation is that the stabilizing polyethylene oxide polymer bound the salt ions, resulting in a thicker and/or stiffer adlayer which in turn caused the increased stability. Since information on the degree of complexation and conformation of the polymer was incomplete, the data were collected and are presented in Chapter 4. Chapter 5 is a characterization of the restabilization phenomena. The results indicate that the effect is highly specific to the type of salt, the molecular weight of the stabilizing polymer, and the amount of free or unadsorbed polymer. Chapter 6 explores why restabilization occurs. Plausible causes discussed in the chapter include: an increase in adsorbed amount caused by decreasing polymer solvency, ion binding as discussed above, and the presence of micelles. At this point in time, it appears that increased adsorption and ion binding are not responsible for the phenomena, but that micelles may be important.

CHAPTER 2: BACKGROUND AND LITERATURE REVIEW

A colloid is a mixture of one material dispersed in another, such that the dimensions of the dispersed material lie roughly between 10 Å and 10 microns[17] (p. IV-1). Colloids can be classified as either lyophilic or lyophobic. The former is thermodynamically dissolved, while the latter is not and maintains a separate identity from the solvent. The stability of lyophobic solids dispersed in aqueous salt solutions (sols) is the focus of this work. Aggregation of sols is prevented by a number of colloidal interactions. The interactions known to be important to this study include van der Waals attraction, electrostatic repulsion, and steric stabilization. Each of these will be reviewed briefly, since they are the subject of many texts[5, 6, 17-19]. The main purpose of this review is to discuss the importance and understanding of the adlayer structure to steric stability and the issues surrounding colloidal stability in salt solutions, including the understanding of the solvent and dissolved polymer. At the end of this chapter, the pertinent experimental methods used to determine colloidal stability and its interactions are discussed, as well as the methods used to understand specific polymer-salt interactions.

A. FORCES AFFECTING COLLOIDAL STABILITY

van der Waals Attraction

Attraction between molecules is created primarily by Keesom (permanent dipole - permanent dipole), Debye (permanent dipole - induced dipole), and London (induced dipole - induced dipole) forces [6, 18](p. 7 ff. and 188, respectively). Of these, London forces are of primary importance to colloid stability . Attractive London forces are created by correlated fluctuations of the system's electron clouds which minimize the potential energy of the system. The numerous interactions act cooperatively in the case of colloids

and the resultant attraction is quite long ranged, on the order of a few nanometers. It is this long range attraction which is responsible for the aggregation of sols.

The attraction or repulsion experienced by a particle is often quantified by the interaction energy, which is negative for attractive interactions such as the London forces. The derivative of the interaction energy will give the force experienced between the particles. The simplest expression for the London interaction energy is given by Hamaker which assumes that the system has two spherical particles with diameters of the same size and that are large compared to their separation distance[18](p.188):

$$V_{vdw} = -\frac{A^* r}{12 H_o} \qquad \text{Eq. 2.1}$$

where: V_{vdw} = interaction energy due to London attraction

A^* = Hamaker constant

r = radius of particle

H_O = separation distance between particles

The long range of the attraction can be seen through the inverse dependence on the separation distance. The Hamaker constant, and hence, the attraction is lower in the presence of a liquid dispersion medium, as opposed to a vacuum. The drawback of this expression is that multibody effects are ignored and oscillation at a single frequency is assumed. The interaction energy is overestimated at long distances since retardation effects are neglected. Retardation is caused by the finite time required for the propagation of electromagnetic radiation. More complete models were first derived by Lifschitz[20].

Electrostatic Repulsion

Electrostatic repulsion is created through the presence of like charges on the particle surface. The surfaces can be charged by a number of mechanisms, including ion adsorption, ion dissolution, and ionization of surface functional groups[5, 18](p.148 and p.213, respectively). In solution, ions which are oppositely charged or counterions will gather around the surface so that the net charge of the interfacial region is zero. This ordering is opposed by thermal diffusion, so that the concentration of ions decreases as the distance from the surface increases. The interfacial structure is often referred to as the electrical double layer, since in the simplest sense, it can be viewed as a capacitor. The thickness of the electrical double layer is given by the Debye length (κ^{-1}), which arises from finding an expression for the surface potential using the Poisson-Boltzmann equation. For flat plates, this is given by equation 2.2[19](p. 206). This equation gives the distribution of counterions and the net excess charge density in the vicinity of the surface. In the case of low surface charges and a symmetrical electrolyte (Debye Hückel approximation), the expression for the potential Ψ at a given distance x from the surface is given by equation 2.3.

$$\frac{d^2\Psi}{dx^2} = -\frac{1}{\varepsilon}\sum_i n_{i\infty} z_i e \exp\left(-\frac{z_i e \Psi}{kT}\right) \qquad \text{Eq 2.2}$$

$$\Psi(x) = \Psi_o \exp(-\kappa x) \qquad \text{Eq 2.3}$$

where: Ψ = potential

Ψ_O = surface potential

x = distance from surface

ε = dielectric constant of solvent

n_∞ = number concentration in the bulk

z = valency

e = charge on an electron

$$\kappa^{-1} = \sqrt{\frac{\varepsilon kT}{8\pi e^2 \sum_i z_i^2 n_{i,\infty}}} = \frac{3.043}{z\sqrt{c}} = \text{Debye length}$$

k = Boltzmann constant

T = temperature

c = molarity of salt

subscript i = indicates for ion type

The second expression for the Debye length is for z:z electrolytes in water. For weak interactions at very large separations, one expression for the interaction energy between spherical colloidal particles of the same size is given by[17](p. V-9):

$$V_{elec} = \frac{64\pi r n_\infty kT\gamma_o^2}{\kappa^2} exp(-\kappa H_o) \qquad \text{Eq. 2.4}$$

where: $\gamma_o = tanh\frac{ze\Psi_o}{4kT}$

Steric Repulsion

The presence of polymer has a profound influence on colloidal stability[6](p. 10 and 412). When only a few parts per million of dissolved polymer are present, then bridging flocculation can result due to the adsorption of a single polymer onto more than one particle surface. When higher concentrations are present, a full sheath of polymer can adsorb to the particle surface, imparting steric stability. At even higher concentrations, the presence of free polymer (dissolved, but not adsorbed) can cause both depletion flocculation and stabilization.

The mechanism underlying steric stabilization was debated since the 1950's[21]. One group, led by investigators such as Mackor, Hesselink, and Bagchi, believed that stabilization is caused by compression of the adsorbed layer, which results in a loss of entropy. This type of stabilization is called entropic or elastic. A second group of investigators, such as Fisher and Napper[6], believed that steric stabilization is primarily caused by interactions of the solvent and polymer that occur during interpenetration of the adsorbed polymer segments. This proposed mechanism is termed osmotic stabilization and can be visualized by imagining two particles with polymer sheaths approaching each other. Once the particles are close enough, the sheaths will overlap, resulting in a region with a high polymer concentration. Under condition of good solvency, the overlap region will have a higher osmotic pressure than the surrounding solvent, causing the flow of solvent between the two particles which forces them apart and prevents aggregation. If the particles are able to approach closer than the thickness of one polymer adlayer, then an elastic repulsion is created due to compression of the polymer.

In either elastic or osmotic stabilization, early models predicted that the stability would increase with the thickness of the adlayer and that the exact conformation was irrelevant. The main difference between the two models is that a change in the solvency from good to poor is predicted to result in flocculation for osmotically stabilized dispersions, while changes in polymer solvency should have little effect on elastically stabilized dispersions.

It is generally agreed that the argument for osmotic stabilization is more convincing, since it has been experimentally determined that the onset of flocculation usually correlates with the onset of poor polymer solvency. A simple osmotic model reflects this correlation for the interaction energy V_{ster} between two spheres of radius a, as shown in equation 2.5[22](p. 480). The chi parameter is a measure of polymer solvency, and is less than 1/2

under conditions of good solvency and greater under poor. As a consequence, the interaction potential is positive or repulsive under conditions of good solvency. At the theta point, the chi parameter is equal to 1/2 and there is no attraction between the polymer segments or between the polymer and solvent segments.

$$V_{ster} = 4\pi kTr\omega^2 N_{av}\left(\frac{v_2^2}{V_1}\right)\left(\frac{1}{2}-\chi\right)\left(1-\frac{H_o}{\delta}\right)^2 \qquad \text{Eq. 2.5}$$

where: ω = mass of stabilizing polymer per unit area

N_{av} = Avogadro's number

v_2 = partial specific volume of polymer

V_1 = molar volume of the solvent

δ = adlayer thickness

The state of polymer solvency can be expressed by more parameters than χ, as shown in Table 2.1. The theory underlying the expressions is called Flory Huggins and is discussed in more detail in Section C. Under conditions of good solvency, the polymer is dissolved because polymer-solvent interactions are favored over polymer-polymer interactions as expressed by the second virial coefficient. In addition, the solvency can be expressed in terms of the θ temperature, due to the fact that a change in temperature typically results in a change in solvency. A lower critical solution temperature (LCST) means that an increase in temperature results in a decrease in solvency, until at the θ point the polymer phase separates. There are of course completely analogous upper critical solution temperatures (UCST), but the LCST is of primary importance to stability for the polymer used in this study.

Table 2.1. Values of the χ Parameter, Second Virial Coefficient B_2, and Temperature with Relation to Polymer Solvency

Parameter	Values during good solvency	Values during poor solvency
χ	$< 1/2$	$> 1/2$
B_2	> 0	< 0
Temperature with LCST	$< \theta$	$> \theta$

Total Interaction Potential

When each type of interaction energy has a separate expression, it is customary to sum them to obtain the total interaction energy as given in Equation 2.6. The validity of this simple summation is questionable, but is often used due to lack of a better method.

$$V_{total} = V_{vdw} + V_{elect} + V_{ster} \qquad \text{Eq. 2.6}$$

In the case when only van der Waals attraction and electrostatic repulsion are present, the theory is referred to as DLVO, after Derjaguin, Landau, Verwey, and Overbeek who first explained stabilization of charged colloids. The shape of the interaction potential curve for electrostatically stabilized colloids is shown in Figure 2.1. Aggregation into the deep primary minimum is irreversible[6](p.21), and its rate is determined by the height of the barrier. Aggregation into the secondary minimum results in loose flocs which may be broken by a small amount of shear[18, 23](p.V-13 and p.193, respectively). In contrast is the curve for sterically stabilized colloids[6](p.312), which show only repulsion in good solvents (curve 1, Figure 2.2), and a pseudo-secondary minimum in poor solvents (curve 2, Figure 2.2).

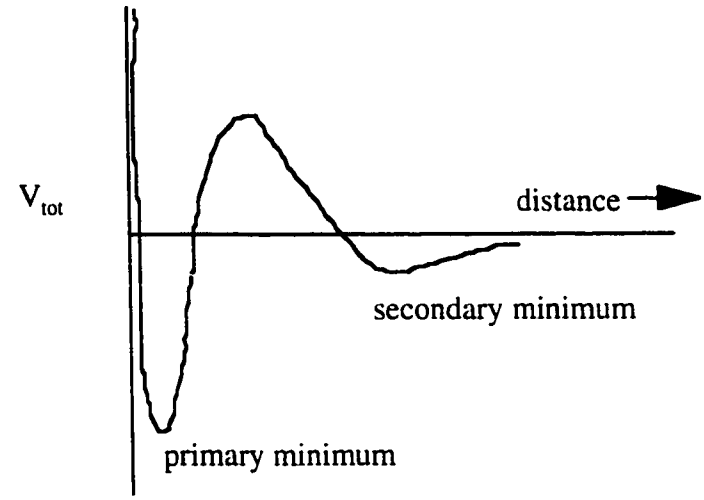

Figure 2.1. Total Interaction Potential for Electrostatically Stabilized Colloids

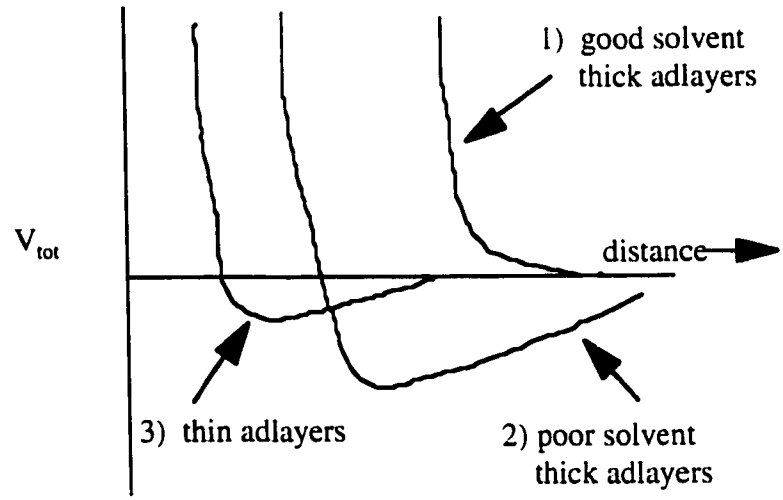

Figure 2.2. Total Interaction Potential for Sterically Stabilized Colloids
(Taken from Figure 13.19 Napper[6])

B. IMPORTANCE OF ADLAYER STRUCTURE

The Importance of Long Tails

The importance of the adlayer structure is only hinted at in the simple expression given by equation 2.5. This expression shows that reducing the adlayer thickness results

in smaller steric repulsion. Once the adlayer is too thin, then aggregation results due to the formation of a pseudo-secondary minimum as shown by curve 3 of Figure 2.2. The aggregation is caused by attractive van der Waals forces, whose magnitude depends not only on the adlayer thickness, but the particle diameter as well. The larger the particle, the more important the van der Waals attraction. Using the simple expression given in equation 2.1, Napper[6](p.125) was able to estimate when the van der Waals attraction is important, using two times the adlayer thickness as the separation distance and a characteristic value of 5×10^{-21} J for A^*. The results are reproduced in Table 2.2. Aggregation results when the van der Waals attraction V_{vdw} is on the order of several kT, and would result no matter how great the barrier imparted by the adlayer. This would result in aggregation at temperatures that result in better than θ conditions.

Table 2.2. London Attraction $|V_{vdw}|/kT$ between Sterically Stabilized Dispersions as a Function of Adlayer Thickness and Particle Radius. (Table 6.7 of Napper[6])

	Particle Radius (nm)				
Adlayer Thickness (nm)	10	50	100	200	500
2.5	0.2	1	2	4	10
5	0.1	0.5	1	2	5
10	0.05	0.25	0.5	1	2.5
25	0.02	0.10	0.2	0.4	1
50	0.01	0.05	0.1	0.2	0.5
100	0.005	0.025	0.05	0.1	0.25
250	0.002	0.01	0.02	0.04	0.1

The subtlety in the expression of equation 2.5 is that the correct adlayer thickness must be used. There are several methods of measuring it, as described in Chapter 3. One of these is the disjoining pressure method in which two polymerically coated surfaces are brought together and the interaction energy is measured as a function of separation distance. This method is believed to reflect the steric interaction. The experimental results qualitatively suggest that significant repulsion can be incurred by long dangling tails[11-13].

Modeling suggests that the tail density required for repulsive interactions is quite low, less than 1% of the adlayer[7-10].

Hydrodynamic measurements are made through the flow of solvent relative to the adlayer, and are attractive due to the relative ease of their execution. Numerous studies show that these measurements are so sensitive that the resulting thicknesses are determined primarily by the dilute tails[24-26], which suggests that they may be appropriate in characterizing steric interactions. Unfortunately, full consensus on the adequacy of hydrodynamic measurements has not been reached. Several studies using disjoining pressure techniques suggest that the density of tails required for repulsive interactions may be so dilute that even hydrodynamic measurements may not detect them[10-13], while other studies show reasonable correlation between the hydrodynamic thickness and the steric thickness measured by disjoining methods[14-16]. This lack of consensus is somewhat complicated by the fact that models of the interaction energy rely on models of the adlayer conformation. Unfortunately, there is no way to experimentally confirm the models of the adlayer[27]. To circumvent this last problem, while still testing the adequacy of the hydrodynamic measurements, an experimentally controlled adlayer was created and tested for its aggregation stability as discussed in Chapter 3. A correlation between the adlayer thickness and stability was found, suggesting that hydrodynamic measurements are indeed adequate in characterizing steric stability.

Enhanced Steric Stabilization

Due to the presence of the χ parameter, equation 2.5 also suggests that there should be a strong correlation between polymer solvency and the point where steric stabilization disappears. This has been shown to be the case for many sterically stabilized colloids in both aqueous and nonaqueous solutions, unless the polymer is poorly anchored or the molecular weight of the polymer is too small as described above[6, 28, 29]. In these last

two cases, steric stabilization is lost before polymer solvency becomes poor, but the phenomena can be readily understood as limiting cases. However, in one special situation, called enhanced steric stabilization, stability is maintained even when the polymer solvency is poor. This result is most surprising because the attraction between segments of the stabilizing polymer must be overcome during poor solvency. Studies of the phenomenon are summarized by Napper[6](p.181), but are also documented in journal articles as well[30, 31].

Dobbie first discovered the phenomena in 1973 for a system using amphipathic polymers with PEO stabilizing blocks. Three types of core particles were tested: polyvinyl acetate and polystyrene with low and high surface carboxyl content. The upper critical flocculation temperature (UCFT) was determined as a function of the ratio of the mass of stabilizing polymer to mass of particles. An UCFT occurs if an increase in temperature causes instability. The UCFT is the lowest temperature at which rapid aggregation occurs. In this case, the aggregation is limited by the diffusion rate of the colloidal particles and viscous drainage as two particles come together. It should be noted that a completely analogous lower critical flocculation temperature (LCFT) can also exist.

In almost all cases, normal behavior was observed; increasing the amount of stabilizing polymer increased the UCFT until the value coincided with the theta temperature. At low polymer concentrations, the UCFT is expected to be lower than the theta temperature due to displacement, or surface migration of the stabilizing polymer, during a Brownian collision. This results in London attraction which leads to aggregation before polymer solvency is poor. Oddly enough, for just the high carboxyl content polystyrene, the UCFT continued to increase by as much as 20°C beyond the theta temperature at intermediate concentrations of polymer, then decreased to the theta

temperature at even higher polymer concentrations. A decrease in pH and a decrease in PEO molecular weight resulted in an increase in the maximum UCFT.

It was determined that exceeding the theta temperature was associated with adsorption of the PEO in a loopy configuration. This loopiness was created by hydrogen bonding between the PEO and carboxylic surface groups. Thus a decrease in pH would result in more un-ionized carboxylic groups, which could hydrogen bond. The presence of too much polymer would prevent the formation of the loops, since the hydrophobic portion would occupy most of the surface. Higher molecular weight PEO would mask the loopiness due to its extension further from the surface.

The exact cause of the increased stability is still unclear. Proponents of osmotic stabilization claim that loopy adsorption results in a decreased polymer segment density at the outer reaches of a colloidal particle, which in turn can result in increased stabilization. In slightly worse than theta conditions, attractive forces exist between the polymer segments. A decrease in the number of segments means that the overall attractive force is decreased. Therefore, worse solvency conditions are required to obtain the overall attractive force required for incipient stability. Proponents of elastic repulsion claim that the loopy configuration results in less interpenetration of the polymer segments and higher configurational losses upon collision of the colloids. In either case, the conformation of the polymer adlayer is viewed as key to the explanation of the phenomenon.

C. ISSUES PERTINENT TO COLLOIDAL STABILITY IN AQUEOUS SALT SOLUTIONS

Colloidal stability in aqueous salt solutions has been studied extensively; however, the understanding is incomplete due to the complexities introduced by the presence of ions in a highly polar medium such as water. To lay the foundation of simpler but pertinent systems, the current state of knowledge with respect to the thermodynamics of and polymers in electrolyte solutions is summarized below, before the issues of colloidal stability are addressed.

Thermodynamics of Electrolyte Solutions

Two opposite approaches to modeling the thermodynamics of concentrated electrolyte solutions have been taken[32, 33]. The first approach initially considered an infinitely dilute system then extended the theory to more concentrated systems. The second approach initially considered either a more concentrated system or a molten salt system, which was then extended to include the presence of water.

The approach from the dilute system can be divided into two different types of models: primitive and non-primitive. In primitive models, the ions are typically represented by charged hard spheres and the solvent by a continuum with uniform dielectric constant, while in non-primitive models the electrolyte or solvent is less idealized. The primitive models can be further divided into classical and statistical mechanical approaches, while non-primitive models are usually statistical.

The most well known and accepted model for electrolyte solutions is the classical Debye Hückel limiting law proposed in 1923. Its development is outlined in physical chemistry texts[34, 35]. The key starting equations are the Boltzmann distribution, which gives the distribution for a large number of ions subjected to thermal agitation in an electric field, and Poisson's equation, which relates the electrostatic potential to the charges

generating the electric field. Therefore, combining the Poisson equation and Boltzmann distribution gives the electrostatic potential for the assumed distribution of charges. The chemical potential is calculated from the electrostatic potential by assuming that an initially uncharged solute molecule is gradually charged by moving infinitely small amounts of charge from infinitely far away. The resultant equation gives a square root dependence on the ionic strength I for the log of the activity coefficient γ:

$$\log\gamma = A_\gamma \left| z^+ z^- \right| I^{1/2} \qquad \text{Eq. 2.7}$$

where: A_γ = Debye Huckel coefficient, function of solution density, dielectric constant, and temperature

z^+, z^- = charge on positive and negative ions, respectively

$I = \frac{1}{2}\sum_i z_i^2 m_i$ = ionic strength

z = charge on ion

m = molality

subscript i = indicates ion i

The system modeled is fairly idealized. The ions are depicted as hard charged points with radial symmetry in a continuous dielectric[33]. A dilute solution is assumed, so that linearization of the Boltzmann distribution is allowed[36]. Unfortunately, this linearization is strictly valid only at infinite dilution.

A number of approaches have been taken to extend the validity of the Debye Hückel limiting law to higher concentrations. Perhaps the most familiar of these uses the parameter α, which is the distance of closest approach of ions to the central ion, and a constant B_γ, which is dependent on the dielectric constant and temperature of the solvent. The

expression is given in equation 2.8. This equation is often referred to as the Debye Hückel equation and is applicable to about 0.05 M[37].

$$\log\gamma = A_\gamma\left|z^+z^-\right|\frac{I^{1/2}}{1+B_\gamma\alpha I^{1/2}} \qquad \text{Eq. 2.8}$$

As can be seen, the limiting law is regained if the ionic strength is extremely low, and the denominator is taken to be one. Another fairly common extension of the limiting law was proposed by Guggenheim in 1935. The terms $B_\gamma\alpha$ are set equal to one and a fitting parameter C_γ is empirically found for each electrolyte (Eq. 2.9). This model is valid up to 0.1 M and often higher[38, 39].

$$\ln\gamma = \frac{A\gamma I^{1/2}\left|z^+z^-\right|}{1+I^{1/2}} + C_\gamma m \qquad \text{Eq. 2.9}$$

Additional approaches[33, 37, 40-43] have been taken to account for the limitations of Debye Hückel theory and extend the predictions to higher salt concentration than can be achieved by the two modifications discussed above. These approaches include accounting for the fact that the dielectric constant is not constant when ions are close to the polar solvent, using an exponential Boltzmann distribution model, and assuming association between ion pairs. Other approaches try to account for the fact that non-Coulombic, short range forces also contribute to the non-ideality of electrolyte solutions. Hydration models account for the fact that water molecules hydrating or solvating an ion are no longer available to hydrate other ions and that energy is required to separate a pair of ions in solution. Virial expansion models account for binary and higher order interactions of ions. Local composition models account for short range forces which are important to the region

immediately surrounding the ion, while outside the region, the system is treated by Debye Hückel theory or some similar model

The drawback with all of these models is that the correction terms are semi-empirical in nature. Even in the case where non-Coulombic forces are considered, the corrections are still semi-empirical since the factors correcting for non-Coulombic forces also correct for deficiencies in the Debye Hückel approach. The advantage of these models is that once the appropriate parameters are found they can be used over a wide concentration range with reasonable accuracy. The hydration model proposed by Stokes and Robinson in 1948 is valid for single electrolyte up to 4-5 M[33, 37], while the local composition model by Cruz and Renon is applicable from 0 to 20 M[43]. One of the most successful models is that proposed by Pitzer[39, 40, 44, 45]. This model is an extension of the Guggenheim model and is a modified virial expansion. The modifications have a fundamental basis since they employ virial expansions dependent on the ionic strength as predicted by statistical mechanical models (Mayer models discussed later). The model is good for complex multicomponent electrolytes up to 20 M and a wide range of temperatures.

To circumvent the problem of having semi-empirical corrections, statistical mechanical models have been used[39, 41, 46]. The two most common primitive models are the cluster expansion and radial distribution models. Cluster expansion or Mayer models were first proposed by Ursell in 1927 then developed by Mayer in the 1950's. In these models, virial coefficients are calculated from mathematical clusters of molecules. In the radial distribution models, thermodynamic quantities are calculated using the potential energy curve between two molecules and the radial distribution function. The radial distribution or pair correlation function gives the probability of finding a molecule a certain distance from a central molecule. The above two theories only account for pure fluids, not

solutions, so the theory must be extended to account for the ions. This extension is accomplished by McMillan Mayer and Mayer electrolyte theories for solutions and electrolyte solutions, respectively. The electrostatic interactions of ionic solutes causes the divergence of the associated integrals. The Mayer electrolyte theory determines ways to express and sum the mathematical clusters to obtain convergence of the integrals and the correct concentration dependence. In non-primitive models, the system considered is more realistic since either the solute is not treated as a hard charged sphere or the solvent is not treated as a continuum. In the most sophisticated model called Schroedinger level models, the "particles" of interest are the nuclei and electrons[47].

The drawback with these and other statistical mechanical models is that enormous amounts of time and computational effort are required for even the most simple systems. The resulting predictions are often either inaccurate or limited to low concentrations or single electrolytes, so are not useful for engineering applications. The statistical mechanical models are; however, key in advancing a fundamental understanding and have been useful in the advancement of semi-empirical models such as that of Pitzer.

There are several theories whose starting point is either a concentrated salt solution or a molten salt[33, 36, 41, 48, 49]. The quasi-lattice models of Bjerrum and Braunstein take advantage of the fact that fused salts form a disordered ion lattice, which is only disrupted when the concentration of water becomes high. Pitzer[44] found that he could adopt the equations van Laar used for non-electrolyte solutions to a wide concentration range, while Stokes and Robinson recognized that concentrated salt solutions could be modeled as water adsorbing to ions in multilayers, reminiscent of Bruenauer-Emmett-Teller (BET) adsorption. The primary drawback with all of these approaches is that the equations do not apply at very low salt concentrations. In the case of the quasi-lattice and van Laar approaches, this failure is presumably due to the fact that the lattice structure is lost at lower salt concentrations, while for the BET model, the assumption is that water-water

interactions are negligible. This deficiency has been addressed by incorporating a Debye Huckel parameter to correct the activity at low salt concentrations in the case of the quasi-lattice and van Laar approaches. Quasi-lattice models were abandoned in the 1970's in favor of the more sophisticated statistical mechanical models described above[50].

As can be seen from the myriad of models proposed, a universally applicable model for the thermodynamics of electrolytes in water is not readily available. Ironically, the simplest systems to model occur at either very low or very high salt concentration regions, not the intermediate concentrations which are of interest. This region is not fully understood. A fundamental understanding will eventually be gained through statistical mechanical models. In the interim, the thermodynamics can be empirically modeled for engineering purposes.

The Behavior of Nonionic Polymer in Aqueous Electrolyte Solution

Non-Specific Effects The thermodynamics of dissolved polymers[23](Chapter 4) is most often described by Flory-Huggins theory. In the athermal derivation of this model, it is not only assumed that the enthalpy change of mixing is zero but also that no volume change upon mixing occurs and that the polymer is a completely flexible chain, with the size of a single polymer segment close to the size of a solvent molecule. The free energy change for the athermal case is purely entropic and given by the first two terms on the right side of equation 2.10. To account for energy changes a more generalized version of Flory Huggins was developed, where the parameter χ is supposed to account for the enthalpy change of mixing. The difficulty with Flory Huggins is that the χ parameter accounts for much more than the enthalpy, including a strong entropic component which prevents a priori predictions. If χ is used as a fitting parameter, then reasonable fits with experimental data are obtained. Assuming that the theory is valid becomes even more tenuous for

aqueous solutions, due to the presence of specific interactions, such as electrostatic, which were assumed not to occur in the development of the theory.

$$\mu_1 - \mu_1^0 = RT \ln \gamma_1 x_1 = RT\left[\ln \phi_1 + \phi_2(1 - \frac{1}{n}) + \chi \phi_2^2\right]$$
$$\mu_2 - \mu_2^0 = RT \ln \gamma_2 x_2 = RT\left[\ln \phi_2 + \phi_1(1 - n) + \chi n \phi_1^2\right] \qquad \text{Eq. 2.10}$$

where: μ = chemical potential

R = gas constant

γ = activity coefficient

x = mole fraction

ϕ = volume fraction

n = degree of polymerization

χ = chi parameter

subscript 1 = solvent

subscript 2 = polymer

As can be imagined, the addition of significant amounts of electrolyte to dissolved polymer complicates the behavior. Some issues can be discussed in generalities; however, the complexities often depend on the particular polymer. One of the most important distinctions is whether the polymer is a polyelectrolyte or is nonionic in character. Since the polymer of interest to this work is polyethylene oxide $(CH_2CH_2O\text{-})_x$, the focus will be placed on nonionic polymers, with special emphasis placed on this particular polymer.

Polyethylene oxide (PEO) is a well studied polymer due to its wide commercial applicability and the fact that it has the simplest structure of all water soluble polymers[51] (p. 19 ff.). The fact that this polymer dissolves in water is surprising considering that all the other homologous polyethers do not {e.g.$([CH_2]_m\text{-}O)_x$ with $m \neq 2$}. One proposed

explanation for this behavior is that it fits better into the structure of water than the other polyethers[52]. Polyethylene oxide shows a lower critical solution temperature close to 90°C by both cloud point and viscometric measurements. By extrapolation of the viscometry data, an upper critical solution temperature of -15°C has been suggested. The solvency of the polymer in water increases between 10 and roughly 45°C before decreasing to its lower critical temperature[52]. Oligomers show complex behavior in water and are believed to have three critical temperatures[27](p. 14).

Static light scattering is often used to characterize polymers, but an understanding of PEO behavior has been complicated by the fact that many researchers discovered non-linear Zimm plots. The curved plots were believed to be caused by large agglomerates, which lead to the claim that the polymer formed gels and was not truly dissolved[53-58]. Later researchers have countered and argue that the polymer is dissolved and that the agglomerates are insoluble organic contaminants[59-62].

Adding an electrolyte to a polymer solution or any dissolved non-electrolyte typically decreases or increases its solubility. These effects are referred to as salting-out and salting-in, respectively. In the overwhelming majority of cases, salting-out occurs. It was first believed that salting-out results from ions binding water molecules, which are then unavailable to solvate the polymer or non-electrolyte[63, 64]. The downfall of this theory is that salting-in cannot be explained.

In the 1920's Debye and McAuley created a model for small non-electrolytes which could predict salting out by accounting for the Coulombic forces between the ions. In the late 1950's, Bailey and Callard[65] employed this model to explain the effectiveness of different salts to decrease the solvency of PEO. The polymer solvency was determined by the cloud point temperature, which is the temperature at which the polymer first precipitates out of solution. In accordance with the Debye - McAuley theory, the effectiveness of the salt in lowering the cloud point increased as the ionic radius of the anions decreased.

Unfortunately, the correct explanation could not be so simple. The theory also predicts that the salt's effectiveness in lowering the cloud point should be proportional to its valency, which was not the case. Napper[28] states that the agreement with theory that Bailey and Callard did find was mere coincidence, since the Debye McAuley model is only applicable to vanishingly small electrolyte concentrations, not the 1 M concentrations used. The Debye-McAuley model also suffers from the fact that quantitative agreement with experiment is not found, and a change from salting-out to salting-in for one electrolyte cannot be predicted[63].

Napper[28] provided his own interpretation for the order of effectiveness in terms of the water structure model of Frank and Wen[66]. In this model, the water surrounding an ion is divided into three different regions. In Region A, the water molecules are immobilized around the surface of the ion. Region B lies outside Region A and is concentric with it. The water is less ordered than in Region A, but the influence of the ion is still felt so that some ordering does occur. The larger the B region the greater the structure breaking ability. Region C lies outside Region B and is structurally normal water. Napper believed that the larger the size of the hydrated ion (i.e. the size to the end of the A region), the less the ability to salt out the polymer.

Other researchers investigating the salting-out of PEO have supported the Frank and Wen model. Ataman[67] and Boucher and Hines[68] note that the order of salting out coincides with the ability of the ion to destroy the structure of water as measured by infrared spectroscopy and nuclear magnetic resonance spectroscopy, so concluded that the model by Frank and Wen is reasonable. Florin and Kjellander[69, 70] explained the phenomena in terms of the free energy of the water surrounding the ion and PEO, while Erlander[71] hypothesized the formation of a pseudo-polyelectrolyte.

The use of the Frank and Wen model created two puzzling situations, which illustrate the lack of understanding about the structure of water and its interaction with

lyophilic colloids. The first of these is that, historically, the structure of water has been used to explain the Hofmeister series. The Hofmeister series was first discovered in 1888 and was originally the order in which salts could precipitate egg albumin, a protein[19, 72]. It was gradually discovered that this order appeared in many other applications, including such things as the heat of hydration of alkali halides, the dielectric constant, and solution densities. As a result, the exact definition of the Hofmeister series varies[18, 22, 72, 73], depending on whether it is considered to be specific to lyophilic colloids or not. In this study, the definition proposed by Voyutsky[74](p.161) will be adopted. In this definition, the Hofmeister series is "the series of ions composed according to their ability to interact with the medium" and is used interchangeably with the lyotropic series. It is therefore, applicable to lyophobic colloids as well. The different measures of the Hofmeister series give a similar ordering, with only *slight* variations. This would lead one to believe that the Hofmeister series should closely coincide with the order of salting out PEO, since the structure of water governs both phenomena. Interestingly, the order of salting out PEO coincides with Hofmeister series for the anions, but the order is directly opposite for the cations[28].

The other puzzling situation is that an alternative model of water structure proposed by many other researchers conflicts with the model proposed by Frank and Wen. One such model is proposed by Collins and Washabaugh[72]. They give the Hofmeister series determined by the order in which salts elute from a Sephadex® column as:

$$SO_4^{2-} \approx HPO_4^{2-} > F^- > Cl^- > Br^- > I^- \approx ClO_4^- > SCN^-$$

The species which elute before Cl^- are called polar kosmotropes or polar water-structure makers, while the species which elute after Cl^- are called chaotropes or water-structure breakers. This is exactly opposite of the Frank and Wen predictions, which show SO_4^{2-} to be a water structure breaker! A more fundamental difference is that Collins and Washabaugh believe that the water layer closest to the ion is not necessarily held tightly, as

Frank and Wen do. The looser the first hydration shell, the greater the structure breaking. Only polar kosmotropes hold the initial water layer tightly. Like supporters of the Frank and Wen model, they used NMR data to support their model. As Collins and Washabaugh state, although the Hofmeister series has been known for 100 years, "no general conceptual framework is yet available to provide a compelling explanation for why these effects occur."

Quite recently, Ninham and Yaminsky[75] have shed much light on the situation. These researchers explain that ion specific effects arise from the artificial separation of electrostatic and van der Waals effects, implying that the simple addition of the interaction potentials discussed earlier is incorrect. They argue that ions not only experience electrostatic effects, but dispersion forces as well. These dispersion forces can dominate the interaction potential at high electrolyte concentrations and are highly specific. In a complex model, they show that ion specificity arises naturally in a complete non-linear treatment, which amplifies the effect of the specific dispersion forces. Hopefully future work will verify how well the model can predict the myriads of experimentally observed, ion specific phenomena.

Specific Effects PEO has been observed to form association complexes with other dissolved compounds, such as polyacrylic acid in water or urea in benzene[76, 77]. The effect is highly dependent on the solvent as well as the dissolved compound, and, in the case of oligomers, the molecular weight of PEO. The complexes of greatest interest are those with neutral salts in aqueous solutions. It has been observed that certain alkali and alkaline earth cations are capable of binding polyethylene oxide such that the electrons of the ethers oxygens are associated with the positive ions. These specific effects will be

discussed in Chapter 4, which focuses on polymer-salt interactions in aqueous salt solutions.

Colloidal Stability in Aqueous Salt Solutions

Although a complete understanding of salt solutions or polymer solubility is still lacking, there are many aspects of colloidal stability in salts which are well established. In the case of electrostatically stabilized colloids, the most well known is the Schulze Hardy Rule. It is known that the Debye length can be decreased through the addition of an indifferent electrolyte. Since this length reflects the range of the electrostatic interactions as shown in equation 2.4, decreasing the length should effectively decrease the stability of the colloid until aggregation results. This decrease in stability is caused by lowering the barrier to coagulation which lies between the primary and secondary minimum, as shown in Figure 2.1. The critical coagulation concentration (CCC) is the lowest salt concentration which results in rapid aggregation limited only by the diffusion of the particles and viscous drainage of the solvent as the two particles come together. Stated in the most general form, the Schulze-Hardy rule is: "The CCC changes by a factor of $(z_i/z_j)^n$ when the counterion valency is changed from z_i to z_j. The exponent lies between 6 and 2." At high surface potentials the value is 6, while at low surface potentials, the value is 2[17].

In the case of sterically stabilized colloids, it is known that electrolytes often decrease the solubility of the stabilizing polymer as discussed in the preceding section. This decrease in solubility will cause a decrease in stability. In this case, the lowest salt concentration which results in rapid aggregation is called the critical flocculation concentration or CFC. As shown in equation 2.5, the critical flocculation concentration should coincide with the onset of poor polymer solvency. Although the chi parameter cannot be predicted a-prior, this correlation has been empirically shown to be the case for

many systems[28, 29]. This correlation has been observed even in complex polyelectrolyte systems where multiple critical points exist[78].

In either electrostatically or sterically stabilized colloids, the addition of electrolyte is typically anticipated to cause a decrease in stability. In the case of electrostatically stabilized colloids, stability in concentrated salts solutions *cannot* occur as predicted by DLVO theory, except in the very special case where heteroaggregation is prevented in a solvent whose dielectric constant is intermediate in value between those of the two types of dispersed phase. However, as early as 1930's, it was documented by Voet that metallic sulfides, metals and silver halide colloids were stable to homoaggregation in concentrated acids and saturated solutions of soluble salts such as calcium chloride[79, 80]. These results were confirmed by Ostwald and Wannow in 1936[81], while Derjaguin discovered in 1962 that repulsive forces existed between crossed gold or platinum wires in concentrated KCl, $MgSO_4$, $ZnSO_4$, and H_2SO_4[82, 83]. The exact mechanism was not understood, but it was found that stability did not exist in all cases, such as silver iodide in half saturated $NaNO_3$ or $Ca(NO_3)_2$[84, 85]. Furthermore, it was discovered that the ability to coagulate hydrophobic electrostatically stabilized sols depended on the exact electrolyte, which is also not predicted by DLVO theory. The order is another manifestation of the Hofmeister series, and in decreasing order of effectiveness, is $Cs^+ > K^+ > Na^+ > Li^+$ for monovalent ions and $Ca^{2+} > Mg^{2+}$ for divalent cations[5].

The explanation used today to explain the unexpected behavior is the presence of hydration forces[5, 86, 87]. These forces were believed to exist as early as the 1930's, but were dismissed as recently as the 1970's since other plausible explanations existed. The definition of a hydration force is a solvation force when the medium is water. Solvation forces are not seen in traditional DLVO theory since the solvent is treated as a continuum. When two surfaces are separated by small distances, then the continuum theory fails and the solvent must be treated as individual particles. In all solutions, a repulsive oscillatory

solvation force is encountered due to changes in the liquid density as two solid surfaces approach each other. At multiples of the solvent molecular diameter, the repulsive force is a maximum due to the high density of the close packed structure.

In the case of water, a repulsive hydration force is encountered whenever the solvent molecules bind to hydrophilic solid surfaces. At large separation distances, it has been found empirically that the force decays monotonically in an exponential fashion as the separation distance increases and can be felt as far as 3-5 nm from the surface. In concentrated salt solutions, cations are observed to bind to hydrophilic surfaces as well as water molecules. The greater the strength and number of bonds between the cation and water molecules, the greater the repulsive hydration force since the energy required to dehydrate the cation and allow interparticle contact is higher. This conclusion was drawn since the order of decreasing strength and range is the order of decreasing hydration: $Mg^{2+}>Ca^{2+}>Li^{+}\approx Na^{+}>K^{+}>Cs^{+}$ as determined by measuring the interaction energy as a function of separation distance. The conclusion is also supported by the Hofmeister series and the fact that latex with COO^{-} and NH_3^{+} groups are stable in concentrated $LiNO_3$, KNO_3, and KBr, but aggregate in $CsNO_3$[88, 89].

Very recently, an alternative explanation of the hydration forces has been offered by Veeramasuneni and coworkers[90], who performed force distance studies between silica and salt crystals in the saturated salts. They note that the oppositely charged surfaces of silica and NaCl attract each other, while the similarly charged silica and KCl crystals repel each other, although electrostatic repulsion should not exist at these high salt concentrations. They explain the interaction energy through van Oss's model of polar acid-base interactions, and note that this mechanism should also explain the selective separation of alkali halide salts in saturated brines (ionic strength ≈4 M). Unfortunately, the van Oss model is not well accepted since it cannot accurately or consistently predict whether a surface is acidic or basic[91]. This study illustrates the fact that full consensus has not been

obtained on the mechanisms underlying surface interactions and, in particular, hydration forces.

It has been observed that strong, monotonic, repulsive short range forces also exist between bilayer and other amphiphilic surfaces, when DLVO and oscillatory solvation forces would predict aggregation. It was long thought that the repulsion was due to the solvation forces described above, and that the force was perhaps smeared out and became non-oscillatory due to the fluid-like nature of the surface, or that perhaps, it was a repulsive hydration force. The problem with either of these conclusions is that it creates several inconsistencies. First, the solvation forces are believed to occur between two smooth rigid solid surfaces. In the case of hydration forces, the forces are believed to exist at high surface charge densities[88], while in the case of oscillatory solvation forces, the repulsion should be equal or greater for charged surfaces. However, the repulsive force between lipid bilayers was often observed to be larger for uncharged surfaces than charged. Due to these and several other discrepancies, Israelachvili and Wennerström[92] hypothesized the existence of molecular-scale protrusions which exist due to thermal fluctuations. Since the protrusions cannot overlap, repulsive forces are created at short separation distances. These forces are referred to as protrusion and sometimes steric forces.

The steric forces just discussed should not be confused with the steric forces imparted by macromolecules and discussed in Section A of this chapter. The latter steric forces are typically considered to be osmotic in origin. As discussed in section B, a correlation between the onset of poor polymer solvency and aggregation does not always occur, and as can be imagined unexpected stability has been observed in concentrated salts. Steric stabilization was observed to occur in 1 M KCl for poly(vinyl alcohol) (PVA) stabilized dispersions, which is a concentrated salt solution giving worse than theta conditions[93]. The exact cause of this stability is unclear. It has been proposed that the origin is the loopy configuration of the adsorbed molecules or enhanced steric stabilization.

Napper[6] has argued, however, that the origin is more unclear since PVA exists as a random block copolymer of PVA and polyvinyl acetate so that the existence of a true theta temperature is somewhat questionable.

Unexpected stability has also been observed in the case of electrosterically stabilized colloids with thin neutral adlayers having PEO stabilizing blocks[94-97]. Due to decreasing solvency and electrostatic stabilization, it is anticipated that the stability should decrease or remain constant as the electrolyte concentration is increased. However, an increase in stability was observed, which is dependent on the type of salt and polymer molecular weight. A systematic characterization of this phenomenon is one purpose of this work, and the results are discussed in Chapter 4.

Different hypotheses for the unexpected stability of the electrosterically stabilized dispersions were offered by the researchers who first discovered the phenomenon, including slow diffusion of salt into the adlayer or cation binding by the PEO, which resulted in a thicker or stiffer adlayer. One alternative hypothesis was offered by Bevan and Prieve[98] in response to the presentation of our work in Chapter 4 at the ACS 72nd Colloid and Surface Science Symposium, June 1998. They argue that osmotic repulsion is not the only stabilizing force observed in sterically stabilized systems, but that researchers overlook the decrease in the attractive van der Waals forces due to the presence of the adlayers, as first noted by Vold and modeled by Parsegian. Furthermore, Bevan and Prieve have predicted a decrease in the attraction due to the introduction of an indifferent electrolyte. They argue that the number of Brownian collisions will remain constant for a given system, but that lowering of the van der Waals attraction could result in too small of an attractive force to result in a stable aggregate. Actual measurements of the reduction in van der Waals attraction is forthcoming.

Other examples of poorly understood stability in concentrated salt solutions exist throughout the literature. In a study of depletion flocculation, Seebergh and Berg[99]

employed a system of free PEO polymer with a molecular weight of 1000 and latex stabilized by block copolymers having PEO stabilizing blocks. As expected, depletion flocculation was observed at relatively high free polymer concentrations. Unexpectedly, at low values (≈1000 mg/L), an increase in free polymer caused an increase in stability. The effect was most pronounced at the higher salt concentrations of 0.4 and 1 M NaCl. As in the sterically stabilized cases studied by Berg and coworkers[94, 100], the cause of the behavior was hypothesized to be cation binding of PEO.

Another example was recently reported by Addai-Mensah and coworkers[101], in which they discovered that gibbsite {$Al(OH)_3$} is stable above pH 13, despite the collapse of the electrical double layer. An analysis of the rheology revealed non-DLVO forces above pH 10. Force distance profiling with atomic force microscopy (AFM) revealed that these non-DLVO forces became important at separation distances less than forty nanometers and could not be solely attributed to hydrodynamic forces. It was hypothesized that either steric or hydration forces were the cause, but further investigation was not conducted. It seems more plausible that the forces encountered are steric in nature since hydration forces have a range of three to five nanometers, not twenty nanometers. In addition, it is believed that "inorganic polymers" exist at the conditions of interest. This study is of notable significance to remediation of the Hanford Site, since the conditions and materials employed reflect the state of the wastes.

Molina-Bolivar and coworkers[102, 103] reported yet another example of unusual stability. They showed that polystyrene particles coated with the protein $F(ab')_2$ showed the typical decrease in stability as a function of increasing NaCl, at low salt concentrations. Above 0.2 M NaCl, the stability showed an unanticipated increase, which is somewhat reversible. These researchers attribute the increase in stability to hydration forces, which they presume would occur on the hydrophilic protein coated surfaces and not the hydrophobic bare latex surfaces. Unfortunately, one questions whether this is really the

case, since protein surfaces are not typically considered rigid, as in the case of minerals. One wonders whether protrusion or steric forces are responsible, since protein is a macromolecule that can be both loose or globular. Furthermore, the reversibility of the aggregation is consistent with steric stabilization. The fractal dimensions of the aggregates should have been compared to those predicted for non-DLVO forces or experimental force distance profiling should have been used to obtain better picture of the mechanisms controlling the restabilization.

D. MEASUREMENT OF COLLOIDAL STABILITY AND INTERACTIONS

Aggregation Kinetics

Aggregation is said to occur when the particles or dispersed phase in a colloid stick to each other. The rate of aggregation thus reflects the stability of the colloid. These kinetics have been modeled and are briefly discussed here. The development used in this work is based on the work of Virden and Berg[104], since their equations were used for determining the aggregation kinetics from photon correlation spectroscopy.

In the early stages of aggregation, the kinetics can be modeled as a bimolecular reaction. In the case of the formation of doublets from singlets only, the rate of disappearance of singlets is:

$$\frac{dn_1}{dt} = -k_{11}n_1^2 \qquad \text{Eq. 2.11}$$

where n_1 = number concentration of singlets

k_{11} = rate constant for doublet formation

t = time

When there is no barrier to aggregation, the rate is determined by the diffusion rate of the particles. In this case, the rate constant was determined by Smoluchowski to be:

$$k_{smol} = \frac{8kT}{3\eta} \qquad \text{Eq. 2.12}$$

where k_{smol} = Smoluchowski rate constant for diffusion limited aggregation

k = Boltzmann constant

T = absolute temperature

η = viscosity of the solvent

The key parameter used to characterize the rate of aggregation is the stability ratio W, and it can be calculated from the rate constants described above. It can be defined as:

$$W = \frac{\textit{Number of collisions between particles}}{\textit{Number of collisions resulting in aggregation}} \qquad \text{Eq. 2.13}$$

The stability ratio is therefore high when the rate of aggregation is low. For a given temperature, solvent and particle concentration, the number of collisions is constant and is reflected by the Smoluchowski rate constant. The number of collisions resulting in an aggregate will be determined by the interparticle forces. The stability ratio can be determined experimentally, and in this case, the equation becomes:

$$W_{exp} = \frac{k_{smol}}{k_{exp}} \qquad \text{Eq. 2.14}$$

The experimental rate constant k_{exp} can be determined by counting particles or through turgidity or light scattering measurements, the last of which will be described below. One might expect that the above stability ratio should be one when rapid aggregation is obtained

in the experimental conditions. It is actually close to 2 due to the presence of viscous drainage effects[105-107] which slow the actual rate of aggregation, but are not accounted for in the Smoluchowski equation. The effects occur because it is difficult for the last bit of fluid to drain between two particles as they come together.

The stability ratio when there is a barrier can be determined theoretically using the total interaction potential. In this case, the rate constant for aggregation in the presence of a barrier is determined as the Smoluchowski rate divided by the theoretically determined stability ratio.

It is customary to plot the stability ratio as a function of added electrolyte on a log-log graph. The lowest concentration where rapid aggregation occurs is called the critical coagulation concentration (CCC) in the case of electrostatically stabilized colloids, and the critical flocculation concentration (CFC) in the case of sterically stabilized colloids. When slow aggregation occurs for electrostatically stabilized colloids and the surface potential is constant, then the stability ratio is predicted to decrease linearly with an increase in the salt concentration[18](p.201).

Photon Correlation Spectroscopy

Photon correlation spectroscopy is a method that can be used to determine the experimental rate constant, which in turn can be used to determine the experimental stability ratio, as described above. The method used in this work is described by Virden and Berg[104], and is briefly outlined here.

When light is scattered from a small volume of colloidal size particles, the intensity will fluctuate due to the Brownian motion of the particles. Two intensities measured at time intervals short compared to the diffusion rate of the colloids should be close to the same value. These intensities are said to be correlated. In contrast, when the intensities are

measured at long time intervals, they will no longer be correlated, and will be more representative of the average intensity. In photon correlation spectroscopy, the intensity $I(t)$ at time t is measured at short time intervals then converted into a normalized intensity auto-correlation function $G^2(\tau)$ which quantifies the fluctuations:

$$G^2(\tau) = \frac{\langle I(t)I(t+\tau)\rangle}{\langle I(t)\rangle^2} \qquad \text{Eq. 2.15}$$

where: τ = delay time or time between successive intensity measurements

The intensity autocorrelation function is linearly related to the square of the electric field autocorrelation function. For a monodisperse system, the electric field autocorrelation function is proportional to $exp(-\Gamma\tau)$, where Γ is the decay rate. For a polydisperse system, the electric field correlation function is a summation of exponentials. Without any a-priori assumption about the distribution, the data can be expressed as a Taylor series about the average decay constant (Γ_{mean}). The first and second moment or cumulant can be related to the intensity auto-correlation function:

$$ln\left(\frac{G^2(\tau)-A}{B}\right) = 2\left[-\Gamma_{mean}\tau + \frac{\mu_2\tau^2}{2!}\right] \qquad \text{Eq. 2.16}$$

where: A,B = Instrument constants

μ_2 = second moment

The use of this equation to fit the data is referred to as the method of cumulants. The useful information comes from the fact that the average decay constant is related to the mean diffusion coefficients D_{mean} (Eq. 2.17), which in turn can be related to the mean particle diameter d_{mean} via the Stokes-Einstein equation (Eq. 2.18). In addition, the second moment reveals information about the polydispersity. When normalized to the square of

the decay constant, the value should be close to 0.02 for monodisperse samples, 0.02 to 0.08 for narrow distributions, and larger for wide distributions[108].

$$\Gamma_{mean} = q^2 D_{mean} \qquad \text{Eq. 2.17}$$

$$d_{mean} = \frac{kT}{3\pi\eta D_{mean}} \qquad \text{Eq. 2.18}$$

where: $q = 4\pi \sin(\zeta/2)/\lambda$ = magnitude of the scattering vector

λ = the wavelength of light in the medium = λ_o/n

λ_o = the wavelength of light in vacuo

n = the refractive index of the medium

ζ = scattering angle

The scattering angle is the angle between the direction of light propagation and the line connecting the sample and the observation point.

The initial slope of a plot of the diameter as a function of time for an aggregating colloid can be used to determine the experimental aggregation constant k_{exp}. In this study, the relationship proposed by Virden and Berg is used (Eq. 2.19).

$$k_{exp} = \frac{1}{\alpha n_o r_{mean,o}} \left(\frac{dr_{mean}}{dt} \right)_o \qquad \text{Eq. 2.19}$$

where: α = optical factor dependent on the particle size, wavelength in the medium, and scattering angle

n_o = number concentration of singlets

$r_{mean,o}$ = initial mean radius of the particles

r_{mean} = measured radius

Direct Measurement of Interaction Forces

The force distance profile can be determined by a number of methods, with surface force apparatus (SFA) measurements, total internal reflection microscopy (TIRM), and atomic force microscopy (AFM) being the three most common techniques. These have been reviewed by Israelachvili[5](p.168 ff.) and will be summarized briefly.

In the surface force apparatus, the force is measured between two crossed cylindrical surfaces with radii of 1 cm. The instrument can measure forces as sensitive as 10^{-8} N, and the distance of separation can be controlled to within 0.1 nm. At close distances, a piezo is used to change the distance between the cylinders. The actual distance is measured using multiple beam interference fringes. The force is calculated as the difference between the distance the piezo moved and the actual distance moved multiplied by the stiffness of the force measuring spring. The SFA can be used to measure forces in aqueous and non-aqueous liquids, even in the presence of adsorbed macromolecules. The refractive index of the material between the two cylinders can be determined, giving an estimation of the amount of polymer or other material adsorbed to the surfaces.

In TIRM, a colloidal particle is allowed to settle to the bottom of a container. In the presence of repulsive forces, there will be a small separation distance between the particle and the container which can be measured using an evanescent wave created from the total internal reflection of an impinging laser beam. The distance fluctuates due to Brownian motion of the particle, so is measured numerous times. These distances are used to determine the potential energy profile assuming a Boltzmann's distribution of energy. The advantage of TIRM is that it can be used to measure extremely small forces (10^{-14} N). Its

detection limit is at least 3 orders of magnitude weaker than SFA or AFM. Its drawback is that its spatial resolution is on the order of 1 nm[98].

Atomic force microscopy (AFM) is similar in principle to SFA measurements, but the force is measured between a tip and a large surface. The tip can be a single atom or a colloidal size particle. Forces as small as 10^{-9} to 10^{-10} N can be measured. Under the very best conditions, displacements of 0.01 nm can be determined, while the separation distance can be as large as 60 nm. The drawback of AFM is that the point of contact must be inferred as the point where the force distance profile becomes linear due to simultaneous movement of the surface and tip. In the case of polymer coated surfaces, the point of contact is more difficult to detect since the polymer may either be displaced or stick to the surface as a consequence of strong adsorption. In contrast, the point of contact may be determined unambiguously in SFA measurements.

E. MEASUREMENT OF POLYMER SOLVENT INTERACTIONS

Solvent Extraction

In solvent extraction, a solute of interest is transferred from one solvent to another in a system where the two solvents are immiscible. Typically, one phase is organic in nature, while the other is aqueous. The partitioning of the solute can be quantified by a number of parameters. In the simplest systems, only one species M is distributed between the two phases and it does not undergo any chemical interactions other than solvation. In this case the thermodynamic partitioning coefficient P_m given in equation 2.20 can be used:

$$P_m = \{M\}_{org}/\{M\}_{aq} \qquad \text{Eq. 2.20}$$

where the parentheses indicate the activity and the subscripts indicate the phase. Unfortunately, chemical interactions often occur or are required for solvent extraction.

Especially in the case of metal ions, various species may exist. In these instances it is more convenient to quantify the extraction by the distribution ratio or extraction coefficient E:

$$E = \frac{\text{Total concentration of the compound in the organic phase}}{\text{Total concentration of the compound in the aqueous phase}} \qquad \text{Eq. 2.21}$$

An alternative is to use the degree of extraction or fraction extracted R:

$$R = \frac{\text{Total mass of the compound in the organic phase}}{\text{Total mass of the compound in the aqueous phase}} \qquad \text{Eq. 2.22}$$

According to De[109] (p. 2), the degree of extraction is more useful than the distribution ratio when the extraction is nearly complete. When the degree of extraction is nearly 1, then the distribution ratio will approach infinity. In these cases, it is difficult to assess the accuracy of the distribution ratio, so it is often reported as infinity. As a result, the degree of extraction is reported in this work.

Most metal salts dissolve readily in water but not in organic solvents, especially hydrocarbons and chlorinated hydrocarbons[110]. The water can coordinate with the metal ion, such that the ion does not unduly disrupt the solvent. Therefore, for metal salts to be extracted, it must form a neutral complex that will dissolve in the organic phase. There are several ways to extract metal salts, including the formation of simple uncharged molecules such as I_2, chelate complexes (polydentate coordination), or ion association complexes.

In this study, the complexes formed are ion association complexes. According to De[109] (p. 8), molecules containing oxygen (such as diethyl ether) are basic and can donate their electrons to the metal atoms and solvate them directly. Presumably this can occur in

the case of the polyethylene oxide. As a consequence, solvent extraction can serve as a screening tool for the strength of the polyethylene oxide-metal complex.

Raman Spectroscopy

In Raman spectroscopy, monochromatic light (usually from a laser) is used to irradiate a sample, which scatters the light[110, 111]. If the scattered light is the same wavelength as the incident, then Rayleigh scattering is said to occur. If the light is at a different wavelength, then the phenomena is called Raman scattering, which is sensitive to the vibrational characteristics of the molecules in the sample. In particular, the vibrations can be correlated with the wavenumber shift, which is the difference in wavenumbers (1/cm) between the scattered and incident light. Shifts can be either positive (anti-Stokes) or negative (Stokes). Since the Stokes lines are more intense, they are usually used in spectroscopy. It is customary to plot the intensity of the scattered light as a function of the shift (1/cm). The abscissa is often labeled frequency and the absolute value of the shift is used.

Raman spectroscopy is very similar to infrared spectroscopy. The main difference is that Raman requires the existence of polarizable bonds, while in infrared the bonds must have a change in the dipole moment. As a result, polar molecules such as water are quite infrared sensitive, but are much less Raman sensitive. Ionic bonds have very weak or non-existent Raman spectra. In many cases, it is advantageous to run both Raman and IR spectra together, since they are complementary.

The conformation of a molecule can be understood by correlating the wavenumber with a particular conformation. This is done through a process called normal coordinate analysis, in which the vibrational motion is derived from the masses and relative movements of the atoms involved. With polymers, the analysis becomes quite complex since there are 3N-5 fundamental vibrations for a linear molecule, where N is the number

of atoms in the molecule. Once this is done, then an understanding of the conformation can be obtained since the peak height or size is proportional to the quantity present.

Additional information can be gained by other features of the spectra. The width of the peak, usually characterized by the full width at half maximum, tends to decrease upon an increase in order. Associations between functional groups can be detected by shifts in the peak frequency. Shifts towards lower frequencies indicate that the bond has become weaker. This weakening can be due to movement of valence electrons away from the atom, such as might occur during cation binding. Shifts towards a lower frequency may also be indicative of a lower mass or of vibrational coupling. Helical structures are evidenced by band splitting. Highly polarized bands are a result of highly symmetric vibrations.

CHAPTER 3: THE EFFECT OF LONG TAILS ON STERIC STABILITY*

A. ABSTRACT

In steric stabilization, the "thickness" of the adsorbed layer on the particles is of key importance in determining the stability of the colloid. There is evidence to suggest that both the adlayer thickness, as measured by hydrodynamic means, and the colloid stability are determined solely by the most outward-extending tails in the adlayer, even when the tail density is quite low. The present study seeks to investigate experimentally and to quantify the relationship between tail density, hydrodynamic adlayer thickness and colloid stability for a model system consisting of a bimodal adlayer of tri-block copolymers anchored to the surface of a latex colloid. The low molar mass component of the adlayer has a thickness too small to impart significant steric stability by itself, therefore isolating the stability attributable to the long tails provided by the high molar mass component. By systematically varying the adlayer composition, the density of tails required to impart marginal stability is determined and compared to the effect of tail density on the hydrodynamic thickness. For the system investigated, the adlayer proportion of long tails required for marginal stability was less than 0.5%, in good agreement with the proportion required to significantly increase the hydrodynamic adlayer thickness. The practical inference is that the most efficient steric stabilizers (on a per unit mass basis) are highly polydisperse mixtures with only a very small proportion of the highest molar mass constituent.

---

* This work was presented at the ACS 71st Colloid and Surface Science Symposium in June 1997. It is also a modified version of the publication in *Langmuir*, **13**, p. 3827-3832 (1997).

B. INTRODUCTION

The efficacy of a steric stabilizer in a given situation depends principally on three factors. First, it must be well anchored to the particle surface such that it does not desorb or migrate laterally upon particle-particle interaction. Thus block copolymers, whose solvent-incompatible blocks provide "anchors," are commonly used for this purpose. Secondly, the unadsorbed portion of the adsorbing copolymer (the "buoy") must have good solvent compatibility (e.g., $\chi < 0.5$). Finally, for effective steric stabilization, the buoy layer must provide sufficient effective thickness to prevent the approach of the colloid particles within range of the attractive van der Waals forces.

The effective thickness of the adlayer may be defined and measured in different ways. Static methods refer to non-invasive techniques which employ scattering or reflection of electromagnetic radiation or subatomic particles. They include small-angle neutron scattering (SANS) [25, 112-116] and ellipsometry [117-120], both of which provide some measure of the polymer segment density distribution. It has been shown [25, 121-123] that the various static methods generally detect only the denser portions of the adlayer near the surface, i.e., the trains (anchors) and small loops, but are insensitive to the presence of far-extending tails, which are at low segment concentrations. Disjoining pressure methods, on the other hand, refer to techniques where polymer-coated surfaces are brought together in instruments such as the surface forces apparatus (SFA) [11, 124] or in film drainage experiments [12], which detect the onset of repulsive interaction between the adlayers, and thus yield the *steric thickness*, δ_S. Such a measure would appear to be directly relevant to the steric stabilization of colloids. While usually giving results reasonably consistent with hydrodynamic thicknesses, described below, disjoining pressure measurements sometimes detect repulsive interactions commencing at surface separations so great that special explanations must be invoked to rationalize them [11-13].

Finally, hydrodynamic methods are those which employ the flow of the solvent relative to the attached polymer and include flow through coated capillaries or porous membranes [125-129] and photon correlation spectroscopy (PCS) [130] of coated dispersions. They yield the *hydrodynamic thickness*, δ_h. Such measurements might be expected to reflect the degree of drainage of the adlayer, but in fact appear to include the full influence of tails, even when the latter are quite sparsely distributed over the surface, provided the molar mass of the buoy polymer is sufficiently large [24-26]. Computed values of the degree of tail extension based on self-consistent field theory also appear to accord with measured values of δ_h [24, 131]. Examples of good agreement between δ_h (measured by PCS) and δ_s (obtained by the surface forces apparatus) have been published, both for adsorbed homopolymers [15, 16] and block copolymers [14, 129].

Several issues regarding the relationship between the hydrodynamic adlayer thickness, adlayer structure, and the stability of colloids supporting such adlayers remain to be investigated. For example, while hydrodynamic thicknesses measured by PCS often accord with steric thicknesses determined by SFA measurements, studies showing such comparisons have not been accompanied with *direct* determinations of colloid stability, as might be quantified by determination of the stability ratio, W. Also, while it has been surmised that only a very low density of tails might be sufficient to confer steric stability [7-9], experiments providing the minimum density for steric stability for any specific system have not been reported. Finally, the ability of hydrodynamic (PCS) measurements to detect the presence of tails at the minimum density required to confer stability has not been demonstrated. The objective of the present report is to explore these issues experimentally for a model system.

The system investigated consisted of a bimodal adlayer of two tri-block copolymers of BAB (buoy-anchor-buoy) type of widely different buoy molar masses adsorbed to the surface of a polystyrene latex dispersed in water, as shown in Figure 3.1. The polymers

used were Pluronics® (BASF Wyandotte), which consist of polyethylene oxide (PEO) buoy blocks and a polypropylene oxide (PPO) anchor block. By varying the proportion of the higher molar mass component, the long tail density could be controlled. The stability characteristics of the system were explored by varying the concentration of the electrolyte $MgSO_4$. The molar mass of the short-tail component was chosen such that its adlayer conferred a marginal degree of stability to the system. Rapid flocculation of this system occurred at a concentration of $MgSO_4$ slightly below that of the θ-point of PEO (0.5 M), but above the CCC for the bare latex. Stability results were then obtained for copolymers of progressively higher buoy molar masses until one was reached for which rapid flocculation required the full θ-concentration of $MgSO_4$. This was used as the long-tail component of the bimodal adlayer. By performing stability experiments on the bimodal systems at salt concentrations exceeding the CFC of the short tail adlayer, but *below* the θ-concentration of PEO, the stability conferred by the long-tail component could be isolated as a function of its fraction in the adlayer. (The preparation of the two-component adlayers of desired composition required separate determination of the binary adsorption isotherms for the system, since the relative concentration of the adsorbed components could not be assumed to be the same as that of the components in the bulk solution.) Parallel PCS experiments with the same systems in water provided a comparison of the collapse in the hydrodynamic thickness vs. long-tail density with the loss of stability vs. long-tail density.

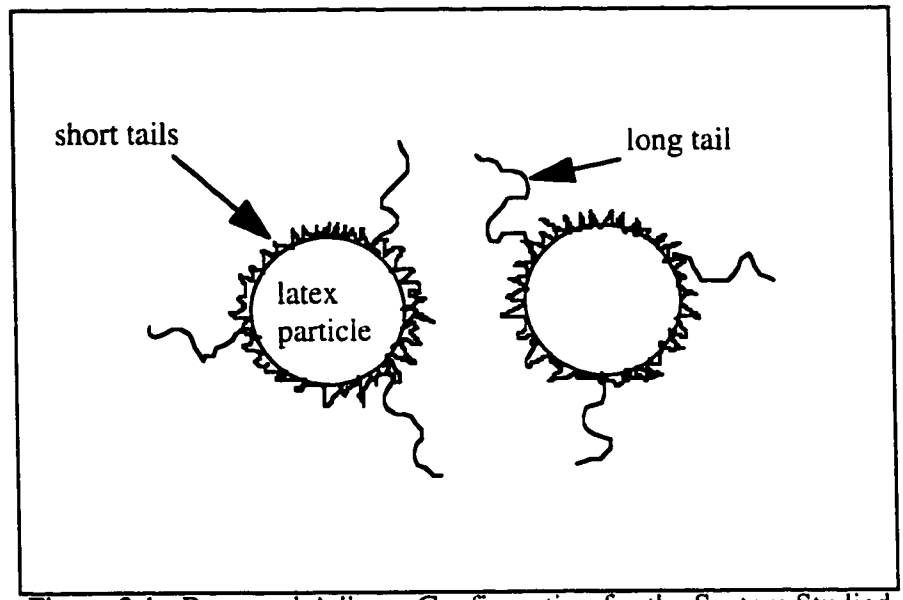

Figure 3.1. Proposed Adlayer Configuration for the System Studied in this Work. (The adlayer is presumed to exist as short tails, which impart little or no steric stability, and long tails, which do impart steric stability.)

C. EXPERIMENTAL SECTION

Materials

Monodisperse polystyrene latices with sulfate functional groups (Interfacial Dynamics Corp., Portland, OR) were used as the model colloid. The latices were suspended in distilled water at a solids concentration of 8.7%. The mean diameter as determined from transmission electron microscopy was 0.168 μm, while the parking area was 3744 $Å^2$/charge group. According to the manufacturer, the dispersion was free of excess surfactant, residual monomer, preservatives, and other additives, and was thus used without further cleaning. The average hydrodynamic diameter of the colloidal particles was approximately 0.197 μm.

The polymers used as steric stabilizers were BAB block copolymers (Pluronics®) of polyethylene oxide/propylene oxide available from BASF Wyandotte Corp. (Wyandotte, MI). The molecular weights of the copolymers are reported in Table 3.1.

Table 3.1 Molar Masses of Pluronics® Copolymers Used in this Study.

Pluronic®	Total Molar Mass	PEO Molar Mass	PPO Molar Mass
L43	1850	650	1250
L64	2900	1150	1750
P75	4150	2100	2050
F108	14000	10750	3250

All water was deionized, doubly-distilled with a pH of 5.5 - 6.0. The $MgSO_4$, NaCl and tannic acid were all reagent grade. The tetrahydrofuran was reagent grade, with 25 ppm butylated hydroxy toluene added as a preservative. All glassware was cleaned using Micro®, a strong detergent available from International Products Corporation (Burlington, NJ). After soaking for several hours, the glassware was rinsed copiously with tap then deionized, doubly-distilled water. All glassware used in light scattering experiments was also rinsed copiously with filtered (0.2 μm nylon) deionized, doubly-distilled water.

Aggregation Experiments

Sterically stabilized dispersions were created by mixing latex and dissolved polymer to a final Pluronics concentration of 300 mg/L and allowing the system to equilibrate for 15-18 hours before testing. The Pluronics® concentration was chosen to allow adsorption in the plateau region of the isotherm [132-134]. The stability of these dispersions and bare latex was tested using dynamic light scattering, as described by Virden and Berg [104]. In the flocculation experiment, 0.5 mL of the dispersion was mixed with 0.5 mL of salt solution for 10 seconds. Fluctuations in light intensity due to Brownian motion of the dispersion were then monitored as a function of time using a Brookhaven light scattering system (Holtsville, NY) with a BI-2030 72 channel digital correlator and a Bi-200SM Goniometer. A Physics Stabilite 35 mW helium-neon laser was used in conjunction with

the system. The temperature of all solutions was 25°C. The scattering angle was 90° and the wavelength was 632.8 nm. The experimental stability ratio was determined from PCS as described in Section D of Chapter 2.

The calculated stability ratios are anticipated to be approximate. Two restrictions apply in the use of equation 2.19. First, only particle translation is considered important so that $qR_g \leq 1$ where q is the scattering vector and R_g is the radius of gyration of the particle[135]. Second, the term α is determined from form factors, which in turn are determined using Rayleigh-Gans-Debye theory. The fundamental assumption[136](Chapter 8) in this theory is that $(4\pi nd/\lambda_o)(n_2/n_1-1) << 1$. Using polystyrene latex particles (n_2 = 1.59) in water (n_1 = 1.33) with a He-Ne source and a 90° scattering angle dictates that $R_g \leq 54$ nm to meet the first restriction and $d << 162$ nm to meet the second. Using the relationship, $d = 2(5/3)^{1/2}R_g$ gives $d \leq 139$ nm for the first restriction. Unfortunately, it was desired to maximize the size of the particles in order to increase the magnitude of the van der Waals forces[6]. Larger van der Waals forces should increase the number of Pluronics® which have the CFC below the theta point of the stabilizing polymer and should increase the difference in the CFC's between colloids with different molecular weight stabilizing blocks, in the case of marginally stable systems as shown in Table 2.2. Therefore, the particle size chosen was somewhat larger than the restrictions dictate.

When performing stability measurements, it is important to choose an appropriate initial particle concentration, because it determines the initial rate of aggregation [104]. An appropriate concentration is high enough to cause a significant change in the hydrodynamic diameter over the time of the experiment, but not so high that the initial aggregation rate, representative of the aggregation of singlets, cannot be determined in the time it takes to perform a single light scattering measurement. High particle concentrations result in artificially high stability ratios because the measured aggregation rate is performed when a significant number of doublets and higher order aggregates have formed, which effectively

reduces the particle number concentration from its initial value and hence, the apparent rate of aggregation. Theoretical work by Virden and Berg [104] suggests that concentrations less than or equal to 10^9 particles/mL are appropriate. The experimental work by Einarson [95] suggests that an appropriate concentration lies between $5x10^9$ - $10x10^9$ particles/mL.

It is also somewhat important to use a constant particle concentration, because it has been shown that aggregation caused by Van der Waals attraction between the core particles is slightly dependent on the particle concentration due to an entropic effect[6]. As a result, the particle concentration affects the rate of aggregation of electrostatic and electrosterically stabilized but not sterically stabilized dispersions . Therefore, choosing a single, appropriate particle concentration for an entire set of experiments involving stabilization mechanisms which are not solely steric requires a balance between a concentration low enough to allow accurate characterization by the light scattering system during rapid aggregation and a concentration high enough to allow accurate characterization during slow aggregation.

The appropriate particle concentration was chosen for this work by performing aggregation experiments for the bare latex at varying particle concentrations in 0.1 M $MgSO_4$,a concentration which allows rapid aggregation. The computed stability ratios are reported in Table 3.2. The aggregation experiment at approximately $1x10^9$ particles/mL was duplicated and the standard deviation is given after the stability ratio. The stability ratio in all cases is higher than the anticipated stability ratio of 1 for rapid flocculation. Viscous drainage effects typically result in experimental stability ratios which are as low as 40% of the Smoluchowski rate[105, 106] so these effects account for some of the deviation from ideality. It is highly probable that some of the additional deviation is caused by the age of the latex dispersions, which were diluted from the latex stock using distilled water 3-4 days prior to the experiments. Young and Prieve[107] have demonstrated that slow aggregation occurs once the latex stock is diluted, and that the extent of aggregation is

significant after a few days. The addition of an adlayer was observed to diminish the effect. (The data in Figure 3.2 was also taken without consideration of this slow aggregation. However, to minimize the effect of slow aggregation, all subsequent experiments were performed so that an adlayer was adsorbed within the same day as dilution of the latex stock.) The data in Table 3.2 also indicate that a slight increase in the stability ratio is observed as the particle concentration increases over the range tested, indicating that the particle concentration is becoming too high to allow measurements before significant aggregation has occurred. Because the change in stability ratio was not large over the range of particle concentrations tested, a particle concentration of $5x10^9$ particles/mL was chosen. This concentration was anticipated to allow reasonably accurate measurements of both rapid and slow aggregation.

Table 3.2. The Stability Ratio Obtained for Various Concentrations of 0.168 μm Latex in 0.1 M $MgSO_4$.

Particle Concentration (number/mL)	Stability Ratio
$9.96x10^8$	6.77+/-0.33
$5.00x10^9$	7.70
$9.96x10^9$	8.74

The CFC was determined for colloids stabilized with only one type of Pluronics® in order to assess which of the polymers imparted full or marginal stability. $MgSO_4$ was the electrolyte chosen to induce flocculation. As shown in Figure 2, the CFC increases with increasing PEO molecular weight, until the molecular weight falls between 1150 and 2100, or 13 to 24 monomer units per tail. At PEO molecular weights at or above 2100, the CFC is roughly 0.7 M $MgSO_4$, which is in reasonable agreement with the θ point of 25°C in 0.5 M $MgSO_4$ found by Boucher and Hines [68]. The data also agree with the cloud point data generated by Bailey and Callard [65]. The data therefore suggest that the

Pluronics® P75 and F108 impart full steric stability, while the other Pluronics® impart only marginal stability. Based on the results given in Figure 3.2, the Pluronics® F108 was chosen for long tails, while the Pluronics® L43 was chosen for the short tails. The electrolyte concentration chosen for the aggregation experiments was 0.3 M $MgSO_4$. These conditions were anticipated to allow steric stabilization by the F108 to occur, while L43 would impart little or no stability.

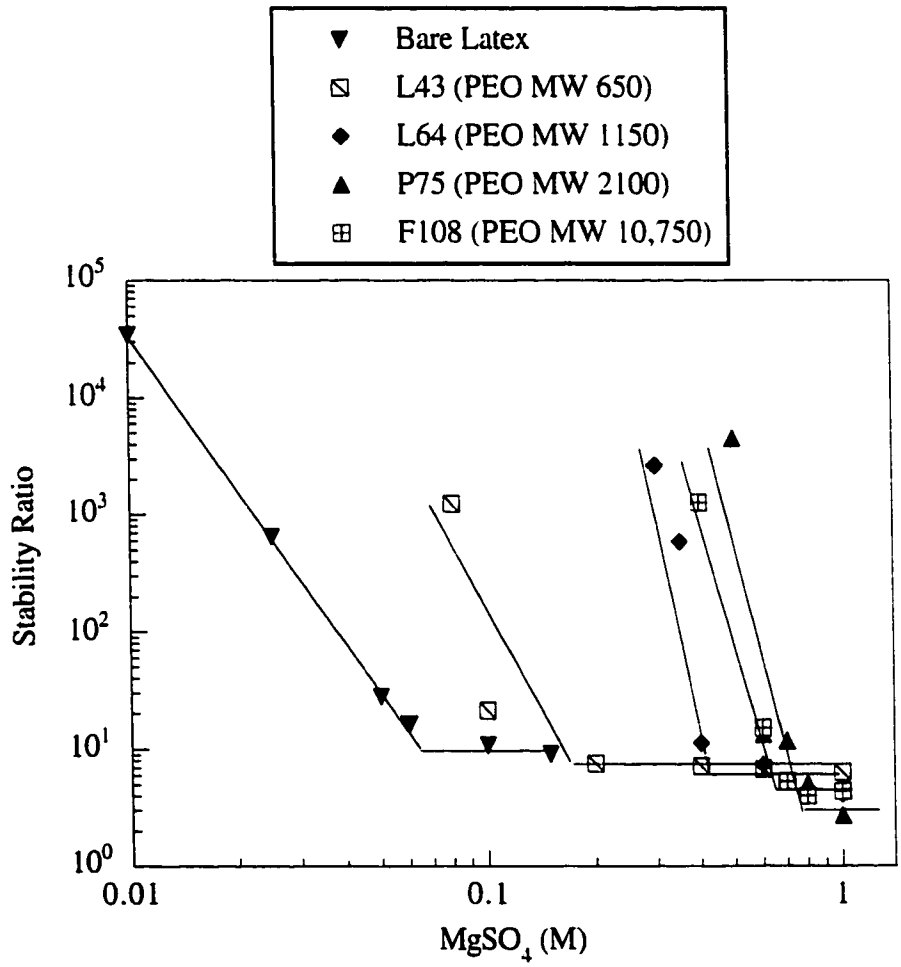

Figure 3.2. Stability Ratios for Bare and Pluronics® Coated Latex Particles as a Function of $MgSO_4$ Concentration.
(The molecular weight of the PEO fraction is given in parentheses).

Adsorption Experiments

The percent F108 on the surface and the total amount adsorbed to the latex were determined as a function of the percent F108 in solution, by using the difference between solution concentrations before and after adsorption. (Here and subsequently, the percent F108, whether weight, number or undesignated, refers to the percent of all the polymer that is comprised of F108). Concentrations before adsorption were determined gravimetrically, while concentrations after adsorption were determined by a combination of size exclusion chromatography and turbidity

In a typical experiment the desired amounts of latex and dissolved polymer were gently stirred for 15 - 18 hours, then the latex was separated from the free polymer and water by ultrafiltration through a 0.1 μm filter. The percent F108 remaining in solution was determined by air drying 12 mL of the solution, then redissolving it in 2 mL tetrahydrofuran at 30°C. This solution was then analyzed by gel permeation chromatography, using a 300x7.5 mm PLgel 10 μm 500 Å column, a Waters 410 Differential Refractometer, and a Perkin Elmer LCI-100 Laboratory Computing Integrator. Due to the difference in refractive indices of the two Pluronics® polymers and the nature of the integrating software, the peak areas did not correspond directly to the weight fractions in solution. To obtain accurate values, a calibration curve was created, which is presented in Appendix A. To test the accuracy of the calibration, two aqueous solutions of known polymer composition (approximately 10 wt% F108) were dried, then redissolved in tetrahydrofuran as described above. The resulting solutions were analyzed using GPC. The percentages F108 obtained by GPC were within 2% of the known gravimetric values, on average. Details of this check are given in Appendix A.

The total amount of Pluronics® remaining in solution after adsorption and separation from the latex was determined using a modification of the turbidimetric technique developed by Attio and Rubio [137]. In this technique, 2.5 mL of sample were

mixed for 30 seconds with 2.5 mL of a solution containing 400 mg/L tannic acid and 0.2 M NaCl. The maximum allowed Pluronics® concentration after mixing was 10 mg/L, so samples were diluted accordingly before mixing. The transmittance was determined at 500 nm, 40-60 minutes after mixing. A solution of 200 mg/L tannic acid and 0.1 M NaCl in distilled water was used to set 100% transmittance. The transmittance was converted to the absorbance using the fact that the absorbance is log (100/%transmittance).

Before converting the absorbance to a concentration, a correction factor was first added. The correction factor was used to account for variations in reagent solutions and lamp intensity and was formulated as the difference in the predicted absorbance and measured absorbance for a standard with a concentration close to that of the sample. The correction factor was found to significantly reduce the variability between duplicate experiments, so was applied to all experiments.

To convert the corrected absorbance to a concentration, different calibration curves were developed for different proportions of the two Pluronics®, since the amount of turbidity developed was dependent on the type as well as the concentration of Pluronics® present. To determine the concentration, two predicted concentrations were computed from the corrected absorbance using calibration curves with the proportion of Pluronics® immediately below and above the actual proportion, as determined by size exclusion chromatography. The actual concentration was then computed using linear interpolation between the two predicted concentrations.

Justification for the parameters chosen for this test as well as the calibration curves are given in Appendix B. An estimation of the accuracy of the test was obtained by employing both gravimetric and turbidimetric techniques to determine total Pluronics concentrations for three different solutions. The results indicate that the turbidimetric

technique yields values to within 1.3% of gravimetric values, on average. Specific details on the accuracy check are given in Appendix C.

D. RESULTS

Adsorption Experiments

Adsorption experiments were performed on the latex, at concentrations used for the light scattering experiments. It was determined that no significant change in the solution concentrations occurred due to adsorption, so the starting concentrations of the polymer were taken as the equilibrium concentrations. Additional experiments were performed at high latex concentrations, where a significant change in polymer concentration occurred so that the amount adsorbed could be computed. Latex was mixed with the dissolved polymer to obtain a starting concentration of 4.2×10^{11} particles/mL and 350 mg/L Pluronics® in water. A solution concentration of 300 mg/L Pluronics® after adsorption was targeted in order to correspond with the conditions used during the aggregation experiments. The weight percent F108 on the surface and the total amount adsorbed as a function of the weight percent F108 in solution are given in Figure 3.3. The percentage of F108 molecules on the surface is given in parentheses, and is indicated as the number percent. Due to the large difference in molar mass, the number percent is an order of magnitude lower than the weight percent. Final concentrations of Pluronics® ranged from 255 to 318 mg/L with an average of 291 mg/L. The experiments corresponding to approximately 20 wt%, 50 wt%, and 80 wt% F108 in solution were repeated. The error bars indicate one standard deviation.

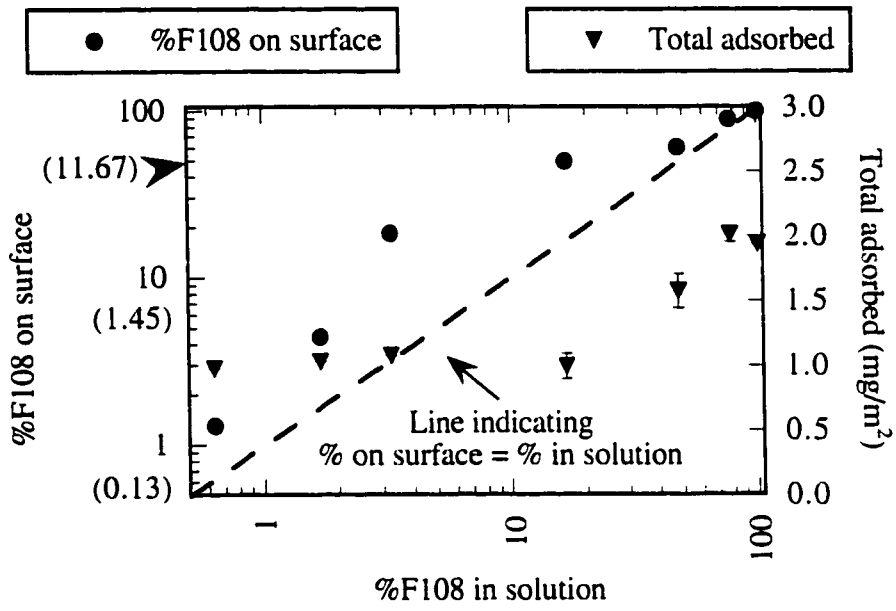

Figure 3.3. Percent F108 on the Surface and Total Amount of Pluronics® Adsorbed to Latex as a Function of Percent F108 in Solution.
(Values indicate weight percents, unless enclosed in parentheses.
Parentheses indicate number percent. Error bars indicate one standard deviation.)

As can be seen, the total weight of Pluronics® adsorbed increases with increasing percent F108. If the curve given in Figure 3.3 is evaluated at 100% L43 and at 100% F108, the data suggest that more F108 adsorbs than L43. This result is in qualitative agreement with the experimental findings of Mallagh [27] and Baker and Berg [132]. Mallagh found that the weight of Pluronics® adsorbed increased as the length of the polyethylene oxide tail increased, for the same length of polypropylene oxide block. His results are in qualitative agreement with Self Consistent Field Theory [27]. Baker also found that the weight adsorbed increased with the length of the PEO tail, even when the PPO blocks were not exactly the same length.

The data in Figure 3.3 suggest that, in solutions of only one type of Pluronics, the density adsorbed by the latex is 1.9 mg/m^2 for F108 and 1.0 mg/m^2 for L43 . The

quantity of F108 adsorbed seems somewhat high compared to that of Kayes and coworkers [133] and Baker and Berg [132], as shown in Table 3.3. It is comparable to the adsorption density found by Li [138]. However, Li determined the adsorption in 0.15 M phosphate buffer saline. Tadros and Vincent have shown that adsorption is higher in salt solutions than in pure water [134]. The data obtained by Mallagh [27] is given in the number of ethylene oxide (EO) and propylene oxide (PO) monomer units since the type of Pluronics® was unnamed. The molecular weight of the polymer studied by Mallagh is similar to that of F108, which has 122 EO units per tail and 56 PO units. The quantity of L43 adsorbed is in good agreement with the data of Seebergh and Berg [99].

Table 3.3. Surface Density of Pure Pluronics® at Plateau Levels of Adsorption.

Pluronic	Γ (mg/m^2)	Reference
F108	1.1	Kayes and Rawlins [133]
F108	1.35	Baker and Berg [132]
$EO_{140}PO_{56}EO_{140}$	1.57	Mallagh [27]
F108	2.1	Li, et al [138]
F108	1.94	This work
L43	1.1	Seebergh and Berg [99]
L43	1.0	This work

The percent F108 on the surface always exceeds the percent F108 in solution. This result differs from the findings of Dhoot and Tirrell [139]. These researchers studied the adsorption of polyvinylpyrrolidone-polystyrene diblock copolymers adsorbed to mica in toluene. They showed that for diblock copolymers with widely differing weights in the non-adsorbing segment, the percent surface coverage for the block with the longer segment will be lower than its percentage in solution. They explained that their results make intuitive sense since the amount of adsorption for a diblock will be governed by its tendency to stay in solution versus its tendency to stay on the surface.

Aggregation Experiments

The stability of the colloid was determined as a function of the F108 surface coverage, by combining the results of light scattering measurements and the results of the adsorption tests shown in Figure 3.3. The particles were observed to flocculate at low surface coverages of F108, as evidenced by the change in hydrodynamic diameter with time, as shown in Figure 3.4. Linear regressions revealed that the hydrodynamic diameter could not be positively correlated with time for surface coverages of 1.1 wt% F108, indicating full stability over the time of testing. This surface coverage corresponds to roughly 1 long tail/1000 nm^2 or 84 long tails per particle. For surface coverages lower than 1.1 wt%, the stability ratio was computed and plotted as a function of the weight or number percent F108 on the surface as shown in Figure 3.5. The error bars indicate the 95% confidence interval for three replicates. These data seem to suggest that some steric stability is still seen as low as 0.4 wt% F108 on the surface, which corresponds to 1 long tail/2700 nm^2 or 33 long tails per particle. However, the stability ratio of the colloid with 0.2 wt% F108 surface coverage is not statistically different than the stability ratio of the colloid with no F108, suggesting that the long tails do not affect the stability at this surface coverage. The stability ratios for both these colloids is 3-4, reasonably representative of rapid flocculation subject to viscous drainage effects [105, 106].

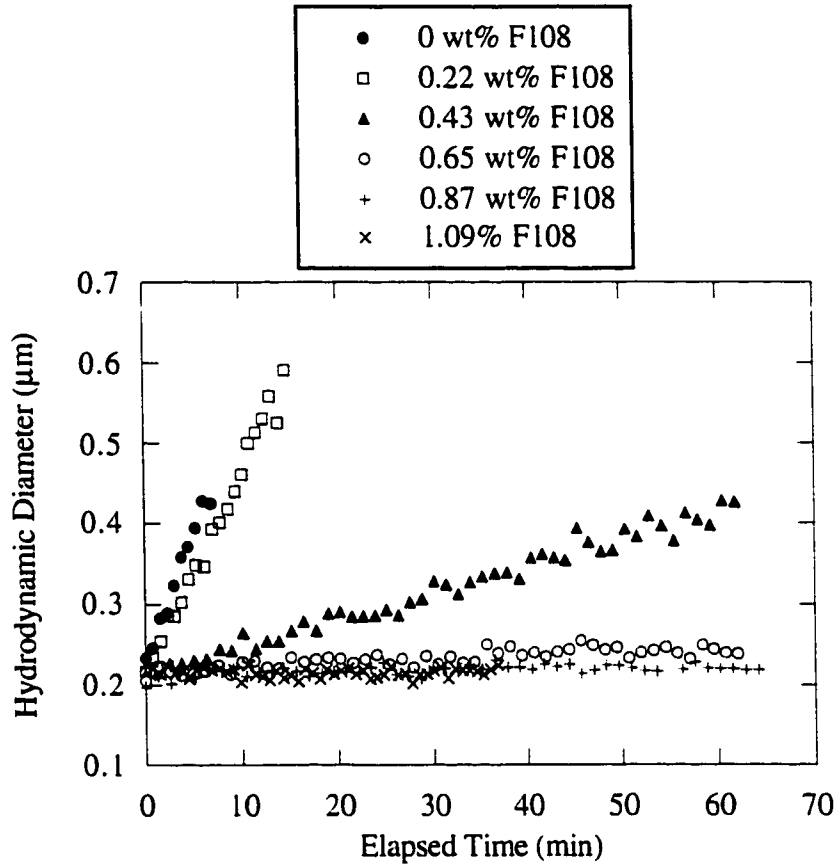

Figure 3.4. Change in Hydrodynamic Diameter of Latex Particles Stabilized with a L43/F108 Pluronics® Adlayer as a Function of Time, upon the Addition of $MgSO_4$. (The legend indicates the weight percent F108 on the surface.)

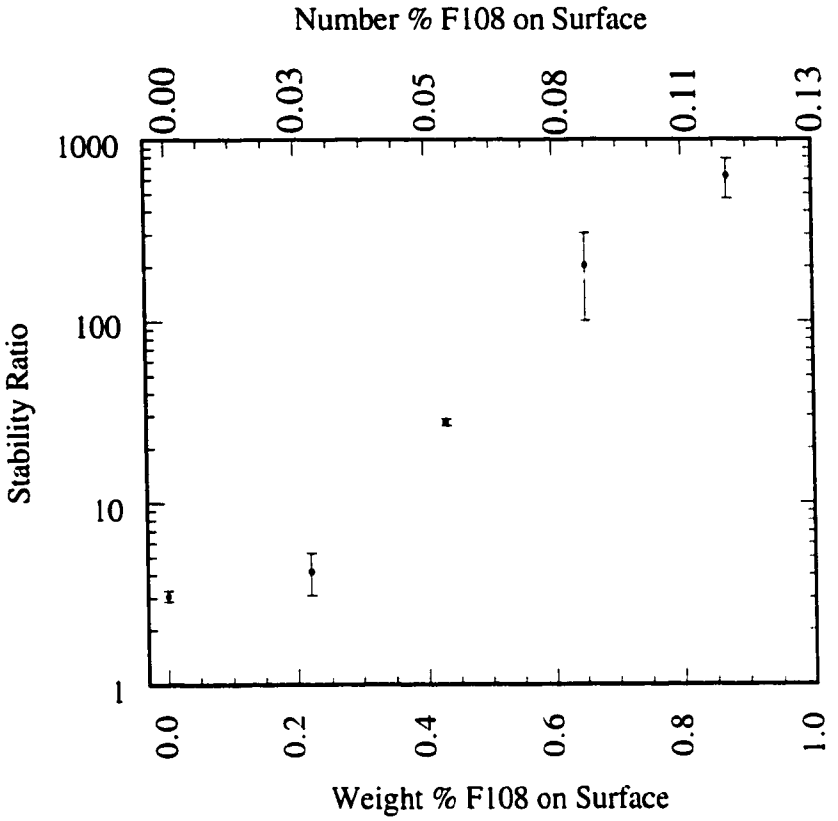

Figure 3.5. Stability Ratio of Latex Particles Stabilized by F108/L43 Pluronics® in 0.3 M $MgSO_4$ as a Function of Percent F108 on the Surface. (Error bars indicate 95% confidence interval.)

Hydrodynamic Diameter Measurements

At and above 1.1 wt% F108 surface coverage, the particles did not flocculate in 0.3 M $MgSO_4$, which resulted in an unchanging hydrodynamic diameter over the 30 to 60 minutes that the measurements were taken. The average particle diameter for this stable colloid is plotted as a function of F108 surface coverage in Figure 3.6 and is represented as a circle. The error bars indicate the 95% confidence interval for 50 to 60 replicates. For the stable colloid, the mean polydispersity is indicated by the diamond symbol. The polydispersity is proportional to the variance of the "intensity" weighted diffusion

coefficient distribution. It is close to zero (0.000 - 0.020) for monodisperse samples, small (0.020 - 0.080) for narrow distributions, and larger for broader distributions[108].

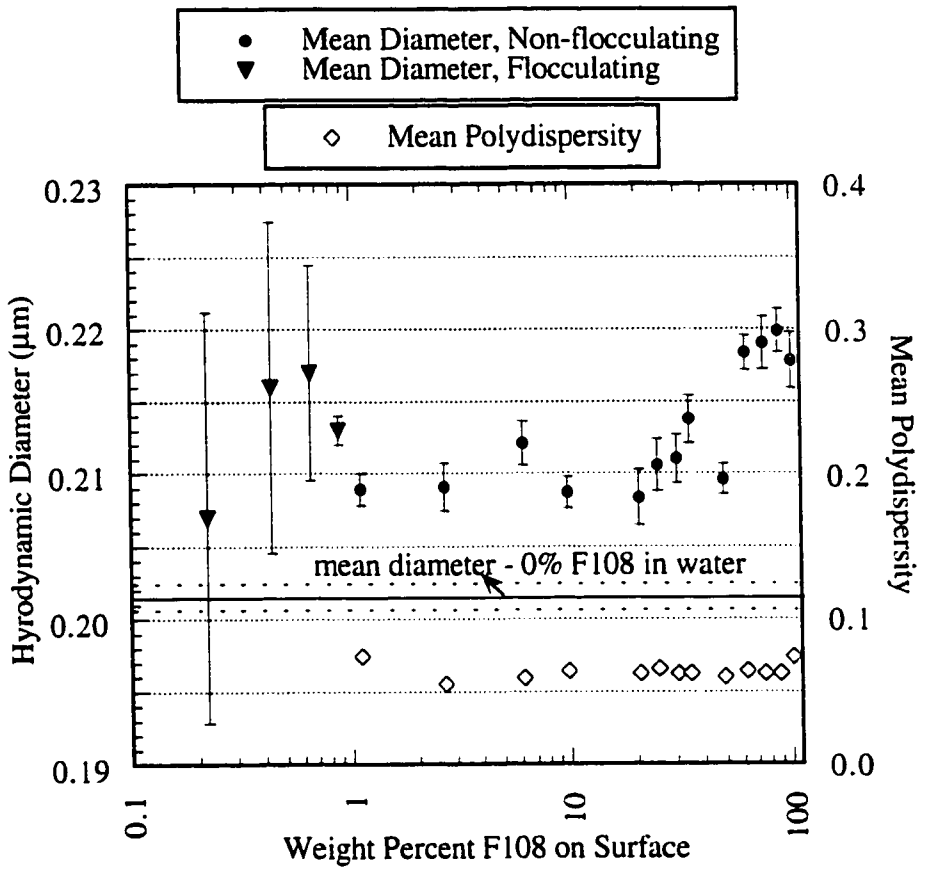

Figure 3.6. Hydrodynamic Diameter and Polydispersity of Latex Stabilized by F108/L43 Pluronics® Adlayer in 0.3 M $MgSO_4$. (Error bars and the dashed lines indicate the 95% confidence interval.)

In the case where flocculation occurs, the hydrodynamic diameter of a singlet can be estimated by linear extrapolation of the curve of hydrodynamic size versus elapsed time to the estimated point where salt is first added. The diameter estimated in this manner was plotted as the upside down triangle. The associated error bars indicate the 95% confidence interval for 3 replicates. Flocculating particles have large polydispersities which increase

with time, due to the formation of doublets and larger aggregates. Therefore a mean polydispersity cannot be indicated for flocculating particles.

The data shown in Figure 3.6 can be compared and contrasted to the data in Figure 3.7, which shows the mean hydrodynamic diameter and mean polydispersity for the colloid in distilled water, as opposed to 0.3 M $MgSO_4$. Estimations of the diameter based on extrapolation of the data are unnecessary since the particles never flocculate. The error bars of the hydrodynamic diameter indicate the 95% confidence interval for 50 to 60 points. Both Figures 3.6 and 3.7 show a horizontal line indicating the average hydrodynamic diameter obtained when the particles have 0% F108 surface coverage and are in distilled water. The dashed lines on either side indicate the 95% confidence interval for roughly 150 data points. The average particle diameter with 0% F108 surface coverage and in 0.3 M $MgSO_4$ is not indicated due to the extremely large variability encountered. This variability is incurred primarily from extrapolation of data with an extremely steep slope. In fact, the variability in data, indicated by the size of the error bars, can be seen to increase monotonically as the rate of flocculation increases and the surface coverage of F108 decreases in Figure 3.6.

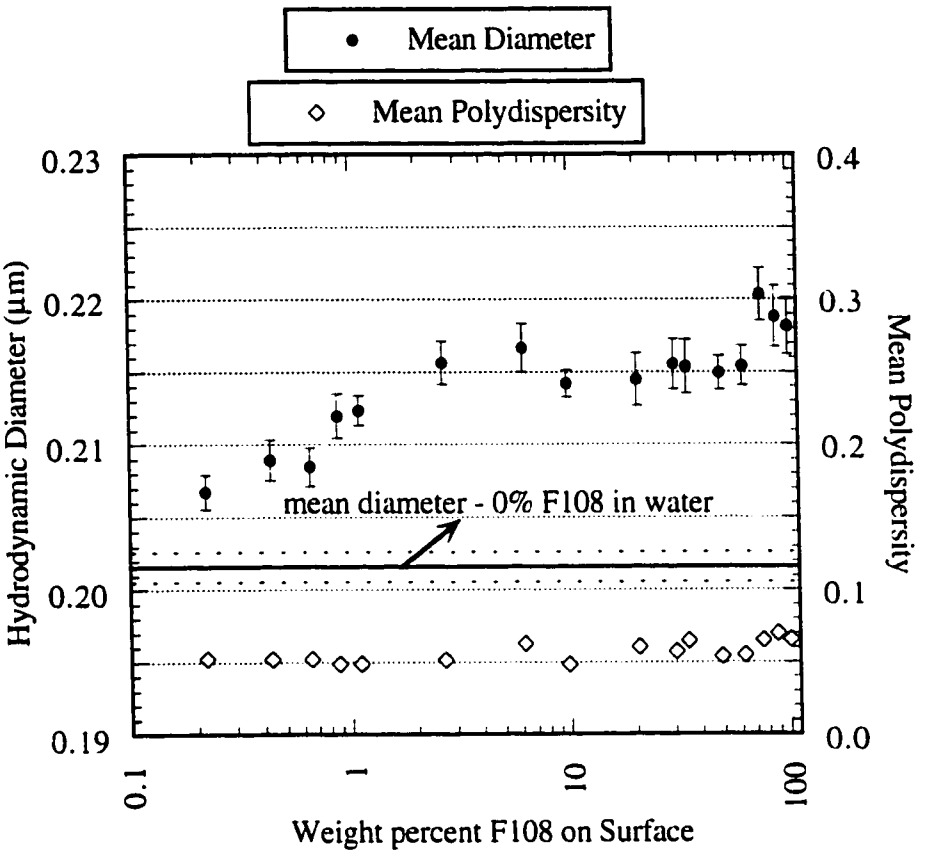

Figure 3.7. Hydrodynamic Diameter and Polydispersity of Latex Stabilized by F108/L43 Pluronics® Adlayer in Distilled Water.

The polydispersity in Figures 3.6 and 3.7 indicate that the stable colloid has a narrow particle size distribution, as expected. Both figures also indicate that the average particle diameter of the stable colloid is generally larger when the surface coverage by F108 is higher. The shape of both curves are in qualitative agreement with the theoretical predictions of Dan-Brandon and coworkers [140]. The hydrodynamic diameters of the colloidal particles are not statistically different in distilled and salt water, when the surface coverage of F108 is 70 wt% or higher. Between 1 wt% and 70 wt% surface coverage by F108, the hydrodynamic diameter in the salt solution is almost always smaller. For all but 2 of the 10 data points in this range, this difference is significantly different with greater

than 95% confidence. Below 1 wt%, one cannot generally conclude that the hydrodynamic diameters are different in the two solutions.

It seems that the trends observed in Figures 3.6 and 3.7 can be explained by the polymer-polymer and polymer-solvent interactions typically used to explain the conformation of adsorbed block copolymers in good solvents [27]. At high surface coverages and in good solvents, the long tails are forced to extend due to crowding, so the hydrodynamic diameters are larger than at lower surface coverages. Furthermore, the diameters are close to the same values despite the change in solvent, since the solvent does not fully control the polymer extension. This long extension is evidenced by the fact that, in both solvents at high F108 surface coverages, the adlayer thickness of 10-11 nm is significantly larger than two to three times the calculated unperturbed radius of gyration of 2 nm [141] and of the same order of magnitude as the calculated contour length of 36 nm. At lower surface coverage by F108, the long tails can take on a more coiled configuration since there is less crowding. Because the pure water is a better solvent than the salt water, the coil is less compact and the hydrodynamic diameter is larger in the former solvent. At medium levels of coverage by long tails, the hydrodynamic diameter remains relatively constant since the particles are covered by a sheath of polymer coils. Although a change in hydrodynamic diameter occurs between high to medium coverage by long tails, the change is not significant enough to affect the incipient stability.

If the mechanisms discussed are responsible for the changes in the hydrodynamic diameter, then it seems plausible that the hydrodynamic diameter should be larger in water, even when the colloid is unstable. However, in these cases, the confidence intervals are extremely large due to the uncertainty in extrapolation, making comparisons between the hydrodynamic diameters in the two media impossible at low long tail coverages.

Even despite the uncertainty, an estimation of the sensitivity of hydrodynamic measurements in 0.3 M $MgSO_4$ can be made. If the mechanism discussed in the previous

paragraph is accepted, then it is permissible to use the hydrodynamic diameter of the colloidal particles with 0% F108 in water and the associated variability as representative of the colloid with 0% F108 in 0.3 M $MgSO_4$. The mechanism suggests that when the particles are fully covered with a single type of Pluronics®, then the adlayer thickness will be relatively independent of the solvent, just as long as the solvency is relatively good. Accepting this hypothesis, an analysis of the data in Figure 3.6 suggests that hydrodynamic measurements are sensitive to a density of long tails less than or equal to 0.4 wt% F108 surface coverage in 0.3 M $MgSO_4$.

This sensitivity can be contrasted to the sensitivity of the hydrodynamic measurements in pure water. A student T test indicates that, with greater than 99% confidence, the average hydrodynamic diameter of the colloidal particles with 0.2 wt% F108 surface coverage is greater than that with 0 wt% F108 surface coverage. This result suggests that the hydrodynamic measurements are sensitive to a density of long tails less than or equal to 0.2 wt% F108 surface coverage in pure water. It seems that the detection limits of the hydrodynamic measurements in pure water are relatively close to 0.2 wt% F108 surface coverage, since the hydrodynamic diameter appears to decrease significantly with a small decrease in F108 surface coverage. A decrease in surface coverage from 2.6 to 0.2 wt% F108 results in a 4.5 nm decrease in the adlayer thickness, for a final adlayer thickness of approximately 3.5 nm. This is a relatively large change for a small change in coverage, considering the adlayer is at most 11 nm. A linear regression over the range of 0.2 to 2.6 wt % F108 surface coverage gives:

$$\textit{hydrodynamic diameter in } \mu m = (0.003)(\textit{wt\% F108}) + 0.207 \qquad \text{Eq. 3.1}$$

The square of the correlation coefficient is 0.85, further suggesting a positive, relatively linear correlation between the two variables. The data suggest that below 2.6 wt% F108 surface coverage, the density of long tails is too low to form a full sheath of polymer coils.

Interestingly, the region where the density of long tails strongly affects the hydrodynamic diameter corresponds well to the region where the density of long tails strongly affects the incipient stability. In fact, a linear regression of the stability in 0.3 M $MgSO_4$ and the hydrodynamic diameter in distilled water over the range of 0.2 to 0.9 wt% F108 surface gives:

$$\textit{stability ratio} = (12095)(\textit{hydrodynamic diameter in } \mu m) - 25073 \qquad \text{Eq. 3.2}$$

The square of the correlation coefficient is 0.83, which suggests a positive, relatively linear correlation between these two variables. This correlation is visually depicted in Figure 3.8.

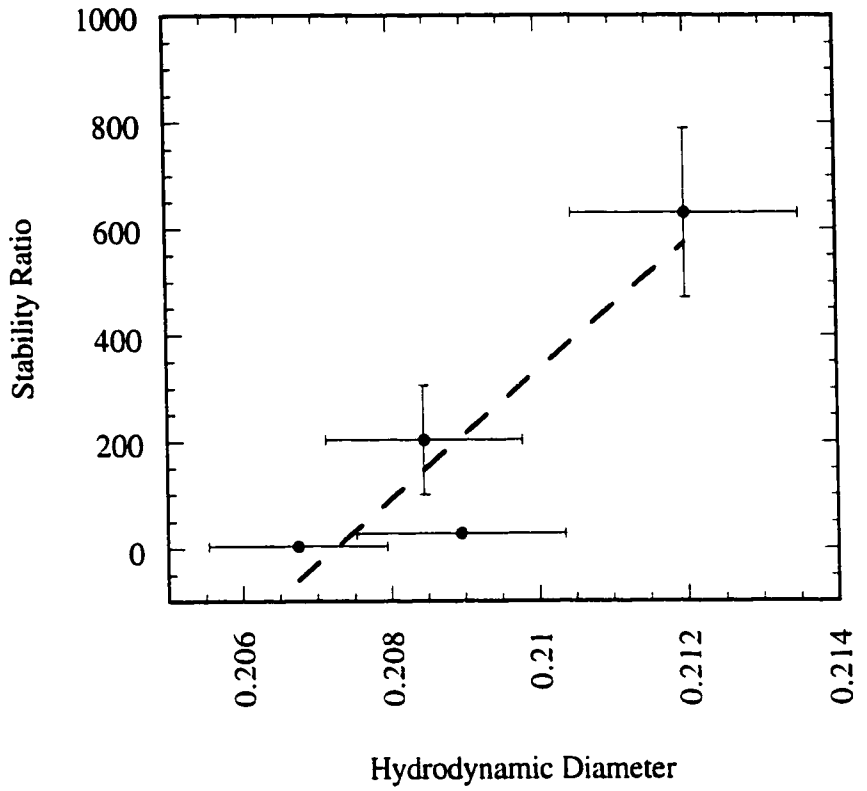

Figure 3.8. Stability Ratio in 0.3 M $MgSO_4$ versus Hydrodynamic Diameter in Distilled Water. (Dashed line indicates the curve fit. Error bars indicate the 95% confidence intervals.)

E. CONCLUSIONS

The results of this study indicate that steric stability and hydrodynamic measurements are sensitive to a low density of long tails. These results are in agreement with expectations of previous literature. A comparison of the two measurements suggests that the density of long tails required to impart full steric stability is somewhat higher than the density of long tails required for detection by hydrodynamic measurements. For the system used in this study and as summarized in Table 3.4, *full* steric stability is imparted at roughly 1 wt% F108 adsorbed or roughly 84 long tails per colloidal particle of radius 168 nm, while the limits of hydrodynamic detection are less than 0.4 wt% F108 or 33 long tails per particle in the same solvent. The minimum density of long tails required to measurably

affect the hydrodynamic diameter compares reasonably well with the minimum density of long tails required to impart some, but not full steric stability. Specifically, there is a linear correlation of the stability ratio with the hydrodynamic diameter at extremely low surface densities of long tails. Both factors experience relatively large changes over a small change in surface coverage by long tails. The hydrodynamic thickness may thus adequately characterize the state of stability for systems with adlayers having a low density of long tails.

Table 3.4. A Comparison of the Sensitivity of Steric Stability and Hydrodynamic Measurements to Tails

Measurement	Weight Percent F108 Adsorbed	Number Percent F108 Adsorbed	Density (tails/particle)
Beginning of Steric Stability	0.2 - 0.4	0.03 - 0.05	17 - 33
Full Steric Stability	1.1	0.14	84
Hydrodynamic Sensitivity in 0.3 M $MgSO_4$	<0.4	<0.05	<33
Hydrodynamic Sensitivity in Distilled Water	< 0.2	<0.03	<17

CHAPTER 4: POLYETHYLENE OXIDE-SALT INTERACTIONS

A. LITERATURE REVIEW - POLYETHYLENE OXIDE SALT COMPLEXES

It was recognized that polyethylene oxide (PEO) formed complexes[142] as early as 1966. A significant amount of research has been conducted since the 1970's to understand the nature of these materials. The focus has been primarily on the solid phase, since the materials form solid polymer electrolytes, which are advantageous over liquid electrolytes in their ability to conform to solid electrodes but maintain separation of chemicals. The information gained from these investigations has application to PEO in aqueous solutions since many similarities exist. Therefore, this literature review discusses not only the interaction of PEO to salt in water, but pertinent aspects of the complex in the solid phase. The first section focuses on the degree of complexation, while the remaining sections focus on the polymer conformation.

Degree of Complexation

It is generally recognized that PEO forms complexes with cations in a manner resembling a crown ether complex. The oxygens donate their electrons to the cation, while the polymer takes on a helical configuration. The ratio of ether oxygens to metal cations generally ranges from 4:1 to 8:1, although both lower and higher ratios have been found[143-145]. This ratio is supported by the fact that low molecular weight oligomers with less than five monomer units generally show poor complexation. Above 5 monomer units, the complexation has been observed to both decrease and remain constant, depending on the study or system [146].

Greater complexation is seen for larger anions, such as I^- and ClO_4^- since the ability to form complexes for any given cation is inversely proportional to the lattice energy or the energy required to separate the ions to infinite distance. Large, polarizable soft base anions such as SCN^- and BH_4^- give very low oxygen to cation ratios (i.e. large degrees of complexation) [144]. The dependence on the cation varies depending on the nature of the environment. For solvent free systems, complexation to smaller cations occurs quite readily (Li^+, Na^+, K^+) and results in crystalline structures. It is usually believed that large cations such as Rb^+ and Cs^+ do not form complexes, since the polymer-salt mixtures are amorphous[144]. In contrast, in polar solvents, such as methanol, the order of selectivity[146] is $K^+ \geq Rb^+ > Cs^+ > Na^+ > Li^+$ (See Table 4.1). Explanations for this dependence are due to differences in the polymer conformation, which will be discussed in more detail. Far fewer data are available for alkaline earth complexes, but the order of complexation is generally taken to be $Ba^{2+} > Sr^{2+} > Ca^{2+} > Mg^{2+}$.

When complexation in solvents is investigated, the focus is generally *not* on aqueous systems. Water has a very strong ability to solvate ions, so complexation is generally poor[146]. There are a few studies, which suggest that complexation does occur in aqueous solutions. Sartori and coworkers[147] used ion selective electrodes and ultrafiltration to quantify the degree of electrolyte binding at low (millimolar) salt concentrations. Yanagida[148] and Kikuchi[149-152] and their respective coworkers employed solvent extraction at higher salt concentrations (0.5 M and 0.01 to 0.1 M, respectively). The metals ions are extracted from the solvent as an ion association complex. Kikuchi describes the distribution ratio in terms of 4 elementary steps: distribution of the polymer between phases, formation of the cation complex with the polymer in the aqueous phase, ion pair formation of the polymer-metal complex with the

anion in the aqueous phase, and distribution of the ion pair between phases. He reasoned that:

- The distribution of the polymer between phases is generally similar for a given molecular weight and type of ion (alkali or alkaline earth)
- The distribution of the ion pair between phases should be similar for the same type of ion, since the molar volume of the ion pair hardly changes upon a change in the cation.

He also showed that the degree of dissociation (ion pair formation) is the same for a given type of ion during the solvent extraction tests. When combined, these deductions suggest that the differences in extraction capability are due primarily to the differences in the ability of PEO to complex various ions.

This final conclusion is further supported by the fact that the order of increasing complexation found by Sartori generally follows the same order of increasing solvent extraction found by Yanagida and Kikuchi, as shown in Table 4.1. The order of extraction ability also generally follows the order found for alkali metals in polar solvents and the inferred order for alkaline earth metal salts, as discussed by Okada[146]. In particular, the ability increases with increasing size for a particular anion. Iodides and thiocyanates show particularly strong complexing capability. The order for the alkali metals clearly increases from Li^+ to Na^+ to the larger cations, K^+, Rb^+, or Cs^+. The exact order of these latter three seems to vary somewhat. Combining the solvent extraction tests suggests that the order of alkaline earth metals is generally taken to be $Mg^{2+} < Ca^{2+} < Sr^{2+} < Ba^{2+}$, as was found in the case of solid polymer electrolytes.

Table 4.1. Order of Ion Binding to PEO in Solutions.

A. Potassium Salts

Order of Ion Binding	Method of Determination	Reference (first author)
$F^- \approx Cl^- < SCN^-$	Ion selective electrodes and ultrafiltration	Sartori[147]
$Cl^- \leq Br^- \approx NO3^- \ll I^- < SCN^-$	Solvent extraction	Yanagida[148]
$Cl^- < F^- < Br^- < NO3^- \ll I^- < SCN^-$	Solvent extraction	This work

B. Sodium Salts

Order of Ion Binding	Method of Determination	Reference (first author)
$Cl^- < NO_3^- < SO_4^{2-}$	Solvent extraction	This work

C. Alkali Metal Salts

Order of Ion Binding	Method of Determination	Reference (first author)
$Li^+ \ll Na^+ < Rb^+ \approx K^+ \approx Cs^+$	Ion selective electrodes and ultrafiltration of chloride salts	Sartori[147]
$Li^+ < Na^+ < Cs^+ < K^+$	Solvent extraction of iodide salts	Yanagida[148]
$Li^+ < Na^+ < Cs^+ < K^+$	Solvent extraction of picrate salts	Kikuchi[149]
$Li^+ < Na^+ < Cs^+ < Rb^+ < K^+$	For polar solvents, using many techniques	(Okada)[146]
$Li^+ < Na^+ \approx K^+$	Solvent extraction	This work

D. Alkaline Earth Metal Salts

Order of Ion Binding	Method of Determination	Reference (first author)
$Mg^{2+} < Ca^{2+} < Sr^{2+} < Ba^{2+}$	Many sources	(Okada)[146]
$Mg^{2+} \leq Ca^{2+} < Ba^{2+}$	Solvent extraction of SCN- salts	Yanagida[148]
$Ca^{2+} < Sr^{2+} < Ba^{2+}$	Solvent extraction of picrates	Kikuchi[150]
$Mg^{2+} \approx Ca^{2+} \approx Ba^{2+}$	Solvent extraction	This work

The dependence on the molecular weight also fits the known dependency. In particular, both Kikuchi and Yanagida found that solvent extraction increased with increasing polymer molecular weight. Kikuchi showed that a PEG with less than 4

monomer units has very poor complexing ability, most likely due to its inability to wrap completely around the cation. This result is in agreement with the findings cited above. Yanagida found poor extraction when the polymer had less than 23 monomer units. This dependence may be a function of the complexation ability as suggested by Yanagida, but also of the ability of the polymer to partition into the organic phase, which was not accounted for in the analysis.

Conformation of PEO in Water

To understand the conformation of PEO complexes in water, the case where no salt is present must be discussed first. The latter has been studied by both infrared and Raman spectroscopy, while the crystalline solid has been studied by these methods as well as x-ray diffraction (XRD). In the crystalline solid the PEO takes on a helical structure which has a repeat unit containing 7 monomer units that create two turns[153]. The length of the repeat unit is 19.3 Å[153]. The conformation is generally trans, gauche, trans (TGT) around the OCCO bonds[154, 155]. The helix has dihedral (two-fold) symmetry, with one axis of symmetry passing through the oxygen atom and the other bisecting the carbon-carbon bond[156, 157].

In the study of aqueous solutions, Raman spectroscopy is advantageous over infrared spectroscopy; the scattering by water is weak, so solvent scattering does not obscure that of the polymer. Matsuura and Fukuhara[158] offered the following classification of the spectral bands, based on a theoretical and experimental analysis of the polymer in water:

1) C-H stretching 3000-2850 1/cm
2) CH_2 scissoring 1500-1450 1/cm
3) CH_2 wagging 1420-1320 1/cm
4) CH_2 twisting 1310-1230 1/cm

5) Hybridized vibrations of skeletal stretching. (C-O and C-C stretching, CH_2 rocking) 1160-810 1/cm

6) Skeletal deformation vibrations below 600 1/cm

From the 1970's to 1980's, the region of focus was between 800-1500 1/cm. Preliminary assignments were made by Koenig and Angood[159], Maxfield and Shepherd[160], and Matsuura and Fukuhara[161]. Matsuura and Fukuhara[158] later made assignments based on a thorough normal coordinate analysis, followed by experimental measurements. Outside the region 800-1500 1/cm, Matsuura and Fukuhara did not make assignments since there was no systematic correlation between the wavenumber and conformation. As can be seen in Table 4.2, the same peaks were seen in these three studies, but the assignments sometimes varied.

From the studies in this era it was found that the conformation of PEO in aqueous solutions exhibits a structure whose order is between that of the disordered melt and the ordered crystalline form. In particular, the widths of the peaks are between the crystalline and molten phase. The shifts in frequency from the crystalline phase are not appreciable, but the addition of water often removes the characteristic splitting of peaks due to the presence of a well ordered helix. This increased order over the melt is caused by hydrogen bonding between the solvent and molecules.

The existence of ordered structure was supported by the analysis of certain key peaks. The main conclusion was that the TGT structure about the O-C-C-O bonds was partially maintained and was still the dominant conformer. In particular, the peak associated with a trans configuration of the carbon-carbon bond (811 1/cm) is quite small in aqueous solutions, thus implying that the gauche C-C bond required for the helix is favorable. Positive evidence for the existence of the TGT structure was found by all three investigators, but the peaks employed to justify this conclusion varied with the

conformational assignments. Koenig and Angood noted that the peak at 846 1/cm was quite strong, while Maxfield and Shepherd noted that this peak was stronger than in the melt. Based on their spectral assignments, this fact suggests the existence of a TGT structure. Matsuura and Fukuhara only assigned the gauche configuration about the C-C bond, which is a necessary but not sufficient requirement for existence of the TGT structure. These authors suggest instead that the peak at 1248 1/cm is "a good key band for identifying the oxyethylene TGT conformation." Maxfield claimed that further evidence for the existence of the TGT structure is supported by maintenance of the peak at 1061 1/cm and the split at 1280 1/cm.

Evidence for disorder in the structure was also found in analysis of particular peaks. The most notable detail is that Matsuura and Fukuhara found a well defined peak at 1045 1/cm, which is characteristic of disordered PEO. Other peaks they found which were associated with a non-solid, disordered structure include shoulders at 832, 1258, and 1301 1/cm, and weak bands at 890, 915-918, and 992-999 1/cm.

The dependence of the conformation on the PEO concentration is somewhat less clear from studies in this era. Maxfield and Shepherd note that the conformation gradually changes from an ordered to a more disordered structure upon the addition of water, until the concentration is 50% by volume. Below this, no additional changes occur. This conclusion is supported by the changes in the peak at 862 1/cm, which decreases upon the addition of water until the 50% value is reached. These conclusion contrast with those of Matsuura and Fukahara, who note that the more dilute solutions are more like the solids. Two factors could account for this discrepancy. First, the molecular weight of the PEO tested by Maxfield and Shepherd was $3x10^6$, while Matsuura and Fukuhara tested an oligomer with 1 to 2 repeat units capped with methyl groups. Secondly, Matsuura and Fukuhara tested predominantly lower PEO concentrations (≤50%), while Maxfield and Shepherd tested predominantly higher PEO concentrations (>50%).

Table 4.2. Raman Vibrational and Conformational Assignments for PEO in Water

Wavenumber (1/cm)*	Vibration**	Conformation***	Reference
282	D-LAM (need isotropic spectrum)	TGT	Yang, Branca
350	D-LAM (need isotropic spectrum)	TGG'	Yang, Branca
807 s 810 ms 811 ms	 $r(CH_2)$ $r(CH_2)$, $t(CH_2)$	TGG of OCCO TTT of OCCO xTx	Koenig Maxfield Matsuura
832 sharp 832 sh 830	end groups u(CO), $r(CH_2)$ skeletal stretch (for isotropic spectrum)	 xGx-xGx of OCCOCCO TGG'	Maxfield Matsuura Yang
846 vs 851 s 850 s	 $r(CH_2)$ u(CO), $r(CH_2)$	TGT of OCCO TGT of OCCO xGx of OCCO	Koenig Maxfield Matsuura
860	skeletal stretch (for isotropic spectrum)	TGT	Yang
884 w 884 w 885 mw	 $r(CH_2)$ u(CO), $r(CH_2)$	GGG of OCCO, TGG, GGG of OCCO xGx-xTx of OCCOCCO	Koenig, Maxfield Matsuura
885	C-OH stretch		Matsuura
911 w 918 w	u(CO), $r(CH_2)$	TGG, GGG of OCCO xGG-TGx of OCCOCCO	Koenig Matsuura
947 w 943 w 947 sh	 $r(CH_2)u(COC)$ $r(CH_2)u(CO)$	TGT of OCCO TGT of OCCO XGT-TGx, xTx-xTx of OCCOCCO	Koenig Maxfield Matsuura
997 w	u(CO)u(CC)	xTT-Gxx	Matsuura
1045 w 1041 m 1045 m	 $r(CH_2)u(COC)$ u(CO)u(CC) $r(CH_2)$	TGG of OCCO TGG of OCCO xTT-TGx, xGT-GGx of OCCOCCO	Koenig Maxfield Matsuura
1063 w 1061 m 1065 m	 $r(CH_2)u(COC)$ u(CO)u(CC) $r(CH_2)$	TGT of OCCO TGT, TTT of OCCO Most conformers	Koenig Maxfield Matsuura
1116 sh 1116 vw 1114 sh	 u(COC) u(CO)u(CC) $r(CH_2)$	TGT of OCCO TGT of OCCO	Koenig Maxfield Matsuura
1123 m 1123 sharp 1124 sh	 u(COC) u(CO)u(CC) $r(CH_2)$	TTT of OCCO TTT, TGT of OCCO	Koenig Maxfield Matsuura

Table 4.2 (cont.)

1135 s 1139 s 1139 ms	u(COC)	T,G	Koenig Maxfield Matsuura
1145 sh	u(CO)u(CC) r(CH_2)		Matsuura
1233 1230 vw	t(CH_2)	TTT, TTG, TGT of OCCO	Koenig Maxfield
1251 m 1248 m	t(CH_2)	TGT of OCCO	Koenig Matsuura
1258 sh	t(CH_2)	TGG of OCCO or xTT-TTx of OCCOCCO	Matsuura
1286 m 1286 s 1287 ms	t(CH_2) t(CH_2)	TTT, TGT of OCCO xxT of OCCO	Koenig Maxfield Matsuura
1302 1298 s 1301 sh	t(CH_2) t(CH_2)	xxG-Txx of OCCOCCO	Koenig Maxfield Matsuura
1372 vw	w(CH_2) u(CH_2)	TGG. GGG of OCCO	Maxfield
1383 w			Koenig
1396 vw	w(CH_2)		Matsuura
1456 m 1452 m 1451 m	sc(CH_2)	TGG, TGT of OCCO	Koenig Maxfield Matsuura
1470 s 1474 s 1474 s	sc(CH_2)	TGT of OCCO All conformers	Koenig Maxfield Matsuura
3200	u(OH)	O-H involved in intramolecular H-bonds	Crupi
3350	u(OH)	O-H fully involved in intermolecular H-bonds	Crupi
3500	u(OH)	O-H with only H atoms bonded	Crupi

*Band intensities: sh (shoulder); vw (very weak); w (weak); mw (moderately weak); m (moderate); ms (moderately strong); s (strong)
Band resolution: sharp (sharp)
**Mode assignments: r (rocking); t (torsion); u (stretching); w (wagging); sc (scissor)
***T=trans, G=gauche or gauche minus, G'=gauche minus or gauche (opposite of G), x=trans or gauche

More recent Raman investigations of PEO in water have focused on bands outside the 800-1500 1/cm range. Crupi and coworkers[162] investigated the O-H stretching spectra between 3200 and 3500 (see Table 4.2). The different peaks are associated with different types of hydrogen bonding. The peaks at 3200 and 3350 1/cm correspond to intramolecular and intermolecular bonding, respectively. The peak at 3500 1/cm

corresponds to situations in which only the H atom is bonded. Crupi concluded that an increase in water content causes an increase in the number of water molecules tightly bound to the lone electrons on the oxygen. The H-bonding to the ether oxygens appears to be stronger than those of the end groups.

Other recent Raman investigations[163, 164] have focused on the region below 600 1/cm. This part of the spectra is created by the skeletal bending and stretching vibrations of a number of conformers. The scattering is highly polarized. In crystalline systems, the characteristic band is called the longitudinal acoustic mode (LAM), and the frequency of the band is inversely proportional to a value called the stem length. In non-crystalline systems, the LAM band becomes the disordered longitudinal acoustic mode (D-LAM) and the stem length becomes the persistence length (length below which the coil can be treated as rigid).

Since the scattering in the D-LAM region is caused by a number of conformers, the assignment of conformers to a particular band is nearly impossible by conventional normal coordinate analysis, as mentioned by Matsuura and Fukuhara. To circumvent this problem, Yang and coworkers used approximate simulations to create a composite spectrum from a specified distribution of chain conformations. They found that the aqueous PEO is dominated by the TGT conformation, while the melt is dominated by the TGG' conformation. The TGT dominated distribution has a D-LAM centered at approximately 282 1/cm and a skeletal stretching band at approximately 860 1/cm. The TGG' dominated distribution has a D-LAM centered at 350 1/cm and a skeletal stretching band at 830 1/cm. The skeletal stretch around 800 1/cm is sensitive to short range order; for instance, any conformers with a TGT OCCO order has skeletal stretching at 860 1/cm. In contrast, the D-LAM region is sensitive to long range order (9 bond conformations).

Branca and coworkers studied the peak in the D-LAM region as a function of the degree of hydration for polyethylene oxide of molecular weight 600. They found that the addition of water caused an increase in the wavenumber of the D-LAM region (over 10

1/cm) and a decrease in the peak width of approximately 20%. Once the polymer was fully hydrated, these two values remained relatively constant. These changes are indicative of increasing order due to the addition of water, as was also suggested by Matsuura and Fukuhara. The conclusions are supported by decreasing compressibility of the system upon the addition of water.

Conformation of PEO in Aqueous Salt Solutions

The conformation of PEO in aqueous salt solutions can be understood from the conformation of pure PEO/salt or crown ether/salt complexes. Sato and Kusumoto[165] found that a highly polarized peak appeared at 870 1/cm when crown ethers were mixed with alkali metal salts. If possible no solvent was used, but sometimes a small amount of methanol was necessary. The peak was attributed to the formation of a complex between the alkali metal and the crown ether in a TGTTG'T conformation about the OCCOCCO bonds. The G and G' conformations indicate the gauche plus followed by the gauche minus conformation or vice versa. The high degree of polarization indicates that the vibration is highly symmetric. The vibrational mode was attributed to a symmetric metal-oxygen breathing mode.

In a very similar manner, Papke, Ratner, and Shriver[166, 167] made solvent free PEO/alkali metal salt complexes. They also observed the peak at 870 1/cm and likewise attributed its appearance to the formation of a complex with the TGTTG'T conformation. This conformation fits well with many of the known data. In particular, x-ray diffraction studies suggest that the repeat unit decreases from 19.25 Å for the pure PEO to 8.1 Å for the KSCN complex[168]. The TGTTG'T creates a more compressed helix than the TGTTGT conformer and has a repeat distance of 9-11 Å. This helix would allow 4 ether oxygen's to complex to the cation, as also suggested by the studies focusing on the degree of complexation. The hole in the center of the helix has a radius of 1.3-1.5 Å, which is

large enough to accommodate Li^+, Na^+, and K^+ but too small to accommodate Cs^+ and Rb^+, thus explaining the dependence on the cation size. The anions sit outside the helix, thus allowing intrachain crosslinking via the anions and a mechanism for cation transport, which is suggested by conductivity studies. The separation of the cation and anion also explains the dependence on the lattice energy. Because the entropy, polymer reorganization and residual coulombic energy are approximately the same for a given cation, the ability to form complexes is inversely proportional to the ability to separate the ions[145].

The TGTTG'T structure seems to fit many of the known properties of PEO/salt complexes, so it is one of the most accepted structures. However, other structures have been proposed. For instance, Chatani and Okamura[169] have proposed a structure in which the cation (Na^+) and anion (I^-) link together in a zig-zag fashion to form the center of the helix. Two NaI units are surrounded by 6 ethylene oxide units, which are in a 2/1 helix. The conformation is TTGTTGTTG' around the OCCOCCOCCO bonds. Parker[170] proposed a structure for KSCN and NaSCN in which the cation was placed inside the cavity in a double stranded helix, while Hibma[171] proposed a KSCN complex in which the cations and anions are outside deformed helices. Recently Bruce[172] claimed that large cations such as Cs^+ and Rb^+ are actually accommodated within a helix, but that the conformation is different. In this case, the helix takes on a TGTTGTTG'TTG'T around the OCCOCCOCCOCCO bonds, such that all C-O bonds are trans, but all C-C bonds are gauche or gauche minus. This configuration results in a wide helix which can accommodate the large cation. Bruce believes that the immediate environment of the cation is composed of the anions and ether oxygens, such that each ion is associated only with one polymer strand and no intrachain ion cross linking occurs. This occurs because the anions generally lie within the dimensions of the helix. Anions which are large can be located in the interchain space and inhibit crystallization.

Unfortunately, the knowledge about the conductive polymers is not complete, so dismissal of these alternative structures is not possible. For instance, the method of conductance is not completely understood[145]. It is believed that the cation transport occurs through large amplitude polymer motions coupled with the breaking of one to two cation-oxygen bonds. The conventional electron hopping mechanism is not occurring. The anions also appear to have some mobility, so it becomes more difficult to rule out the other conformers. In addition, Shriver[145] points out that "one outstanding problem is the effect of polymer orientation on conductivity." This seems to suggest that the conformation may change depending on the orientation. The fact that Chatani and Okamura[169] saw a different configuration may not be due to a discrepancy in data interpretation but due to the fact that they hotdrew the cast films to 30 times the original length.

Finally, the depiction of the TGTTG'T conformation is not without its flaws. As mentioned previously, the peak at 870 1/cm is attributed to a metal oxygen breathing mode. However, it is known that the Raman intensity is a function of the polarizability of the bond. Ionic bonds are not very polarizable so their Raman spectra are very weak or non-existent. In contrast, infrared bonds are sensitive to existing dipoles. The peak at 870 1/cm is not infrared active as observed by Papke[166, 167], but is Raman active, suggesting that the vibration is not ionic in character. Furthermore, no change in the Raman shift is observed when the cation is changed, further suggesting that the metal cation is not involved[173]. Takeuchi and coworkers[174] performed a normal coordinate analysis and concluded that the 870 1/cm peak was due to C-O stretching coupled with CH_2 rocking in the TGTTG'T conformation around the OCCOCCO bonds. Some researchers prefer this interpretation of the peak.

Work by Siew and coworkers[173, 175, 176] seems to support the existence of the TGTTG'T conformation in the aqueous solutions. By normalizing the spectra to a particular peak, then taking the difference between the spectra with and without salt, she

has been able to show the existence of a peak around 870 1/cm. This peak exists for both alkali and alkaline earth metals and increases in intensity in the order: $Li^+<Na^+<K^+$ and $Mg^{2+}<Ca^{2+}<Sr^{2+}<Ba^{2+}$. This order is consistent with the known degree of complexation in aqueous solutions as discussed above. The Rb^+ and Cs^+ caused a decrease in intensity relative to the value for K^+. In other words, the increase in intensity and implied complexation was greater for ions with a radius between 0.133-0.135 nm (e.g. Ba^{2+} and K^+), which is almost exactly the helical hole size. The increase was larger for Ba^{2+} than for K^+, suggesting that the effect is stronger for the divalent cations. The effect of the halide anions (Cl^-, Br^-, and I^-) was negligible when tested for the K^+ complexes. The intensity of the peak increased with increasing molecular weight for degrees of polymerization between 7 and 40.

What is curious is that the degree of complexation generally increases from smaller to larger cation sizes in aqueous salt solutions, while the solid complexes form most readily for the smaller cations. This apparent discrepancy can most likely be explained by complexation of water, as discussed by Kikuchi and coworkers[152]. They measured the amount of water bound by the PEO/salt complex by determining the amount of water extracted into the organic phase during solvent extraction. They discovered that the amount of water complexed decreased in the order $Li^+>Na^+>K^+\approx Rb^+\approx Cs^+$, which is approximately the order of decreasing hydration energy. They concluded that the helix forms around the bulky hydrated Li^+ ion, so the polymer becomes distorted. This distortion is also seen for certain crown ethers. The work by Horikoshi and coworkers[177] supports this conclusion, since they found a different structure for hydrated $MgCl_2$ than for the water free $CaCl_2$ complex. Therefore, it appears that hydration of the cations may explain the differences in the degrees of binding seen in the solid and in solutions.

B. PURPOSE OF THE STUDY

Although there has been a significant amount of research performed, it is apparent that a thorough understanding of PEO-salt complexation in aqueous solutions does not exist. This situation is partially due to the fact that the propensity towards complexation is dependent on the anion as well as the cation; tests must be conducted for each salt. Not surprisingly, the database for the salts used in the restabilization study is incomplete. Therefore one purpose of this study is to determine the complexation ability of the pertinent salts. These include a series of potassium, sodium, and chloride salts. Because the goal was to understand the ability of the salts to complex at high salt concentrations, solvent extraction was chosen over methods such as equilibrium dialysis. Equilibrium dialysis suffers from the fact that the amount of salt bound is determined by difference. Therefore, in cases when small amounts are bound at high salt concentrations, the complexation ability becomes more error prone than when direct determination is possible. As discussed above, the work of Kikuchi and coworkers[149-151] suggests that solvent extraction should be representative of the complexation ability for a particular type of salt. This should allow a comparison among the different alkali and alkaline earth metal cations. Comparison between the two groups may be less valid.

As discussed in the literature review, the degree of complexation is dependent on the molecular weight of the polymer, especially when the molecular weight is low. Since the Pluronics® used in the restabilization study have relatively low molecular weight, the effect of molecular weight was also tested. The solvent extraction ability was determined for each salt at a molecular weight of 8000, which is relatively high, and 600, which is representative of the molecular weight resulting in the greatest degree of restabilization. In addition, the extraction ability was determined for KSCN, using several different molecular weights of polyethylene oxide.

Raman spectroscopy was performed for a few polymer salt solutions to determine if the polymer conformation affected the degree of extraction or restabilization, as discussed in the next chapter.

C. EXPERIMENTAL SECTION

Materials

Polyethylene oxides of varying molecular weight were used in the solvent extraction and Raman spectroscopy. The molecular weights had a number average of 400 (Aldrich Chemical Company; Milwaukee WI, Catalog # 20,239-8), 600 (Aldrich 20,240-1), 1000 (Aldrich 20,242-8), and 8000 (Sigma Chemical Company; St. Louis, MO; Catalog # P-2139). All the salts used were reagent grade, except the LiCl and $NaNO_3$, which had a purity of 99%. The water used was either deionized, doubly-distilled or Millipore treated with a pH of 5.5 - 6.0.

Solvent Extraction Experiments

A Burrell Wrist-Action shaker (Burrell Corp., Pittsburgh, PA) was used to perform the solvent extraction tests. A suitable concentration of PEO for the solvent extraction tests was determined by shaking 20 mL of PEO dissolved in water against 20 mL methylene chloride for approximately 20 minutes at room temperature. Concentrations which were too high resulted in white emulsified samples that did not separate rapidly after shaking. The highest concentration (30 g/L) which gave rapid separation was used in the subsequent tests. A measured quantity of the organic phase was separated then dried until a constant weight was obtained (Mettler AE 200; Mettler Instrument Corporation; Hightstown, NJ). The amount of extracted PEO was calculated using the amount of dried extract and the percentage of the organic phase separated. As can be seen from Table 4.3, the percentage

of PEO extracted varies as the molecular weight. However, this percentage remained constant for the varying PEO concentrations tested.

Table 4.3. Percentage of PEO Extracted from an Aqueous Solution into Methylene Chloride as a Function of Molecular Weight, with No Salt Present.

Molecular Weight	Percent Extracted
400	16
600	35
1000	79
8000	100

A suitable time for extraction was determined by shaking 4 samples of 20 mL of 0.5 M KSCN and 30 g/L PEO against 20 mL methylene chloride. The shaking time for each sample was varied: 5, 10, 20 and 30 minutes. Again a measured quantity of the organic phase was separated from the mixture then dried until a constant weight was obtained. The total amount of extract was determined using the difference in the weight of the jar with and without extract, as well as the percentage of the organic phase which was separated. The amount of potassium in the sample was determined by dissolving the sample in water and analyzing by flame atomic emission spectroscopy (Perkin Elmer 2380 Atomic Absorption Spectrophotometer). The amount of PEO was determined as the difference between the amount of extract and salt. As can be seen from Figures 4.1a and 4.1b, the amount of KSCN and PEO extracted is constant as a function of extraction time for both 600 and 8000 MW PEO.

An extraction time of 20 minutes was arbitrarily chosen for subsequent runs. Otherwise the tests were performed in the same manner described in the previous paragraph. The starting concentration of PEO in the aqueous phase was 30 g/L , while the concentration of the cation was 0.5 M. The concentration of the cation was determined by flame atomic emission spectroscopy (Perkin Elmer 2380 Atomic Absorption Spectrophotometer) for the potassium and sodium salts and by inductively coupled plasma

atomic emission spectroscopy in the case of the chloride salts (excluding the potassium and sodium chloride salts). Calibration standards were made with the appropriate polymer and concentration that were representative of the samples tested. To test the extraction ability of the salts alone, identical tests were run except no PEO was used.

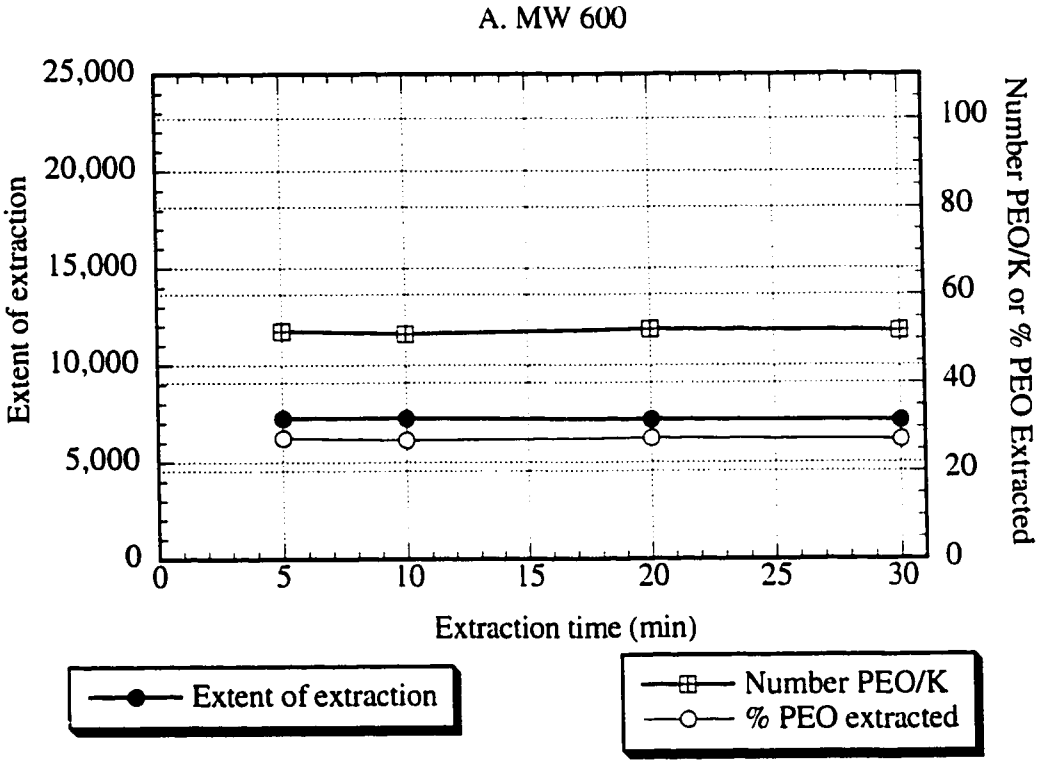

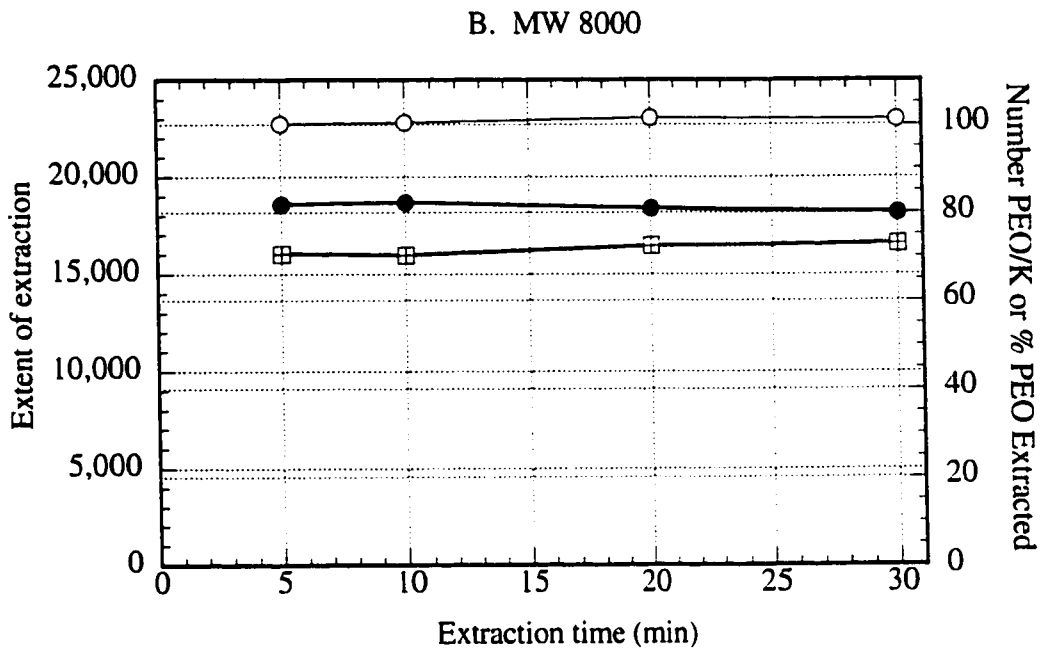

Figure 4.1. Quantities Extracted as a Function of Time from 30 g/L PEO, 0.5 M KSCN.

Raman Spectroscopy Experiments

Raman spectra were acquired on liquid samples in quartz cuvettes using a 90° scattering configuration and a Spex (Edison, NJ) Model 1877 Triple spectrometer. The 488.0-nm line of a Spectra Physics (Mountain View, CA) 164 Ar ion laser was used for excitation and the detector was a Princeton Instruments (Trenton, NJ) LN/CCD detector. The slit width was 400 μm and the exposure time was 100 s. Spectral analysis was performed using Galactic Industries (Salem, NH) Grams 386 software. The estimated uncertainty of the peak frequencies was ±1 cm^{-1}. Unless otherwise indicated, solutions

were 100 g/L PEO. Lower concentrations (≈20 g/L) resulted in such a poor signal that the peaks around 800 1/cm were partially obscured by solvent scattering.

D. RESULTS

Solvent Extraction

The results of the extraction tests are given in Figures 4.2 through 4.4 below, for potassium, sodium and chloride salts, respectively. Black bars indicate the case where no PEO was present, the circle and dot pattern has been used to indicate 600 molecular weight PEO, and the stripes have been used to indicate 8000 molecular weight PEO.

Part A of each figure gives the extent of extraction. In general, the amount of salt extracted in the absence of PEO is negligible compared to that in the presence of polymer. The one exception is for the sodium salts. In this case, the amount extracted by the sodium salts is so low, that it is very likely contamination from the glassware played a role. A small amount of KI was extracted without polymer present. Presumably this small amount occurred as the I_3^- as discussed by De[109]. A comparison of the three Part A figures for the polymer shows that PEO has the strongest ability to extract KSCN. KI is a close second. These trends for the potassium salts are consistent with the results from Yanagida [148]. All the sodium and chloride salts show poor extraction. However, the order of extraction can be tentatively assigned as in Table 4.1, and it is in general agreement with the known order of ion binding. The extraction by the divalent chlorides was so low that the extraction abilities were not differentiated. For cases with low extraction, the ratio of ethylene oxide groups to cations in the methylene chloride phase are much less accurate. This ratio is therefore only presented for the potassium salts (Part C).

Part B of each figure gives the percentage of PEO extracted into the organic phase. In all cases, the 8000 molecular weight polymer is extracted almost completely, while between 30 and 60% of the 600 molecular weight polymer is extracted. In the latter case,

higher percentages generally correlate with greater ability of the salt to decrease the polymer solvency. This correspondence is followed exactly in the case of the potassium and sodium salts; for these the ability to salt out PEO decreases as $KF>KCl\geq KNO_3>KBr\approx KSCN>KI$ and $Na_2SO_4>NaCl>NaNO_3$ (see Chapter 6 for details). The correspondence is less clear for the chloride salts. In this case the order of salting out is $MgCl_2\approx CaCl_2\approx BaCl_2$ for the alkaline earth metal salts, while the amount of PEO extracted is $MgCl_2\approx CaCl_2>BaCl_2$. The order of salting out alkali earth metal salts is $KCl\geq NaCl>LiCl$, while the extraction was $NaCl\geq KCl\approx LiCl$. The discrepancy with $BaCl_2$ may be due to the paucity of cloud point data, as shown in Chapter 6.

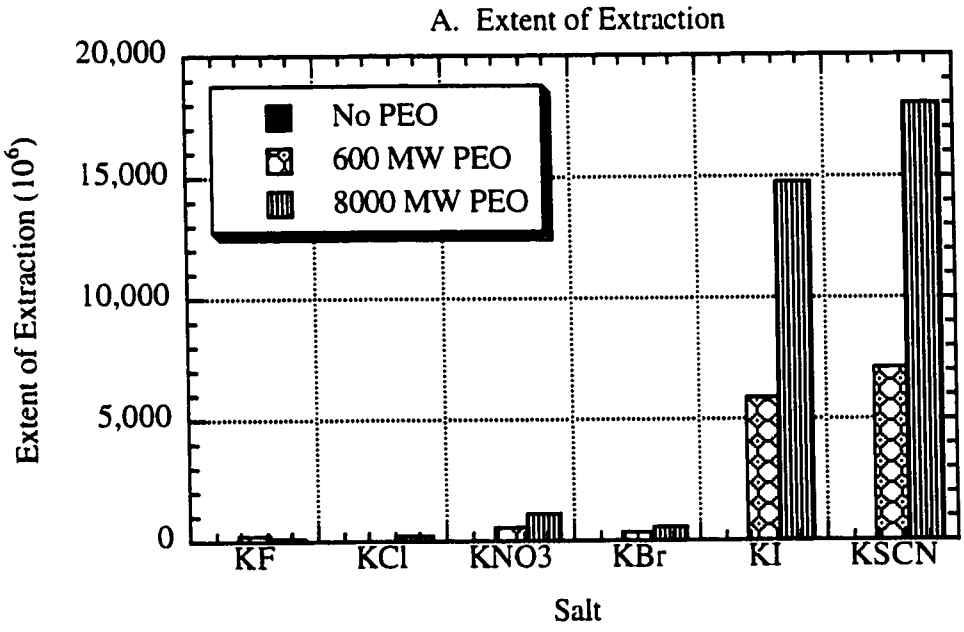

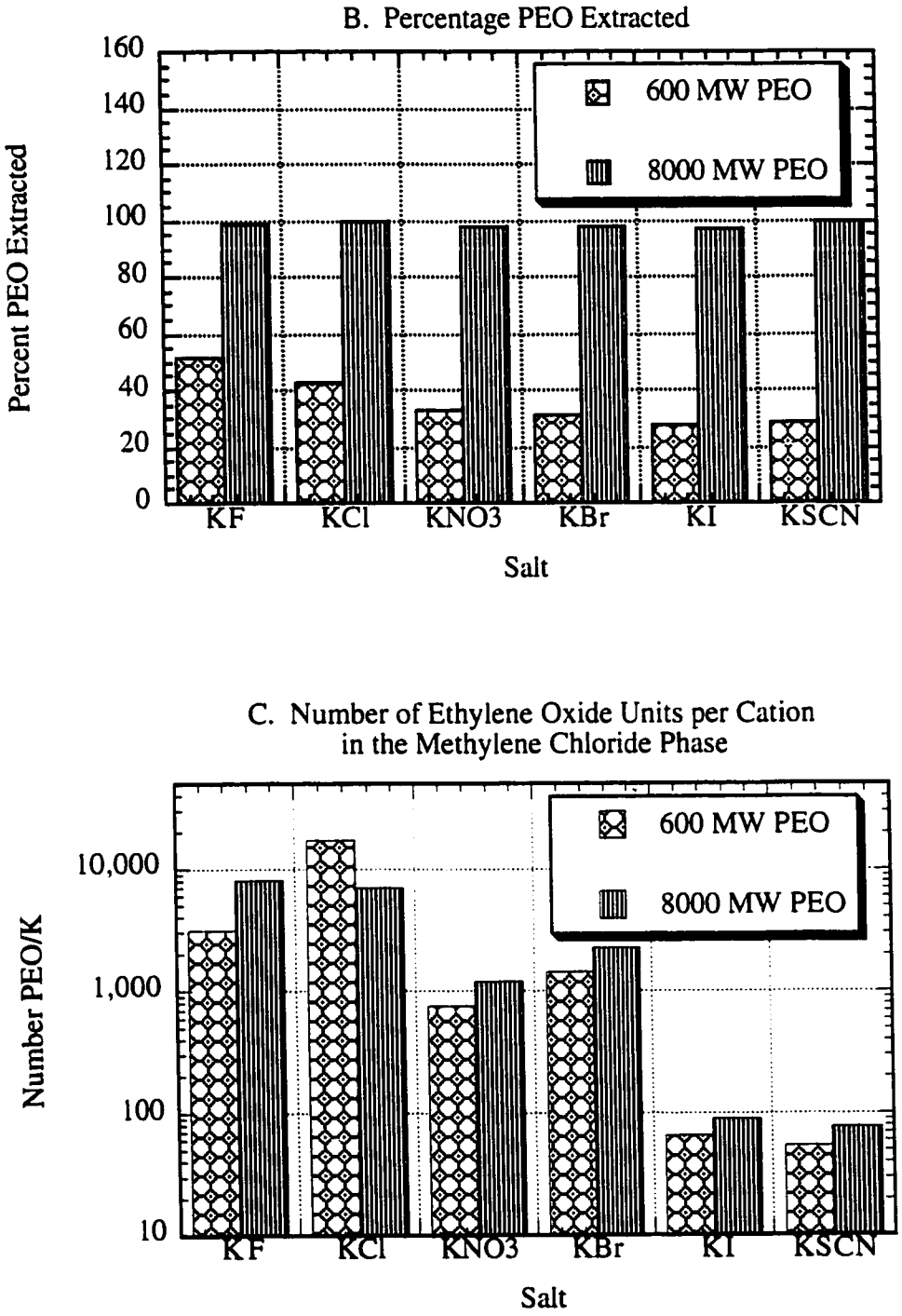

Figure 4.2. Results for Solvent Extraction of Potassium Salts

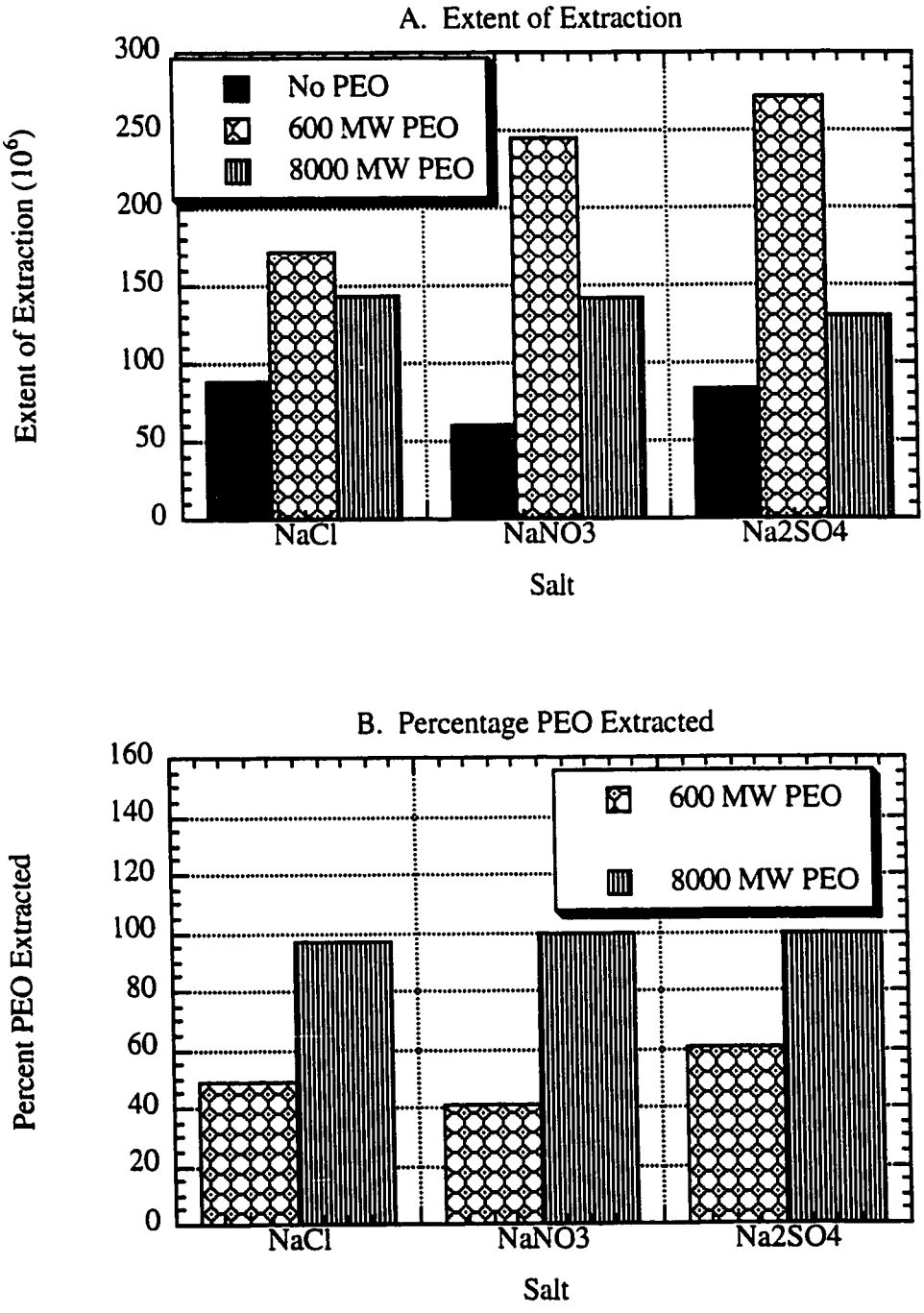

Figure 4.3. Results for Solvent Extraction of Sodium Salts

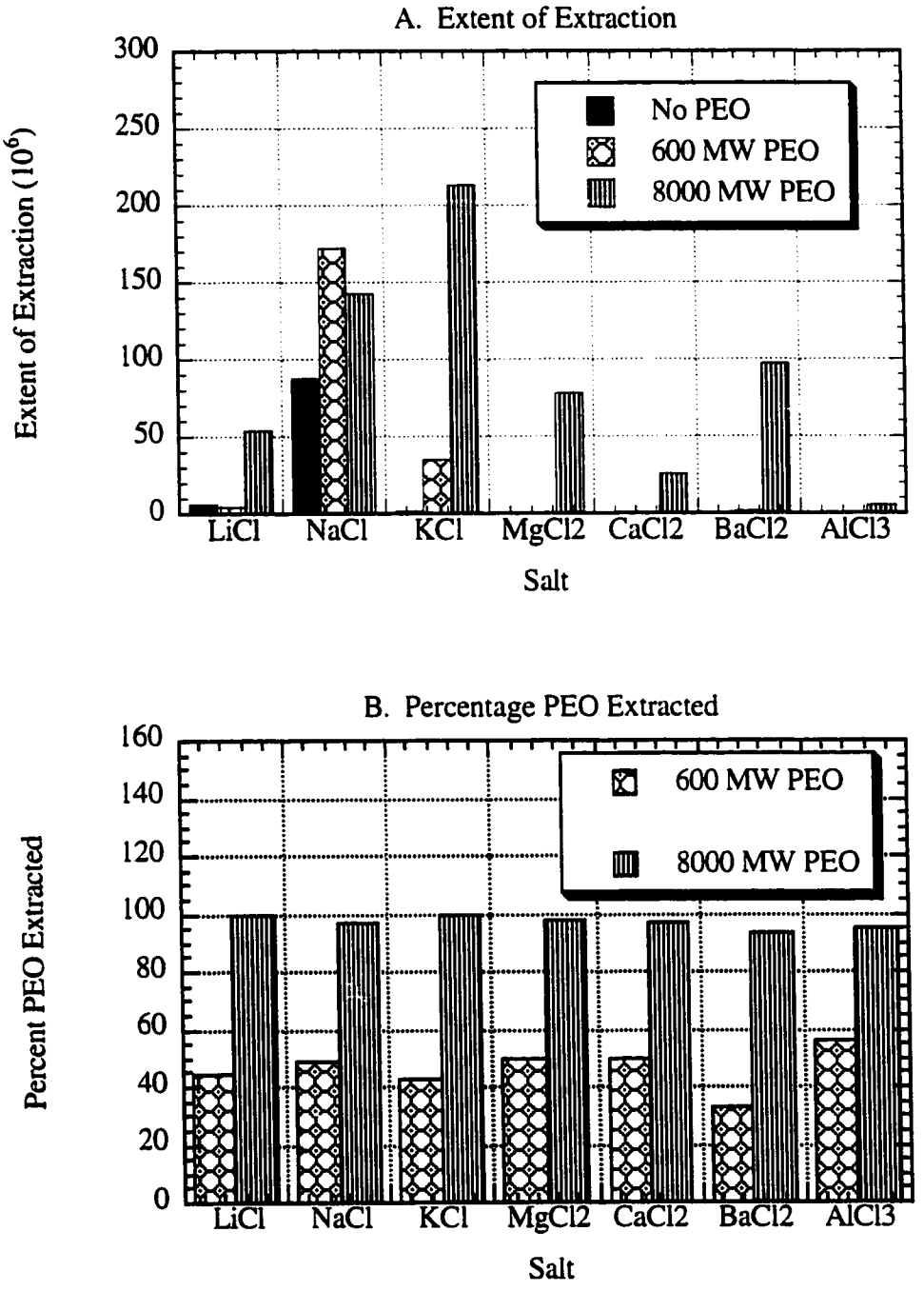

Figure 4.4. Results of Solvent Extraction of Chloride Salts

As stated earlier, Kikuchi assumed that the amount of PEO extracted is relatively constant for a type of salt and a particular polymer. This assumption justifies his claim that solvent extraction primarily reflects the complexation ability of the polymer. Although the exact values for PEO extraction vary in this study, the assumption is still reasonably valid, considering that the amount of cation extracted varies by orders of magnitude. In fact, the amount of PEO extracted is relatively constant for the two different types of chloride salts: alkali and alkaline earth (Figure 4.4B).

It seems that, for a variety of molecular weights, an accurate portrayal of the complexation ability is the number of EO/cation in the organic phase. However, too much stock in these values should not be taken when the extent of extraction of the cation is low. For the potassium salts, which have the most reliable values, the ratio of EO/cation (Part C) is almost always lower for the 600 MW PEO than for the 8000 MW PEO. In other words the number of ethylene oxide units required to move a cation to the organic phase is typically lower for the lower molecular weight, which suggests that the complexing power of the ethylene oxide is greater for the lower molecular weight. This trend occurs despite the fact that the extent of extraction is larger for the higher molecular weight. The larger extent of extraction is not caused by greater complexing power but by the larger amount of PEO extracted into the organic phase, as shown in Part B of the figure.

To confirm the results suggested in the previous paragraph, extraction tests were performed for additional molecular weights of PEO. KSCN was used since it shows the greatest extent of extraction, thus readily allowing accurate determination of the amount of salt. The results are presented in Figure 4.5. As can be seen, these results support the conclusions just drawn. Part A of the figure shows that the extent of extraction increases with increasing molecular weight until a molecular weight of 8000 is reached, at which point it decreases slightly. Part B of the figure indicates that the percentage of PEO extracted increases monotonically until 100% is extracted at a molecular weight of 8000.

More importantly are the trends in Part C. The ratio of EO/cation increases as the molecular weight increases from 600 to 18500, indicating decreasing ability to complex with increasing molecular weight as suggested in the prior results. The higher molecular weight polymers may have difficulty in extracting salt, because, as suggested by the PMR studies by Yanagida and coworkers[178], the OH- are important in complexation when the solvent is water. The EO/K^+ ratio shows a decrease between 400 and 600 molecular weight. This trend may be due to decreasing ability of PEO to encase the salt. Additional tests should be run to confirm this since the accuracy in the amount of PEO extracted is somewhat lower for the 400 molecular weight sample.

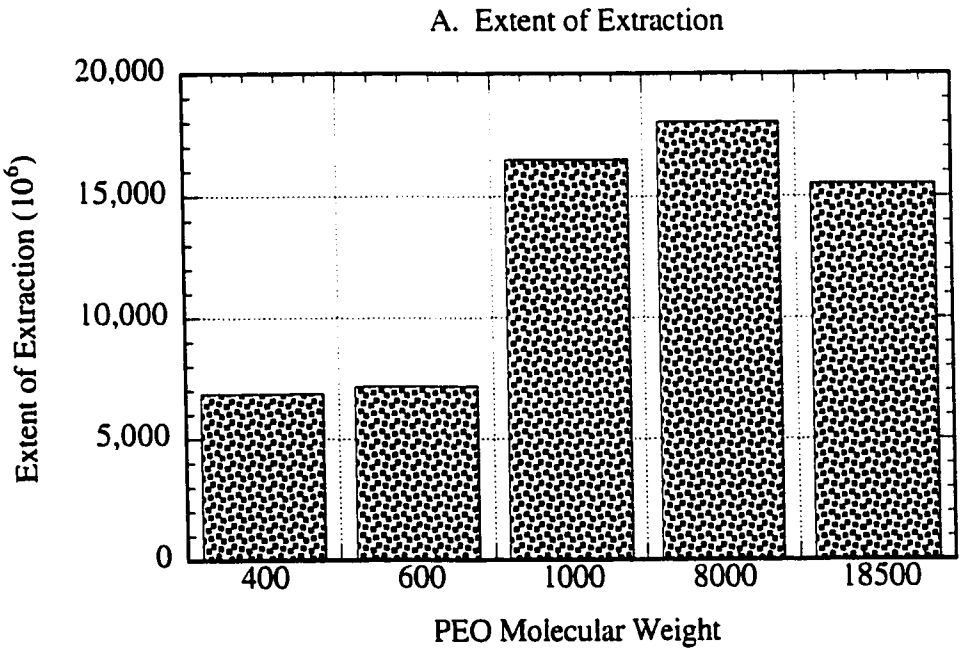

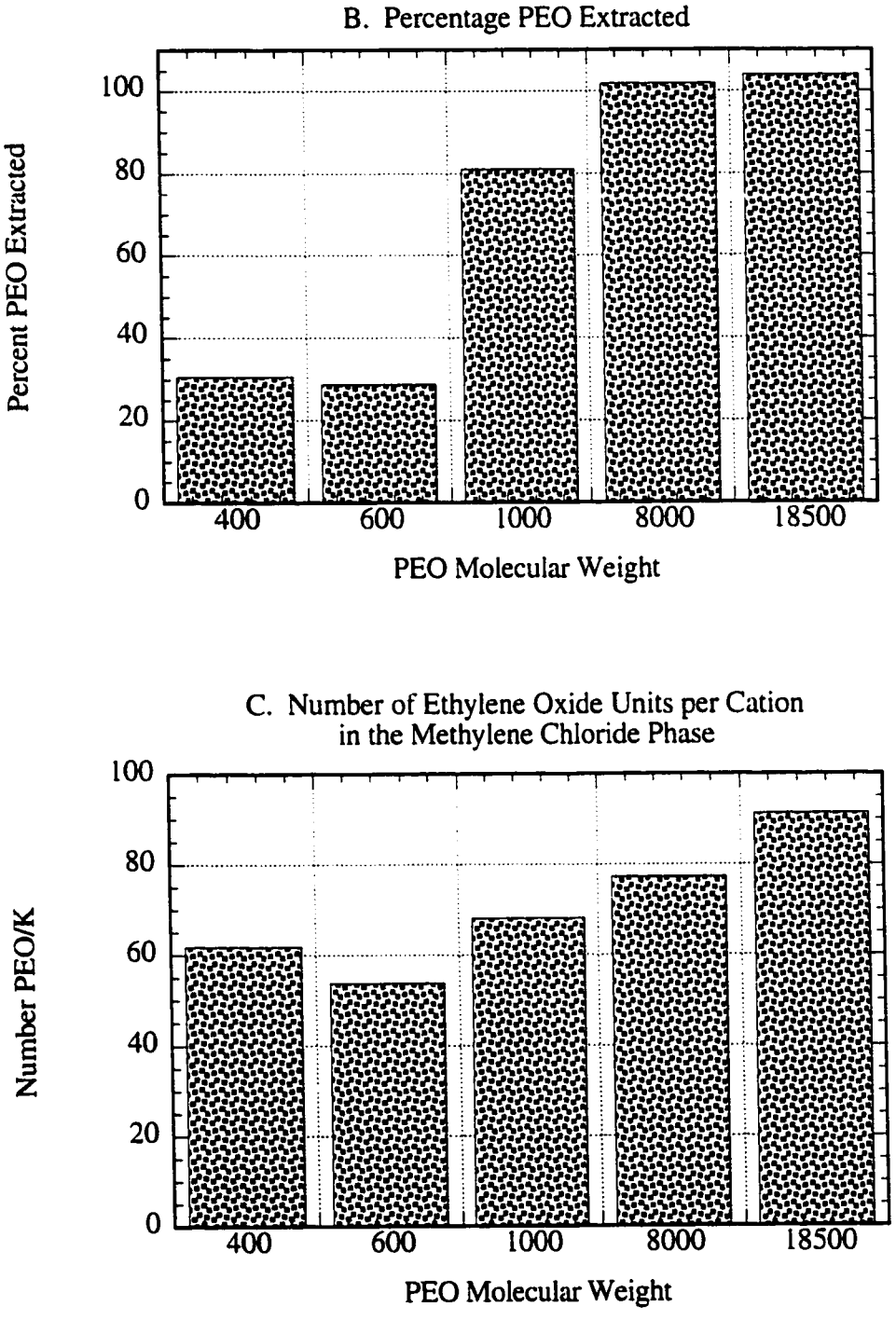

Figure 4.5. Results of Solvent Extraction Tests for KSCN Using Varying Molecular Weight Polyethylene Oxide

Raman Spectroscopy

As discussed in the literature review, there are many different proposed conformations for polymer-salt complexes. It seems plausible that different conformations may affect processes such as solvent extraction or, as discussed in the next chapter, restabilization. Therefore to explore the possibility of conformational changes, Raman spectroscopy was performed for aqueous PEO-salt solutions.

The salts chosen were KSCN and $BaCl_2$. These were chosen for two reasons. First, these solvent extraction tests suggest that orders of magnitude more KSCN is extracted than $BaCl_2$. This occurred although the complexation studies by Yanagida[148] and Sartori[147] and their respective coworkers suggests that KSCN binds quite well, while the spectroscopy by Siew and coworkers[173, 175, 176] suggests a similar nature for $BaCl_2$. In fact, Siew suggests that Ba^{2+} forms stronger complexes than K^+, while this work and that of Yanagida's show that extraction is significantly less for Ba^{2+} than for K^+. Yanagida noted that, in general, the extraction of the alkaline earth salts was poorer than the alkali metal salts. Although he speculated that this difference is caused by changes in solvency of the complex in the organic phase, it seems plausible that other explanations may exist. A second and more important reason for the spectroscopy measurements is that $BaCl_2$ exhibited quite strong restabilization, while KSCN did not, as shown in the following chapter. If the restabilization can be linked to ion complexation, then the apparent discrepancy may be linked to the polymer conformation.

A difference in conformation in aqueous salt solutions may be hypothesized since larger anions are cited as disrupting the helical structure, as discussed in the literature review. The change in the cation may also be important. Kikuchi has shown that the degree of hydration is lower for Ba^{2+} than for K^+ in the extracted complex, although its hydration energy is much higher. This difference is presumably due to the presence of two

anions in the case for Ba^{2+}. As Kikuchi[152] has suggested in the case of Li^{+}, the degree of hydration may significantly change the polymer conformation.

To establish a baseline for comparison, the Raman spectra was collected for PEO of differing molecular weights (200 g/L). The spectra are shown in Figure 4.6. To a large extent, the spectra are extremely similar. The existence of a TGT helical structure is supported, no matter whose peaks assignments are used. The work of Maxfield and Koenig and their coworkers suggests a TGT structure due to the presence of peaks at 840 1/cm, 1065 1/cm, and 1474 1/cm, while the work of Matsuura and Fukuhaara suggests a TGT structure due to the presence of a peak at 1250 1/cm.

Non-helical or disordered structures exist as suggested by the presence of shoulders at 810 1/cm and 1040 1/cm, and a peak at 1140 1/cm. The work by Matsuura and Fukuhara would suggest that the extremely large peak at 1474 and the smaller peak at 1065 are suggestive of disorder, not the TGT structure assigned by Maxfield and Koenig and their coworkers.

There are certain small differences in the spectra caused by varying the molecular weight. In particular, the shoulder peak at 1040 1/cm is pronounced at higher molecular weights. According to Maxfield and Koenig and their coworkers, this trend suggests greater predominance of the TGG structure around the OCCO bond, while the work of Matsuura and Fukuhara suggests the greater predominance of the xTT-TGx, xGT-GGx conformers of OCCOCCO. Perhaps the most noticeable change is that the peak at 885 1/cm decreases with increasing molecular weight, until it has disappeared by a molecular weight of 8000. Although this peak can be assigned to vibrations of the main PEO chain, the strong molecular weight dependence suggests that it is most likely associated with the C-OH stretching of the endgroups.

To test the scattering of the salt, the Raman spectra were collected at the highest salt concentrations used, as seen in Figures 4.7 and 4.8. As a comparison, the spectra for the

salts with PEO present were also plotted. A concentration of 1.2 M $BaCl_2$ was chosen since this value is close to the solubility limit and results in restabilization, as discussed in the next chapter. A value of 4 M was chosen for KSCN, since this results in destabilization of the colloidal particles. As can be seen, significant scattering occurs below 800 1/cm for both salts. The scattering by KSCN in this region is more significant. Around 500 1/cm, the scattering for KSCN is greater than even the large peak at 1474 1/cm caused by the presence of PEO. As discussed by Papke and coworkers[166, 167] the presence of KSCN results in fluorescence, but the Raman spectra are still acceptable. Since the scattering by the salt solutions was so significant in the lower regions, the subsequent spectra are plotted for Raman shifts above 700 1/cm. Although there is still a slope to the baseline in this region, this value was chosen to allow inclusion of the SCN^- peak at 750 1/cm and the PEO peaks around 800 1/cm.

The spectra for molecular weights of 600 and 8000 in $BaCl_2$ and KSCN are shown in Figures 4.9 to 4.12. The peak at 1475 1/cm was not plotted since very little change was observed. Its elimination allowed the other peaks to be scaled to a larger size. As can be seen from the graphs, the addition of salt results in spectra which are very similar. There are a number of changes due to the presence of salt which are common to all salts and molecular weights. In particular, the peaks clustered between 800-900 shrink in relation to the other peaks. The shoulder at 810 grows in relation to the peak around 840 1/cm, so that at the highest salt concentration, the two peaks are comparable in height. This might suggest that the trans C-C bond is growing at the expense of the gauche C-C bond. The maxima centered at 840 1/cm moves to a lower frequency, about 10 1/cm lower at the highest salt concentration tested. Possible causes for this trend include:

- A shift in the peak wavenumber associated with the gauche C-C bond
- The growth of a peak around 830 1/cm, which is associated with the xGx-xGx structure of OCCCOCCO or the TGG' structure of OCCO

- Growth of the peak at 810 1/cm to such a large extent that the peak at 840 1/cm shows an apparent shift .

Only careful deconvolution of the peaks can reveal the correct answer. The peak at 1065 1/cm does not shift in its wavenumber (perhaps slightly for PEO MW 600 in $BaCl_2$), while the peak at 1140 1/cm grows slightly in relationship to it. The peaks at 1250 and 1287 1/cm do not shift much in wavenumber, but the peak at 1250 1/cm grows noticeably in relationship to the peak at 1287 1/cm. In fact, the peak at 1250 grows in relation to all the other peaks, while the peak at 1287 decreases. The peak at 1250 is the TGT conformer associated with the helical structure of PEO crystals without salt (according to Matsuura and Fukuhara), while the peak at 1287 1/cm is the xxT and possibly the TTT and TGT structures of OCCO. It should be noted that although these changes are similar over the concentrations tested, the changes occur more rapidly for $BaCl_2$ (i.e. $BaCl_2$ was tested over a smaller concentration range).

There are also a few changes which appear to be particular to the type of salt. Most noticeable is the peak at 750 1/cm for the KSCN spectra. This peak is the SCN- peak, which would be anticipated to grow with increasing salt concentration as is seen. Another noticeable difference is that there is a peak for only KSCN, which increases in intensity with increasing salt concentration at 920 1/cm. This peak is also attributable to the scattering of SCN-, as can be seen by comparing the spectra in Figures 4.7 and 4.8.

The most important difference between the salts is that the shoulder peak at 865 1/cm does not appear for KSCN at any of the concentrations, even 4 M, although it appears for $BaCl_2$. This difference is very important, since it is believed that this peak is attributable to the TGTTG'T helix of alkali and alkaline earth complexes. The Raman difference spectra that Siew used to strongly delineate this peak are not presented. The fluorescence by the KSCN causes a noticeable slope in the baseline in this region. Since the slope changes with KSCN concentration, such comparisons may not be valid.

Two additional differences are caused by the type of salt. The first is that the peak at 885 1/cm appears to shift to a higher wavenumber only for PEO of MW 600 in $BaCl_2$, but does not in the case of KSCN (Figure 4.13). This change for $BaCl_2$ suggests that there are changes in the endgroups associated with the addition of salt. The second change seen is that the peak at 1140 1/cm shifts significantly to a lower wavenumber for $BaCl_2$, but not for KSCN (Figure 4.14). The assignment of this peak is not clear from the work of Koenig, Maxfield, or Matsuura and their respective coworkers. Matsuura and Fukuhara note that the wavenumber conformation correlations were not definitive in this region in their 1986 work.

The differences seen in the types of salt raises the obvious question: is the change caused by the cation or the anion? Spectra of the PEO in KCl solutions suggests that the changes are associated with the change in the cation. These spectra show that there is no appearance of a shoulder peak at 865 1/cm and no shift in the peaks at 885 1/cm and 1140 1/cm upon the addition of KCl. In fact, the spectra are remarkably similar if the scattering by SCN^- is taken into account.

It was noticed that the solutions with 2 and 4 M KSCN having PEO of molecular weight 600 turned yellow over time. To test if there were significant conformational changes associated with this color, Raman spectra were performed for freshly made solutions. As can be seen in Figure 4.15, the spectra for freshly made and one day old solutions are virtually identical, eliminating aging as an explanation for the change in the spectra. The one day old solutions are the spectra previously presented.

A comparison of this work with the work by Siew reveals some striking differences. First, the peak close to 810 1/cm in this study appears to grow relative to the peak at 850 1/cm until it is equal in size. In contrast, in Siew's work, this peak remains a shoulder. Perhaps the most notable difference is that the peak at 865 1/cm dominates in Siew's work, while this peak is either a small shoulder or does not appear at all. This

result cannot be explained by differences in the concentrations of materials used, since they are remarkably close. Siew uses a concentration of 0.30 mol/kg of $C_{12}H_{25}(OCH_2CH_2)_8OH$, with an ether oxygen to barium ratio of 2, 3, 4, and 8. This gives a polymer concentration of 159 g/kg, a PEO concentration of 106 g/kg, and $BaCl_2$ concentrations of 0.3, 0.6, 0.8, and 1.2 M. The most logical explanation for the differences is the presence of an alkane group. Three plausible explanations could explain the large peak seen in Siew's work:

- The presence of an alkane group changes the conformation of the PEO to a predominantly TGTTG'T conformation
- The peak is associated with vibrations of the alkane chain.
- The peak maxima associated with TGTTG'T conformation has significantly shifted in its wavenumber in this study

The second hypothesis seems entirely plausible since skeletal stretches of the alkane chain exist in the region between 800-900 1/cm. If this were the case, one plausible explanation of the changes in conformation seen in Siew's work is micellization of the surfactant upon the addition of salt, as discussed by other researchers[179]. Micellization results in significant changes in the environment of the alkane or hydrophobic group.

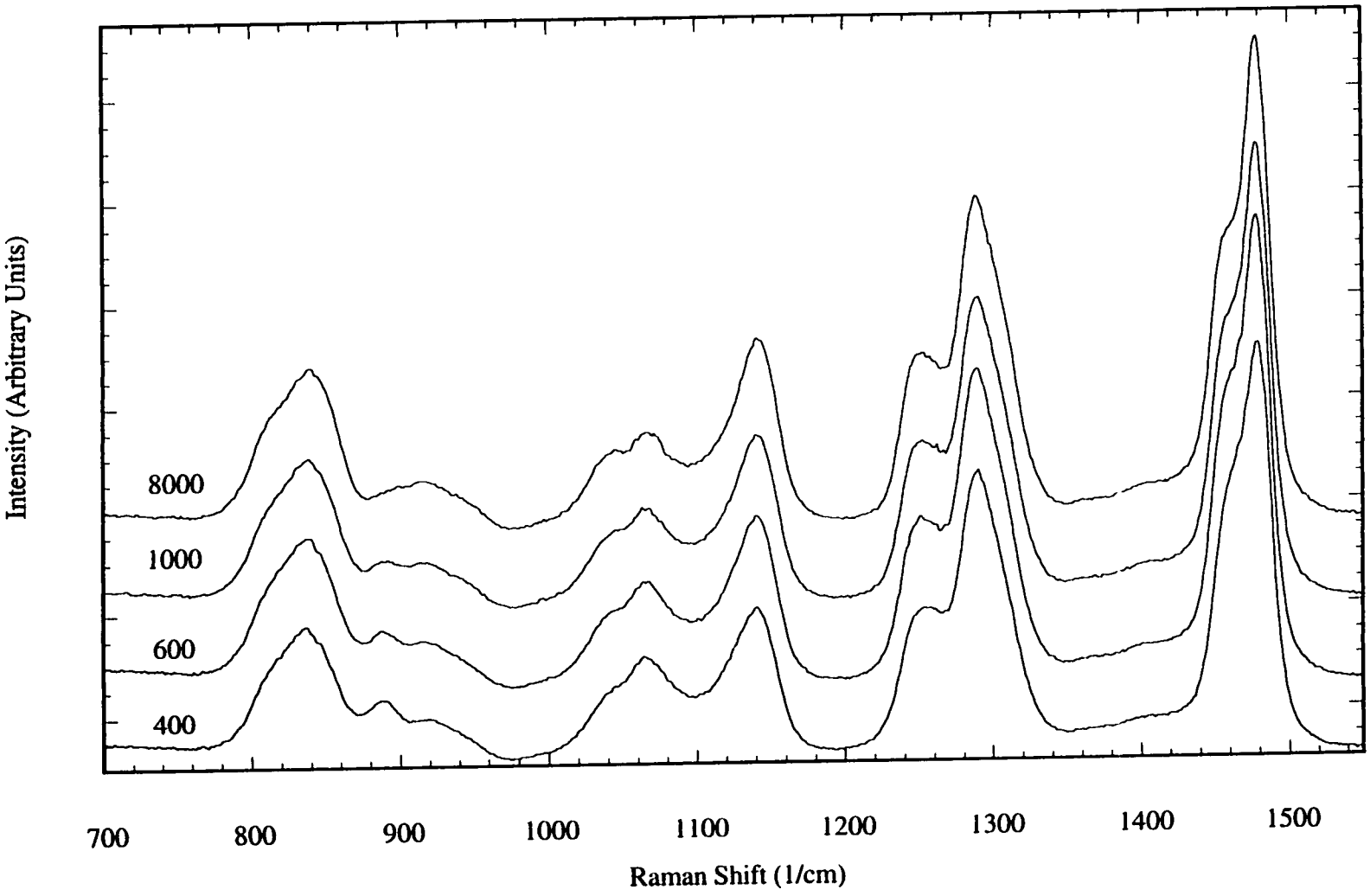

Figure 4.6. Raman Spectra of Aqueous PEO, with Molecular Weights Varying Between 400-8000

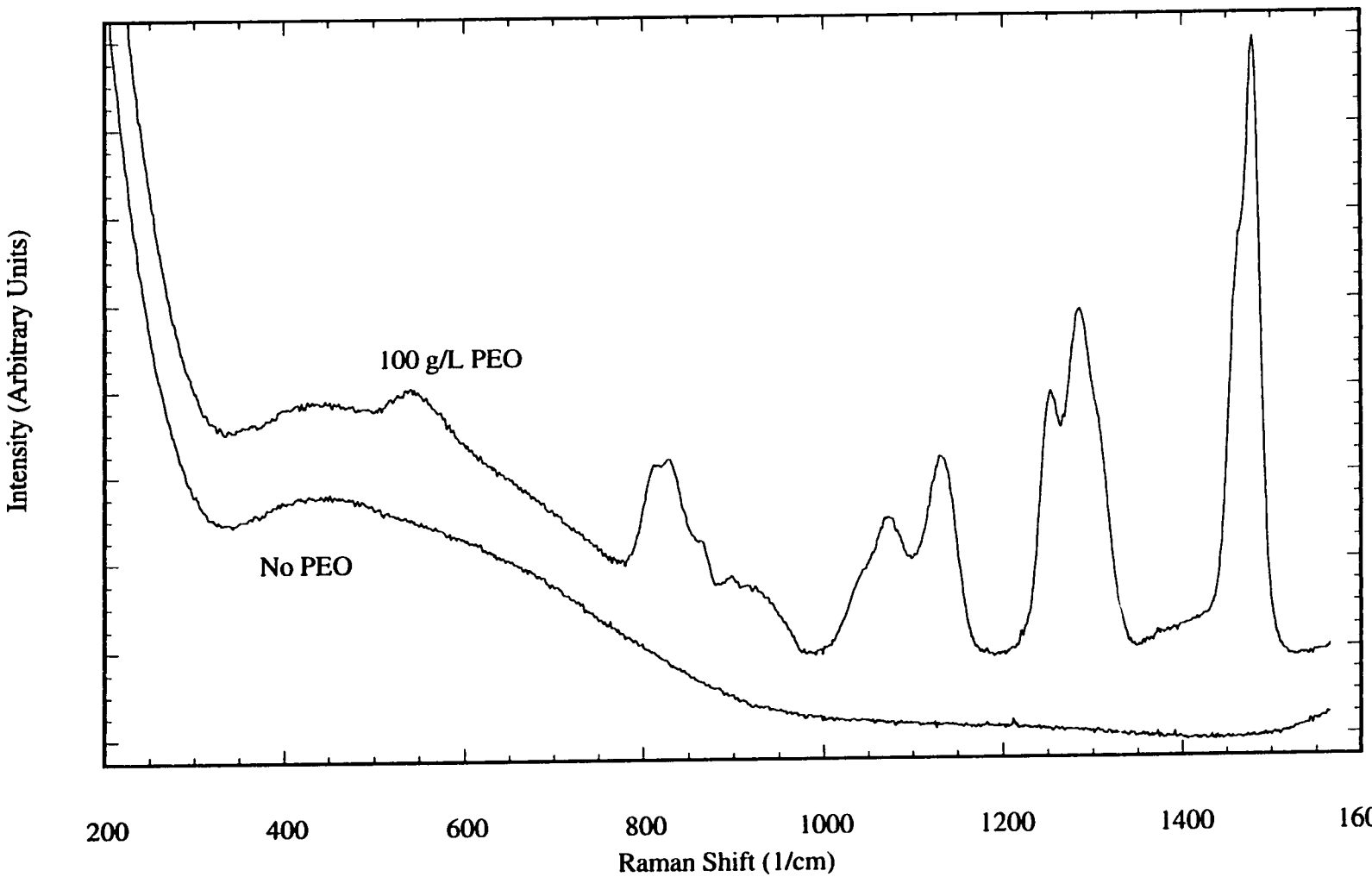

Figure 4.7. Raman Spectra of 1.2 M $BaCl_2$ with and without 600 Molecular Weight PEO

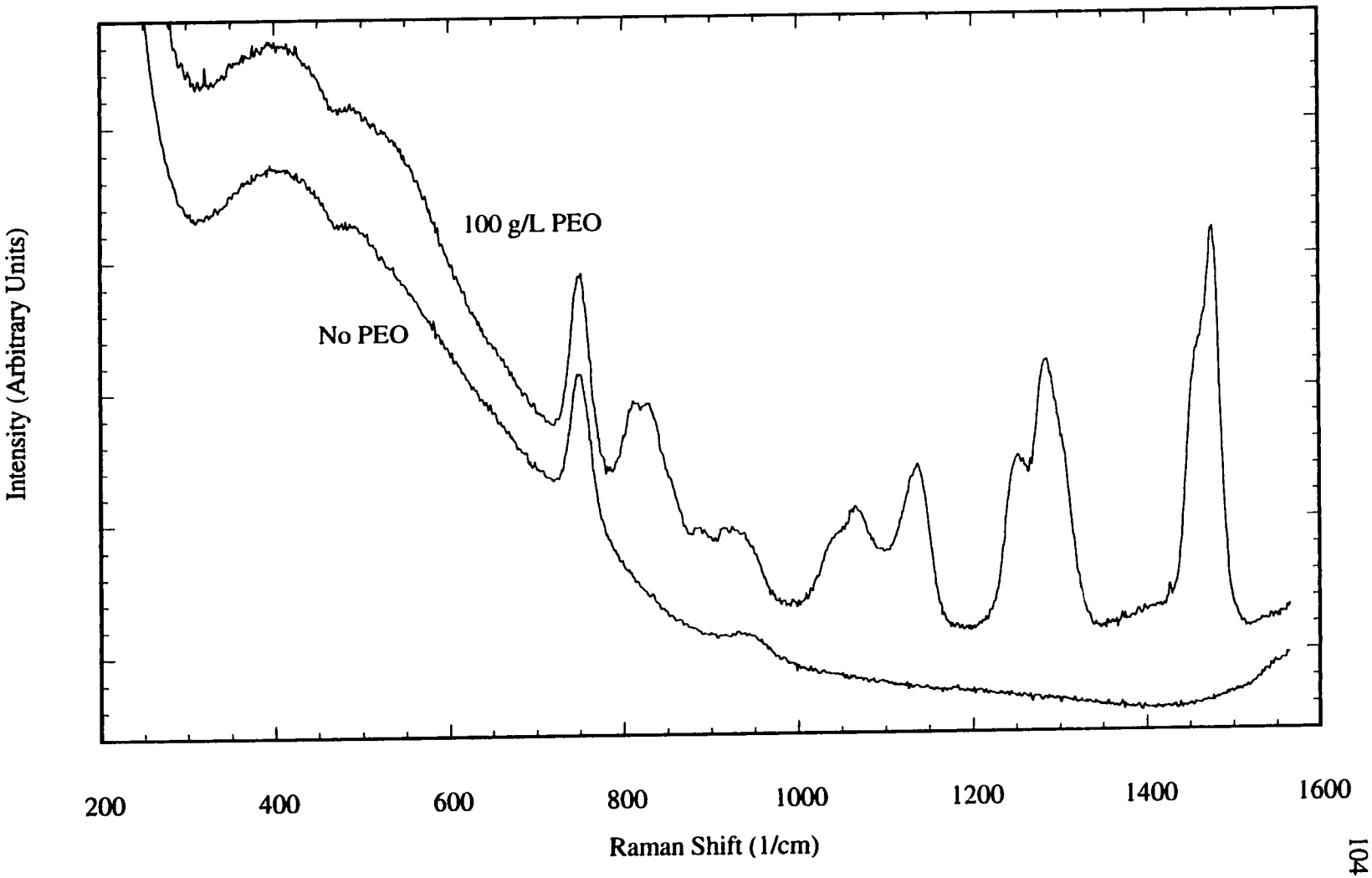

Figure 4.8. Raman Spectra of 4 M KSCN with and without 600 Molecular Weight PEO

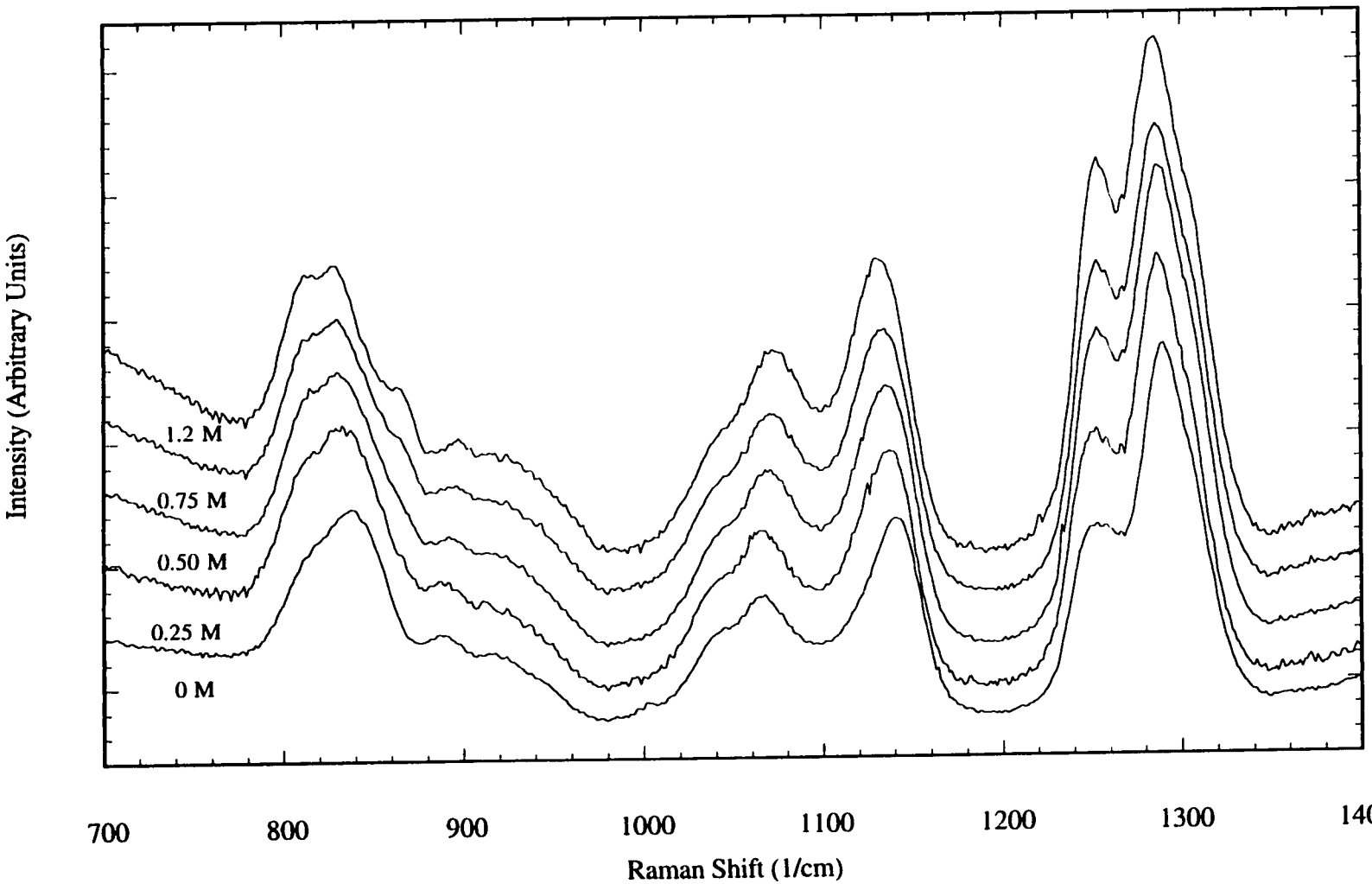

Figure 4.9. Raman Spectra of Aqueous PEO of Molecular Weight 600 with Varying $BaCl_2$ Concentrations

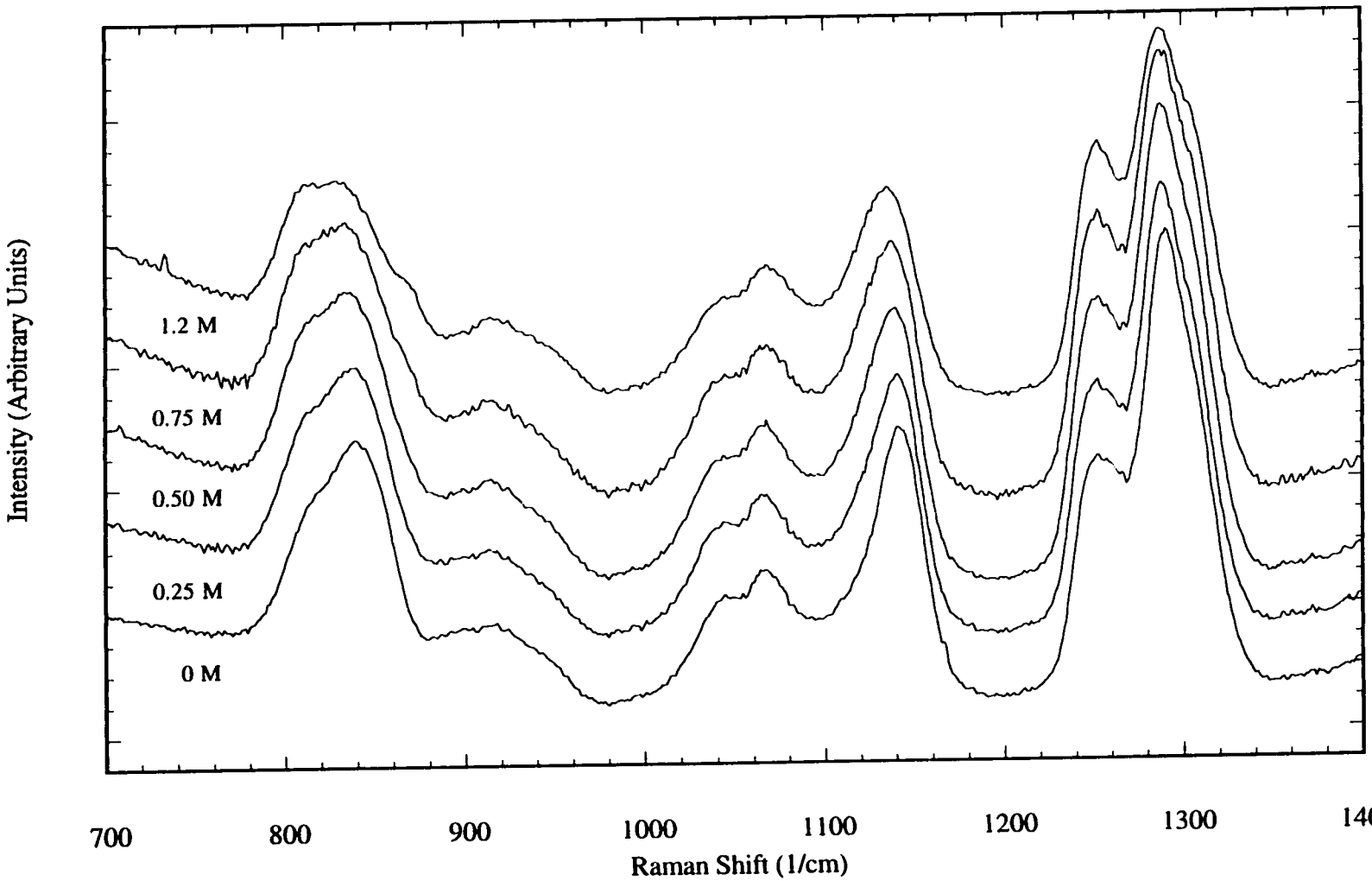

Figure 4.10. Raman Spectra of Aqueous PEO of Molecular Weight 8000 and Varying $BaCl_2$ Concentrations

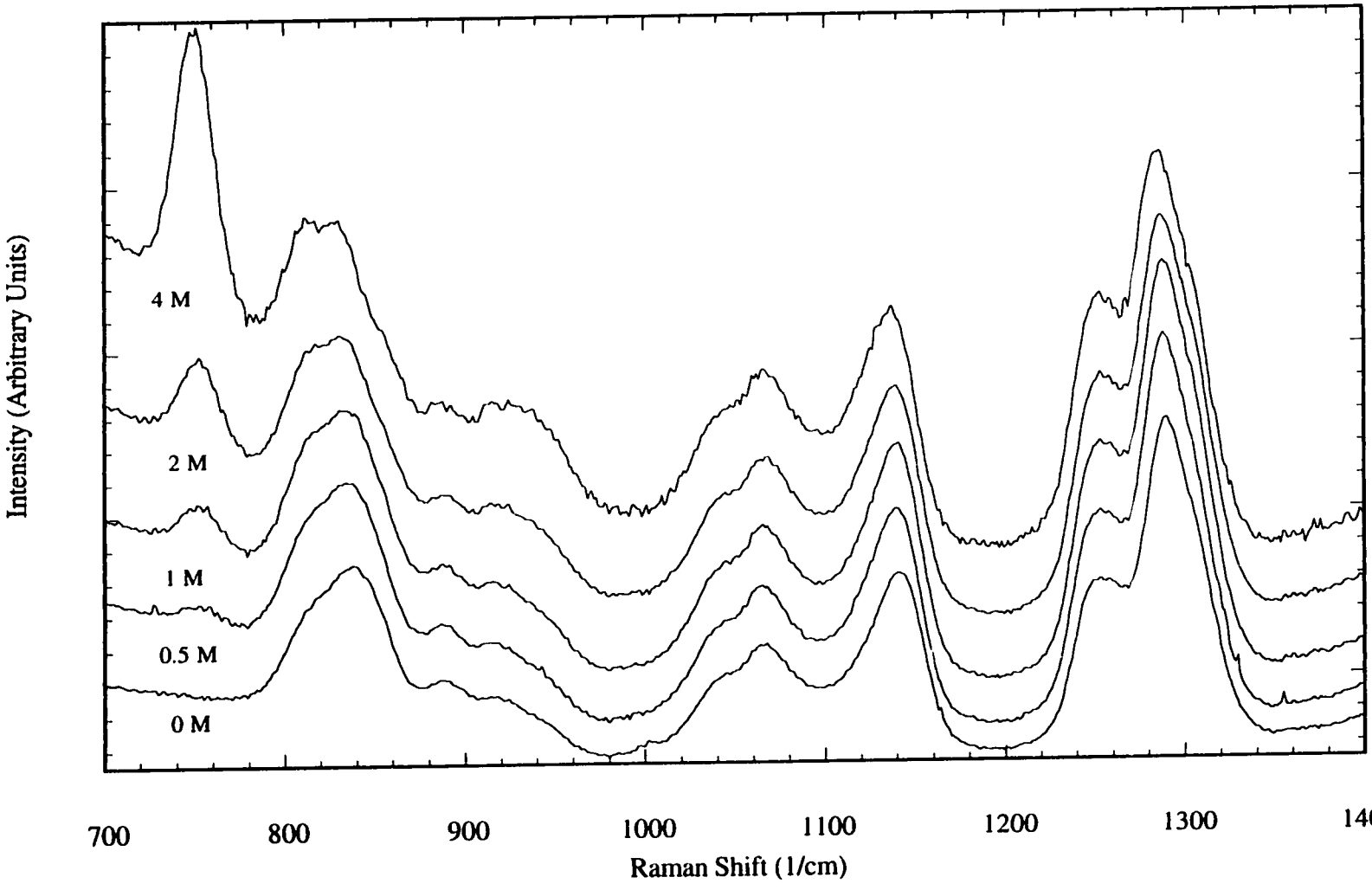

Figure 4.11. Raman Spectra of Aqueous PEO of Molecular Weight 600 with Varying KSCN Concentrations

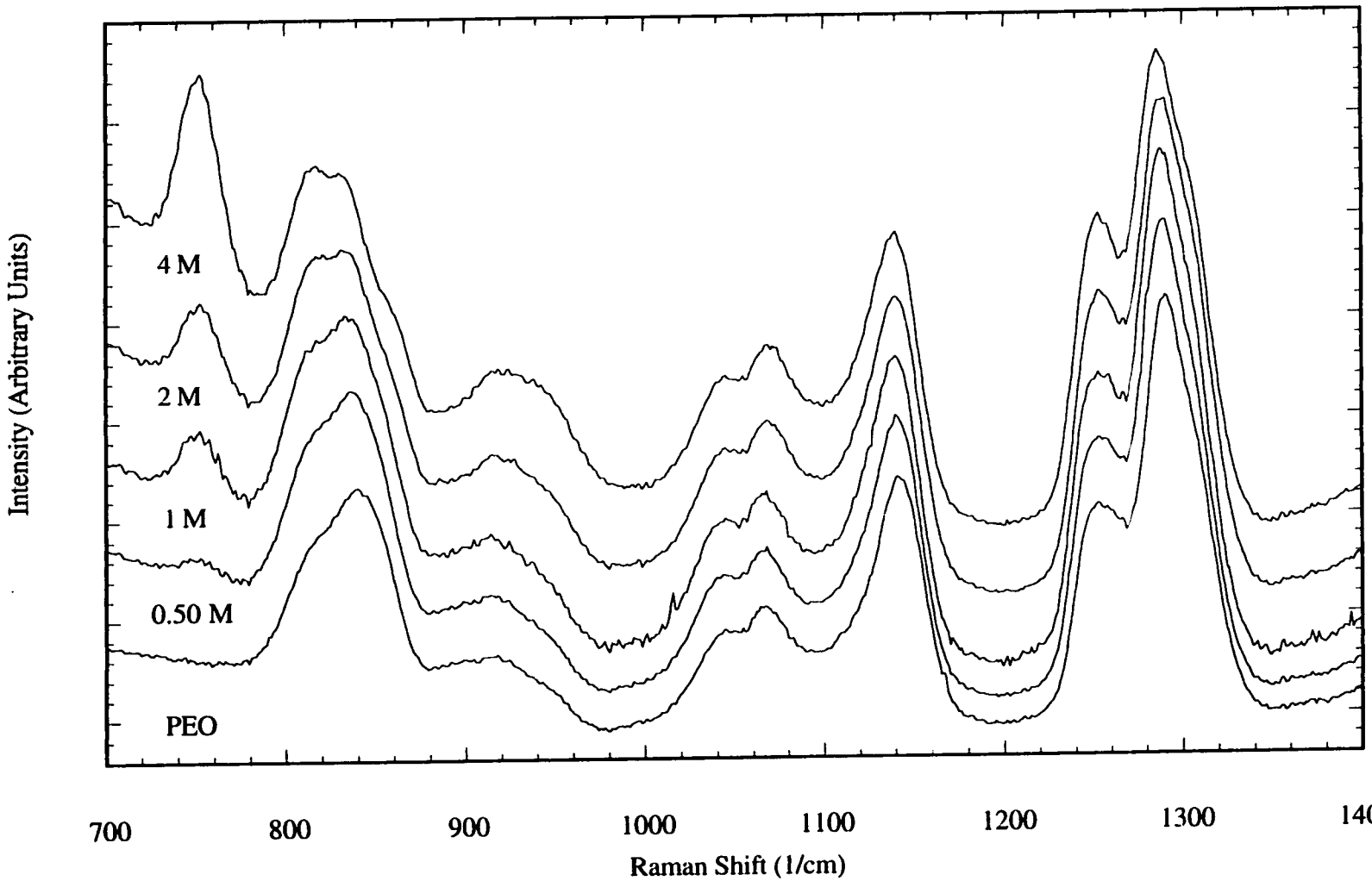

Figure 4.12. Raman Spectra of Aqueous PEO of Molecular Weight 8000 with Varying KSCN Concentrations

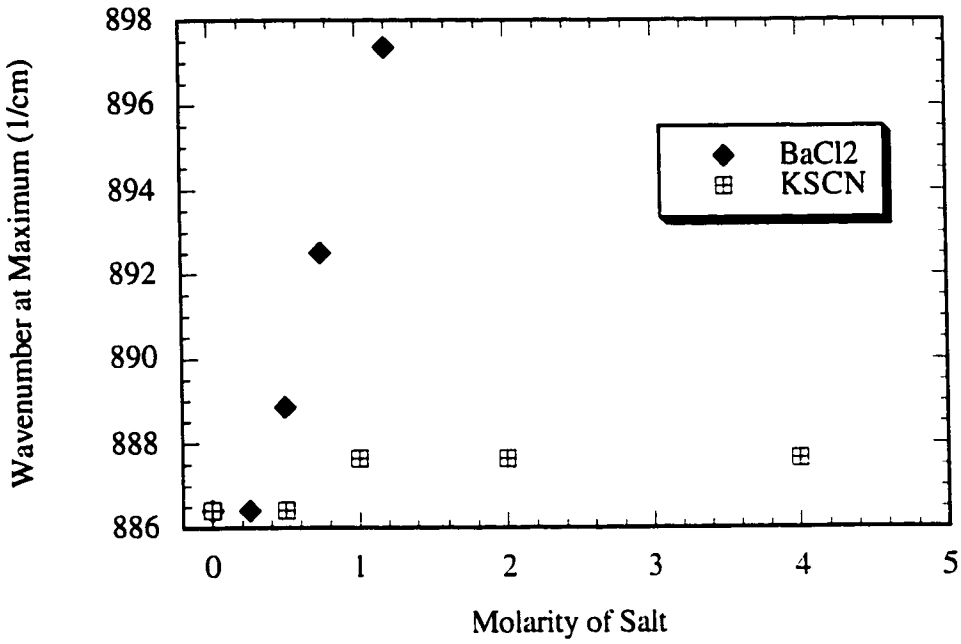

Figure 4.13. Change in the Peak Frequency at 885 1/cm as a Function of Salt Concentration for PEO of Molecular Weight 600

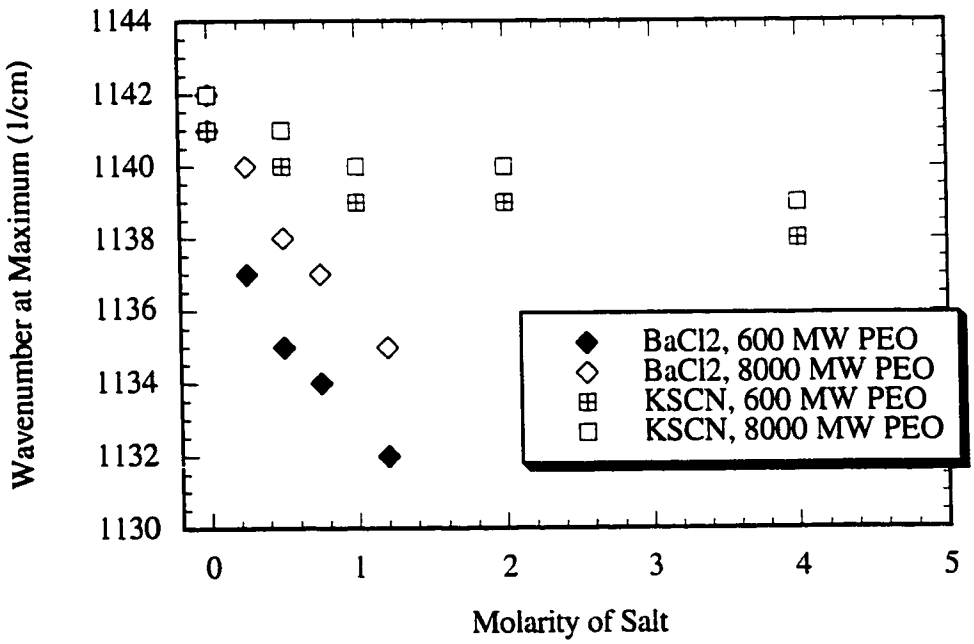

Figure 4.14. Change in Peak Frequency at 1140 1/cm as a Function of Salt Concentration

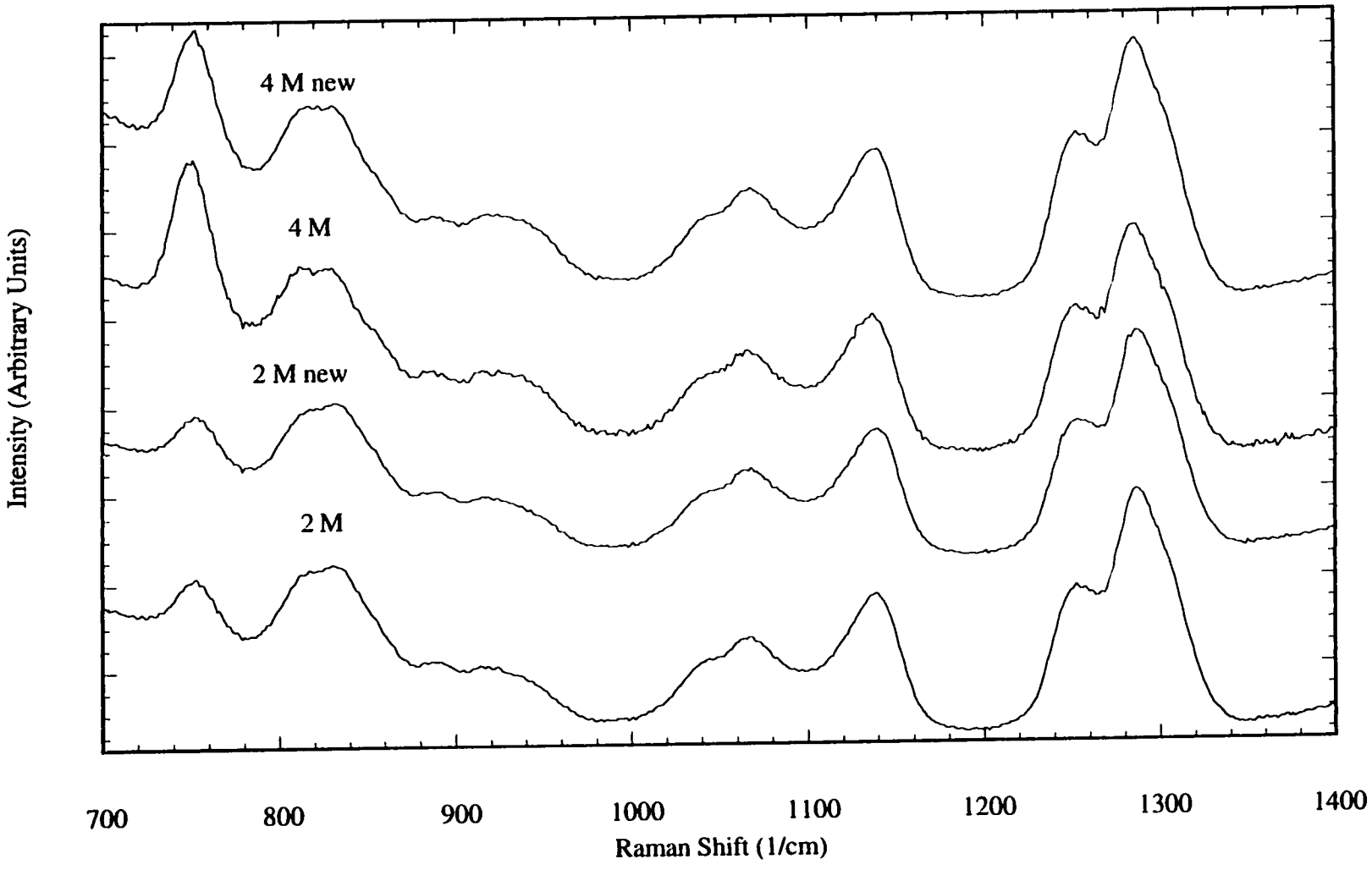

Figure 4.15. Raman Spectra of Freshly Made and 1 Day Old Solution of Aqueous PEO of Molecular Weight 600 with KSCN

Discussion and Conclusions

This work shows that the solvent extraction increases in the following order:

Potassium Salts: $Cl^- < F^- < Br^- < NO3^- \ll I^- < SCN^-$

Sodium Salts: $Cl^- < NO_3^- < SO_4^{2-}$

Monovalent Chlorides: $Li^+ < Na^+ \approx K^+$

Divalent Chlorides: $Mg^{2+} \approx Ca^{2+} \approx Ba^{2+}$

Ion binding by the chloride salts is particularly low, while it is high for KI and KSCN. For a type of salt, these results are in rough agreement with the known order of binding, suggesting that the solvent extraction does reflect the complexation ability. Comparison between groups becomes more tentative.

Raman spectroscopy of aqueous PEO solutions with either KSCN, KCl, or $BaCl_2$ suggest that changing the salt only slightly changes the spectra and hence the detected conformation. The noticeable changes occurred on changing the cation from K^+ to Ba^{2+}. Since the bare K^+ and the Ba^{2+} ion are the same size, it appears that changing the valence causes slight differences in the structure and ability to affect the bonds. These changes may be enough to partially account for the greater extraction ability of K^+ than Ba^{2+} for both the chloride salts (this work) and SCN^- salts (Yanagida's work). The Raman spectra reveal almost no differences in conformation due to changing of the anion from SCN^- to Cl^-. Therefore, changes in extraction ability caused by changes in the anion are not caused by conformational changes that are detectable by this Raman spectroscopy.

The Raman spectra do reveal that the TGTTG'T structure is not predominant in these solutions, although they are believed to otherwise in solid complexes and in aqueous salt solutions containing PEO-alkane surfactants.

CHAPTER 5: RESTABILIZATION OF ELECTROSTERICALLY STABILIZED COLLOIDS IN HIGH SALT MEDIA*

A. INTRODUCTION

Electrosteric stabilization occurs due to a combination of electrostatic and steric repulsion, both of which were discussed in Chapter 2. This type of stabilization can be manifested in one of two forms, either a thin adlayer overlying a charged surface or a thick, charged adlayer.

This work focuses on the former, and in particular, on the case of neutral thin adlayers comprised of block copolymers, whose advantages are cited in Chapter 3. For these types of colloids, a plot of the stability ratio as a function of salt concentration is anticipated to take on the qualitative features depicted in Figure 5.1[100] when the salt decreases the solvency of the stabilizing polymer. At low salt concentrations, the stability ratio is high due to the presence of both electrostatic and steric repulsion. As electrostatic screening increases due to an increase in salt concentration, the stability ratio decreases. At intermediate salt concentrations, the stability ratio will remain constant while the polymer solvency is good, but the electrostatic repulsion is negligible. The stability ratio will decrease again when the polymer solvency becomes poor, until rapid aggregation is obtained. The exact shape and location of the curve can vary depending on the system. For relatively low molecular weight stabilizing polymers, increasing the molecular weight will increase the stability ratio for a given salt concentration, when the solvency of the stabilizing polymer is good[97, 100]. The plateau region in the intermediate salt region may shrink or disappear altogether, if the points where electrostatic and steric repulsion become

* This work was presented at the ACS 72nd Colloid and Surface Science Symposium, June 1998.

negligible are near the same salt concentration. The most important aspect of this graph is that the stability ratio is always either decreasing or remaining constant.

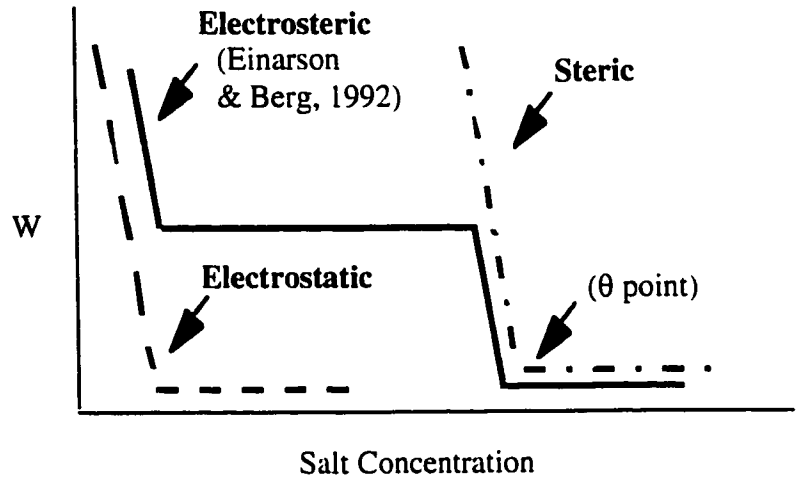

Figure 5.1. Anticipated Plot of the Stability Ratio versus Salt Concentration Obtained in the Case of Thin Electrosteric Adlayers.

For certain electrosterically stabilized colloids, some very odd behavior was observed[94, 97, 100], as depicted schematically in Figure 5.2. The stability first decreased due to the loss of electrostatic stabilization, then seemed to remain relatively constant. Surprisingly, at even higher salt concentrations, the stability actually increased upon an increase in salt concentration. This increase is extremely odd since all electrostatic stabilization is gone, and the solvency of the stabilizing polymer is decreasing (but not yet poor). This very unexpected increase in stability is defined in this work as *restabilization* .

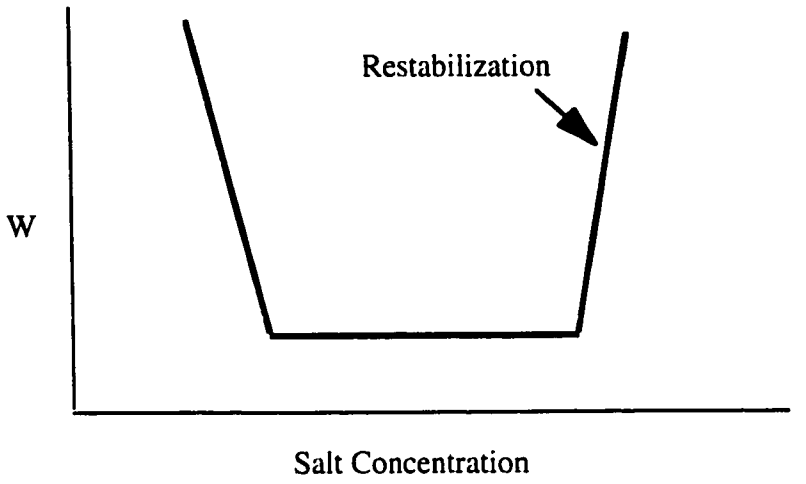

Figure 5.2. Plot of Stability Ratio versus Salt Concentration Illustrating Restabilization of Electrosterically Stabilized Colloids.

Since this type of restabilization has been observed in only a handful of cases, the objective of this study was to systematically characterize the unexpected behavior and determine its cause. Chapter 5 presents the characterization of the behavior, while Chapter 6 is a discussion of the possible causes. The characterization consists primarily of dynamic light scattering measurements which were used to quantify the incipient aggregation rate. The materials employed were aqueous salt solutions containing polystyrene latex stabilized by B-A-B block copolymer, where B = polyethylene oxide and A = polypropylene oxide. Both the molecular weight and concentration of the block copolymer were varied for numerous salts. To understand the nature of the interaction underlying restabilization, force distance profiling was conducted using the surface force apparatus.

B. EXPERIMENTAL SECTION

Materials

The core particle consisted of a polystyrene latex with sulfate functional groups (Interfacial Dynamics Corp., Portland, OR). The latices were suspended in distilled water at a solids concentration of 7.2%. The mean diameter from transmission electron microscopy was 110+/-8 nm (standard deviation of the diameter). The parking area was 1789 $Å^2$/charge group, which is equivalent to a surface charge density of 0.9 $\mu C/cm^2$. According to the manufacturer, the dispersion was free of excess surfactant, residual monomer, preservatives, and other additives, and was thus used without further cleaning.

The polymers used as steric stabilizers were BAB block copolymers with polyethylene oxide B blocks and polypropylene oxide A blocks. The B blocks are anticipated to serve as stabilizing moieties, while the A blocks anchor the polymer to the latex surface. The polymers are tradenamed Pluronics® and are available from BASF Wyandotte Corp (Wyandotte, MI). The molar masses, cloud point and HLB of the copolymers are reported in Table 5.1. These values were given by the manufacturer[180].

Table 5.1. Molar masses, cloud points and HLB of Pluronics® copolymers used in this study. The cloud point is for 1% aqueous solutions. The numbers in parentheses indicate the number of monomer units.

Pluronic®	Total Molar Mass	PEO Molar Mass	PPO Molar Mass	Cloud point (°C)	HLB
L35	1900	950 (22)	950 (16)	73	19
L64	2900	1150 (26)	1750 (30)	58	15
P75	4150	2100 (48)	2050 (35)	82	12-18

All water was deionized, doubly-distilled with a pH of 5.5 - 6.0. Filtered (0.2 μm nylon) deionized, doubly-distilled water was used in all light scattering experiments. All salts and chemicals were reagent grade, except LiCl and $NaNO_3$, which had purities of 99%. All glassware was cleaned using Micro®, a strong detergent available from

International Products Corporation (Burlington, NJ). After soaking for several hours, the glassware was rinsed copiously with tap then distilled water. All glassware used in light scattering experiments was also rinsed copiously with filtered, deionized, doubly-distilled water.

Aggregation Experiments

Sterically stabilized dispersions were created and tested via light scattering for incipient aggregation as described in Chapter 3. Unlike the study in Chapter 3, the conditions used for these experiments fit the requirements for Rayleigh-Gans-Debye (RGD) theory and translational diffusion more closely. The requirements are that $d << 162$ nm and $d \leq 139$ nm for RGD and translational diffusion, respectively. The hydrodynamic size of the latex used in this study was roughly 112 nm in distilled water.

During the creation of all dispersions, a concentration of 300 mg/L free polymer was targeted in order to allow adsorption in the plateau region of the isotherm. In the aggregation experiment, the dispersion was mixed with the desired salt solution for 20-30 seconds, to allow thorough mixing of the sometimes concentrated salt with the dispersion. To determine the particle size, the procedure for the aggregation experiment was followed, except filtered, deionized, doubly-distilled water was used, instead of salt solution. When possible, the viscosities and refractive indices for the salt solutions were taken from handbooks[181]. When unavailable, the values were determined using a #50 Cannon Fenske Capillary Viscometer, a Woods Model RF-600 Differential Refractometer, and a Mettler/Paar DMA 45 Calculating Digital Density Meter. The measured values are presented in Appendix C.

In a manner similar to that described in Chapter 3, the particle concentration was chosen by performing aggregation experiments for varying concentrations of the bare latex

at conditions which result in rapid aggregation (1 M NaCl). A plot of the stability ratio as a function of particle concentration is presented in Figure 5.3. Since the stability ratio is normalized by the Smoluchowski limit, the stability ratio during rapid aggregation should be between to 2 to 3[105-107]. A particle concentration of $2x10^9$ part/mL was chosen since it is the highest concentration that gives a stability ratio in this range. Lower particle concentrations give values closer to 2, but are so low that slow aggregation was difficult to detect. The same particle concentration was used in the aggregation experiments and in the experiments used to determine the particle size.

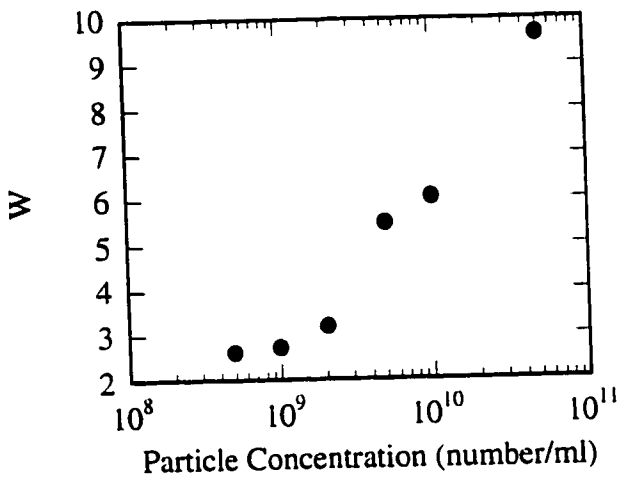

Figure 5.3 Plot of Stability Ratio versus Particle Concentration for 0.11 μm Polystyrene Latex in 1 M NaCl.

Force Distance Profiling

Force distance profiling was performed using the surface force apparatus (SFA). Mica sheets were cleaved and glued to silica support disks using Epon 1004 (Shell) hot melt epoxy. The surfaces were mounted into the apparatus which was then purged with N_2 for 0.5 hour. The surfaces were then brought together in air and the zero contact position

measured. The surfaces were removed from the surface forces apparatus (SFA) and hydrophobized by exposure to a vapor of $C_{16}SiCl_3$ for 0.5 hour. The surfaces were then rinsed with ethanol and dried with a stream of N_2. The surfaces were placed back into the SFA and purged with N_2. The surfaces were brought together and the contact corresponded to 11 D separation as compared to the previous measurements of air contact. The birefringence of the mica in both air contact and monolayer contact was similar.

A 500 mL solution of 300 mg/L L35 Pluronics® was allowed to equilibrate overnight. The water had been ion exchanged and was freshly distilled before use. The entire apparatus (approximately 400 ml capacity) was filled with the Pluronic® solution and 7.3 ml of a 0.55M $BaCl_2$ solution was then injected into the apparatus to give 0.01 M $BaCl_2$ in the apparatus. The forces were measured using a double variable spring with a spring constant k=1.48 x 10^5 M dynes/cm. The mean radius R of this contact position was 2.72 cm.

The apparatus was left overnight. 100 ml of a saturated $BaCl_2$ solution was then injected into the [Pluronics®/0.01M $BaCl_2$] solution to give 0.5 M $BaCl_2$. The solubility of $BaCl_2$ in water at room temperature is 37.5 g/100 ml or 1.8 M. The contact position was changed due to contamination. The interaction forces of the Pluronics® in 0.5 M solution was then measured. The mean radius of this contact position was 1.48 cm.

C. CHARACTERIZATION OF RESTABILIZATION

Effect of Pluronics® Molecular Weight

The prior work seemed to suggest that restabilization only occurs for relatively low molecular weight polymers. A systematic study of the effect of polymer molecular weight was tested for a number of different salts, as presented in Figures 5.4 - 5.10. Each symbol represents the mean for 1-4 runs at those conditions. Error bars are present when more than one run was conducted, and they represent one standard deviation. Upward pointing arrows at the top of the symbol indicate that the stability ratio was immeasurably high. In general, stability ratios above a few thousand are somewhat approximate. In these cases the slopes of the plot of the hydrodynamic diameter versus time are so low that the correlation coefficient is very small. Differentiating stability ratios above 10,000 is extremely difficult, and at these conditions, the system can be considered stable. Lines are used to connect the points for a particular molecular weight and are not curve fits, but are used to guide the eye. In all cases, 60 mg/L free polymer was present during the aggregation experiment.

As anticipated, increasing the molecular weight of the polymer always causes an increase in the stability ratio at the lower salt concentrations in the region where electrostatic repulsion is decreasing or gone but where the solvency of the stabilizing polymer is good. The more interesting effects occur at high salt concentrations, where restabilization is anticipated to occur. The lowest molecular weight polymer L35 can only cause restabilization in the case of $BaCl_2$, while the intermediate molecular weight polymer L64 causes the odd behavior for a number of salts: LiCl, NaCl, $NaNO_3$, KCl, KNO_3 and $BaCl_2$. At high enough molecular weights (P75), the system remains completely stable (e.g Figure 5.5 or 5.6, plots for NaCl or $NaNO_3$ respectively). The results suggest that $BaCl_2$ shows a greater ability to restabilize a colloid, while KSCN has little or no tendency to

cause the phenomenon. The remaining salts are intermediate in their capability. The results also suggest that restabilization is most likely to occur for intermediate molecular weights. As a consequence, the subsequent studies were performed primarily for L64 coated latex.

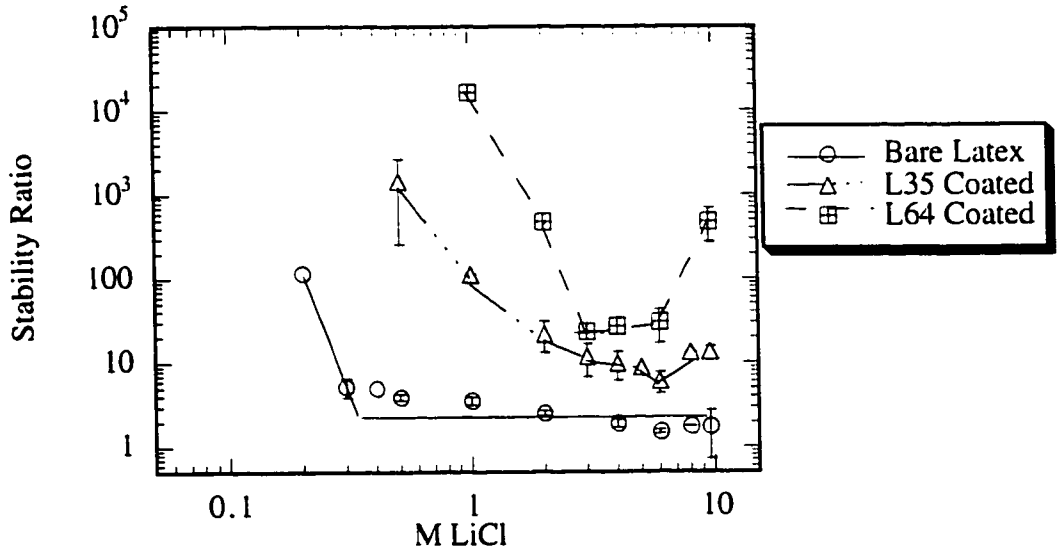

Figure 5.4 Stability Ratio of Pluronics® Coated 0.11 μm Latex in Aqueous LiCl Solutions, 60 mg/L Free Polymer, Various Molecular Weights

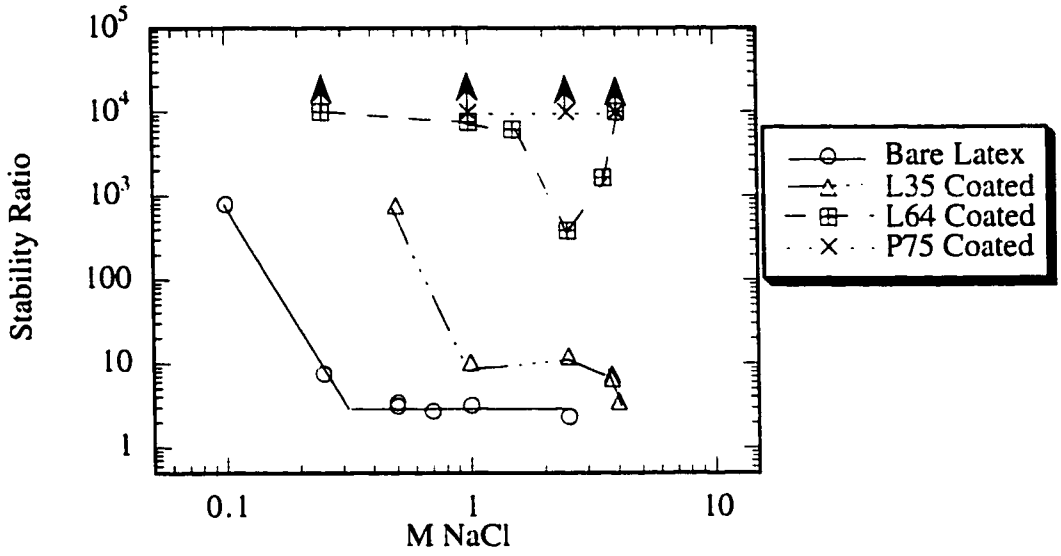

Figure 5.5 Stability Ratio of Pluronics® Coated 0.11 μm Latex in Aqueous NaCl Solutions, 60 mg/L Free Polymer, Various Molecular Weights

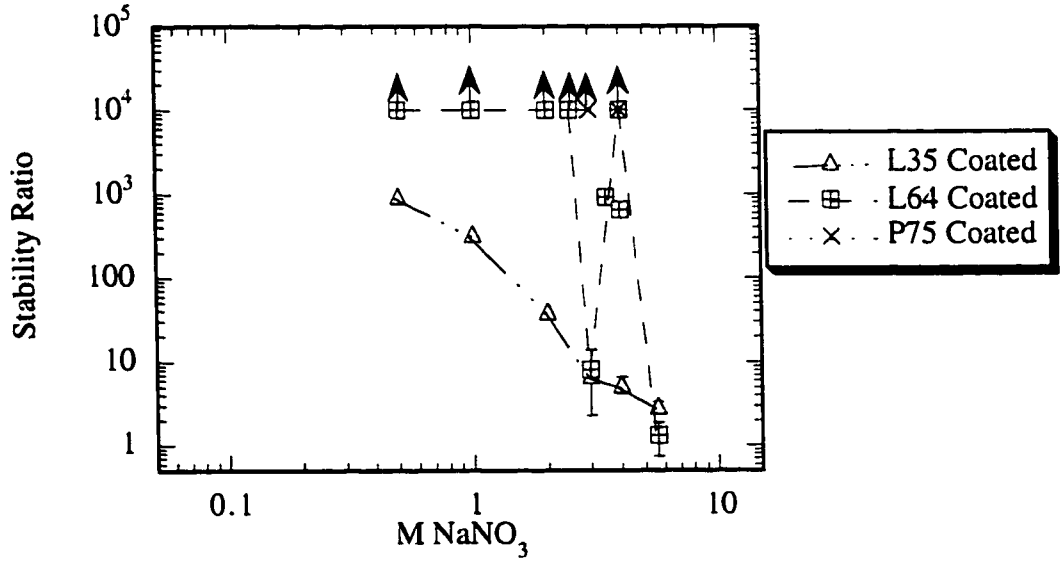

Figure 5.6 Stability Ratio of Pluronics® Coated 0.11 μm Latex in Aqueous $NaNO_3$ Solutions, 60 mg/L Free Polymer, Various Molecular Weights

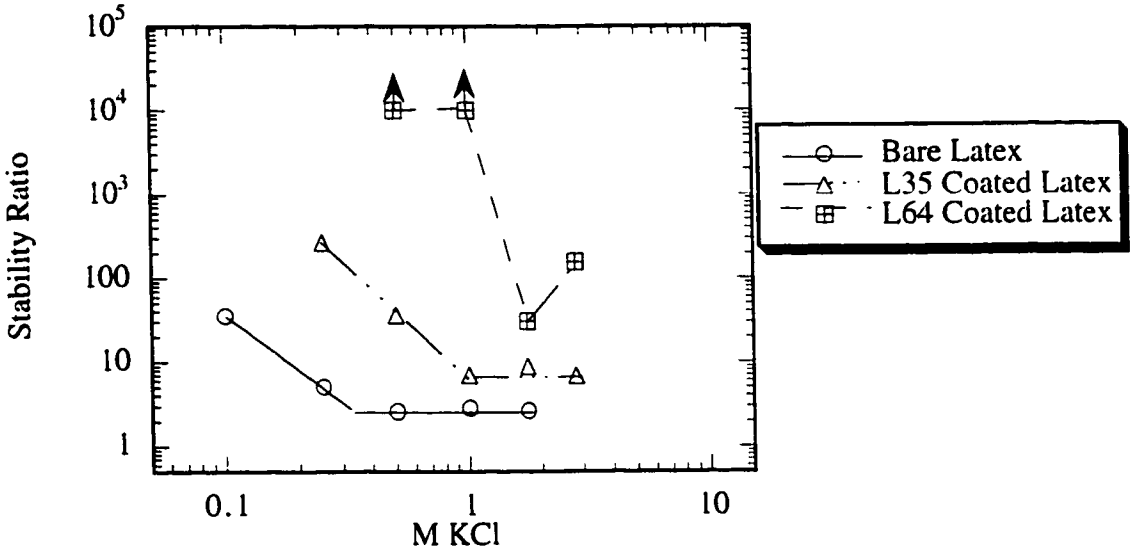

Figure 5.7 Stability Ratio of Pluronics® Coated 0.11 μm Latex in Aqueous KCl Solutions, 60 mg/L Free Polymer, Various Molecular Weights

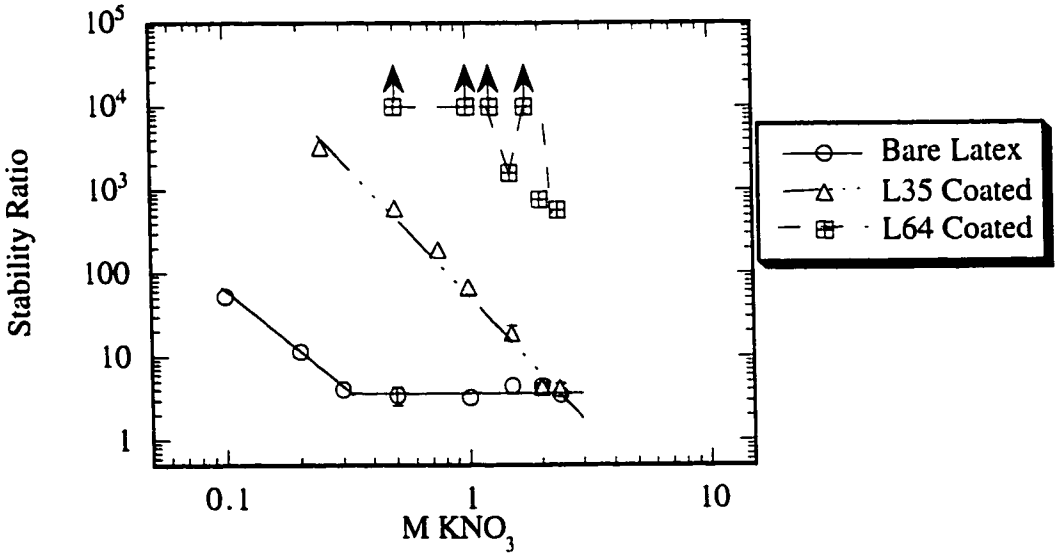

Figure 5.8 Stability Ratio of Pluronics® Coated 0.11 μm Latex in Aqueous KNO_3 Solutions, 60 mg/L Free Polymer, Various Molecular Weights

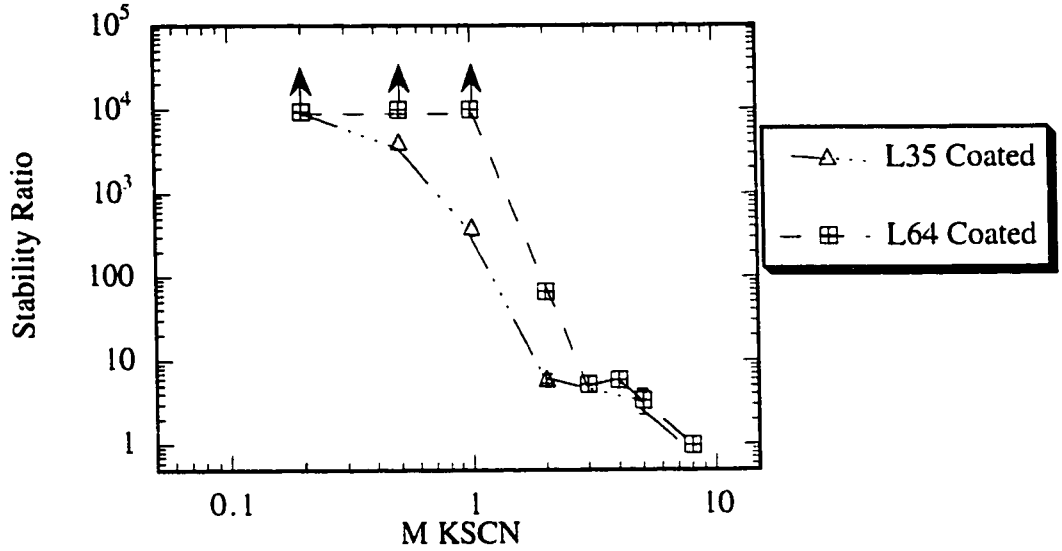

Figure 5.9 Stability Ratio of Pluronics® Coated 0.11 μm Latex in Aqueous KSCN Solutions, 60 mg/L Free Polymer, Various Molecular Weights

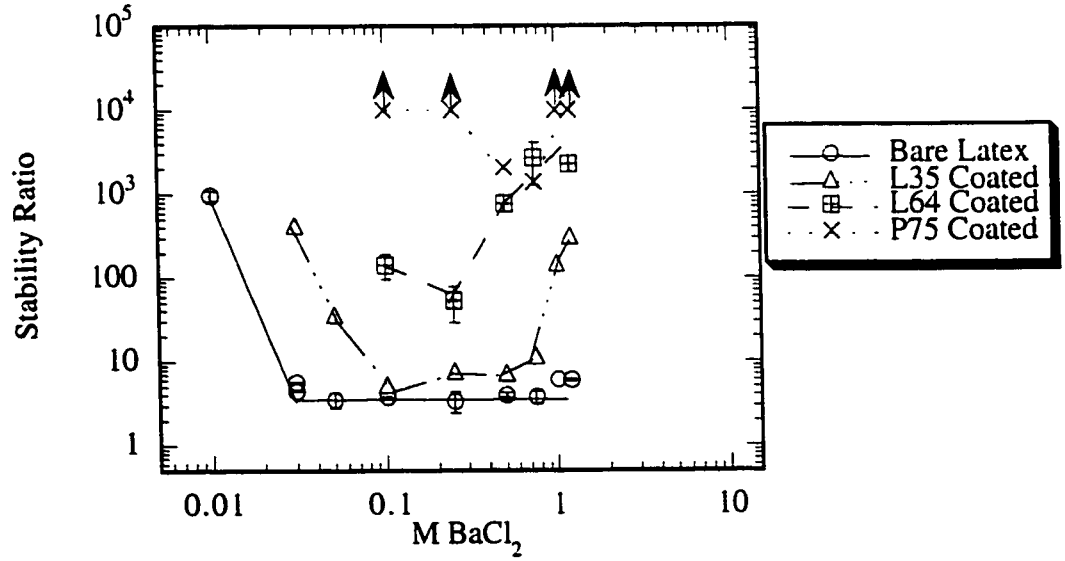

Figure 5.10 Stability Ratio of Pluronics® Coated 0.11 μm Latex in Aqueous $BaCl_2$ Solutions, 60 mg/L Free Polymer, Various Molecular Weights

In the plots for L35 and L64 coated latex in KSCN (Figure 5.9) and L64 in $NaNO_3$ (Figure 5.6), the stability ratio reaches a surprising value close to 1 at the highest salt concentrations tested. The values should be at least 2, when viscous drainage effects are taken into account[107]. As shown in Figure 5.11a, mixing 60 mg/L L64 with the appropriate amount of KSCN revealed that extremely large polymer agglomerates form upon the addition of salt, which continue to grow in size. These agglomerates were visible by eye and suggest that the cloud point of the polymer had been reached. These agglomerates dominate the light scattering signal as can be seen by comparing Figures 5.11a to 5.11b, which shows the change in hydrodynamic diameter of the L64 coated latex with 60 mg/L free polymer present. For both systems, an apparent stability ratio was calculated from the initial slope and the parameters used during the aggregation experiment (i.e. particle concentration and size). The plots and calculated stability ratios are almost identical with and without latex, suggesting that the aggregation of the 0.11 μm latex particles does not contribute much to the signal. The same polymer agglomerates were observed to form in 5.6 M $NaNO_3$. These conclusions are further supported by the fact that extrapolation of the data by Boucher and Hines[68] suggests that the theta temperature of polyethylene oxide is 25°C when the salt concentration is above 4 M $NaNO_3$.

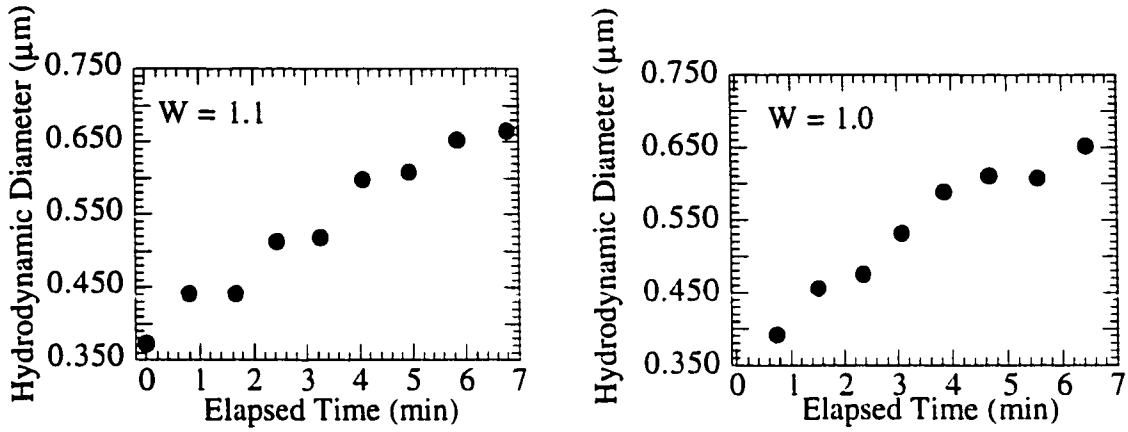

A. 60 mg/L L64 B. L64 Coated Latex and 60 mg/L L64

Figure 5.11. Hydrodynamic Diameter as a Function Time in 8 M KSCN

The most interesting aspect of this part of the study is that the small increase in PEO molecular weight from L35 to L64 causes a drastic change in the probability for restabilization. As suggested by Table 5.2, the approximate change in PEO molecular weight is only 2 monomer units for each block and the increase in adlayer thickness in distilled water is immeasurably small. This change from L35 to L64 corresponds to an increase of 21% for the PEO molecular weight but an 84% increase for the PPO molecular weight. Which of these changes governs restabilization will depend on the mechanism, which is discussed in Chapter 6.

Table 5.2. Adlayer Thicknesses of Pluronics® Coated 0.11 μm Latex in Distilled Water.

Pluronics®	PEO Length for Each Block (Monomer Units)	Adlayer Thickness (nm)
L35	11	1.1
L64	13	1.2
P75	24	2.5

Effect of Free Pluronics® Concentration

Another aspect which was investigated was the effect of free polymer or polymer which is not adsorbed to the surface of the latex, but is dissolved in solution. The amount of free polymer was controlled by adsorbing the polymer at varying latex concentrations but at a final free Pluronics® concentration of 300 mg/L. The dispersion was then diluted to a concentration of $2x10^9$ particle/mL during the light scattering experiment. The free polymer concentrations tested were 60, 0.6, and 0.01 mg/L. In the cases for 0.6 and 0.01 mg/L free polymer, the particle concentration during adsorption was extremely high. In these cases, the experiments were facilitated by diluting the dispersion to an intermediate concentration of $1x10^{10}$ part/mL. This diluted stock was then used throughout the day for light scattering experiments. With one exception all experiments employed L64 Pluronics®.

The results were graphed in the same manner described in the section the Effect of Polymer Molecular Weight and are presented in Figures 5.12 to 5.27. In general it can be concluded that decreasing the amount of free polymer decreases the probability that restabilization will occur. For the case of LiCl, $NaNO_3$, KNO_3, $MgCl_2$, and L35 coated $BaCl_2$ (Figures 5.12 to 5.16), a decrease from 60 to 0.6 mg/L free polymer causes the loss of the restabilization behavior. The salts NaCl, KCl, and $AlCl_3$ have a stronger propensity for restabilization and are capable of restabilizing the colloid in 0.6 mg/L free polymer , but not in 0.01 mg/L free polymer (Figures 5.17 to 5.19). Only $BaCl_2$ and KBr are capable of restabilization at all free polymer concentrations (Figures 5.20 and 5.21). For $BaCl_2$, the restabilization in 0.01 mg/L free polymer is small but noticeable. In many cases, restabilization does not occur at all (Figures 5.22 and 5.27). These results are summarized in Table 5.3, which classifies the salts by the lowest free polymer concentration at which restabilization occurs. The strength or capability of restabilization increases from left to

right in the table. As can be seen, restabilization is dependent not only on the cation but the anion of the salt as well. Chloride salts show a particularly strong propensity towards restabilization; with size of the seven exhibiting the behavior. The exception is $CaCl_2$. Nitrate salts are similarly strong; both nitrate salts exhibit restabilization.

One intriguing possibility with these results is that $CaCl_2$ may show restabilization with a free polymer concentration that is intermediate between 0.6 and 60 mg/L. It seems especially plausible since restabilization by $CaCl_2$ was seen by Virden and Berg[94]. It seems that one would expect some aggregation using $CaCl_2$ at 60 mg/L free polymer since its salting out capability is similar to that of $BaCl_2$ and $MgCl_2$ (see Chapter 6 Figure 6.3), however none exists. A similar situation exists for KBr. KBr salts out PEO more strongly than KI (see Chapter 6 Figure 6.4), but in 60 mg/L free polymer it exhibits very little decrease in the stability ratio, while KI does. The stability ratio for KBr at these conditions is so high that it is difficult to conclude what is happening. This apparent anomaly is reconciled by the fact that restabilization is occurring, but is not apparent until a lower free polymer concentration is reached.

To test whether restabilization can be detected for $CaCl_2$, aggregation experiments were performed for L64 coated Pluronics® with free polymer concentrations of 10 and 30 mg/L over the same salt concentrations presented in Figure 5.25. The stability ratio was immeasurably high at all conditions, suggesting again that restabilization may be occurring but is not seen.

Based on these limited data, it appears that the anion is largely responsible for restabilization. Anions such as chloride and nitrate cause the behavior, while anions such as sulfate, thiocyanate, fluoride, and iodide do not. The cations, as in the case of the chlorides, determine the relative ordering for a particular anion.

In a manner similar to KSCN and $NaNO_3$ mentioned earlier, both KF and Na_2SO_4 (Figures 5.22 and 5.26) exhibit surprisingly low apparent stability ratios at higher salt concentrations when 60 mg/L free polymer is present. Again, the formation of growing polymer agglomerates at the cloud point is the explanation. The test performed for the 60 mg/L free polymer in KSCN was also performed for these two salts. At KF concentrations of 2, 5, and 10 M and Na_2SO_4 concentrations of 1 and 1.6 M, the solution turned visibly cloudy and formed agglomerates which increased in size over time. As described before, an apparent stability ratio was calculated in the case where growing agglomerates occurred in Na_2SO_4. Again, the stability ratio calculated from the agglomerates was 1, suggesting that the polymer agglomerates dominated the light scattering signal over the latex. The stability ratio could not be calculated in the case of KF due to the large amount of flare. The growing agglomerates were not observed in 0.5 and 1 M KF or 0.5 M Na_2SO_4.

In agreement with our data, extrapolation of the data from Boucher and Hines[68] suggests that the theta temperature reaches 25°C in roughly 0.6 M Na_2SO_4, while the data of Florin and Kjellander[70] suggest that the cloud point reaches 25°C in roughly 1.3 M KF. It seems reasonable that the stability ratio for the L64 coated latex in KF with 0.6 mg/L free polymer present reaches the anticipated diffusion limited aggregation rate. There is so little free polymer that their formation into agglomerates does not interfere with the light scattering signal.

It should be noted that the pH was either measured or adjusted in the case of $AlCl_3$ to ensure that Al^{3+} was the predominant species[182]. The pH was adjusted to 4 for $AlCl_3$ concentrations less than $2x10^{-4}$ M. Otherwise the pH took on the values indicated in Table C.1.

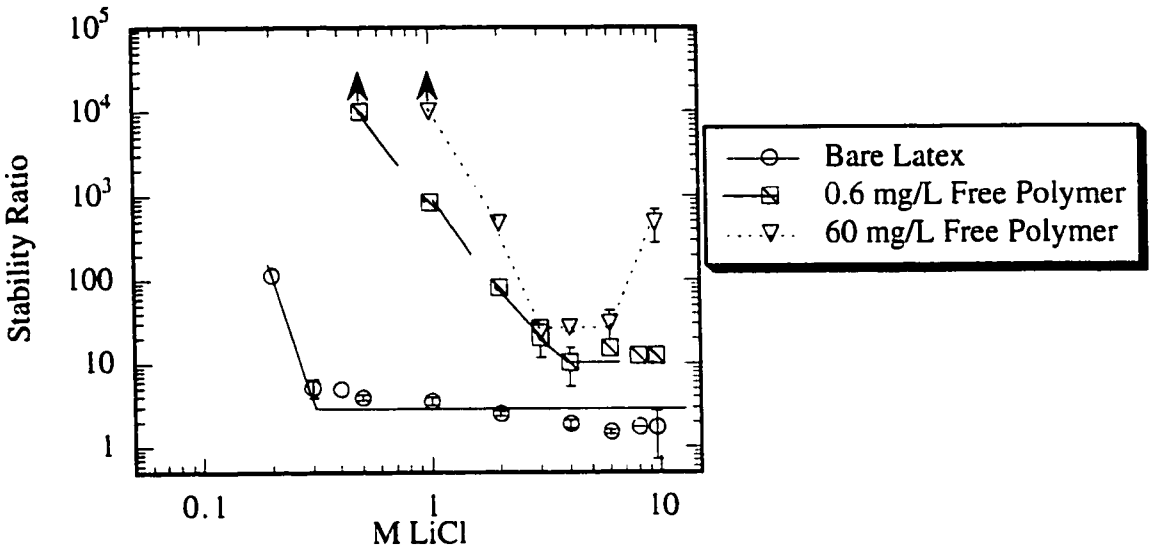

Figure 5.12 Stability Ratio of Pluronics® L64 Coated 0.11 µm Latex in Aqueous LiCl Solutions, Varying Free Polymer Concentrations

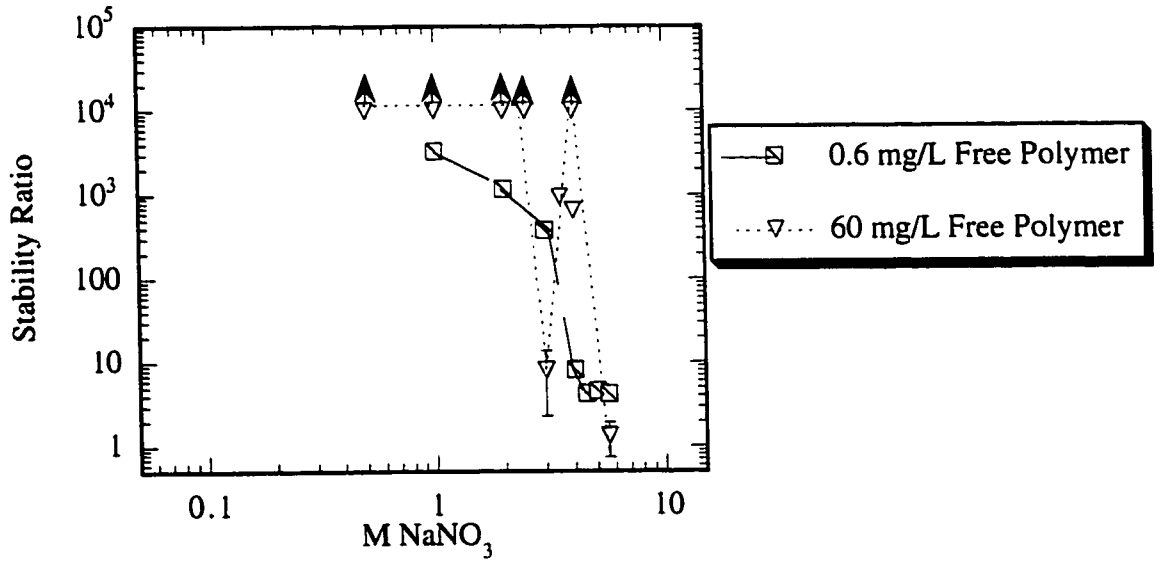

Figure 5.13 Stability Ratio of Pluronics® L64 Coated 0.11 µm Latex in Aqueous NaNO3 Solutions, Varying Free Polymer Concentrations

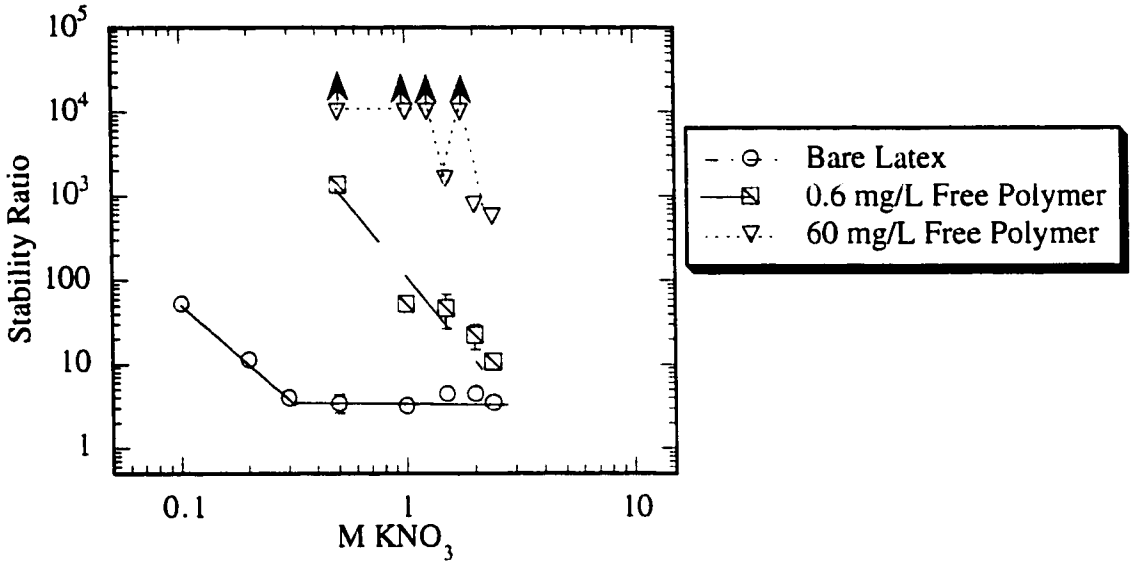

Figure 5.14 Stability Ratio of Pluronics® L64 Coated 0.11 µm Latex in Aqueous KNO_3 Solutions, Varying Free Polymer Concentrations

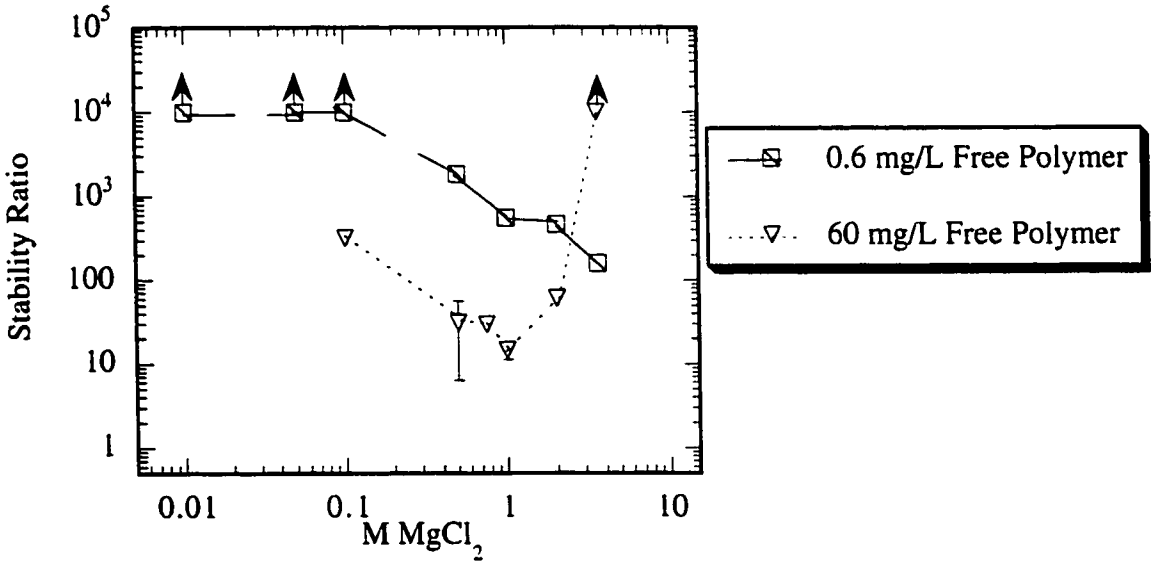

Figure 5.15 Stability Ratio of Pluronics® L64 Coated 0.11 µm Latex in Aqueous $MgCl_2$ Solutions, Varying Free Polymer Concentrations

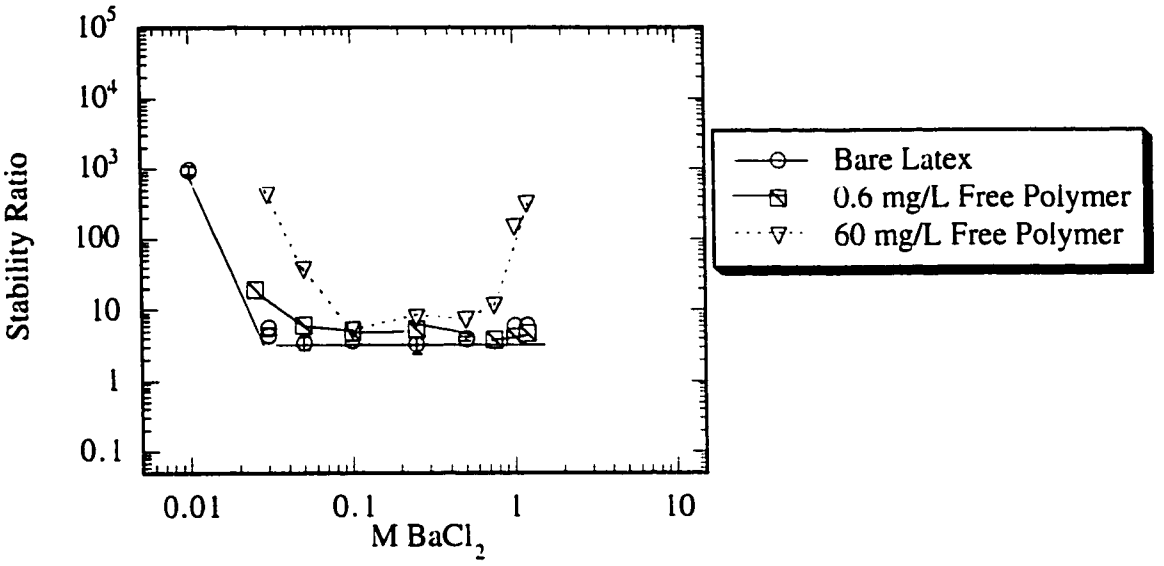

Figure 5.16 Stability Ratio of Pluronics® L35 Coated 0.11 μm Latex in Aqueous $BaCl_2$ Solutions, Varying Free Polymer Concentrations

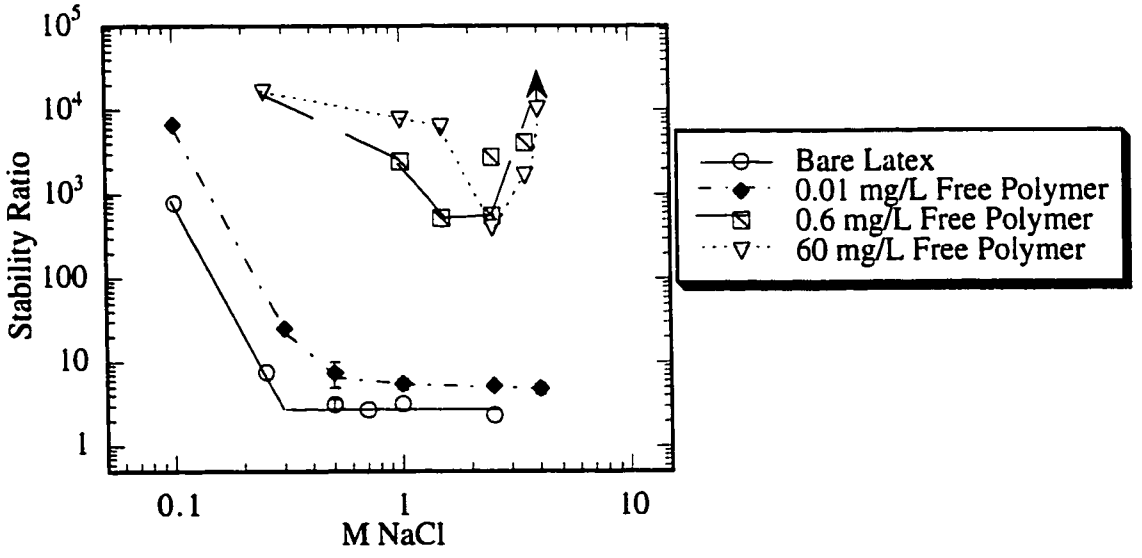

Figure 5.17 Stability Ratio of Pluronics® L64 Coated 0.11 μm Latex in Aqueous NaCl Solutions, Varying Free Polymer Concentrations

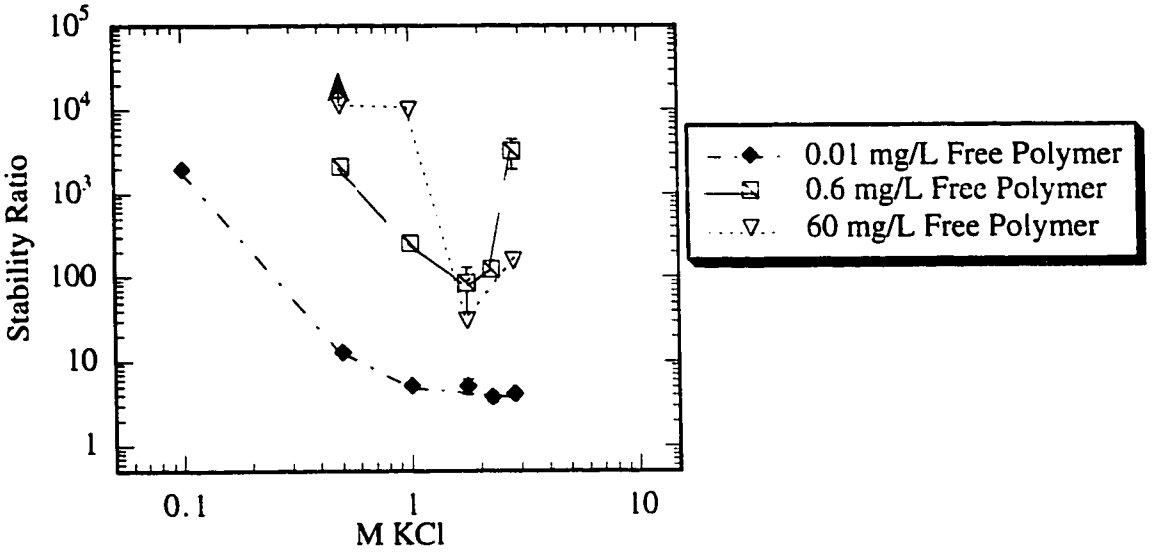

Figure 5.18 Stability Ratio of Pluronics® L64 Coated 0.11 µm Latex in Aqueous KCl Solutions, Varying Free Polymer Concentrations

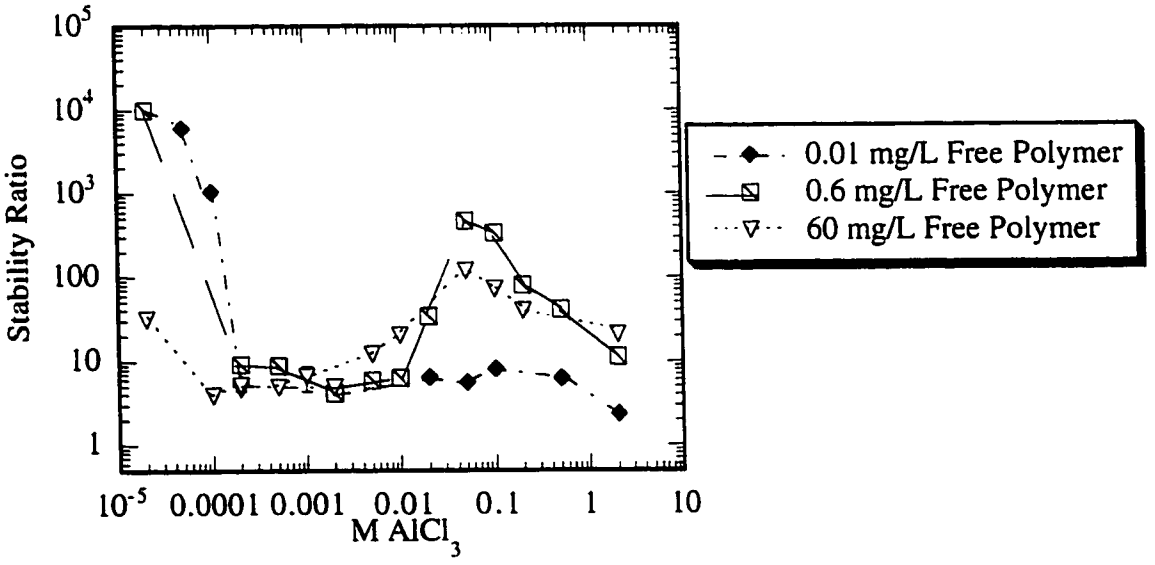

Figure 5.19 Stability Ratio of Pluronics® L64 Coated 0.11 µm Latex in Aqueous $AlCl_3$ Solutions, Varying Free Polymer Concentrations

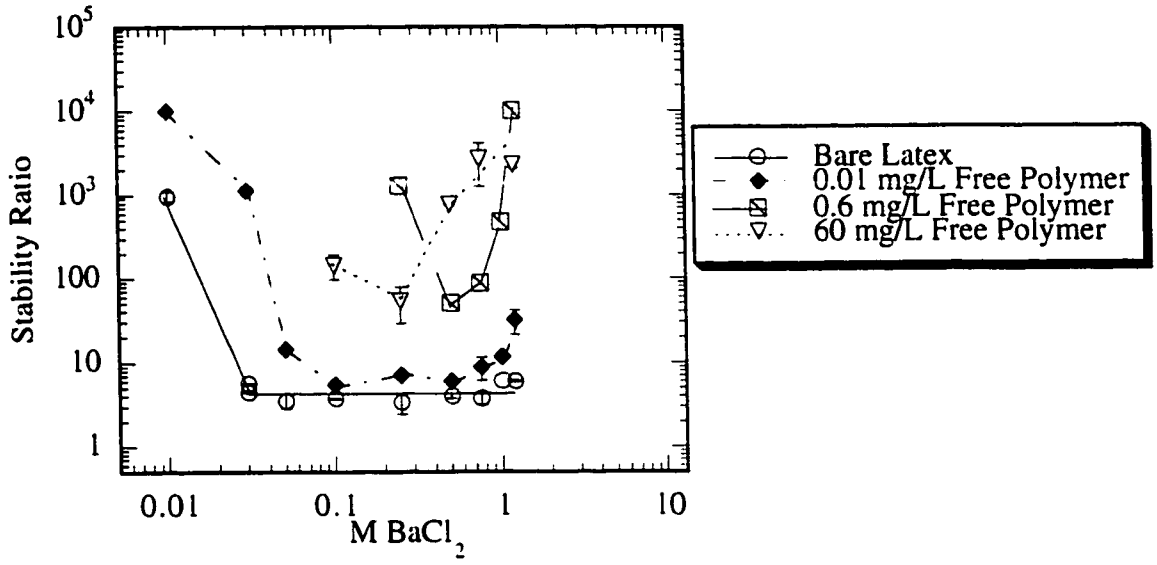

Figure 5.20 Stability Ratio of Pluronics® L64 Coated 0.11 μm Latex in Aqueous $BaCl_2$ Solutions, Varying Free Polymer Concentrations

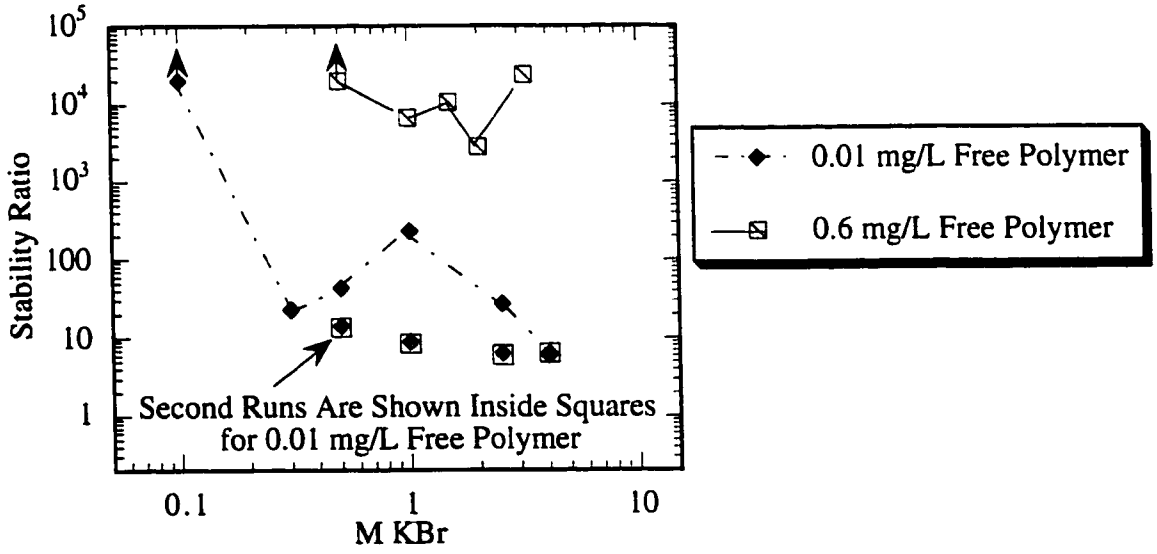

Figure 5.21 Stability Ratio of Pluronics® L64 Coated 0.11 μm Latex in Aqueous KBr Solutions, Varying Free Polymer Concentrations

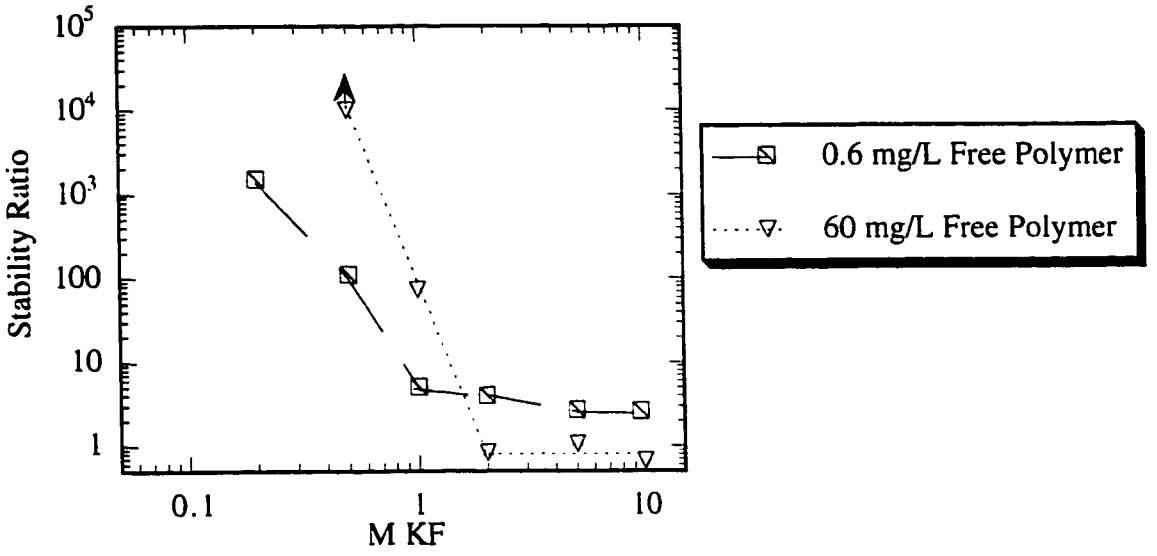

Figure 5.22 Stability Ratio of Pluronics® L64 Coated 0.11 μm Latex in Aqueous KF Solutions, Varying Free Polymer Concentrations

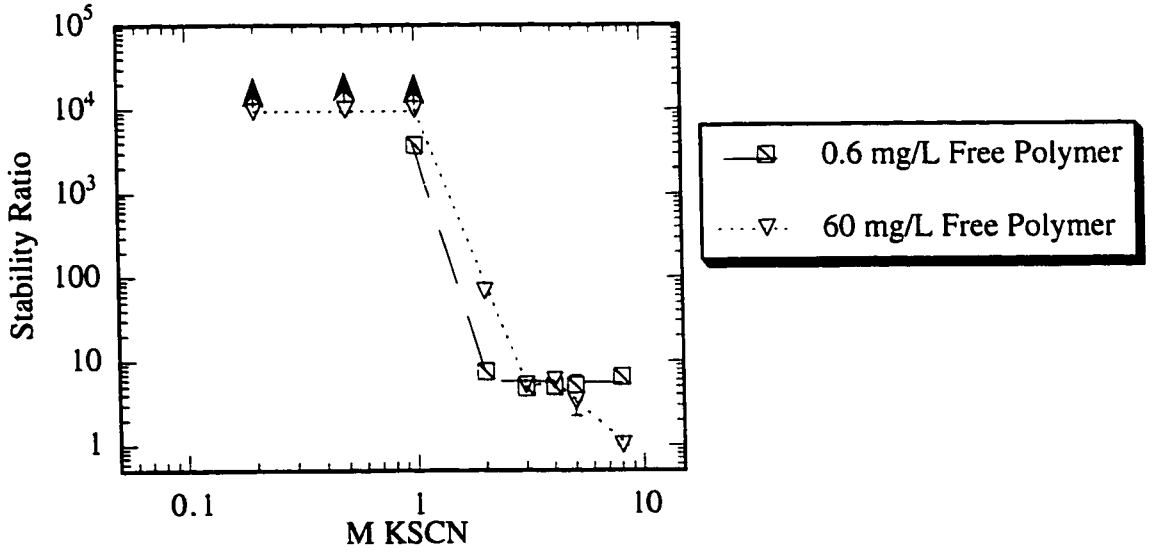

Figure 5.23 Stability Ratio of Pluronics® L64 Coated 0.11 μm Latex in Aqueous KSCN Solutions, Varying Free Polymer Concentrations

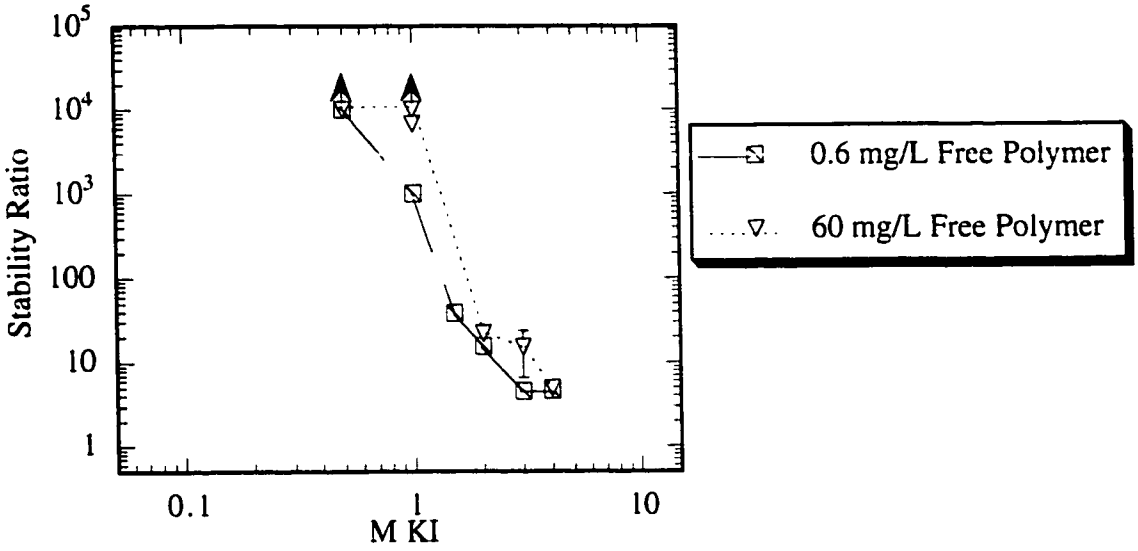

Figure 5.24 Stability Ratio of Pluronics® L64 Coated 0.11 µm Latex in Aqueous KI Solutions, Varying Free Polymer Concentrations

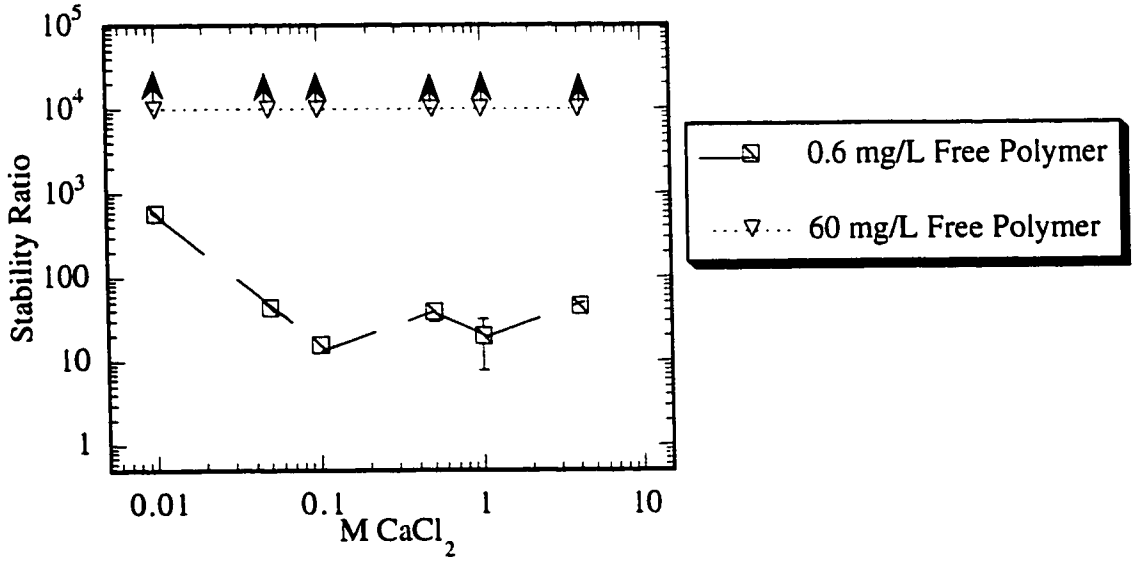

Figure 5.25 Stability Ratio of Pluronics® L64 Coated 0.11 µm Latex in Aqueous $CaCl_2$ Solutions, Varying Free Polymer Concentrations

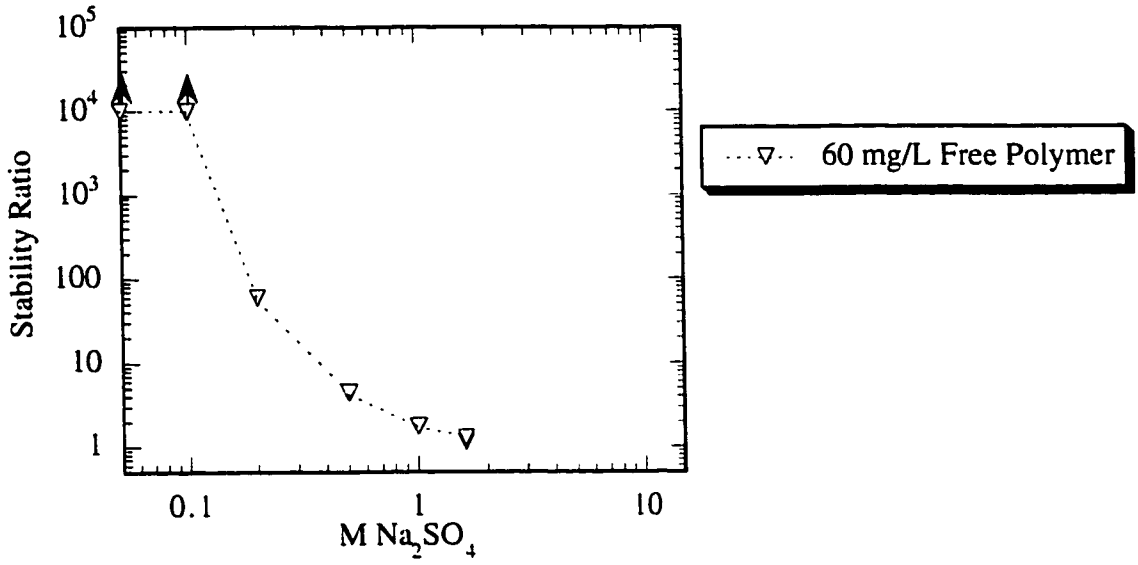

Figure 5.26 Stability Ratio of Pluronics® L64 Coated 0.11 µm Latex in Aqueous Na2SO4 Solutions, Varying Free Polymer Concentrations

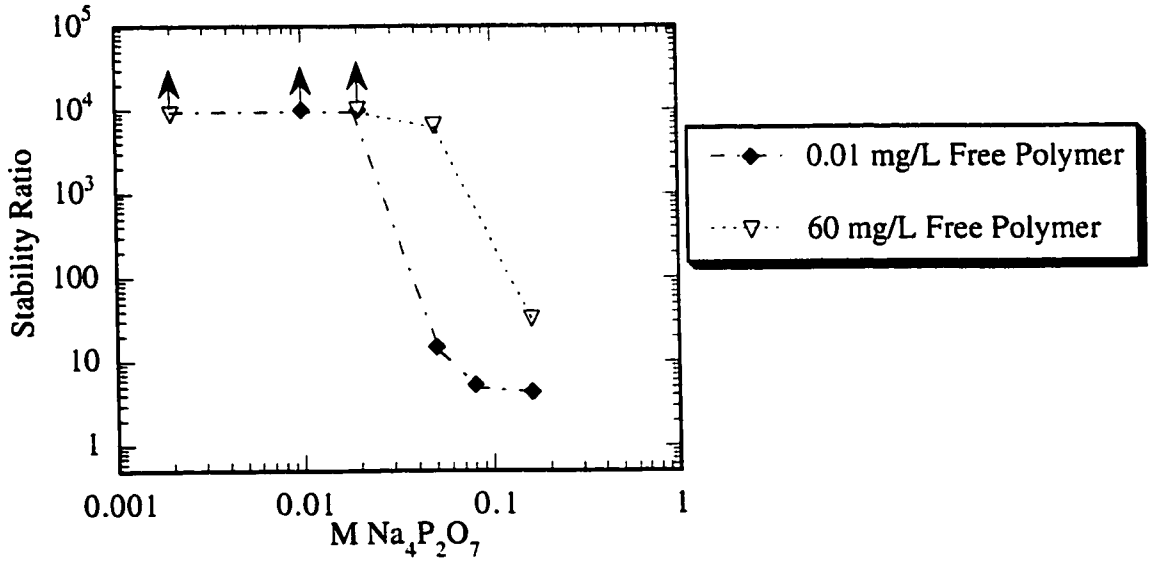

Figure 5.27 Stability Ratio of Pluronics® L64 Coated 0.11 µm Latex in Aqueous Na4P2O7 Solutions, Varying Free Polymer Concentrations

Table 5.3. Lowest Free Polymer Concentration at Which Restabilization Occurs for Pluronics L64 Coated 0.11 μm Latex in Aqueous Salt Solutions.

No Restabilization	At 60 mg/L Free Polymer	At 0.6 mg/L Free Polymer	At 0.01 mg/L Free Polymer
KF KI KSCN $CaCl_2$ Na_2SO_4 $Na_4P_2O_7$	LiCl $NaNO_3$ KNO_3 $MgCl_2$	NaCl KCl $AlCl_3$	$BaCl_2$ KBr

Desorption of Pluronics®

As shown in the previous section, decreasing the amount of free Pluronics® decreases the probability or the amount of restabilization. Close scrutiny of the results suggest that this one action has an additional effect: desorption. Three pieces of evidence suggest that dilution of the sterically stabilized latex to an intermediate concentration of $1x10^{10}$ part/mL resulted in desorption at the lower free polymer concentrations of 0.01 and 0.6 mg/L, which in turn decreased the stability imparted to the colloid. This decrease is not anticipated to be as strong when 60 mg/L free polymer is present. Until just prior to dilution, the colloid is kept at a free polymer concentration of 300 mg/L, which is in the plateau region of the isotherm.

The first piece of evidence for desorption is that, for monovalent electrolytes, increasing the free polymer concentration *always* increases the stability ratio in the region where electrostatic screening is increasing and causing a decrease in the stability. This trend can be discerned by studying the appropriate graphs presented in Figure 5.12 - 5.27 or the more convenient summary presented in Table 5.4.

Table 5.4. Relative Values of the Stability Ratio for Various Monovalent Salts as a Function of Free Polymer Concentration, in the Region where Electrosteric Stabilization is Important.

	Relative Value of the Stability Ratio		
Monovalent Salt	0.01 mg/L	0.6 mg/L	60 mg/L
LiCl	not available	lower	higher
$NaNO_3$	not available	lower	higher
NaCl	lowest	middle	highest
KCl	lowest	middle	highest
KBr	lower	higher	not available
KF	not available	lower	higher
KSCN	not available	lower	higher
KNO_3	not available	lower	higher
KI	not available	lower	higher

Unfortunately, this relative order is not maintained in the case of higher valency salts, as shown in Table 5.5. However, it may be argued that higher valency salts show poorer reproducibility. Overbeek[183] showed that the critical coagulation concentration for a negatively charged gold sol changed by a factor of 3 when the trivalent salt was changed from $Al_2(SO_4)_3$ to $Ce(NO_3)_3$. This argument is further supported by comparing the critical coagulation and critical flocculation concentrations for this and Einarson and Berg's work [95, 96, 100] when $AlCl_3$ is used as the electrolyte at a pH low enough to cause Al^{3+} to be the dominant species. The results suggest that critical concentrations can vary by an order of magnitude!

Table 5.5. Relative Values of the Stability Ratio for Di- and Trivalent Salts as a Function of Free Polymer Concentration, in the Region where Electrosteric Stabilization is Important.

	Relative Value of the Stability Ratio		
Salt	0.01 mg/L	0.6 mg/L	60 mg/L
$MgCl_2$	not available	higher	lower
$BaCl_2$ - L35	not available	lower	higher
$AlCl_3$	highest	middle	lowest
$BaCl_2$	lowest	highest	middle
$CaCl_2$	not available	lower	higher
$Na_4P_2O_7$	lower	not available	higher

The second piece of evidence is shown in Figure 5.21. In the case of KBr with 0.01 mg/L free polymer, a second run always resulted in a significant decrease in the stability ratio, to the point where restabilization no longer occurred. A slight decrease for the subsequent runs was observed for NaCl, KCl, and $BaCl_2$ with 0.01 mg/L, but it was not enough to significantly change the value of the stability ratio, as seen in Figure 5.16, 5.17, and 5.19. This decrease was not noticed in runs with 0.6 mg/L, suggesting that the driving force for desorption is not as great.

The third piece of evidence is given by changes in the adlayer thickness. Sterically stabilized latex was created by adsorbing Pluronics® L64 to the 0.11 μm latex so that 300 mg/L free polymer was remaining (plateau region of the isotherm). This stock was then diluted so that the final particle concentration was $1x10^{10}$ part/mL and the free polymer concentration was approximately 0.4 mg/L. This stock was immediately diluted to a final particle concentration of $2x10^9$ part/mL and the hydrodynamic adlayer thickness was determined to be 1.4 nm from measurements repeated 90 times on this sample. The $1x10^{10}$ part/mL was allowed to sit for four hours before another sample was diluted to $2x10^9$ part/mL and the hydrodynamic diameter determined again. This time the adlayer thickness was 0.7 nm, suggesting that it is decreasing due to desorption. Unfortunately,

the change in the adlayer thickness is of the same order of the detection limits of the dynamic light scattering measurements, which is rather unsatisfying.

Further evidence of desorption can be found in the literature, as shown by Freij-Larsson[184] and Tiberg[185] and their respective coworkers. These researchers used ellipsometry to measure the amount of Pluronics adsorbed to hydrophobized silica. They allowed adsorption for 1-2 hours, then commenced washing with pure water. Freij-Larson found that more than 30% of the polymer desorbed within 15 minutes for Pluronics PE 94 at a bulk concentration of 3000 mg/L. The structure of PE94 is $HO(CH_2CH_2O)_{21}(CH_3CH_2CHO)_{47}(CH_2CH_2O)_{21}H$. The anchor block of PPO is relatively large, considering that the largest anchor block for Pluronics® occurs for F108 and is 56 units long. Tiberg and coworkers found that the desorbed amount increases with increasing bulk concentration, and varies between roughly 20 and 70% for bulk concentrations between 10 and 10,000 mg/L. The Pluronics used was PE6200, which has a structure of $HO(CH_2CH_2O)_6(CH_3CH_2CHO)_{37}(CH_2CH_2O)_6H$. The anchor block is significantly smaller than that for PE94, but is still significantly longer than the anchor block of L64 or L35 used in this study. The desorption of these smaller polymers may be even more severe.

Strength of Restabilization

As shown, the probability or amount of restabilization can be increased by increasing the concentration of salt , concentration of free polymer, or the molecular weight of the polymer if the polymer is of low molecular weight. Salts which require less polymer, less salt, or a lower molecular weight to exhibit restabilization can be said to show a stronger propensity towards the phenomena. In the case of the salt concentration, the strength of restabilization can be characterized by using the onset of restabilization. The onset is defined as the point where an increase in the salt concentration results in an

increase in the stability ratio. Salts exhibiting stronger restabilization have a lower onset. The onsets for the various salts have been determined from the graphs presented in Figures 5.12 - 5.27 and are presented in Table 5.6. The salts have been divided into groups, according to the type of salt: chloride, potassium, or sodium.

The last column in Table 5.6 presents the molarity of the salt when the theta temperature is 25°C. The data are either taken directly or extrapolated from values in the literature[65, 67, 68, 70]. It should be noted that in every case, the onset is lower than the estimated theta point of PEO, which suggests that restabilization occurs when the solvency of the stabilizing polymer is good.

The data for L35 coated latex with 60 mg/L free polymer and L64 coated latex with 0.01 mg/L free polymer are not presented in Table 5.6 since restabilization was seen only for $BaCl_2$ in the former and $BaCl_2$ and KBr in the latter. In these cases, the values for the onset in $BaCl_2$ are in reasonable agreement with the values in the table; the onset was 0.8 M and 0.5 M for L35 coated latex, 60 mg/L free polymer and L64 coated latex, 0.01 mg/L free polymer, respectively. In the case of KBr, restabilization is so strong that the system is completely stable with 0.6 mg/L free polymer and exhibits restabilization at 0.3 M with 0.01 mg/L free polymer.

Table 5.6. Onset of Restabilization for L64 Stabilized 0.11 μm Latex with 0.6 and 60 mg/L Free Polymer. (The theta point for PEO is also presented for comparison)

A. Chloride Salts

	Molarity at the Onset of Restabilization		
Cation of Chloride Salt	0.6 mg/L Free Polymer	60 mg/L Free Polymer	Approximate Molarity Where θ=25°C for PEO
Li^+	no restabilization	6.0	»4
Na^+	2.5	2.5	4.5
K^+	1.8	1.8	3.8
Ba^{2+}	0.5	0.25	>2
Ca^{2+}	no restabilization	completely stable	»4
Mg^{2+}	no restabilization	1.0	»4

B. Potassium Salts

	Molarity at the Onset of Restabilization		
Anion of Potassium Salt	0.6 mg/L Free Polymer	60 mg/L Free Polymer	Approximate Molarity Where θ=25°C for PEO
F-	no restabilization	no restabilization	1.3
SCN-	no restabilization	no restabilization	»2
NO3-	no restabilization	1.5	3.2
I-	no restabilization	no restabilization	»4
Cl-	1.8	1.8	3.8
Br-	completely stable	not tested	>4

C. Sodium Salts

	Molarity at the Onset of Restabilization		
Anion of the Sodium Salt	0.6 mg/L Free Polymer	60 mg/L Free Polymer	Approximate Molarity Where θ=25°C for PEO
SO_4^{2-}	not tested	no restabilization	0.6
Cl^-	2.5	2.5	4.5
NO_3^-	no restabilization	3.0	4.0

Table 5.7 shows the salts in order of increasing restabilization strength using all criteria: molarity at the onset, free polymer concentration, and number of Pluronics®

exhibiting restabilization. Salts which do not cause restabilization are on the far left of the series and are italicized. In terms of strength, there is reasonable internal consistency among the aggregation data. Specifically, the salts which have a low molarity at the onset of restabilization are also capable of restabilization at low free polymer concentrations and at a wider range of molecular weights. The molarity of the onset is a more sensitive screen than the other two, since the salt molarity was varied over a wide range. On the other hand, only three different molecular weights and three different free polymer concentrations were employed for any one salt.

There are two cases where the data are not consistent in terms of strength: $MgCl_2$ and KNO_3. In the case of $MgCl_2$, restabilization only occurs in the presence of 60 mg/L free polymer, which is the highest concentration tested, while the molarity of the onset occurs at the relatively low concentration of 1 M when 60 mg/L free polymer is present. In the case of KNO_3, the KNO_3 and KCl switch places in the order of the onset depending on the amount of free polymer present. The molarity at restabilization is so close that this discrepancy may not be significant (Table 5.6 Part B).

Table 5.7. Salts in Order of Increasing Strength of Restabilization

A. Chloride Salts

Criteria	Order of Salts
Molarity at the Onset of Restabilization	Ca^{2+}=*Li^{+}*=*Mg^{2+}*>Na^{+}>K^{+}>Ba^{2+} (0.6 mg/L free polymer) Ca^{2+}>Li^{+}>Na^{+}>K^{+}>Mg^{2+}>Ba^{2+} (60 mg/L free polymer)
Free Polymer Required for Restabilization	Ca^{2+}>Li^{+}=Mg^{2+}>Na^{+}=K^{+}>Ba^{2+}
Number of Pluronics Which Show Restabilization	Li^{+}=Na^{+}=K^{+}<Ba^{2+} Remaining salts not tested

B. Potassium Salts

Criteria	Order of Salts
Molarity at the Onset of Restabilization	F^-=*SCN*$^-$=*I*$^-$>Cl^- >NO_3^->Br-
Free Polymer Required for Restabilization	F^-=*SCN*$^-$=*I*$^-$>NO_3^->Cl^- >Br-
Number of Pluronics Which Show Restabilization	*SCN*$^-$<NO_3^-=Cl^- Remaining salts not tested

C. Sodium Salts

Criteria	Order of Salts
Molarity at the Onset of Restabilization	NO_3^->Cl^- (SO_4^{2-} not tested) (0.6 mg/L free polymer) *SO*$_4^{2-}$ >NO_3^->Cl^- (60 mg/L free polymer)
Free Polymer Required for Restabilization	*SO*$_4^{2-}$ >NO_3^->Cl^-
Number of Pluronics Which Show Restabilization	NO_3^->Cl^- (SO_4^{2-} not tested for more than one polymer)

Effect of Valency

The effect of valency was tested by performing aggregation tests for salts having anions and cations of different valencies, while keeping the valency of the opposite ion at one. The results have already been presented in Figures 5.12 through 5.27, but are summarized more succinctly in Table 5.8. For the data thus far, there is no clear dependency on valency, primarily because the effect is extremely salt specific.

Table 5.8. The Dependency of Restabilization on the Valency of the Salt.

Valency	Number of Salts Showing Restabilization	Number of Salts Not Showing Restabilization
Monovalent Cation and Anion	6	4
Divalent Cation	2	1
Trivalent Cation	1	0
Divalent Anion	0	1
Tetravalent Anion	0	1

The salt $Na_4P_2O_7$ was also tested to determine the effect of a known dispersant[186-188]. This salt is known to adsorb to the surfaces of minerals and oxides, causing an increase in the negative potential at the same pH. This increase, in turn, causes an increase in colloidal stability. As can be seen from Figure 5.27, no restabilization was seen, suggesting that either this salt does not adsorb to the surface of polystyrene latex or that the mechanism of this restabilization is different than that caused by known dispersants. In order to draw firm conclusions about the effect of a dispersant, more research needs to be performed.

Force Distance Profiling

To gain a greater understanding of the mechanism controlling restabilization, force distance profiling was conducted. Pluronics® L35 with $BaCl_2$ salt was chosen since the restabilization was very pronounced (see Figure 5.10 or 5.16). The force distance profiles on approach are presented in Figure 5.28 for 0.01 M and 0.5 M $BaCl_2$. The free Pluronics® concentration was such that adsorption in the plateau region could occur, preventing complications caused by desorption. The distance presented is the distance from monolayer/monolayer contact measured in air. The profiles on separation are not presented. It appeared that there was hysteresis in the measurements. Measurements after the surfaces had previously been brought together appeared to be longer range. This

behavior was not fully investigated, but one possibility was that the surfaces were damaged upon contact. As can be seen, the separation distance at the onset of repulsion as well as the magnitude of repulsion increases as the salt concentration increases. In particular, the onset of repulsion occurs at a separation distance of 3.5 nm in 0.01 M salt and 16.5 nm in 0.5 M salt. This behavior is consistent with the appearance of restabilization.

One must note that these conditions are not identical to those presented in Figure 5.10. The concentration in the aggregation experiment was 60 mg/L, while that in the force distance measurements was 300 mg/L. An increase in stability ratio, indicative of increased repulsion is observed at 0.8 M for the aggregation experiment, while an increase in repulsion is observed at 0.5 M for the force distance measurement. This would suggest that restabilization is increased upon an increase in the Pluronics® concentration, which is consistent with the results presented earlier.

Greater understanding of the mechanism behind restabilization can be gained by comparing the distance at the onset of repulsion with the contour lengths of the Pluronics®. If the Pluronics® adsorbs so that the PPO block exists as trains and the PEO block exists as tails, then only the PEO tail is available to impart repulsion from the surface. The contour length of a PEO tail is approximately 4 nm, assuming it contains 11 ethylene oxide units. This result suggests that even at the stiffest, most extended configuration, two PEO tails engaged in a steric interaction are insufficiently long to impart the repulsion seen at 0.5 M, but are reasonably consistent with the distance of repulsion seen for 0.01 M. The contour length of the entire L35 Pluronics® is 14 nm. Therefore, the distance at the onset of repulsion in 0.5 M is consistent with a more complex configuration, such as the entrapment of a Pluronics® between two Pluronics® coated surfaces.

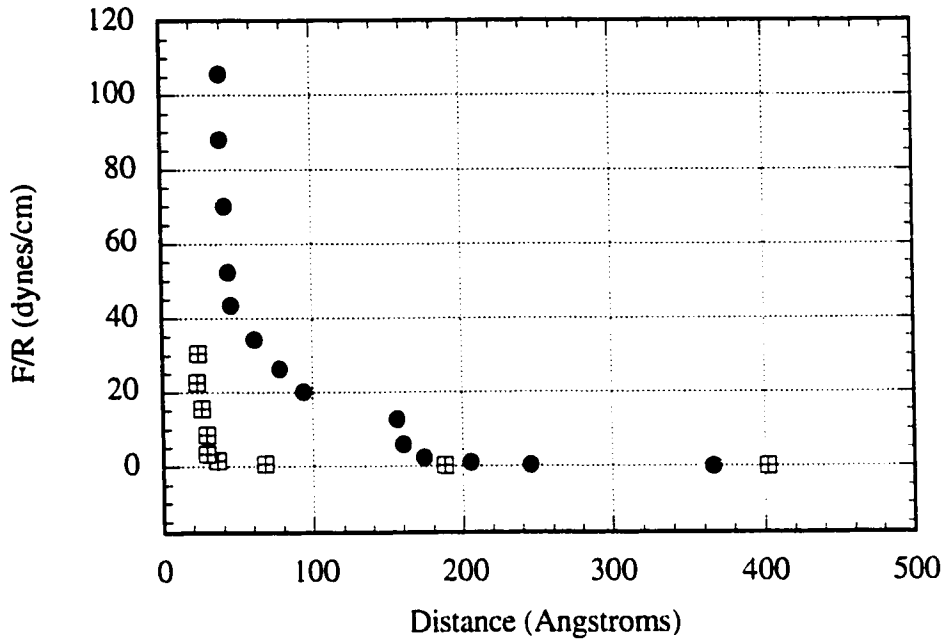

Figure 5.28. Measurement of Interaction Energy by SFA as a Function of Separation Distance for 300 mg/L Pluronics L35 in Aqueous $BaCl_2$ Solutions.

SUMMARY OF WORK

Restabilization has been defined as an increase in the stability ratio of a colloid upon an increase in salt concentration. In prior work, restabilization was seen for charged latices with thin neutral adlayers. The behavior was unexpected since electrostatic repulsion was negligible and the solvency of the stabilizing polymer was good but decreasing. Common knowledge would suggest that the stability ratio should decrease or remain constant upon an increase in salt concentration. This chapter presents a systematic characterization of the behavior. The model system employed was a polystyrene latex with sulfate functional groups, having a layer of adsorbed triblock copolymer. The copolymer has polyethylene oxide stabilizing blocks on either side of a polypropylene oxide anchor block.

This work indicates that restabilization requires intermediate molecular weight adlayers to occur, and that a decrease in the amount of free or unadsorbed polymer can decrease the probability for restabilization. Most importantly, restabilization is a highly specific phenomenon, depending strongly not only on the cation but the anion of the salt as well. The limited amount of data suggest that the anions determine whether the phenomena can occur, while the cations determine the relative order for a particular anion. Chloride salts show a particularly strong propensity towards restabilization; with six of the seven tested exhibiting the behavior. The one exception is $CaCl_2$. A comparison of the polymer solvency and stability ratios suggest that restabilization may be occurring for this salt, but it is not detected.

CHAPTER 6: INVESTIGATION OF THE RESTABILIZATION MECHANISM

A. INTRODUCTION

As discussed in Chapter 5, the purpose of this chapter is to discuss the possible causes for restabilization. The researchers who first observed this phenomena could only speculate on the cause since its characterization was not their main goal. It is known that cations can bind polyethylene oxide in a manner resembling a crown ether complex[76, 77, 143, 147]. As a result, the group from the University of Washington hypothesized that the stabilizing polymer was binding the cation, which stiffened and/or lengthened the adlayer enough to cause a measurable increase in stability. The group from the University of Akron did not observe the behavior for the lowest molecular weight adlayers. They concluded that the unusually high stability ratio was caused by slow incorporation of salt into the thicker adlayers, causing a "time delay for aggregation." It also seems plausible that, since the solvency of the polymer is decreasing, additional adsorption may occur[134], causing enough of an increase in the adlayer thickness to slow aggregation. Alternatively, restabilization may be linked to block copolymer micellization, which is induced by an increase in salt concentration[189].

Of these hypotheses, the least likely seems to be that proposed by the researchers from Akron. It has been shown in previous studies[7-9] and in Chapter 3 that the most outward extending tails are responsible for the majority of stabilization. Due to the proximity of the tails to the solvent, it seems unlikely that the proposed time delay should occur. As a result, no attempt has been made to investigate this mechanism. Instead, this chapter discusses the plausibility of inducing restabilization by increased polymer

adsorption caused by decreased polymer solvency, ion binding, or block copolymer micelles.

B. EXPERIMENTAL SECTION

Materials and Aggregation Experiments

The materials and aggregation experiments were discussed in Chapter 5.

Adsorption Experiments

To determine the adsorbed amount, the desired concentration of latex and dissolved polymer were gently stirred for 15-18 hours, then the latex was separated from the free polymer and water by ultrafiltration through a 0.05 μm Isopore® Polycarbonate Membrane Filter (VMTP04700) from Millipore (Bedford, MA). The total amount of Pluronics® remaining in solution after adsorption onto and separation from the latex was determined using the turbidimetric technique outlined in Chapter 3 with the calibration curves given in Appendix B.

C. DISCUSSION OF POSSIBLE MECHANISMS

Additional Adsorption Caused by Decreased Pluronics® Solvency

Measurements of Additional Adsorption The results in the study of the Pluronics® concentration lead to the obvious question: if removal of free polymer reduces restabilization, is additional adsorption occurring as the salt concentration increases? This increased adsorption could in turn result in a thicker adlayer, which would prevent aggregation. As a counter-argument, restabilization is seen at 0.01 mg/L free polymer, which is only enough to increase the adsorbed amount by 15%. This result might suggest adsorption is unimportant; however, to obtain more concrete evidence, adsorption tests were performed and the aggregation data re-examined for more detail.

The goal of the adsorption test was to determine if the addition of salt resulted in an increase in the adsorbed amount. This test was performed for the case of L35 coated latex in 1.2 M $BaCl_2$ solutions with 60 mg/L free polymer since this system exhibits quite pronounced restabilization and force distance profiling results are available at similar conditions. The procedure followed in this experiment was chosen to closely mimic the conditions experienced during the aggregation experiment. The adsorption density was determined to be close to 1 mg/m^2 in pure water with roughly 300 mg/L free polymer concentration present. Enough salt was then added to result in restabilization and reduce the free polymer to 60 mg/L. The adsorbed amount was determined as a function of time since the addition of salt as shown in Figure 6.1. The error bars indicate one standard deviation for two determinations of the adsorbed amount. The typical duration of a light scattering experiment ranges from a few minutes to 2 hours. Therefore, the results suggest that less than 0.1 mg/m^2 is adsorbed to the surface within the time frame of a typical light scattering experiment. Since the detection limit of the test is close to this value, one can only conclude that very little, if any, additional adsorption has occurred.

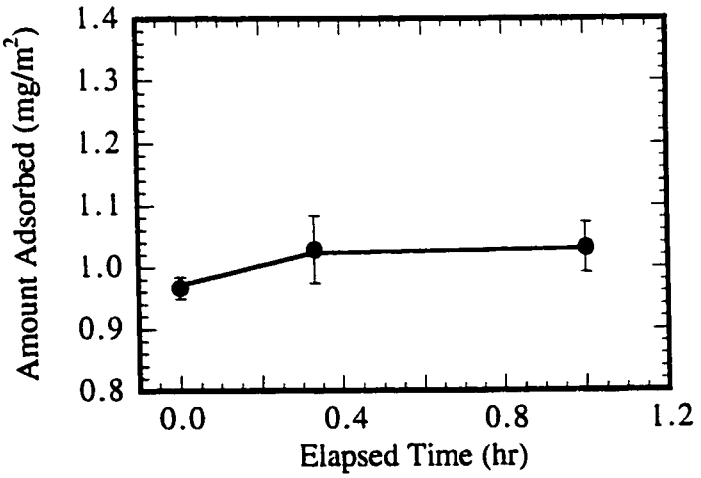

Figure 6.1. The Amount of L64 Pluronics® Adsorbed to the Surface of 0.11 μm Latex in 1.2 M $BaCl_2$ and 60 mg/L Free L64 as a Function of Time Since the Addition of Salt. The Point at Time Zero Indicates the Amount Adsorbed in Distilled Water.

This conclusion can also be obtained by re-examining the aggregation data in which the average hydrodynamic size of the latex particles is plotted as a function of time since the addition of salt. An example plot is given in Figure 6.2, which depicts the hydrodynamic diameter for L35 coated latex in 1.2 M $BaCl_2$ and 60 mg/L free polymer as a function of time. The size of the polymer coated latex particles in distilled water is given as the solid line for comparison. The plot shows that the average particle diameter of the restabilized latex is close that of the coated latex in distilled water. In Chapter 3 it was shown that dynamic light scattering measurements can detect the presence of an adlayer which is comprised of less than 1% weight of long tails. Therefore, the similarity in hydrodynamic diameters suggests that a large increase in the adlayer thickness caused by significant additional adsorption is not the likely cause of restabilization.

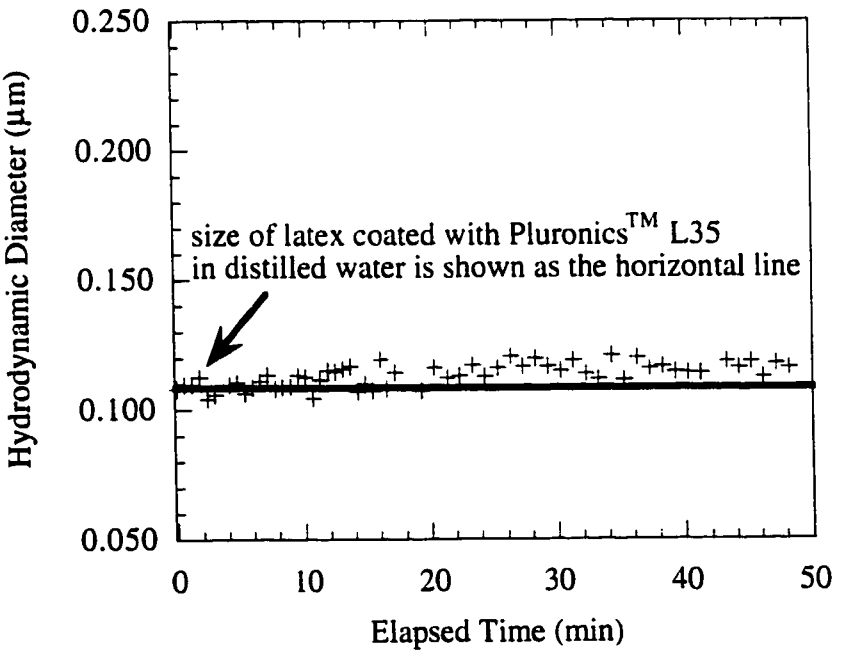

Figure 6.2. The Hydrodynamic Diameter of L64 Coated 0.11 μm Latex in 1.2 M $BaCl_2$ and 60 mg/L Free L64 as a Function of Time Since the Addition of Salt.

Comparison to the Order of Salting Out Tadros and Vincent [134] have shown that decreasing the polymer solvency can increase the amount of Pluronics® adsorbed. In particular, they show that Na_2SO_4 increases the adsorbed amount more than KCl due to its poorer solvency. Baring specific interactions, these results suggest that an increase in adsorption caused by the addition of electrolyte should follow the order of salting out PEO. Therefore, to further investigate if additional adsorption is responsible for restabilization, the onset of restabilization can be compared to the order of salting out.

Theta or cloud point temperatures from the literature[65, 67, 68, 70] were used to establish the order of salting out. Data presented by Ataman, Florin, and Boucher and their coworders were plotted for comparison in Figure 6.3 - 6.5. Data from Bailey and Callard were not used simply because there were little data for each salt, and the numbers could not be read as accurately from the graphs as the tabulated data presented in the other publications. Both Ataman and Boucher with their respective coworkers presented theta temperatures, while Florin and Kjellander presented cloud point temperatures for 1 wt% PEO. The molality data presented in Florin and Kjellander's work were converted to molarity using handbook data[181], except in the case of KF for which there were no data. In this case, the molality was used instead. The maximum error is anticipated to occur at the higher salt concentrations and should be on the order of 10%. The order of salting out was estimated for KSCN from the CFT of sterically stabilized colloids[29].

It can be seen from Figures 6.3 - 6.5 that values from the different sources agree well . The values are somewhat more disparate in the case for LiCl, but the order of salting out established in the literature is consistent. This order is summarized in Table 6.1 and can be compared to the order of the onset of restabilization. If restabilization is caused by additional adsorption (without specific interactions), then the molarity of the onset should decrease with increasing ability to decrease solvency. As can be seen, the order of salting

out does not follow the order of restabilization. In the case of the chloride salts, $BaCl_2$ and LiCl are similar in their ability to salt out PEO, but $BaCl_2$ is extremely strong in its ability to restabilize, while LiCl is poor. KCl, KNO_3, and KBr are the only potassium salts and NaCl is the strongest sodium salt to show restabilization, but all are intermediate in ability to salt out PEO. These results suggest that the order of salting out does not correlate with the strength of restabilization, further supporting the conclusion that increased adsorption caused by decreased solvency is not the cause of the phenomena.

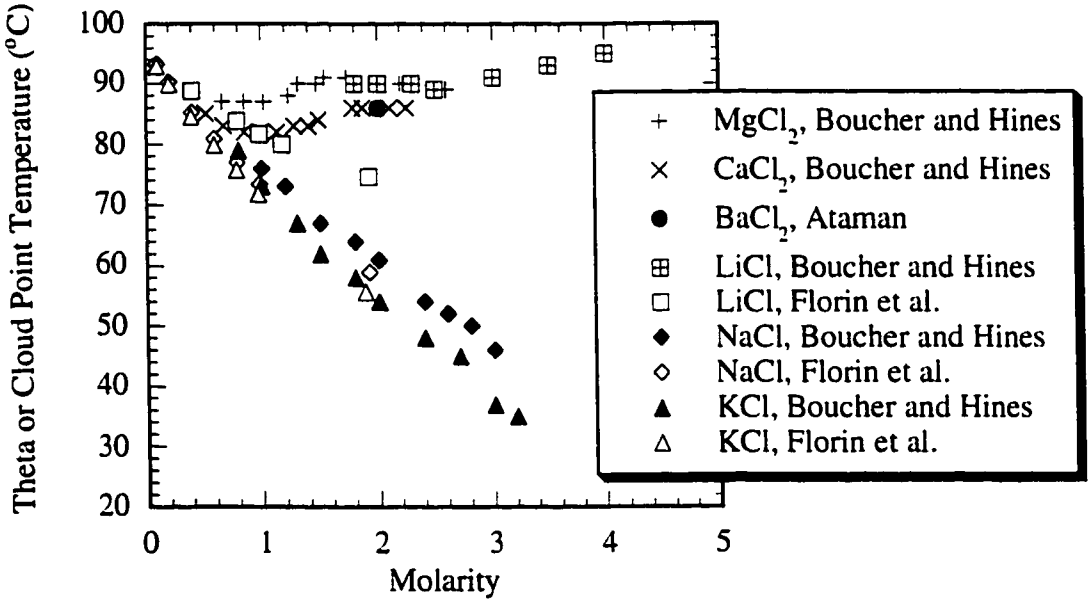

Figure 6.3. Theta or Cloud Point Temperatures for Chloride Salts

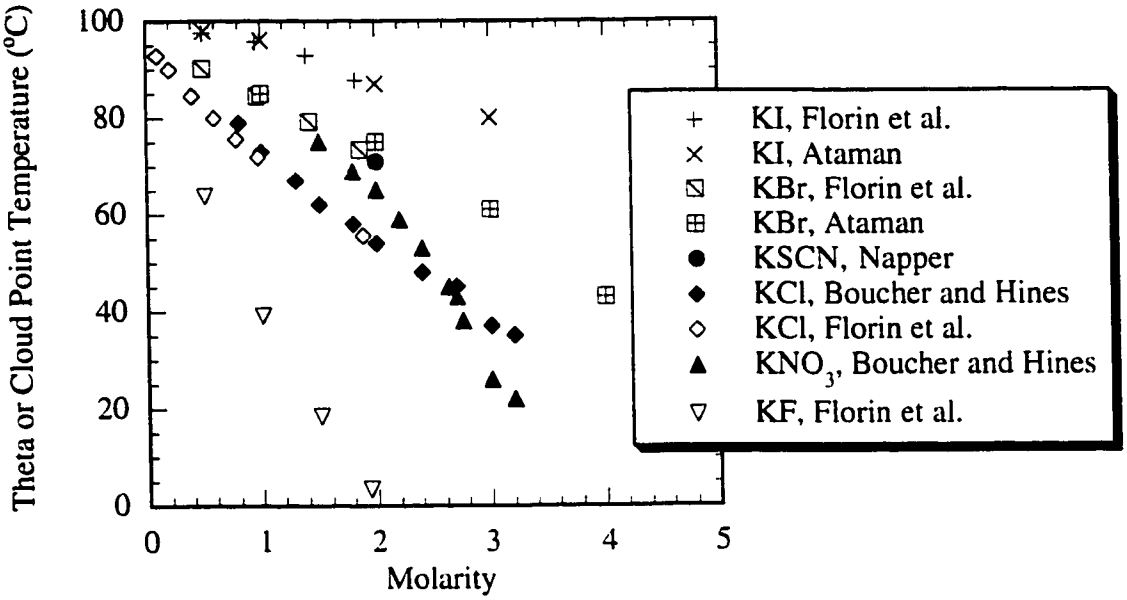

Figure 6.4. Theta or Cloud Point Temperatures for Potassium Salts

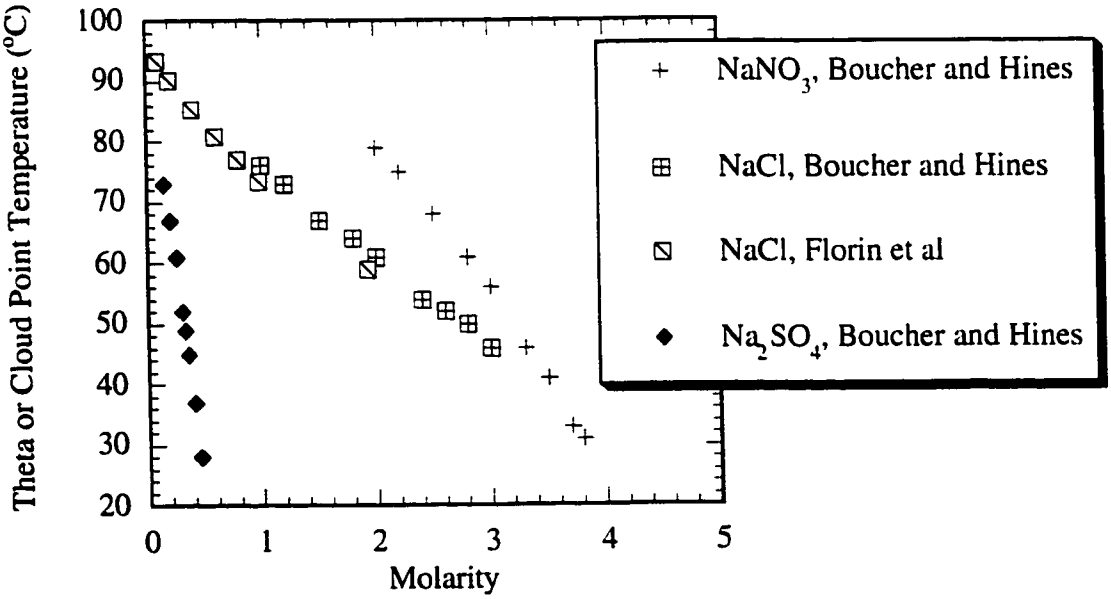

Figure 6.5. Theta or Cloud Point Temperatures for Sodium Salts

Table 6.1. The Order of Ion Binding, Salting Out, and the Molarity at the Onset of Restabilization

A. Alkali and Alkaline Earth Metal Salts

Series	Order of Salts
Molarity at the Onset of Restabilization	$Ca^{2+}=Li^{+}=Mg^{2+}>Na^{+}>K^{+}>Ba^{2+}$ (0.6 mg/L free polymer) $Ca^{2+}>Li^{+}>Na^{+}>K^{+}>Mg^{2+}>Ba^{2+}$ (60 mg/L free polymer)
Salting Out	$Mg^{2+}\approx Ca^{2+}\approx Ba^{2+}\leq Li^{+}<Na^{+}\leq K^{+}$
Ion Binding	$Li^{+}<Na^{+}\approx K^{+}$; $Mg^{2+}\approx Ca^{2+}\approx Ba^{2+}$ (Solvent extraction, this study) $Li^{+}<< Na^{+}<Rb^{+}\approx K^{+}\approx Cs^{+}$ (Sartori)[147] $Na+<Ba^{2+}$ (Cross)[143] $Li^{+}<Na^{+}<Cs^{+}<Rb^{+}<K^{+}$; $Mg^{2+}<Ca^{2+}<Sr^{+}<Ba^{2+}$ (Okada, Kikuchi, and Yanagida)[146, 148-152]

B. Potassium Salts

Series	Order of Salts
Molarity at the Onset of Restabilization	$F^{-}=SCN^{-}=I^{-}>Cl^{-}>NO3^{-}>Br^{-}$
Salting Out	$I^{-}<SCN^{-}\approx Br^{-}< NO3^{-}\leq Cl^{-}<F^{-}$
Ion Binding	$Cl^{-}<F^{-}<Br^{-}<NO3^{-}\ll I^{-}<SCN^{-}$ (Solvent extraction, this study) $F^{-}\approx Cl^{-}<SCN^{-}$ (Sartori)[147] $Cl^{-}\leq Br^{-}\approx NO3^{-}\ll I^{-}<SCN^{-}$ (Yanagida)[148]

C. Sodium Salts

Series	Order of Salts
Molarity at the Onset of Restabilization	$NO3^{-}>Cl^{-}$ ($SO4^{2-}$ not tested) (0.6 mg/L free polymer) $SO4^{2-}>NO3^{-}>Cl^{-}$ (60 mg/L free polymer)
Salting Out	$SO4^{2-}>Cl^{-}>NO3^{-}$
Ion Binding	$Cl^{-}<NO3^{-}<SO4^{2-}$ (solvent extraction)

Ion Binding

Comparison to the Order of Ion Binding and Spectroscopic Measurements As discussed earlier, it is plausible that ion binding is responsible for restabilization. The drastic change in restabilization upon a slight change in PEO molecular weight (from 11 to 13 units/tail) could be explained by the strong dependence of ion binding on molecular weight when oligomeric PEO is involved. Ion binding could cause a

stiffer and/or thicker adlayer, either through conformational changes in the polymer or through intermolecular binding. Intermolecular binding could link two or more polymers together to essentially form a high molecular weight polymer. To obtain concrete evidence of this possibility, the strength of restabilization as shown by the onset was compared to the strength of binding. If the molarity of the onset decreases with increasing binding ability, then ion binding may be responsible for restabilization.

Solvent extraction tests were performed as described in Chapter 4 to perform a rough screening for binding ability. What was concluded is that the chloride salts show extremely poor solvent extraction, and therefore ion binding. In contrast, the majority of salts which show restabilization are chloride salts. This leads to one conclusion: ion binding is not responsible for restabilization.

Comparisons within salt series lead to the same conclusion for the majority of cases. Table 6.1 presents the solvent extraction results performed in this study as well as ion binding data obtained by Sartori[147], solvent extraction data obtained by Yanagida[148], and summary data presented in reviews by Okada[146] and Cross[143]. The information presented by Okada is primarily for organic solvents, while the other data are for aqueous systems. Solvent extraction and direct measurements of binding for the potassium salts indicate that ion binding is high for KSCN and KI, but is considerably less for KCl, KBr and KNO_3. The strength of restabilization is exactly opposite; restabilization is seen for KCl, KBr and KNO_3, but nor for KSCN and KI. The only salt which shows poor (actually no) restabilization and poor ion binding is KF. The trend is similar for sodium salts; binding is poor for both NaCl and $NaNO_3$, but restabilization is seen for both of these.

If comparisons were limited to monovalent chloride salts, one might be led to erroneously believe that there is a correlation between ion binding and restabilization. The information in Table 6.1 indicates that the order of increasing binding ability and increasing

restabilization strength is $Li^+<Na^+<K^+$. Fewer studies have been performed for divalent salts, but the order of ion binding in organic solvents is $Mg^{2+}<Ca^{2+}<Ba^{2+}$, while the solvent extraction tests performed for this research reveals roughly equal (but extremely poor) ion binding by all three of the divalent chlorides. The experimental results indicate that Ba^{2+} has quite strong restabilization. Whether Ca^{2+} or Mg^{2+} has greater restabilizing ability is not clear. Mg^{2+} does show restabilization, while Ca^{2+} does not show a decrease followed by an increase in stability as the salt concentration is varied. However Ca^{2+} does show unexpected, immeasurably high stability given the solvent quality at the higher salt concentrations.

One might argue that ion binding is still a viable option, since the studies discussed above cannot distinguish between different polymer conformations or between intra- or inter- molecular binding. Changes in either conformation or type of binding could result in changes in colloidal stability. With respect to the former, the Raman spectroscopy results presented in Chapter 4 indicate that the configuration of the polymer is largely the same, regardless of the type of salt. Some smaller changes occur on changing the valence (from K^+ to Ba^{2+}), but these changes cannot account for restabilization which occurs for both when the anion is chloride.

Role of the Polymer Type The possibility for intermolecular binding is still not clear from the preceding discussion. The force distance profiling suggests than an increase in the salt concentration causes an increase in the separation distance at the onset of repulsion. However, as discussed in the section on additional adsorption, large amounts of adsorption and large increases in the adlayer thickness as measured by PCS are *not* seen. It seems somewhat plausible to reconcile these two facts if small amounts of tethered polymer are responsible for the increase in the adlayer thickness. In other words, this may be a special case where the polymers are apparent using SFA but not PCS.

To understand more fully what is occurring, a test was performed in which L35 Pluronics® was adsorbed to the latex particles with a free polymer concentration of 300 mg/L. The concentrations chosen were such that the free Pluronics® concentration was 0.6 mg/L during the aggregation experiment. As can be seen from Figure 6.6, there is no restabilization in this case (patterned squares). In contrast, restabilization is seen when 60 mg/L free Pluronics® is present (white triangles). Presumably, if it is intermolecular binding between PEO units, then addition of free PEO to the dispersion should help recover the restabilization behavior. Dissolved PEO was added to a sample of the L35 stabilized latex, then stirred for 30 seconds. The desired amount of salt was then added and stirred for an additional 30 seconds. The final concentration of free L35 was 0.6 mg/L and the final concentration of the PEO (MW = 8000) was 60 mg/L. As can be seen from Figure 6.6, the addition of PEO does not cause restabilization (black circles). In contrast, this experiment was repeated using dissolved L35 instead of PEO. As shown in Figure 6.6, the restabilization behavior seen with 60 mg/L was fully recovered, although the 60 mg/L free Pluronics® was added just prior to the addition of salt (black triangles). These results suggest that the presence of the triblock copolymer is required for restabilization. In other words, intermolecular binding between PEO blocks is not the likely cause of restabilization.

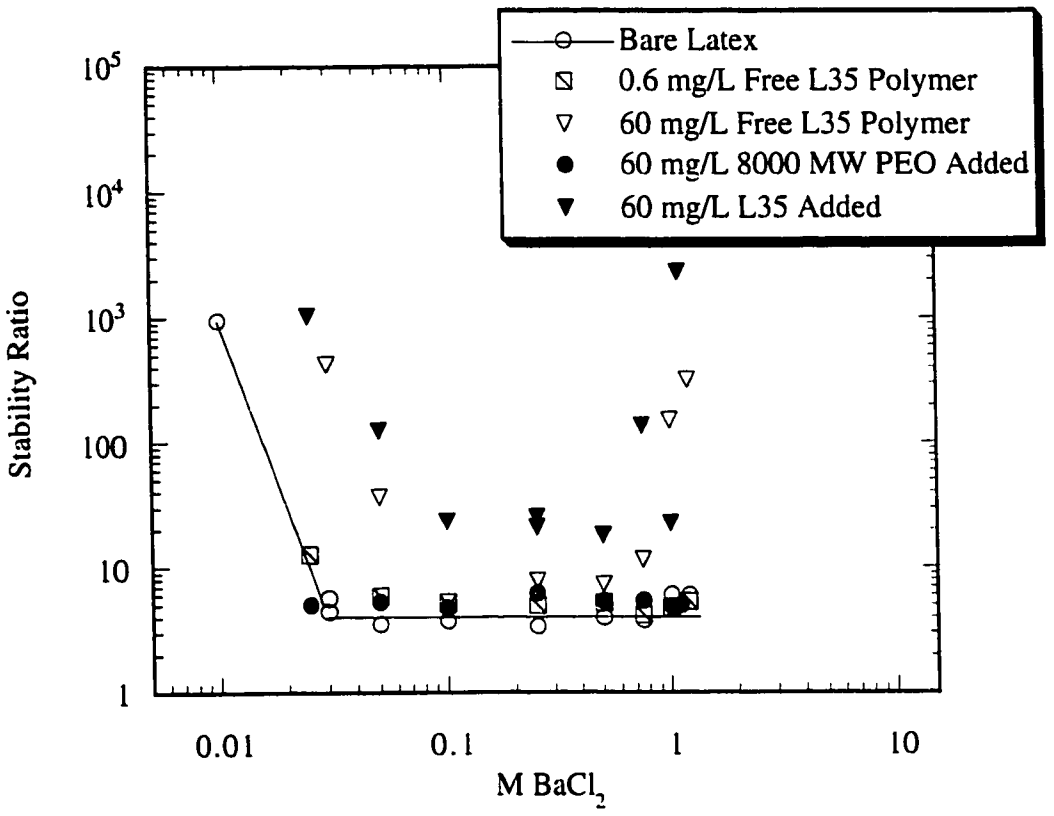

Figure 6.6. Effect of the Free Polymer Type on the Stability Ratio of L35 Coated Latex as a Function of $BaCl_2$ Concentration.

Polymer Micelles/Agglomerates

As will be discussed below, typical spherical micelles in addition to relatively large aggregates comprised of the block copolymer can form upon the addition of salt. The aggregates are much larger than the typical small spherical micelle. Any polymer aggregates (micelles included) are called agglomerates in this text to avoid confusion with aggregates of the latex spheres.

It seems plausible that agglomerates could be responsible for restabilization. The results discussed in the prior section can be used as an argument in favor of this mechanism

since the presence of the triblock would be required. To explore the possibility of this stabilization mechanism, a literature review of Pluronics® micellization was performed. A summary of the findings is presented in the first section. Next are the results for some simple experiments on the current system. These results and those presented previously are then compared to the findings in the literature.

Current State of Knowledge for Pluronics® Micelles and Agglomerates There is a large amount of literature discussing the behavior of PEO-PPO-PEO triblock copolymers; by 1991, there were "over 1000 articles on many applications in the medical and pharmaceutical industries alone."[190] Review articles[190-192] by experts in the area provide a good overview of micellization in pure water, and the most pertinent aspects are briefly summarized below.

In contrast Alexandridis and Holzwarth[189] state that, "there is very little information published on the effects of additives on (PEO-PPO-PEO triblock copolymers)." Currently, there are only a half dozen papers which discuss the topic. Of these, only a few[189, 193-195] discuss the effects of inorganic salts on the copolymers, and all of them employed relatively high polymer concentrations (1% or 10,000 mg/L). As far as is known, there is no literature which documents the formation of agglomerates at a concentration of 0.006% or 60 mg/L, which is the highest free polymer concentration in the latex aggregation experiments. The key results discussing the addition of inorganic salts are summarized below.

For many years, it was debatable whether PEO-PPO-PEO triblock copolymers or polaxamers (tradenamed Pluronics®) formed micelles as other surfactants do. The difficulty was that early work using light scattering revealed no micelles, while dye solubilization and surface tension techniques did. An important paper by Zhou and Chu[196] documented that micelles do form for Pluronics® F68 and can be detected by

dynamic and static light scattering. The unimers and micelles were quite small (2.3 and 8 nm, respectively) and required developing an autocorrelation function for a few hours using a 200-400 mW 488 nm laser for dynamic light scattering. These conditions allowed the detection of the micelles, which other researchers missed.

The polaxamer micelles show unusual behavior. Unlike the case for block copolymers of PEO and alkanes, the CMC is highly temperature dependent and decreases with increasing temperature. A change of 10°C can result in a change of the CMC by a factor of 10-100. In contrast, block copolymers of PEO and alkanes show a 35-45% change in CMC for a 25°C temperature change. This strong temperature dependence is attributed to hydrophobic interactions between the PPO blocks, which are believed to cause micellization. These hydrophobic interactions result in a large endothermic enthalpy, which is compensated by an even larger, positive entropy change. The temperature dependence arises from the fact that PPO only dissolves in cold (<10-15°C), but not warm or hot water. Support for the existence of this mechanism is gained by the fact that the PPO blocks are key in controlling micellization. The CMC decreases exponentially and the CMT decreases linearly with increasing PPO length. Ten to thirteen polypropylene oxide units per surfactant molecule are sufficient to induce micellization. In contrast, the length of the PEO block only weakly affects the CMC or CMT.

Another unusual aspect about Pluronics® is that the CMC or CMT is often not sharp. As a result, the values vary according to the technique as well as the data interpretation. As an example, the CMC varies over an order of magnitude for L64 Pluronics® at 25°C, as shown in Table 6.2. Perhaps it is this wide variation which makes the vendor[180] claim that micelles are not formed, but that aggregates are formed over a broad polymer concentration range, typically above 1000 ppm. This value far exceeds the typical CMC for nonionic surfactants, which is often below 100 ppm. Plausible explanations for the poorly delineated CMC include: the formation of monomolecular

micelles at concentrations lower than multimolecular micelles, rearrangement of the adsorbed polymer at the air water interface in surface tension measurements, and broad molecular weight distributions of the Pluronics®.

Table 6.2. CMC of Pluronics® L64 at 25°C. Information is taken from the review by Chu and Zhou[190].

CMC (mg/L)	Technique	Reference
70,000	dye solubilization	Alexandridus et al[197]
44,000	light scattering	Pandya et al[198]
110,000	surface tension	Wanka et al[199]
11,000	surface tension	Reddy et al[200]

In surface tension measurements, the CMC may also be difficult to delineate due to a minimum in the plot of the surface tension versus Pluronics® concentration at a location very close to this critical point. In this case, the most plausible explanation is the existence of a contaminant, which is especially notable for Pluronics® L64. It is most likely that more hydrophobic diblock copolymers of PEO-PPO exist in the Pluronics® due to the manner in which the triblock is manufactured. Detection of the contaminant has been difficult since its behavior mirrors the changes in the CMC. Specifically, the anomalous behavior becomes more noticeable at lower concentrations when the temperature is higher. In light scattering, large agglomerates composed of the hydrophobic portion cause intense scattering in the transition region between unimers and micelles. For Pluronics L64® this scattering can be removed by washing in hexane, which removes the hydrophobic contaminant[201]. The anomalous behavior can then be recovered by introduction of a more hydrophobic Pluronics®. Fluorescence probing suggests that the diblock comprises 2% of the material, while HPLC suggests that 3% is diblock, through the existence of a bimodal peak. A CONTIN analysis used in light scattering suggests that the large particles created

by the contaminant constitute only a few thousandths to a few percent of the total weight, so that the unimers and/or typical micelles are overwhelming in number.

Both the CMT and cloud point (CP) can be changed by the addition of inorganic salts. This effect is largely attributed to changes in the structure of water, which is often described as a function of the bare ion radius. A differential scanning calorimetry (DSC) study[189] indicated that increasing the anion size of sodium salts significantly increased both the CP and CMT of Pluronics® L64 in aqueous solutions. The dependence on the cation size was less clear since the dependence was very small and the order of increasing CP and CMT for chloride salts was $Na^+<K^+<Li^+$. Li^+ is the smallest, while K^+ is the largest.

Theories such as McDevitt Long are often used to explain the dependence of the ion size in changing the CP or CMT[179]. In McDevitt Long theory, the greater the electrostriction or decrease in total volume upon mixing the salt and water, the lower the CP or CMT. Small ions cause the greatest electrostriction so are anticipated to lower the CP or CMT the most. The small ions essentially squeeze out the polymer from solution. In an alternative viewpoint proposed by Florin[70], salt deficient zones around the polymer are created when the poorly polarizable polymer repulses the ions. The repulsion is strongest for small ions. As the temperature is raised, the repulsive forces between the PEO chains are reduced and the water surrounding the polymer is released. Incorporation of the water into the bulk results in a negative free energy, which eventually results in salting out. Highly polarizable, large ions are not repulsed by the polymer, and can even positively adsorb.

The anomalous behavior seen with the cations was attributed to the fact that Li^+ is so strongly hydrated that the hydrated and not the bare ion radius is important[189]. Alternative viewpoints may be equally valid since the effects of salts on aqueous polymer solutions are not fully understood. Studies of micellization of other surfactants and cloud

points of PEO suggest that the dependence on the cation size is, in general, more difficult to understand. In the case of salting out PEO, the anions proceed in the order of the well known Hofmeister series, while the cations run counter[6]. One study of micellization suggests that the dependence of the CMC is actually on the charge-to-radius ratio[202]. The charge to radius ratio can be used to determine the solvation free energy, which is an indicator of the salt's ability to make or break the structure of water. In this case the CMC varied inversely as the charge to radius ratio for anions and directly on the ratio for cations.

Typically, the CMT is believed to be controlled by the increasing insolubility of the PPO block, while the cloud point is controlled by the insolubility of the PEO blocks. Despite these differences in proposed mechanisms, the DSC measurements discussed above indicate that the temperature of the CP or CMT is raised or lowered by the same amount relative to the pure water case for a given salt solution, thus resulting in parallel behavior. Stated differently, the difference between the CMT with and without salt was equal to the difference between the CP with and without salt for Pluronics® L64 in aqueous solutions of lithium, sodium, and potassium chlorides and sodium chloride and bromide. Similarly, other studies[194] show that a universal curve is obtained when the intrinsic viscosity (an indicator of the size and shape of the agglomerates) is plotted as a function of the difference between the cloud point and the actual temperature for the case of no salt, KCl and KF. In the DSC study, the parallel relationship of the CMT and CP was found to be inapplicable in the case of NaI, which was found to decrease the CMT of Pluronics® but increase the cloud point. This anomaly was attributed to specific interactions between I^- and PEO headgroups. Another exception to this rule was found for KF by Bahadur and coworkers[193]. In this study, a comparison of cloud point and light scattering measurements indicate that for Pluronics® F68 the CMT is lowered much less (19°C) than the cloud point (50°C) in 1 M KF. Interestingly, if the trends of the data sets

from Alexandridis and Bahadur are combined (and the effect of the polymer molecular weight ignored), the results suggest that increasing the anion size increases the CMT or CP as discussed above, but the dependence is less strong in the case of the CMT. Small differences between the results[189] for Br^- and Cl^- ions support this conclusion. These differences suggest that more studies on the behavior of Pluronics® in salt solutions are required before a full understanding is gained. In the interim, the parallel behavior proposed by Alexandridis will be used.

The hydrodynamic diameter and the aggregation number of the polymer in salt solution was shown to monotonically increase as a function of temperature, for the case of Pluronics® F68, L64 and P85 in aqueous KF[193, 194]. Close to the cloud point for the polymer, the agglomerates become quite large (30-140 nm). These results contrast with the results for Pluronics® in pure water. The hydrodynamic size is essentially a step function for F68 in water with the step occurring at the CMT[203]. Thus the size remains constant although the aggregation number continuously increases with temperature. The typical micelles in water are quite small (8 nm). Large agglomerates have been seen in distilled water. As mentioned earlier, Pluronics® L64 in water often forms large agglomerates in the transition region where unimers change to micelles due to the presence of a hydrophobic contaminant.

Formation of Polymer Agglomerates

To gain a better understanding of the Pluronics® behavior at the conditions during restabilization, tests were performed to determine if agglomerates of the dissolved Pluronics® could scatter significant amounts of light during the latex aggregation experiments. The tests consisted of mixing the desired amount of salt and polymer and measuring the light scattering in the same manner used for the latex aggregation experiments. In all tests, the final polymer concentration was 60 mg/L, while the salt

concentrations were varied. All the salt/polymer combinations tested during the latex aggregation experiments were tested in this manner.

For $BaCl_2$, KCl, KNO_3, NaCl, $NaNO_3$, and LiCl, a mixture of L35 Pluronics® with the salt at the highest concentration used in the latex aggregation experiments resulted in very little light scattering and no discernible correlation function. In contrast, polymer agglomerates which increased in size were observed in 60 mg/L L35 Pluronics® with 8 M KSCN. This behavior is characteristic at the cloud point, as discussed in Chapter 5. Very little light scattering and no discernible correlation function were observed in 5 M KSCN.

Two types of polymer agglomerates were observed to form in certain L64 mixtures. The first type of polymer agglomerate increased in size over time and, as mentioned, is indicative of the system reaching the cloud point. In the case of KSCN, $NaNO_3$, KF, and Na_2SO_4, these growing agglomerates resulted in stability ratios less than 2, as discussed earlier. Interestingly, growing polymer agglomerates were also observed in the case of KI between 1 and 4 M. At these concentrations, the stability ratio was somewhat difficult to determine during the latex aggregation tests, although the stability ratio did not drop below 2. These concentrations do not correspond to the PEO cloud point, as indicated in Figure 6.4.

The second type of polymer agglomerate formed at most within a few minutes, and remained constant in size over the 5-50 minutes of testing. These large stable agglomerates are anticipated to be either the large micelles which form close to the cloud point of the polymer or contaminant agglomerates which form in the transition region between unimers and micelles. A typical example plot of the hydrodynamic size of the agglomerate as a function of time is given in Figure 6.7, which is for 4 M NaCl. A summary of the type and character of the polymer agglomerates is given in Table 6.3. The term KHz in the fourth column of the table refers to the scattered light intensity and is equivalent to the number of

photons per second that are detected. The pinhole of 800 μm refers to the final pinhole size before the photomultiplier tube.

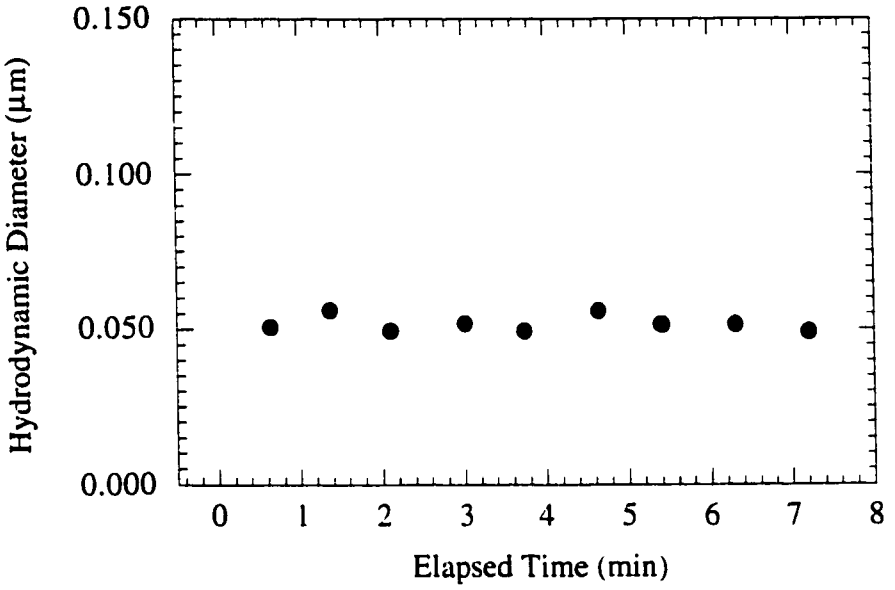

Figure 6.7. Plot of Hydrodynamic Size versus Time for 60 mg/L L64 Pluronics® in 4 M NaCl

Table 6.3. Formation of Agglomerates from 60 mg/L L64 Polymer in Concentrated Salt Solutions.

A. Chloride Salts

Salt	Conc (M)	Mean Diameter of Agglomerate (nm)	Photon Count Pinhole 800 μm (KHz)	Molarity at Onset of Restabilization with 60 mg/L Free Polymer	Molarity when θ=25°C for PEO
LiCl	9.6	agglomerates not detected	2	6.0	»4
NaCl	2.0	agglomerates not detected	1	2.5	4.5
	2.5	0.057	8		
	4.0	0.052	14		
KCl	1.0	agglomerates not detected	<1	1.8	4
	1.8	0.099	17		
	2.8	0.094	55		
$MgCl_2$	3.6	agglomerates not detected	2	1	»2.6
$CaCl_2$	4.0	agglomerates not detected	1	completely stable	»4
$BaCl_2$	1.2	agglomerates not detected	2	0.25	>2
$AlCl_3$	0.1	agglomerates not detected	2	0.01	unknown
	0.5	0.123	5		
	2.0	0.078	12		

B. Potassium Salts

Salt	Conc (M)	Mean Diameter of Agglomerate (nm)	Photon Count Pinhole 800 μm (KHz)	Molarity at Onset of Restabilization with 60 mg/L Free Polymer	Molarity when θ=25°C for PEO
KF	0.5	agglomerates not detected	<2	no restabilization	1.3
	1	0.179	8		
	2	n/a - increasing	n/a		
	5	n/a - increasing	n/a		
	10	n/a - increasing	n/a		
KCl	1.0	agglomerates not detected	<1	1.8	4
	1.8	0.099	17		
	2.8	0.094	55		
KNO_3	2.4	agglomerates not detected	1	1.5	3
KBr	2.0	agglomerates not detected	1	not tested - onset at 0.5 M in 0.01 mg/L free polymer	»4
	3.2	0.133	25		
KI	1	agglomerates not detected	1	no restabilization	»3
	2	n/a - increasing	n/a		
	3	n/a - increasing	n/a		
	4	n/a - increasing	n/a		
KSCN	4	agglomerates not detected	2	no restabilization	»2
	5	n/a - increasing	n/a		
	8	n/a - increasing	n/a		

C. Sodium Salts

Salt	Conc (M)	Mean Diameter of Agglomerate (nm)	Photon Count Pinhole 800 μm (KHz)	Molarity at Onset of Restabilization with 60 mg/L Free Polymer	Molarity when θ=25°C for PEO
NaCl	2.0	agglomerates not detected	1	2.5	4.5
	2.5	0.057	8		
	4.0	0.052	14		
$NaNO_3$	2.0	agglomerates not detected	2	3.0	≈4
	3.0	0.068	6		
	4.0	0.052	10		
Na_2SO_4	0.5	agglomerates not detected	2-4	no restabilization	0.45
	1.0	n/a - increasing	n/a		
	1.6	n/a - increasing	n/a		
$Na_4P_2O_7$	0.16	agglomerates not detected	1	no restabilization	unknown

The salts NaCl, KCl, $AlCl_3$, KF, KBr, and $NaNO_3$ all induce the formation of polymer agglomerates which stay constant in size over the time of testing, while the remaining salts do not. The scattering by the agglomerates is not negligible compared to the light scattering by the polymer coated latex; the scattering intensity of the 0.11 μm latex singlets at the experimental conditions was approximately 55 KHz. A simple calculation was used to determine the impact of the agglomerates on the size measured during the latex aggregation experiments when restabilization occurs. It is known[204] that the measured decay constant is intensity weighted as shown in equation 6.1.

$$\Gamma = \frac{\sum f_i M_i^2 P_i(\theta)\Gamma_i}{\sum f_i M_i^2 P_i(\theta)} = \frac{\sum f_i I_i \Gamma_i}{\sum f_i I_i} \qquad \text{Eq 6.1}$$

where: f_i = number fraction of particles with molecular weight Mi

$P_i(\theta)$ = structure factor for particle i at scattering angle θ

Γ_i = decay constant for particle i

I_i = intensity of scattered light from particle i

Since $\Gamma \propto diffusivity \propto \frac{1}{d}$, we can then obtain:

$$\frac{1}{d} = \frac{\sum f_i I_i \frac{1}{d_i}}{\sum f_i I_i} = \frac{\sum I_i / d_i}{\sum I_i} \qquad \text{Eq. 6.2}$$

where the intensity of all particles with molecular weight M_i is designated as $I_i=f_iI_i$, so that no particular knowledge of the molecular weight distribution of particles is required. Since the system is presumably bimodal the equation reduces to:

$$\frac{1}{d} = \frac{I_l / d_l + I_p / d_p}{I_l + I_p} \qquad \text{Eq. 6.3}$$

where the subscript l and p designate the latex and polymer, respectively. To test the simplest case, calculations were performed where almost complete restabilization had occurred in the presence of polymer agglomerates. Approximate values of 55 KHz for the intensity and 110 nm for the diameter were used for the polymer coated latex. The values of intensity and diameter used for the polymer are given in Table 6.4 below, as well as the

size predicted from PCS. In the last column of the table are maximum measured sizes from the aggregation experiments. These values are reasonably representative of the entire population since very little change in diameter over time was observed. As can be seen, the measured and predicted values are extremely close. The presence of polymer agglomerates decreases the apparent size of the latex particles between 3.6 to 16%. The small change seen in 2.8 M KCl is fortuitous, since the size of the agglomerates is close to the size of the latex. A smaller diameter would have had a larger impact. The more important implication is that a size of 110 nm for the polymer coated latex is consistent with the results, suggesting that there is no large increase in the diameter of the latex due to the presence of a significantly thicker adlayer or attached agglomerates.

Table 6.4. Predicted and Measured Values of the Apparent Hydrodynamic Diameter Obtained from PCS for Latex and Polymer Agglomerate Systems.

Salt	M	Polymer Intensity (KHz)	Polymer Agglomerate Size (nm)	Calculated Size (nm)	Measured Size (nm)
KCl	2.80	55	94	101	106
NaCl	4.00	14	52	90	91
$NaNO_3$	4.00	10	52	94	92

Comparison of the Results to the Literature

As mentioned previously, the existence of small typical micelles or large stable agglomerates may be responsible for restabilization. The Pluronics® exhibiting restabilization (L35 and L64) are capable of micellization since there are over 10-13 PPO units. Unfortunately, the literature does not have data for the low Pluronics® concentrations used (60 mg/L). With the cloud point data from Pandya [205] or the CMT data from Alexandridis[189] and their respective coworkers, one can estimate the salt concentration where the micelles should first form for 60 mg/L Pluronics® L64 at 25°C using the two rules of thumb presented earlier:

- A 10°C change in the CMC is equal to a change in a concentration decade of the Pluronics®
- The difference between the CMT with and without salt is equal to the difference between the CP with and without salt

It was found that virtually all the salts tested could be classified into four categories, using these estimates and the data presented in the preceding section.

In the first category, restabilization and large but stable polymer agglomerates were *not* experimentally observed. The two salts which fell into this category include KSCN and KI. Micellization is not predicted to occur for KI, using the data from Pandya and coworkers[205] and the two rules of thumb presented above. Micellization in KSCN solutions has been shown[194] to be similar to that in water.

In the second category, no restabilization occurred, although micellization was predicted (Table 6.5) using just the cloud point data from Pandya and coworkers[205]. Salts in this category include KF and Na_2SO_4. Large stable polymer agglomerates were observed for KF. This category at first seems to preclude the possibility of agglomerates as the cause; however, closer examination reveals that this is not the case. For both salts, the molarity at which micellization is predicted and/or large agglomerates seen coincides closely with the molarity at which the PEO solvency becomes poor (Data taken from Figures 6.4 and 6.5). As discussed in Chapter 5, restabilization is only seen when the PEO solvency is good. Therefore, these results are still consistent with restabilization by micelles.

Table 6.5. Molarity at the Formation of Polymer Agglomerates, Predicted Micellization, and Poor PEO Solvency for KF and Na_2SO_4.

Salt	Agglomerate Formation	Predicted Micellization	Poor PEO Solvency
KF	1 M	1.2 M	1.2 M
Na_2SO_4	no agglomerates	0.5 M	0.5 M

In the third category, restabilization coincides with the appearance of large, stable polymer agglomerates and predicted micellization (Table 6.6). Values for predicted micellization were available from the work of both Pandya and Alexandridis. The agglomerates could be comprised of the hydrophobic contaminant that scatter light in the transition region between unimers and micelles or the large agglomerates seen above the CMC but close to the cloud point in the presence of salts. Infomation from the three categories just discussed give positive evidence that micellization is responsible.

Table 6.6. Molarity at the Formation of Polymer Agglomerates, Predicted Micellization, and Poor PEO Solvency for NaCl, KCl, and $NaNO_3$.

			Predicted Micellization		
Salt	Restabilization	Agglomerate Formation	Pandya	Alexandridis	Poor Solvency
NaCl	2.5	2.5	2.5	1.8	4.5
KCl	1.8	1.8	2.2	2.2	3.8
$NaNO_3$	3.0	3.0	>2	not available	4.0

In the fourth category, restabilization was seen but no large stable polymer agglomerates formed at the molarity of the onset. These salts include: LiCl, KNO_3, KBr, $MgCl_2$, $BaCl_2$, $AlCl_3$. In general, very little is known about the micellization/cloud point data for these salts. In particular, micellization is predicted occur around 2 M for $MgCl_2$, using cloud point data and the estimation scheme outlined above. This contrasts somewhat with the 1 M concentration at which restabilization occurs; however the prediction scheme developed by Alexandridis was for monovalent salts only. Very small micelles have been observed in 1 M KBr at 30°C[194]. The fact that there were no large stable agglomerates detected in $MgCl_2$, KBr or these other salts does not preclude the possibility that restabilization is caused by micelles. It may simply mean that the micelles were too small to detect. In this study, only large particles can be detected since the correlation function was developed over 30-60 seconds using a 25 mW laser 633 nm. This can be compared to the

conditions used by Zhou and Chu to detect the micelles (≈8 nm); a development time of a few hours using a 200-400 mW 488 nm laser. Therefore, the fourth category indicates a lack of information as opposed to evidence against restabilization.

The only two salts which have not been classified according to this scheme are $CaCl_2$ and $Na_4P_2O_7$. Very little information on the effect of $Na_4P_2O_7$ on PEO is given in the literature. As discussed earlier, $CaCl_2$ gives unusually high stability but no restabilization is seen, so it is difficult to firmly interpret the results. In addition very little information on its ability to micellize or decrease the solvency of L64 is given in the literature. Due to the lack of information, no attempt was made to classify these salts.

Additional arguments in favor of restabilization by micelles/stable agglomerates can be made using the data presented in Chapter 5 and earlier in this chapter. As just discussed, the dependence on the type of salt can be explained by classification into four categories. Other details on the salt dependence can also be elucidated. As discussed in Chapter 5, restabilization appears to be more dependent on the anion than the cation. This dependence is quite logical if restabilization is caused by micellization, since micellization is determined largely by the anion[189]. Micellization can also explain the variation in the onset for the monovalent chlorides. The molarity at the onset is higher for LiCl because its ability to salt out and decrease the predicted CMT of Pluronics® L64 is poor compared to the ability of NaCl (Table 6.7). Similar arguments hold in the comparison of KCl and LiCl and the comparison of NaCl and $NaNO_3$. The distinction between KCl and NaCl is much smaller, so the order between these two varies, according to the investigation. It is difficult to understand the relationship with the divalent salts since very little data on the CP and CMT behavior is available.

It is interesting to note that, in general, the molarity at the onset decreases (i.e. the strength of restabilization increases) with increasing cation radius (Table 6.7). The one exception is $CaCl_2$, which exhibits odd behavior as discussed in Chapter 5. If

restabilization is caused by micellization, then this suggests that the ability to decrease the CMT is directly proportional to the cation radius size for a given valence, which is similar to the findings of Zhang, Somusundaran, and Maltesh[202] for alkane-sugar block copolymers.

Table 6.7. Order of Salting Out Pluronics® L64, Micellization of L64, Ion Radius Compared to the Onset of Restabilization

A. Chloride Salts

Series	Order of Salts
Molarity at the Onset of Restabilization	$Ca^{2+}=Li^{+}=Mg^{2+}>Na^{+}>K^{+}>Ba^{2+}$ (0.6 mg/L free polymer) $Ca^{2+}>Li^{+}>Na^{+}>K^{+}>Mg^{2+}>Ba^{2+}$ (60 mg/L free polymer)
Salting Out L64[195]	$Mg^{2+} < Na^{+} < K^{+}$
Decreasing the CMC of L64[189]	$Li^{+} < K^{+} \leq Na^{+}$
Ion Radius	$Li^{+}<Na^{+}<K^{+}$ $Mg^{2+}<Ca^{2+}<Ba^{2+}$

B. Potassium Salts

Series	Order of Salts
Molarity at the Onset of Restabilization	$F^{-}=SCN^{-}=I^{-}>Cl^{-}>NO_3^{-}>Br^{-}$
Salting Out L64[195]	$SCN^{-}<I^{-}<Br^{-}<Cl^{-}<F^{-}$
Decreasing the CMC of L64[189]	No data
Ion Radius	$F^{-}<Cl^{-}<NO_3^{-}<Br^{-}<I^{-}<SCN^{-}$

C. Sodium Salts

Series	Order of Salts
Molarity at the Onset of Restabilization	$NO_3^{-}>Cl^{-}$ (SO_4^{2-} not tested) (0.6 mg/L free polymer) $SO_4^{2-}>NO_3^{-}>Cl^{-}$ (60 mg/L free polymer)
Salting Out L64[195]	$SCN^{-}<NO_3^{-}<Cl^{-}<SO_4^{2-}$
Decreasing the CMC of L64[189]	$SCN^{-}<I^{-}<Br^{-}<Cl^{-}$
Ion Radius	$Cl^{-}<NO_3^{-}<SO_4^{2-}$

Returning to the arguments in favor of restabilization by micellization. It is quite logical that restabilization is seen in the presence of the triblock but no the pure PEO polymer; the presence of the triblock copolymer is required for micelles/stable agglomerates

to form. Furthermore, restabilization is strongly affected by the concentration of free Pluronics®, which in turn affects the concentration of micelles. Changing from the low (L35) to the middle (L64) molecular weight strongly affects the size of the PPO block, which is key in controlling micellization. Hence, the large dependence of restabilization on Pluronics® molecular weight , and specifically PPO molecular weight.

Further evidence to support restabilization caused by micelles is found in the micelle size. The micelles, even in salt solutions, are often 5-30 nm in diameter, which is the same magnitude by which the repulsion in the SFA experiments is increased [190](Table 7 p. 90). One possibility is that the micelles which are caught in between two polystyrene particles cause interference with aggregation. This scenario seems plausible. The estimated concentration of micelles is 2.5×10^{17} micelles/mL, using an aggregation number of 50, a molecular weight of 2900 and concentration of 60 mg/L for L64. Considering that there are 2×10^{9} particles/mL of the polystyrene latex gives roughly 100,000 micelles per latex particle. Essentially the polystyrene latex would be surrounded by the micelles. These micelles would not be detected by the light scattering measurements used to measure the aggregation rate due to their small size, but may be detected in the interaction energy profile.

An argument against micellization as the cause is that restabilization occurs at roughly 0.01 mg/L free Pluronics®. One might wonder if this is enough to cause micellization. Counter arguments include the fact that the estimates where micellization should occur were very conservative (the CMC can be lowered by a factor of 100 for a 10°C change) and that there is no CMT data for the salts (KBr and $BaCl_2$) which showed restabilization at this low polymer concentration. Finally, calculations reveal that even with this low concentration the maximum concentration of micelles would be 4×10^{10} micelles/mL with an aggregation number of 50. This gives essentially 20 micelles per latex particle, which may be enough to slow but not stop aggregation, as is seen.

Consideration of Other Mechanisms

In the course of trying to understand the mechanism governing restabilization, the pertinence of other parameters was evaluated. These parameters were found not to be important. The information and analysis are presented below.

Hofmeister Series The Hofmeister series is believed to reflect the ion's size, polarizability, and ability to structure water. The Hofmeister series is thus important to electrostatic and often steric stabilization. It should be noted that the order of salts in the Hofmeister series is not hard and fast, but takes on *minor* variations depending on the manner in which it is determined. The Hofmeister series for cations and anions is presented in Table 6.8. The Hofmeister series for the cations (chloride series) is in the order of decreasing ability to salt out proteins. The Hofmeister series for the anions is published more often. A few proposed series are given in the tables for the potassium salts. In the case of the sodium salts, the only series including the correct anions is the order of salting out egg albumin.

A comparison with the order of the onset indicates that restabilization cannot be governed by the Hofmeister series alone. For the chloride salts, $BaCl_2$ and LiCl appear in the center of the series, but $BaCl_2$ is extremely strong in its ability to restabilize, while LiCl is extremely poor. For the potassium salts and sodium salts, the strongest restabilizing salts occur in the center of the Hofmeister series.

It should be noted that the Hofmeister series, as defined here, is not the same as the order of salting out PEO. The order of the anions is the same but the order of the cations is opposite[29].

Table 6.8. Order of the Hofmeister Series and the Strength of Restabilization

A. Chloride Salts

Series	Order of Salts
Molarity at the Onset of Restabilization	$Ca^{2+}=Li^{+}=Mg^{2+}>Na^{+}>K^{+}>Ba^{2+}$ (0.6 mg/L free polymer) $Ca^{2+}>Li^{+}>Na^{+}>K^{+}>Mg^{2+}>Ba^{2+}$ (60 mg/L free polymer)
Hofmeister Series[18]	$Mg^{2+}>Ca^{2+}>Sr^{+}>Ba^{2+}>Li^{+}>Na^{+}>K^{+}$ $>NH_4^{+}>Rb^{+}>Cs^{+}$

B. Potassium Salts

Series	Order of Salts
Molarity at the Onset of Restabilization	$F^{-}=SCN^{-}=I^{-}>Cl^{-}>NO_3^{-}>Br^{-}$
Hofmeister Series	Order of salting out egg albumin[18]: $citrate^{3-}>SO_4^{2-}>Cl^{-}>NO_3^{-}>I^{-}>SCN^{-}$ Order of elution from a dextran size exclusion gel (Sephadex G-10®)[72]: $SO_4^{2-}\approx HPO_4^{2-}>F^{-}>Cl^{-}>Br^{-}>I^{-}\approx ClO_4^{-}>SCN^{-}$ Order of adsorbability from water[19]: $ClO_4^{-}<NO_3^{-}<F^{-}<Cl^{-}<Br^{-}<I^{-}<SCN^{-}$

C. Sodium Salts

Series	Order of Salts
Molarity at the Onset of Restabilization	$NO_3^{-}>Cl^{-}$ (SO_4^{2-} not tested) (0.6 mg/L free polymer) $SO_4^{2-}>NO_3^{-}>Cl^{-}$ (60 mg/L free polymer)
Hofmeister Series[18]	$citrate^{3-}>SO_4^{2-}>Cl^{-}>NO_3^{-}>I^{-}>SCN^{-}$

Ion Activity Coefficients It is known that ion activity coefficients can show minima and maxima at high salt concentrations, indicating large deviations from ideality. It seems plausible that these deviations may be largely responsible for the unexpected stability behavior. To explore this possibility, activity data were collected from the literature[206] and plotted as a function of salt concentration. The activity data were given in terms of molality, so were converted to molarity using handbook data[181]. To make a comparison, the stability curves for L64 coated latex with 60 mg/L free polymer are shown on the same

plot. As can be seen from Figure 6.8, there is no consistent correspondence for the two data sets. The activity or stability can both show a minima, but many times only one parameter does. As in Chapter 5, upward pointing arrows indicate immeasurably high stability ratios.

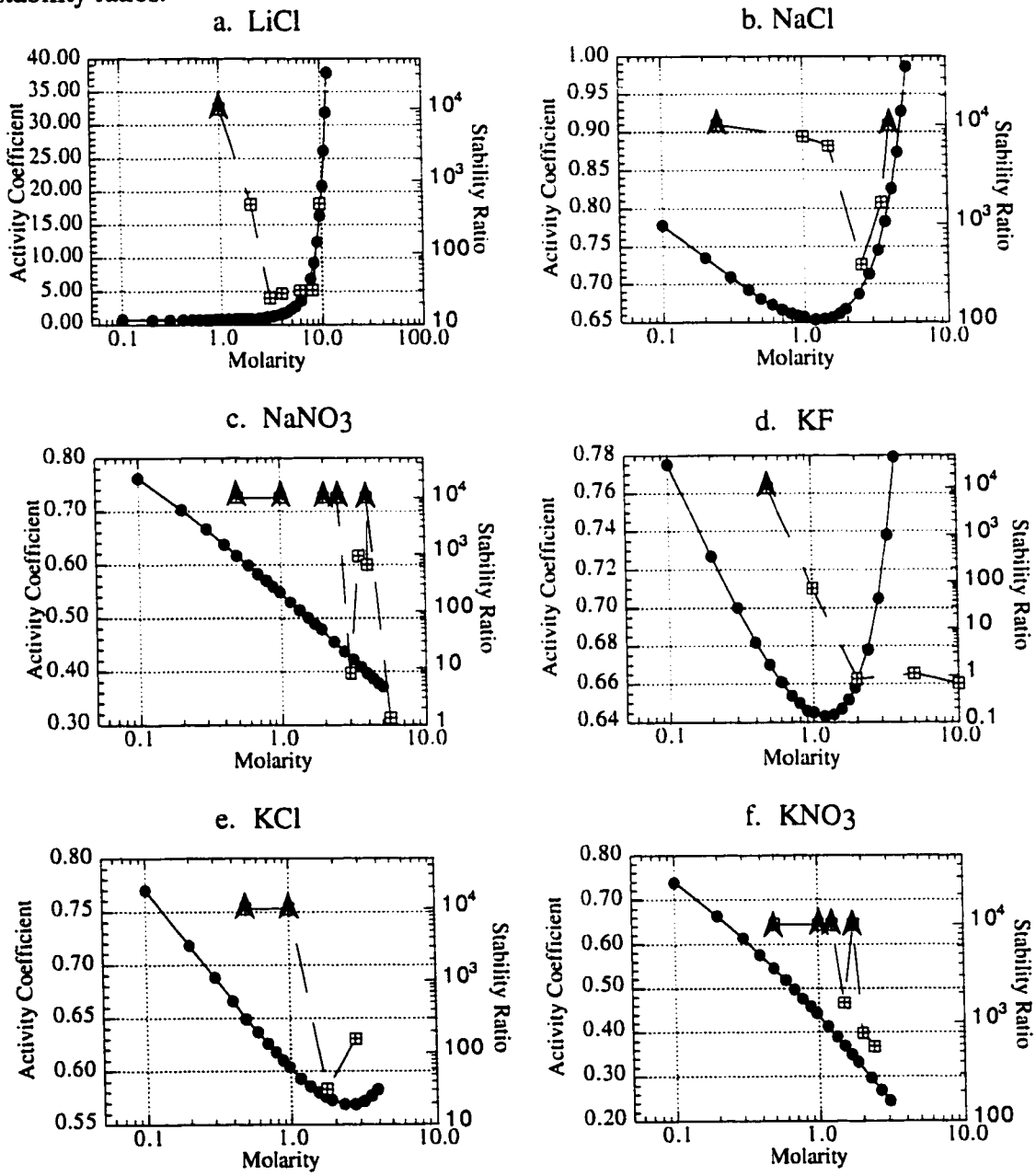

Figure 6.8. Plots of Mean Ion Activity Coefficients and Stability Ratios for L64 Latex with 60 mg/L Free Polymer as a Function of Salt Concentration. Patterned squares indicate the stability ratio, while dark circles indicate the activity coefficients.

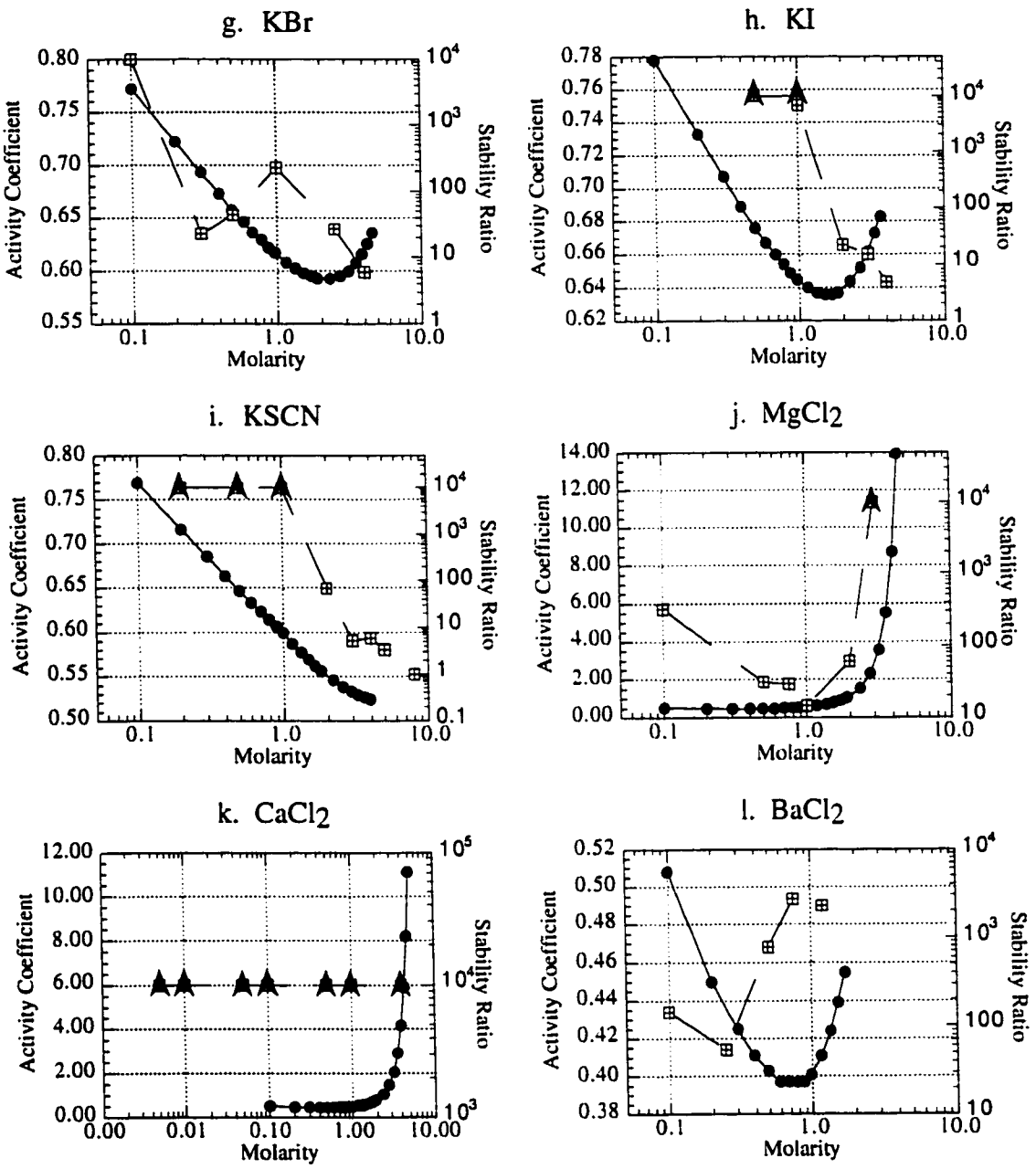

Figure 6.8. (Continued)

Relation to Bubble Coalescence One interesting effect of electrolytes is that they can prevent bubble coalescence at high concentrations[207, 208]. At first glance, this

effect may seem to have bearing on restabilization due to certain resemblances. At low salt concentrations, bubble coalescence (aggregation) occurs until a critical salt concentration is reached, at which point it stops. The effect, like restabilization, is dependent on the particular type of salt. To determine if this effect has any bearing, a closer examination was taken.

There are several details which suggest that the effect which governs bubble coalescence is not related. In particular, this effect prevents the aggregation of *hydrophobic* bubbles. In fact, Craig has hypothesized that the same effect is responsible for the hydrophobic effect itself. Since the formation of microbubbles has often been observed on the approach of two hydrophobic surfaces, Craig has hypothesized that dissolved gases accumulate close to these surfaces, releasing the high energy water. Fluctuations in the density of the "adsorbed" gas result in the long range attraction. As a result, the removal of dissolved gases or addition of the correct electrolyte may prevent the long range attractive force. Support for this claim comes from the fact that the concentration at which bubble coalescence ceases correlates extremely well with the solubility of gases in aqueous electrolytes. In the study of restabilization, hydrophobic polystyrene latex surfaces are employed; however, they are covered by a hydrophilic polymer. In fact, this hydrophilic polymer is required for restabilization; the effect was not observed for the uncoated, more hydrophobic latex.

Further support for the lack of correlation comes from the dependence on the salts. As has been shown in this study, restabilization is highly dependent on the type of anion. The effect is strong for chlorides, but also occurs for nitrates and bromides. As discussed by Paulson and Pugh[209], in the case of flotation (a process highly dependent on bubble coalescence), the "cations play a more important role than the anions." A detailed look at the individual salts further supports the conclusion drawn. In particular, both alkali and alkaline earth chlorides can cease bubble coalescence, just as in the case of restabilization.

However, Na_2SO_4 does and KI is predicted to prevent bubble coalescence, but restabilization clearly does not occur for either.

SUMMARY AND CONCLUSIONS

A systematic characterization has allowed elimination of several possible causes for restabilization. Although there is an effect of free polymer, studies of the adsorbed amount and the hydrodynamic diameter suggest that large amounts of adsorption of the free polymer do not cause restabilization. Comparisons to the order of ion binding, the Hofmeister series, the ion activity coefficients, and the ability to affect bubble coalescence suggest that these parameters also do not control the phenomena.

At this point, one plausible explanation is that restabilization is caused by the presence of unadsorbed micelles. Evidence corroborating this mechanism is as follows:

1) Large polymer agglomerates are often present at the onset of restabilization. The formation of large agglomerates near the CMC has been reported in the literature. Crude calculations using literature data suggest that the formation of micelles is possible at the conditions used during aggregation experiments.
2) Restabilization is seen in the presence of free or dissolved Pluronics® but not free PEO.
3) Restabilization is affected by the free Pluronics® concentration, which in turn affects the concentration of micelles.
4) The dependence on the polymer molecular weight can be explained. Changing from the low to the middle molecular weight Pluronics significantly changes the size of the PPO block, which is key in determining micellization.
5) An increase in distance at the onset of repulsion of approximately 13 nm is seen using F-d profiling. This distance corresponds reasonably well with the known size of micelles.

If restabilization is caused by micelles, then the dependence on the various salts can be explained. Salts which increase the critical micelle temperature do not cause restabilization; there are no micelles present. Salts which decrease the CMT extremely rapidly also do not cause restabilization; the formation of micelles and the loss of PEO solvency occur at very close molarities so that the loss of solvency prevents effective stabilization by the micelles. Therefore, it is only the salts which show an intermediate ability to decrease the CMT and the CP which are capable of restabilization.

At this point in time, it is not decisive whether micelles cause restabilization; it can only be concluded that there is not enough direct evidence to dismiss the micelles as a possibility. In spite of these tentative arguments, one may still speculate on the type of mechanism which may be present. As mentioned, the distance at the onset of repulsion increases in the force distance profile, with increasing salt concentration. The hydrodynamic diameter of the latex during restabilization is unchanged from that in distilled water. A mechanism consistent with these two observations is restabilization by micelles which are not permanently attached.

One obvious choice for mechanisms is depletion stabilization. This type of stabilization can occur for relatively large colloidal particles in the presence of smaller dissolved macromolecules, micelles, or undissolved spheres. When the two large colloidal particles approach, then the smaller particles are caught in between. At a separation distance roughly equal to the smaller particle size, an increase in the free energy occurs since the only way that the large particles can approach even closer is for the solvent between them to demix such that the smaller particles move outside this zone. If there are enough small particles, then the energy of demixing is greater than 10-20 times kT so that depletion stabilization results. On even closer approach the interaction becomes attractive, since the approach will push out the solvent in between the particles and allow it to mix with the bulk fluid. If the concentration of particles is insufficient to impart stability, then

aggregation may occur due to this attractive force at closer distance. This phenomena is called depletion aggregation. As can be imagined, depletion aggregation dominates at low small particle concentrations, while depletion stabilization dominates at high values.

To determine whether depletion stabilization is occurring for this system would require a significant amount of research since many issues are not clearly resolved. For instance, in the case where dissolved polymer is the "small particle", it has been shown both theoretically and experimentally that the higher the molecular weight the lower the volume fraction required for stabilization[6]. In contrast, for small hard particles, the repulsion is predicted to increase if the size ratio of large to small particle increases[210]. In other words, smaller hard particles are more capable of repulsion. Whether the micelles behave more like a dissolved macromolecule or a hard sphere is debatable. A second point is that Napper[6] argues that only small amounts of free polymer are required for stabilization, while Scheutjens and Fleer argue that high volume fractions are required since their model predicts that the interaction between the large particles is attractive at all separation distances at low volume fractions. Napper has shown experimentally that less than 4% by volume of a 300,000 molecular weight PEO is required to stabilize latices. The effect of polymer solvency is also debatable. Feigin and Napper predicted that a decrease in solvency would cause a decrease in depletion stability, while Scheutjens and Fleer argued that the depletion interactions are amplified until just before phase separation occurs[6]. A very recent study by Chatterjee and Schweizer[211] suggests that depletion *attraction* is enhanced just before phase separation. The issue of polymer solvency may be convoluted by the presence of a steric layer on the large particles. As Napper has shown, the depletion and steric interaction are not simply additive.

Mechanisms other than depletion stabilization may be possible. Perhaps a small amount of intermolecular bridging is ineffective in the case of dissolved PEO but is effective for the much larger micelles. If transitory intermolecular bridging between PEO

units occurs then the micelles could be temporarily attached to the large latex particles such that their presence is detected by SFA but not PCS. An argument in favor of this mechanism is that the conformation for PEO surfactants and pure PEO (this work) appear to be different as measured by Raman spectroscopy. An argument against this mechanism is that the attachment would have to be perfectly timed such that an increase in the hydrodynamic diameter is not observed but an increase in the separation distance at the onset of repulsion is.

Alternatively, the formation of micelles may impact steric stabilization itself. The formation of micelles will decrease the osmotic pressure in the bulk. As a consequence, the osmotic flow into the overlap region during steric repulsion would be increased, thus increasing the repulsive force. This change may be enough to counteract the decrease in solvency caused by the addition of salts. Since micelles often have an aggregation number of 50 or so, the decrease may be quite significant. An argument in favor of this mechanism is that a low concentration of dissolved polymer is permissible since the driving force for the mechanism is proportional to the aggregation number and not the concentration. Unfortunately this mechanism cannot explain the increase in the distance at the onset of repulsion caused by increasing salt concentration. However, it seems difficult to rule out this mechanism entirely since SFA and hydrodynamic measurements often give inexplicably different thicknesses as discussed in the literature review (Chapter 2) and Chapter 3.

REFERENCES

1. Gephart, R. E.; Lundgren, R. E., *Hanford Tank Clean Up: A Guide to Understanding the Technical Issues*; Pacific Northwest National Laboratory: Richland, WA, 1997.

2. Allen, G. K., *Estimated Inventory of Chemicals Added to Underground Waste Tanks, 1944 through 1975*; Atlantic Richfield Hanford Company: Richland, WA, 1976.

3. Swanson, J. L., *Initial Studies of Pretreatment Methods for Neutralized Cladding Removal Waste (NCRW) Sludge, Report #PNL-7716, UC-700*; US Department of Commerce: Richland, WA, 1991.

4. Bunker, B. C.; Virden, J. W.; Rector, D. R.; Smith, P. A.; Keefer, K. D.; Martin, J. A.; Berg, J. C., *Environmental Management Science Program Proposal Submittal: Colloidal Agglomerates in Tank Sludge: Impact on Waste Processing*; Battelle Pacific Northwest National Laboratory: Richland, WA, 1996.

5. Israelachvili, J., *Intermolecular & Surface Forces*; San Diego: Academic Press, 1995.

6. Napper, D. H., *Polymeric Stabilization of Colloidal Dispersions*; Academic Press: New York, 1983.

7. Sonntag, H.; Ehmke, B.; Miller, R.; Knapschinski, L., *Adv. Colloid Interface Sci.*, **1982**, *16*, 382.

8. Sonntag, H.; Ehmke, B.; Miller, R.; Knapschinsky, L. In *The Effect of Polymers on Dispersion Properties* ; Tadros, T. F., Ed.; Academic Press: 207, 1982.

9. Gotze, T.; Sonntag, H.; Rabinovitch, Y., *Colloid Polym. Sci.*, **1987**, *265*, 134.

10. Gotze, T.; Sonntag, H., *Colloids Surf.*, **1988**, *31*, 181.

11. Israelachvili, J. N.; Tandon, R. K.; White, L. R., *J. Colloid and Interface Sci.*, **1980**, *78*, 430.

12. Lyklema, J.; van Vliet, T., *Discuss. Faraday Soc.*, **1976**, *65*, 1978.

13. Cain, F. W.; Ottewill, R. H.; Smitham, J. B., *Faraday Discuss. Chem. Soc.*, **1978**, *65*, 33.

14. Cohen Stuart, M. A.; Van Den Boomgaard, T.; Zourab, S. M.; Lyklema, J., *Colloids Surf.*, **1984**, *9*, 163.

15. Klein, J.; Luckham, P., *Nature*, **1982**, *300*, 429.

16. Klein, J.; Luckham, P. F., *Macromolecules*, **1984**, *17*, 1041.

17. Berg, J. C., *Surface and Colloid Science*; University of Washington: Seattle, 1996.

18. Shaw, D. J., *Introduction to Colloid and Surface Chemistry*; Butterworth & Co.: Boston, 1980.

19. Hunter, R. J., *Introduction to Modern Colloid Science*; Oxford University Press: New York, 1993.

20. Lifschitz, E. M., *Sov. Phys. - JETP (Engl. Transl.)*, **1956**, *2*, 73.

21. Sato, T., *J. Coat. Technol.*, **1993**, *65*, 113.

22. Hunter, R. J., *Foundations of Colloid Science*; Oxford University Press: New York, 1987.

23. Berg, J. C., *Macromolecules in Solution and at Interfaces: An Introductory Overview*; University of Washington: Seattle, 1998.

24. Cohen Stuart, M. A.; Waajen, F. H. W. H.; Cosgrove, T.; Vincent, B.; Crowley, T. L., *Macromolecules*, **1984**, *17*, 1825.

25. Cosgrove, T.; Vincent, B.; Crowley, T. L. In *Polymer Adsorption and Dispersion Stability* ; Goddard, E. D. , Vincent, B., Ed.; American Chemical Society: Washington, D.C., 1984.

26. Anderson, J. L.; Kim, J., *J. Chem. Phys.*, **1987**, *86*, 5163.

27. Fleer, G. J.; Cohen Stuart, M. A.; Scheutjens, J. M. H. M.; Cosgrove, T.; Vincent, B., *Polymers at Interfaces*; Chapman & Hall: New York, 1993.

28. Napper, D. H., *J. Colloid Interface Sci.*, **1970**, *33*, 384.

29. Napper, D. H.; Netschey, A., *J. Colloid Interface Sci.*, **1971**, *37*, 528.

30. Dobbie, J. W.; Evans, R.; Gibson, D. V.; Smitham, J. B.; Napper, D. H., *J. Colloid Interface Sci.*, **1973**, *45*, 557.

31. Smitham, J. B.; Napper, D. H., *Colloid Polym. Sci.*, **1979**, *257*, 748.

32. Braunstein, J., *Inorg. Chim. Acta*, **1968**, *2*, 19.

33. Braunstein, J. R. In *Ionic Interactions from Dilute Solutions to Fused Salts, Vol. 1: Equilibrium and Mass Transport* ; Petrucci, S., Ed.; Academic Press: New York, 1971.

34. Castellan, G. W., *Physical Chemistry, 3rd edition*; The Benjamin/Cummings Publishing Company, Inc.: Menlo Park, CA, 1983.

35. Atkins, P. W., *Physical Chemistry, 4th edition*; W.H. Freeman and Company: New York, 1990.

36. Benetto, H. P., *Prog. Chem.; Sect. A. Phys. Inorg. Chem.*, **1973**, *70*, 223.

37. Maurer, G., *Fluid Phase Equilib.*, **1983**, *13*, 269.

38. Berg, J., *Lecture Notes in Thermodynamics*; University of Washington: Seattle, 1997.

39. Pitzer, K., *Acc. Chem. Res.*, **1977**, *10*, 371.

40. Pitzer, K., *J. Phys. Chem.*, **1973**, *77*, 268.

41. Vaslow, F. In *Water and Aqueous Solutions, Structure, Thermodynamics, and Transport Processes* ; Horne, R. A., Ed.; Wiley Interscience: New York, 1972.

42. Renon, H., *Fluid Phase Equil.*, **1986**, *30*, 181.

43. Liu, Y.; Harvey, A. H.; Prausnitz, *Chem. Eng. Commun.*, **1989**, *77*, 43.

44. Pitzer, K., *Ber. Bunsen-Ges. Phys. Chem.*, **1981**, *85*, 952-959.

45. Felmy, A. R.; Weare, J. H.,"The Development and Application of Aqueous Thermodynamic Models: The Specific Ion-Interaction Approach," presented at the *1990 Annual Meeting of the Soil Science Society of America*, San Antonio, Texas, 1990.

46. Anderson, H. C. In *Modern Aspects of Electrochemistry* ; Conway, B. E. , Bockris, J. O., Ed.; Plenum Press: New York, 1975.

47. Friedman, H. L., *Ann. Rev. Phys. Chem.*, **1981**, *322*, 179.

48. Braunstein, J. R., *J. Phys. Chem.*, **1967**, *71*, 38.

49. Ally, M. R.; Braunstein, J., *Fluid Phase Equilib.*, **1993**, *87*, 213.

50. Gubbins, K. E., *Chem. Eng. Prog.*, **1989**, *85*, 38.

51. Molyneux, P., *Water-Soluble Synthetic Polymers: Properties and Behavior*; Boca Raton, Florida: CRC Press, Inc., 1984.

52. Molyneux In *Water: A Comprehensive Treatise* ; Franks, F., Ed.; Plenum Press: New York, 1975.

53. Bailey Jr., F. E.; Kucera, J. L.; Imhof, L. G., *J. Polym. Sci.*, **1958**, *32*, 517.

54. Strazielle, P. C., *Makromol. Chem.*, **1968**, *119*, 50.

55. Bortel, E.; Kochanowski, A., *Makromol. Chem. Rapid Commun.*, **1980**, *1*, 205.

56. Kambe, Y.; Honda, C., *Polym. Comm.*, **1984**, *25*, 154.

57. Polik, W. F.; Burchard, W., *Macromolecules*, **1988**, *16*, 978.

58. Bazzi, G. A. *Ph.D. Thesis*, Wayne State University, 1988.

59. Devanand, K.; Selser, J. C., *Nature*, **1990**, .

60. Devanand, K.; Selser, J. C., *Macromolecules*, **1991**, *24*, 5943.

61. Kinugasa, S.; Nakahara, H.; Fudagawa, N.; Koga, Y., *Macromolecules*, **1994**, *27*, 6889.

62. Porsch, B.; Sundelof, L. O., *Macromolecules*, **1995**, *28*, 7165.

63. Long, F. A.; McDevit, W. F., *Chem. Rev.*, **1952**, *51*, 119.

64. Sergeeva, V. F., *Russ. Chem. Rev. (Engl. Transl.)*, **1965**, *34*, 309.

65. Bailey, J., F.E.; Callard, R. W., *J. Appl. Polym. Sci.*, **1959**, *1*, 56.

66. Frank, H. S.; Wen, W.-Y., *Discuss. Faraday Soc.*, **1957**, *24*, 133.

67. Ataman, M., *Colloid and Polym. Sci.*, **1987**, *265*, 19.

68. Boucher, E. A.; Hines, P. M., *J. Polym. Sci., Polym. Phys. Ed.*, **1976**, *14*, 2241.

69. Kjellander, R.; Florin, E., *J. Chem. Soc., Faraday Trans. 1*, **1981**, *77*, 2053.

70. Florin, E.; Kjellander, R.; Eriksson, J. C., *J. Chem. Soc., Faraday Trans. 1*, **1984**, *80*, 2889.

71. Erlander, S. R., *J. Colloid Interface Sci.*, **1970**, *34*, 53.

72. Collins, K. D.; Washabaugh, M. W., *Q. Rev. Biophys.*, **1985**, *18*, 323.

73. Walker, P. M. B., *Cambridge Dictionary of Science and Technology*; Cambridge University Press: New York, 1988.

74. Voyutsky, S., *Colloid Chemistry*; Mir: Moscow, 1978.

75. Ninham, B. W.; Yaminsky, V., *Langmuir*, **1997**, *13*, 2097.

76. Bailey, J., F.E.; Koleske, J. V., *Poly(ethylene Oxide)*; Academic Press: San Francisco, 1976.

77. Bailey, F. E.; Koleske, J. V. In *Nonionic Surfactants: Physical Chemistry* ; Schick, M. J., Ed.; Marcel Dekker: New York, 1987.

78. Buscall, R., *J. Chem. Soc., Faraday Trans. 1*, **1981**, *77*, 909.

79. Voet, A., *J. Phys. Chem.*, **1936**, *40*, 307.

80. Voet, A., *J. Colloid Interface Sci.*, **1969**, *30*, 149.

81. Ostwald, W.; Wannow, H. A., *Kolloid Z.*, **1936**, *76*, 159.

82. Voropaeva, T. N.; Derjaguin, B. V.; Kabanov, B. N., *Kolloidn. Zh.*, **1962**, *24*, 396.

83. Derjaguin, B. V.; Voropayeva, T. N.; Kabanov, B. N.; Titiyevskaya, A. S., *J. Colloid Sci.*, **1964**, *19*, 113.

84. Fleer, G. Y.; Lyklema, J., *J. Colloid Interface Sci.*, **1969**, *29*, 170.

85. Fleer, G. J.; Lyklema, J., *J. Colloid Interface Sci.*, **1969**, *31*, 440.

86. Pashley, R. M., *Adv. Colloid Interface Sci.*, **1982**, *16*, 57.

87. Israelachvili, J. N., *Chem. Scr.*, **1985**, *25*, 7.

88. Healy, T. W.; Homola, A.; James, R. O.; Hunter, R. J., *Faraday Discuss. Chem. Soc.*, **1978**, *65*, 156.

89. Delgado-Calvo-Flores, J. M.; Peula-Garcia, J. M.; Martinez-Garcia, R.; Callejas-Fernandez, J., *J. Colloid Interface Sci.*, **1997**, *189*, 58.

90. Veeramasuneni, S.; Yueha, H.; Yalamanchili, M. R.; Miller, J. D., *J. Colloid Interface Sci.*, **1997**, *188*, 473.

91. Volpe, C. D.; Siboni, S., *J. Colloid Interface Sci.*, **1997**, *195*, 121.

92. Israelachvili, J. N.; Wennerstrom, H., *Langmuir*, **1990**, *6*, 873.

93. Tadros, T. F. In *The Effect of Polymers on Dispersion Properties* ; Tadros, T. F., Ed.; Academic Press: London, 1982.

94. Virden, J. W.; Berg, J. C., *J. Colloid Interface Sci.*, **1992**, *153*, 411.

95. Einarson, M. B. *Ph.D. Thesis*, University of Washington, 1992.

96. Einarson, M. B.; Berg, J. C., *J. Colloid Interface Sci.*, **1993**, *155*, 165.

97. Sung, A.-M.; Piirma, I., *Langmuir*, **1994**, *10*, 1393.

98. Bevan, M., *Direct Measurement of the Net van der Waals Attraction in the Presence of Sterically Stabilizing Polymer Layers: Henkel Corporation Research Fellowship Application*; Carnegie Mellon University: Pittsburgh, 1997.

99. Seebergh, J. E.; Berg, J. C., *Langmuir*, **1994**, *10*, 454.

100. Einarson, M. B.; Berg, J. C., *Langmuir*, **1992**, *8*, 2611.

101. Addai-Mensah, J.; Dawe, J.; Hayes, R.; Prestidge, C.; Ralston, J., *J. Colloid Interface Sci.*, **1998**, *203*, 115.

102. Molina-Bolivar, J. A.; Galisteo-Gonzalez, F.; Hidalgo-Alvarez, R., *J. Colloid Interface Sci.*, **1998**, *208*, 445.

103. Molina-Bolivar, J. A.; Ortega-Vinuesa, J. L., *Langmuir*, **1999**, *15*, 2644.

104. Virden, J. W.; Berg, J. C., *J. Colloid Interface Sci.*, **1992**, *149*, 528.

105. Honig, E. P.; Roebersen, G. J.; Wiersema, P. H., *J. Colloid Interface Sci.*, **1971**, 97.

106. Spielman, L. A., *J. Colloid Interface Sci.*, **1970**, 562.

107. Young, W. D.; Prieve, D. C., *Langmuir*, **1991**, *7*, 2887.

108. Seebergh, J. E.; Berg, J. C., *Colloids Surf., A*, **1995**, *100*, 139.

109. De, A. K., *Solvent Extraction of Metals*; Van Nostrand Reinhold: New York, 1970.

110. Christian, G. D.; O'Reilly, J. E., *Instrumental Analysis*; Allyn and Bacon: Boston, 1986.

111. Fadini, A.; Schnepel, F.-M., *Vibrational Spectroscopy: Methods and Applications*; Halsted Press: New York, NY, 1989.

112. Cebula, D. J.; Thomas, R. K.; Harris, N. M.; Tabony, J.; White, J. W., *Faraday Discuss. Chem. Soc.*, **1978**, *65*, 76.

113. Barnett, K. G.; Cosgrove, T.; Vincent, B.; Burgess, A. N.; Crowley, T. L.; King, T.; Turner, J. D.; Tadros, T. F., *Polymer*, **1981**, *22*, 283.

114. Barnett, K.; Cosgrove, T.; Crowley, T. L.; Tadros, T. F.; Vincent, B. In *The Effect of Polymers on Dispersion Properties* ; Tadros, T. F., Ed.; Academic Press: New York, 1982.

115. Cosgrove, T.; Crowley, T. L.; Vincent, B.; Barnett, K. G.; Tadros, T. F., *Faraday Symp. Chem. Soc.*, **1981**, *16*, 101.

116. Cosgrove, T.; Crowley, T. L.; Vincent, B. In *Adsorption from Solution* ; Ottewill, R. H., Rochester, C. H. , Smith, A. L., Ed.; Academic Press: New York, 1983.

117. Abeles, F.,"Optical Properties of Inhomogeneous Films," presented at the *Ellipsometry in the Measurement of Surfaces and Thin Films: Symposium Proceedings*, Passaglia, E., Stromberg, R. R. , Kruger, J., Ed.; National Bureau of Standards Miscellaneous Publication 256: Washington, D.C., 1963.

118. Lyklema, J., *Fundamentals of Interface and Colloid Science*; Academic Press: San Diego, 1991.

119. McCrackin, F. L.; Colson, J. P.,"Computational Techniques for the Use of the Exact Drude Equations in Reflection Problems," presented at the *Ellipsometry in the Measurement of Surfaces and Thin Films: Symposium Proceedings*, Passaglia, E., Stromberg, R. R. , Kruger, J., Ed.; National Bureau of Standards Miscellaneous Publication 256: Washington, D.C., 1963.

120. Stromberg, R. R.; Passaglia, E.; Tutas, D. J.,"Application of Ellipsometry to the Study of Adsorption from Solution: Symposium Proceedings," presented at the *Ellipsometry in the Measurement of Surfaces and Thin Films*, Passaglia, E., Stromberg, R. R. , Kruger, J., Ed.; National Bureau of Standards Miscellaneous Publication 256: Washington, D.C., 1963.

121. Killman, E.; Maier, H.; Kaniut, P.; Gutling, N., *Colloids Surf.*, **1985**, *15*, 261.

122. Killman, E.; Sapuntzjis, P., *Colloids Surf., A.*, **1994**, *86*, 229.

123. Malmsten, M.; Tiberg, F., *Langmuir*, **1993**, *9*, 1098.

124. Israelachvili, J. N., *Philos. Mag. A*, **1981**, *43*, 753.

125. Ohrn, O. E., *J. Polym. Sci.*, **1955**, *16*, 137.

126. Ohrn, O. E., *Ark. Kemi*, **1958**, *12*, 397.

127. Priel, Z.; Silberberg, A., *J. Polym. Sci., Polym. Phys. Ed.*, **1978**, *16*, 1917.

128. Varoqui, R.; Dejardin, P., *J. Chem. Phys.*, **1977**, *66*, 4395.

129. Webber, R. M.; Anderson, J. L.; Jhon, M. S., *Macromolecules*, **1990**, *23*, 1026.

130. Pecora, R., *Dynamic Light Scattering*; Plenum Press: New York, 1985.

131. Scheutjens, J. M. H. M.; Fleer, G. J.; Cohen Stuart, M. A., *Colloids Surf.*, **1986**, *21*, 285.

132. Baker, J. A.; Berg, J. C., *Langmuir*, **1988**, *4*, 1955.

133. Kayes, J. B.; Rawlins, D. A., *Colloid Polym .Sci.*, **1979**, *257*, 622.

134. Tadros, T. F.; Vincent, B., *J. Phys. Chem.*, **1980**, *84*, 1575.

135. Lindsay, H. M.; Lin, M. Y.; Weitz, D. A.; Sheng, P.; Chen, Z., *Faraday Discuss. Chem. Soc.*, **1987**, *83*, 153.

136. Kerker, M., *The Scattering of Light and Other Electromagnetic Radiation*; Academic Press: New York, 1969.

137. Attio, Y. A.; Rubio, J., *Br. Polym. J.*, **1975**, *7*, 135.

138. Li, J.; Carlsson, J.; Huang, S.; Caldwell, K. D. In *Hydrophilic Polymers: Performance with Environmental Acceptance.* ; Glass, J. E., Ed.; American Chemical Society: 248, 1996.

139. Dhoot, S.; Tirrell, M., *Macromolecules*, **1995**, *28*, 3692.

140. Dan-Brandon, N.; Argillier, J. F.; Tirrell, M., *Rev. Inst. Fr. Petr.*, **1992**, *47*, 244.

141. Brandrup, J.; Immergut, E. H., *Polymer Handbook*; John Wiley & Sons: New York, 1989.

142. Lundberg, R. D.; Bailey, F. E.; Callard, R. W., *J. Polym. Sci., Part A-1*, **1966**, *4*, 1563.

143. Cross, J. In *Nonionic Surfactants: Chemical Analysis* ; Cross, J., Ed.; Marcel Dekker, Inc.: New York, 1987.

144. Armand, M., *Solid State Ionics*, **1983**, *9 & 10*, 745.

145. Shriver, D. F.; Papke, B. L.; Ratner, M. A., *Solid State Ionics*, **1981**, *5*, 83.

146. Okada, T., *Analyst*, **1993**, *118*, 959.

147. Sartori, R.; Sepulveda, L.; Quina, F.; Lissi, E.; Abuin, E., *Macromolecules*, **1990**, *23*, 3878.

148. Yanagida, S.; Takahashi, K.; Okahara, M., *Bull. Chem. Soc. Jpn.*, **1977**, *50*, 1386.

149. Kikuchi, Y.; Takahashi, N.; Suzuki, T.; Sawada, K., *Anal. Chim. Acta*, **1992**, *256*, 311.

150. Kikuchi, Y.; Suzuki, T.; Sawada, K., *Anal. Chim. Acta*, **1992**, *264*, 65.

151. Kikuchi, Y.; Nojima, Y.; Kita, H.; Suzuki, T.; Sawada, K., *Bull. Chem. Soc. Jpn.*, **1992**, *65*, 1506.

152. Kikuchi, Y.; Kubota, M.; Suzuki, T.; Sawada, K., *Bull. Chem. Soc. Jpn.*, **1994**, *67*, 2111.

153. Tadokoro, H.; Chatani, Y.; Yoshihara, T.; Tahara, S.; Murahashi, S., *Makromol. Chem.*, **1964**, *73*, 109.

154. Matsuura, H.; Miyazawa, T., *Bull. Chem. Soc. Jpn.*, **1968**, *41*, 1798.

155. Miyazawa, T., *J. Chem. Phys.*, **1961**, *35*, 693.

156. Miyazawa, T.; Fukushima, K.; Ideguchi, Y., *J. Chem. Phys.*, **1963**, *37*, 2764.

157. Yoshihara, T.; Tadokor, H.; Murahashi, S., *J. Chem. Phys.*, **1964**, *41*, 2902.

158. Matsuura, H.; Fukuhara, K., *J. Polym. Sci., Polym. Phys. Ed.*, **1986**, *24*, 1383.

159. Koenig, J. L.; Angood, A. C., *J. Polym. Sci., Part A-2*, **1970**, *8*, 1787.

160. Maxfield, J.; Shepherd, I. W., *Polymer*, **1975**, *16*, 505.

161. Matsuura, H.; Fukuhara, K., *J. Mol. Struct.*, **1985**, *126*, 251.

162. Crupi, V.; Jannelli, M. P.; Magazu, S.; Maisano, G.; Majolino, D.; Migliardo, P.; Ponterio, R., *J. Mol. Struct.*, **1996**, *381*, 207.

163. Branca, C.; Magazu, S.; Maisano, G.; Migliardo, P.; Villari, V., *J. Phys.: Condens. Matter*, **1998**, *10*, 10141.

164. Yang, X.; Su, Z.; Wu, D.; Hsu, S. L.; Stidham, H. D., *Macromolecules*, **1997**, *30*, 4796.

165. Sato, H.; Kusumoto, Y., *Chem. Lett.*, **1978**, 635.

166. Papke, B. L.; Ratner, M. A.; Shriver, D. F., *J. Phys. Chem. Solids*, **1981**, *42*, 493.

167. Papke, B. L.; Ratner, M. A.; Shriver, D. F., *J. Electrochem. Soc.*, **1982**, *129*, 1434.

168. Fenton, D. E.; Parker, J. M.; Wright, P. V., *Polymer*, **1973**, *14*, 589.

169. Chatani, Y.; Okamura, S., *Polymer*, **1987**, *28*, 1815.

170. Parker, L. M.; Wright, P. V.; Lee, C. C., *Polymer*, **1982**, *22*, 1305.

171. Hibma, T., *Solid State Ionics*, **1983**, *9/10*, 1101.

172. Bruce, P. G., *Electrochim. Acta*, **1995**, *40*, 2077.

173. Siew, D.; Cooney, R. P.; Taylor, M. J.; Easteal, A. J., *J. Chem. Soc., Faraday Trans.*, **1990**, *86*, 1109.

174. Takeuchi, H.; Takakai, A.; Harada, I., *J. Mol. Struct.*, **1986**, *146*, 197.

175. Siew, D. C. W.; Cooney, R. P.; Taylor, M. J., *J. Raman Spectrosc.*, **1991**, *22*, 183.

176. Siew, D. C. W.; Cooney, R. P.; Taylor, M. J., *Appl. Spectrosc.*, **1993**, *47*, 1784.

177. Horikoshi, K.; Hata, K.; Kawabata, N.; Ikawa, S.-I.; Konaka, S., *J. Mol. Struct.*, **1990**, *239*, 33.

178. Yanagida, S.; Takahashi, K.; Okahara, M., *Bull. Chem. Soc. Jpn.*, **1978**, *51*, 1294.

179. Carale, T. R.; Pham, Q. T.; Blankschtein, D., *Langmuir*, **1994**, *10*, 109.

180. BASF Corporation, *BASF Performance Chemicals: Pluronics and Tetronic Surfactants*, Mt. Olive, NJ, 1996.

181. *CRC Handbook of Chemistry and Physics*; Lide, D. R.; Frederikse, H. P. R., Ed.; CRC Press, Inc.: New York, 1997.

182. Baes, C. F.; Mesmer, R. E., *The Hydrolysis of Cations*; John Wiley & Sons: New York, 1976.

183. Overbeek, J. T. G. In *Colloid Science* ; Kruyt, H. R., Ed.; Elseview: Amsterdam, 1952.

184. Freij-Larsson, C.; Nylander, T.; Jannasch, P.; Wesslen, B., *Biomaterials*, **1996**, *17*, 2199.

185. Tiberg, F.; Malmsten, M.; Linse, P.; Lindman, B., *Langmuir*, **1991**, *7*, 2723.

186. Riddick, T. M., *Control of Colloid Stability Through Zeta Potential*; Creative Press: New York, 1968.

187. *Kirk-Othmer Encyclopedia of Chemical Technology*; Kroschwitz, J. I.; Grant, M. H., Ed.; John Wiley & Sons: New York, 1991.

188. *Kirk-Othmer Encyclopedia of Chemical Technology*; Kroschwitz, J. I.; Grant, M. H., Ed.; John Wiley & Sons: New York, 1991.

189. Alexandridis, P.; Holzwarth, J. F., *Langmuir*, **1997**, *13*, 6074.

190. Chu, B.; Zhou, Z. In *Nonionic Surfactants: Polyoxyalkylene Block Copolymers* ; Nace, V. M., Ed.; Marcel Dekker, Inc.: New York, 1996.

191. Alexandridis, P., *Curr. Opin. Colloid Interface Sci.*, **1997**, *2*, 478.

192. Chu, B., *Langmuir*, **1995**, *11*, 414.

193. Bahadur, P.; Li, P.; Almgren, M.; Brown, W., *Langmuir*, **1992**, *8*, 1903.

194. Bahadur, P.; Pandya, K.; Almgren, M.; Li, P.; Stilbs, P., *Colloid Polym. Sci.*, **1993**, *271*, 657.

195. Pandya, K.; Lad, K.; Bahadur, P., *J. Macromol. Sci., Pure Appl. Chem.*, **1993**, *A30*, 1.

196. Zhou, Z.; Chu, B., *J. Colloid Interface Sci.*, **1988**, *126*, 171.

197. Alexandridus, P.; Holzwarth, J. F.; Hatton, T. A., *Langmuir*, **1994**, *10*, 2604.

198. Pandya, K.; Bahadur, P.; Nagar, T. N.; Bahadur, A., *Colloids Surf., A*, **1993**, *30*, 1.

199. Wanka, G.; Hoffman, H.; Ulbricht, W., *Macromolecules*, **1994**, *27*, 4145.

200. Reddy, N. K.; Fordham, P. J.; Attwood, D.; Booth, C., *J. Chem. Soc., Faraday Trans.*, **1990**, *86*, 1569.

201. Kositza, M. J.; Bohne, C.; Alexandridis, P.; Hatton, T. A.; Holzwarth, J. F., *Langmuir*, **1999**, 322.

202. Zhang, L.; Somasundaran, P.; Maltesh, C., *Langmuir*, **1996**, *12*, 2371.

203. Zhou, Z.; Chu, B., *J. Colloid Interface Sci.*, **1988**, *126*, 171.

204. Thomas, J. C., *J. Colloid Interface Sci.*, **1987**, *117*, 187.

205. Pandya, K.; Lad, K.; Bahadur, P., *J. Macromol. Sci., Pure Appl. Chem.*, **1993**, *A30*, 1.

206. Robinson, R. A.; Stokes, R. H., *Electrolyte Solutions*; Butterworths: London. 1965.

207. Craig, V. S. J.; Ninham, B. W.; Pashley, R. M., *J. Phys. Chem.*, **1993**, *97*, 10192.

208. Weissenborn, P. K.; Pugh, R. J., *Langmuir*, **1995**, *11*, 1422.

209. Paulson, O.; Pugh, R. J., *Langmuir*, **1996**, *12*, 4808.

210. Mao, Y.; Cates, M. E.; Lekkerkerker, H. N. W., *Physica A*, **1995**, *222*, 10.

211. Chatterjee, A. P.; Schweizer, K. S., *Macromolecules*, **1999**, *32*, 923.

212. Baker, J. A. *Ph.D. Thesis*, University of Washington, 1987.

213. Nuysink, J.; Koopal, L. K., *Talanta*, **1982**, *29*, 495.

APPENDIX A: SIZE EXCLUSION CHROMATOGRAPHY: CALIBRATION CURVES AND ACCURACY TEST RESULTS

A. CALIBRATION CURVES

For the test procedure described in Chapter 3, calibration curves were developed to relate the peak areas determined by size exclusion chromatography to the known weight percentages of Pluronics in tetrahydrofuran (THF), since the relative areas did not correspond directly to the relative percentages in solution. These differences were caused by the difference in refractive indices of the two Pluronics® (F108 and L43) and the nature of the integrating software. The integrator used was a Perkin Elmer LCI-100. The sensitivity of the software to peak detection and the sampling rate were determined as recommended by the manufacturer. Since very little drift in the baseline occurred, a horizontal baseline connecting basepoints was used.

The calibration curves were creating by determining the relative peak areas for solutions with known concentrations of Pluronics®. In all cases, the total concentration of Pluronics® was 2000 mg/L, while the relative concentrations were varied. An average peak area was determined from three runs on the chromatography system, then linearly correlated with the known solution concentration. Since the peak area did not linear correlate with the known concentration over the entire range, several linear correlations were created over smaller ranges. An acceptable range resulted in a linear correlation coefficient (R) greater than 0.99. Figures depicting the data and the resulting correlations are given in Figure A.1. The error bars indicate one standard deviation.

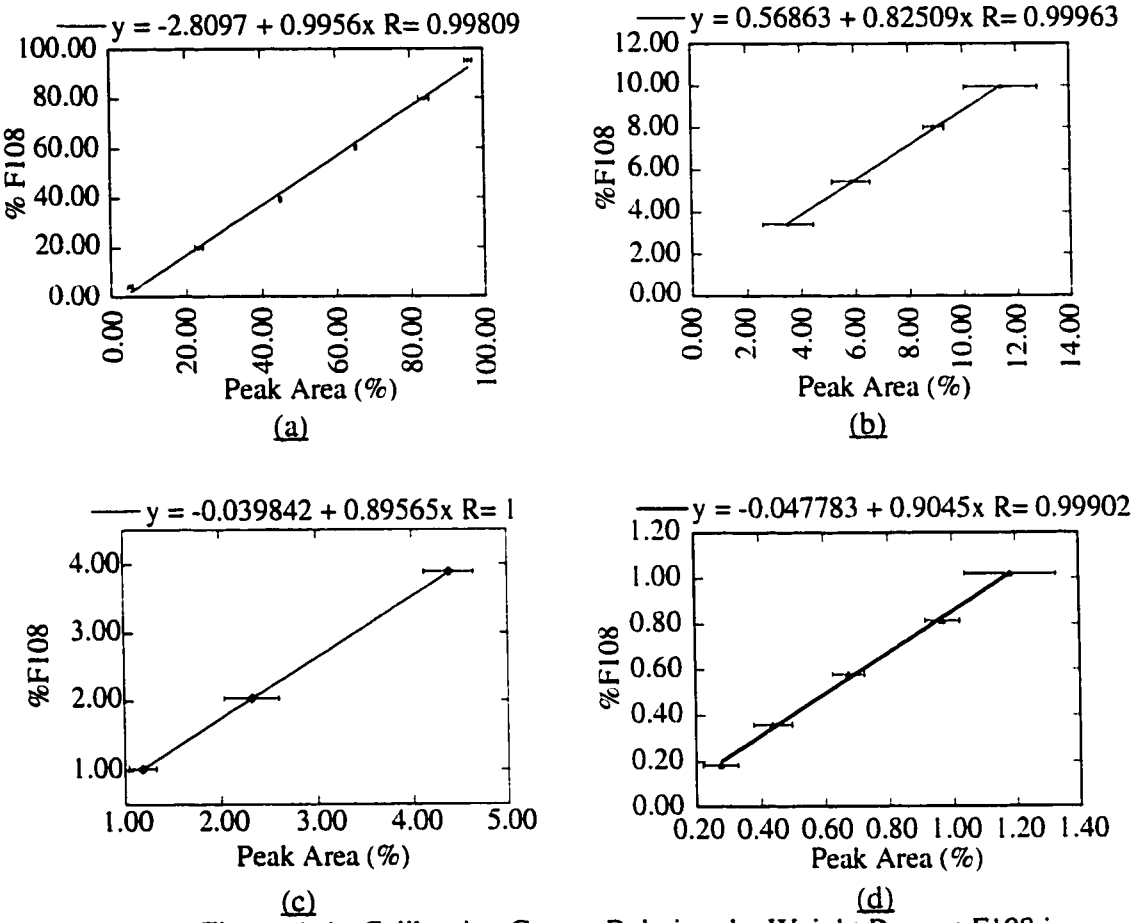

Figure A.1. Calibration Curves Relating the Weight Percent F108 in Tetrahydrofuran Solution to the Peak Areas Obtained by Size Exclusion Chromatography. (Linear regressions of the mean values are given in the equations above the appropriate graph. Error bars indicate one standard deviation.)

B. RESULTS OF ACCURACY TEST

Two samples were tested to determine the accuracy of the calibration curves given in Figure A.1. For each sample, twelve milliliters of an aqueous solution containing 300 mg/L total Pluronics® and approximately 10 wt% F108 were air dried. The solids were then dissolved in 2 mL of tetrahydrofuran for 3 hours at 30°C. Each sample was analyzed three times by size exclusion chromatography as described in Chapter 3, then converted to a concentration using the calibration curves given in Figure A.1. The percent F108 determined by gravimetric and chromatographic techniques is given in Table A.1 below.

The standard deviation of the replicates is given after the mean value for the chromatographic values.

Table A.1. Comparison of the Weight Percent Measured by Chromatography and Gravimetric Techniques, for 10 wt% F108. (The mean weight percent ± standard deviation is given for the chromatographic values.)

Duplicate	Wt% F108 by Gravimetric Techniques	Wt% F108 by Chromatography	% Error
1	9.93	10.23 ± 0.88	3.02
2	9.93	9.97 ± 0.22	0.40

APPENDIX B: TURBIDIMETRIC TECHNIQUE: DETERMINATION OF PARAMETERS, CALIBRATION CURVES, AND ACCURACY TEST RESULTS

A. DETERMINATION OF PARAMETERS

To determine an appropriate wavelength to use for the turbidimetric technique, the procedure, as described in Chapter 3, was performed at a number of different wavelengths. For Pluronics® F108, no peak in the absorbance occurs over the wavelengths tested as shown in Figure B.1, possibly explaining why a number of wavelengths are employed for this method [137, 212, 213]. A wavelength of 500 nm was arbitrarily chosen for the test.

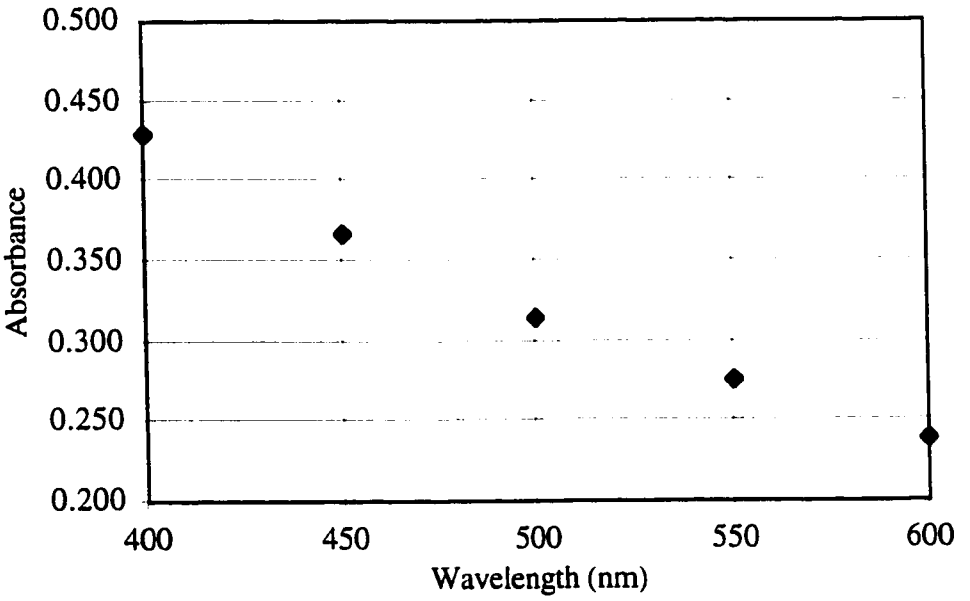

Figure B.1. Absorbance of 10 mg/L F108 Pluronics®/Tannic Acid Complex at Various Wavelengths, 40-60 Minutes after Mixing. (Final concentrations of tannic acid and NaCl were 200 mg/L and 0.1 M, respectively.)

Nuysink and Koopal[213] have indicated that the absorbance can be a strong function of time at high concentrations of the polymer and reagents. To determine an acceptable upper concentration limit of the polymer and an appropriate measurement time after mixing, the absorbance was determined as a function of time for various concentrations of both F108 and L43 Pluronics® at 500 nm. As indicated in Figures B.2 and B.3, a concentration of 10 mg/L does not exhibit a strong time dependence so was chosen as the acceptable upper concentration limit for the polymer. For this concentration, the absorbance changes insignificantly between 40 and 60 minutes after mixing, so this time was deemed appropriate to make measurements. Curves developed for the F108 and L43 Pluronics® at a wavelength of 600 nm and for Polyox (Union Carbide) at 500 nm and 600 nm showed the same qualitative characteristics as the graphs depicted.

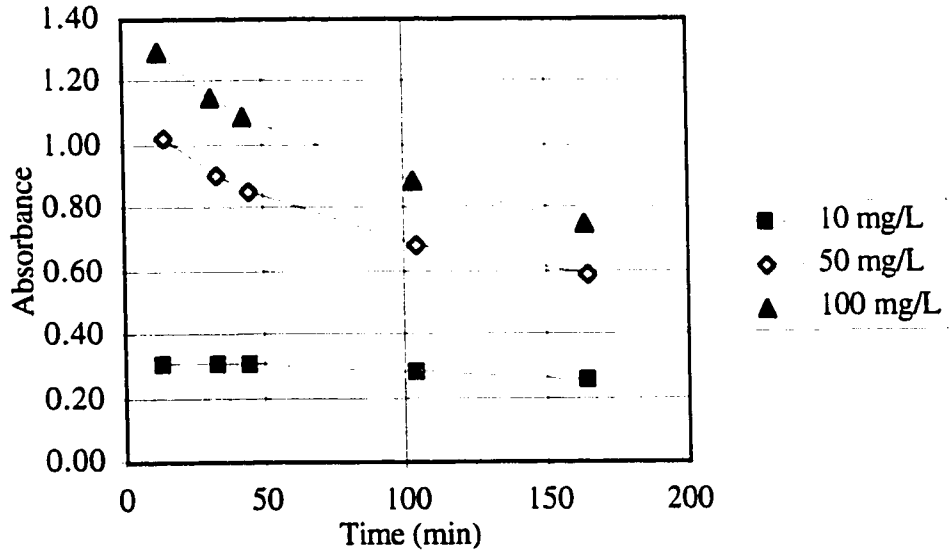

Figure B.2. The Absorbance of F108/Tannic Acid complex at 500 nm as a Function of Time after Mixing. (Final concentration of tannic acid and NaCl were 200 mg/L and 0.1 M, respectively. Final concentrations of Pluronics® indicated in legend.)

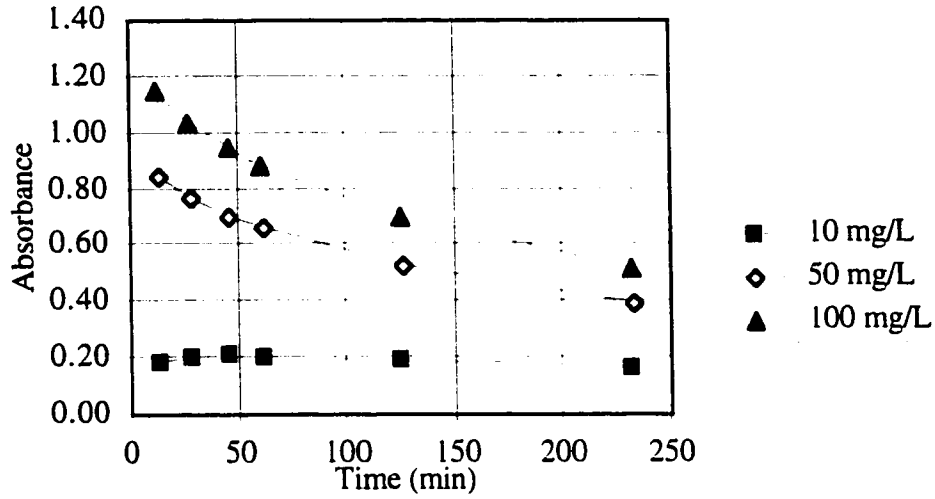

Figure B.3. The Absorbance of L43/Tannic Acid Complex at 500 nm as a Function of Time after Mixing. (Final concentration of tannic acid and NaCl were 200 mg/L and 0.1 M, respectively. Final concentrations of Pluronics® indicated in legend.)

B. CALIBRATION CURVES

Calibration curves, developed using gravimetrically determined concentrations of Pluronics® polymer, are presented in Figure B.4. Calibrations curves were created for various proportions of the two Pluronics®, F108 and L43, since the turbidity generated was dependent on the type as well as the quantity of Pluronics® in solution. Each sample was run in triplicate, and the error bars indicate one standard deviation. Linear regressions were performed for each calibration curve using the mean value of the replicates and are presented with the graph. The calibration curves for L35 in distilled water and 0.3 M $BaCl_2$ were also developed for the adsorption tests performed in Chapter 6 and are presented in Figure B.5.

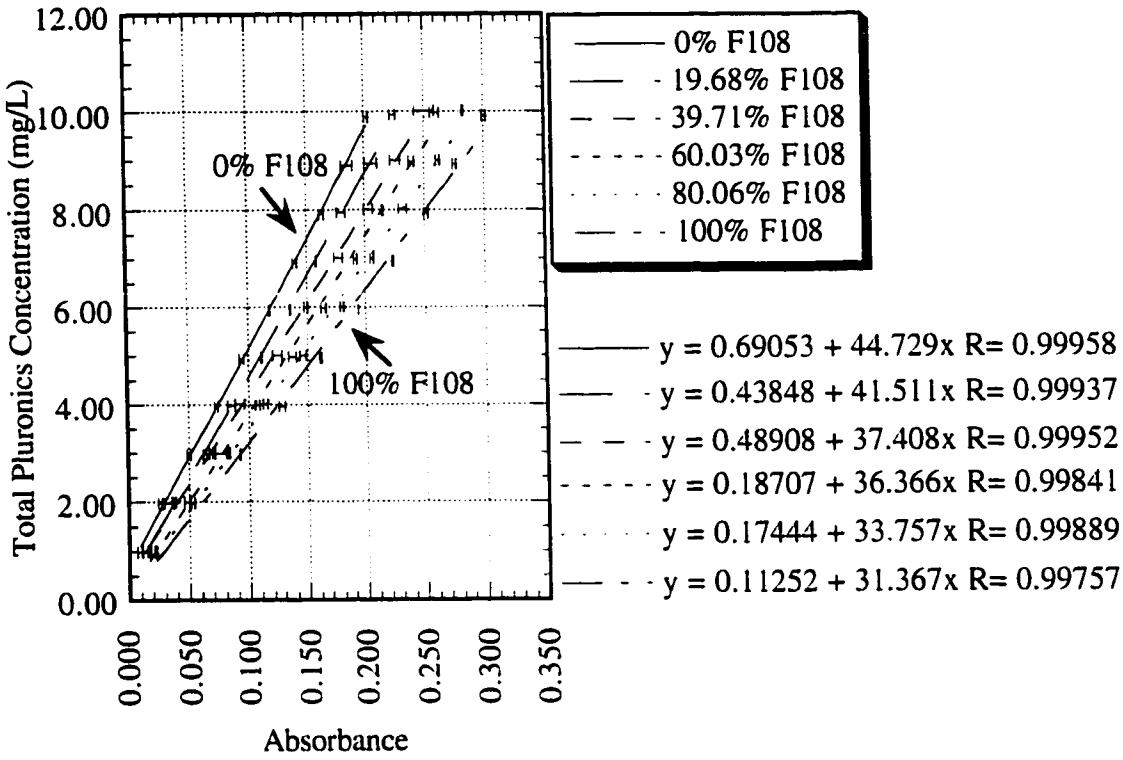

Figure B.4. Calibration Curves of Pluronics® Concentration as a Function of the Absorbance of the Tannic Acid Complex, for Various Proportions of F108/L43 Pluronics®. (All measurements taken at 500 nm 40-60 minutes after mixing. Final concentration of tannic acid and NaCl were 200 mg/L and 0.1 M, respectively.)

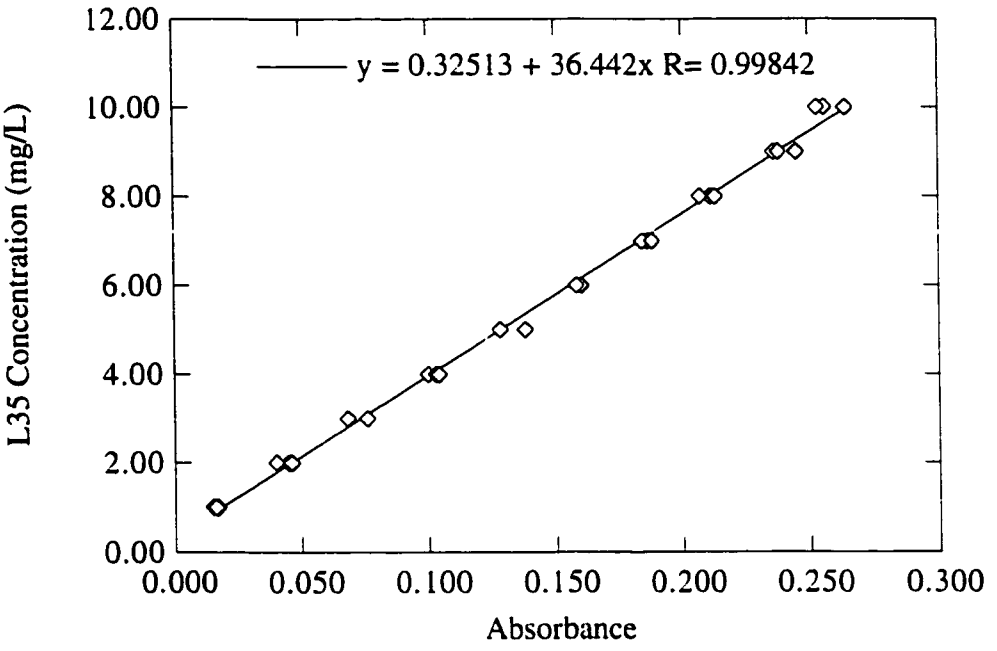

(a) Calibration in Distilled Water

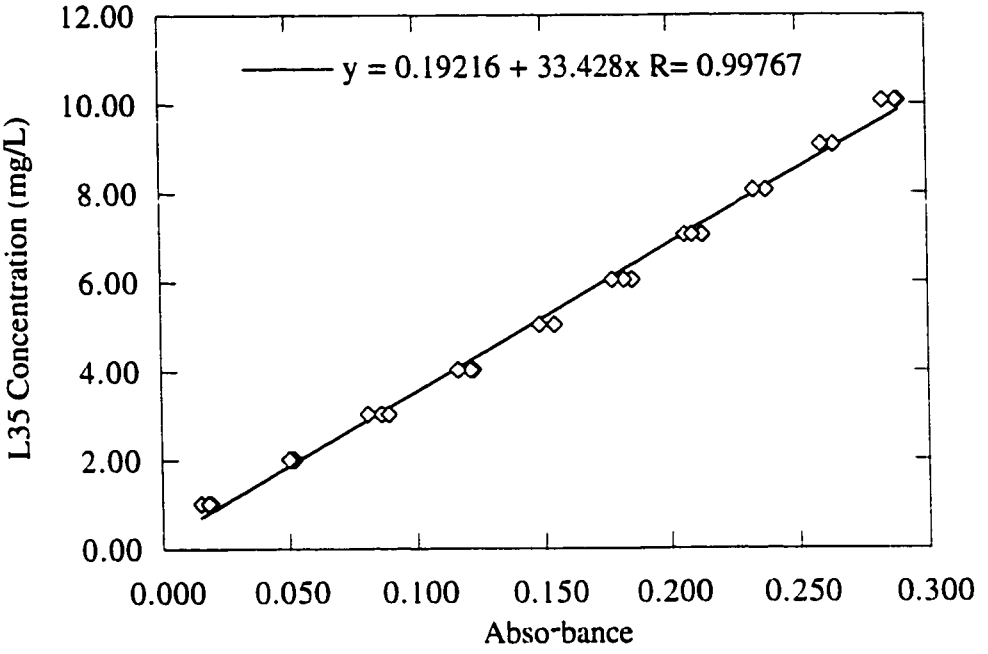

(b) Calibration in 0.3 M $BaCl_2$

Figure B.5. Calibration Curves of L35 Pluronics® Concentration as a Function of the Absorbance of the Tannic Acid Complex. (All measurements taken at 500 nm, 40-60 minutes after mixing. Final concentration of tannic acid and NaCl were 200 mg/L and 0.1 M, respectively.)

C. TEST OF ACCURACY

The accuracy of the turbidimetric technique was tested by determining the total concentration of Pluronics® in solution both gravimetrically and by the turbidity method. Three solutions were tested, and the turbidimetric technique was replicated three times for each solution. The results are presented in Table B.1. As indicated the absolute value of the error between the gravimetric and turbidimetric technique is less than 2%, and is 1.3% on average.

Table B.1. Comparison of the Concentrations Predicted by the Turbidimetric Technique and by Gravimetric Measurements, for Various Relative Concentrations of F108 and L43 Pluronics®.

%F108	Gravimetric Concentration of Pluronics (mg/L)	Predicted Turbidimetric Concentration and Standard Deviation(mg/L)	Error (%)
10.05	300.79	305.91±7.69	1.70
59.97	296.23	296.69±2.85	0.15
60.03	19.93	19.55±0.12	-1.92

APPENDIX C: REFRACTIVE INDEX, VISCOSITY, AND DENSITY OF AQUEOUS SALT SOLUTIONS

When possible, handbook values of the refractive index, viscosity, and density of aqueous salt solutions were used[181]. Although the handbook values were reported for 20°C and the experimental temperatures were 25°C, the error incurred in the stability ratios were felt to be negligible. First, the refractive index is only a weak function of the temperature and wavelength. Secondly, the viscosity actually cancels out of the expression for the stability ratio since it appears in both the denominator for the Smolukowski rate constant and the denominator of the Stokes Einstein expression.

When unavailable, the values were determined in the laboratory at a temperature of 25°C. The refractive index was determined using a Woods Model RF-600 Differential Refractometer, using either distilled water or aqueous sucrose solutions as the reference solution. The manufacturer claims the sensitivity is 3×10^{-6} refractive index units. The kinematic viscosity was determined using a #50 Cannon Fenske capillary viscometer, which was calibrated using distilled water. The density was determined using a Mettler/Paar DMA 45 Calculating Digital Density Meter. The dynamic viscosity was calculated as the product of the kinematic viscosity and density. Three to five measurements were taken for one solution for the refractive index and kinematic viscosity. Only one measurement was taken for the density. The values for the measurements are given in Tables C.1 through C.6. In the case of aluminum chloride, the pH was measured for each solution. In each case shown, the pH was below 4.5, indicating that the dominant species was Al^{3+}. In very rare cases, either the density or kinematic viscosity was not measured, but an estimate of the value was used to calculate the dynamic viscosity. The estimate was calculated using linear interpolation.

The reproducibility of the kinematic viscosity measurements was made by determining the viscosity for four different 1 M $BaCl_2 \cdot 6H_2O$ solutions. Measurements were taken five times for each solution. The average and standard deviation is given for these measurements in Table C.7. As can be seen, the difference between any two averages is less than 1%.

Table C.1. Refractive Index, Density, Kinematic Viscosity and Dynamic Viscosity for Aqueous $Al_2Cl_3 \cdot 6H_2O$.

		Refractive Index			Kinematic Viscosity (cS)		
Molarity	pH	Mean	Standard Deviation	Density (g/ml)	Mean	Standard Deviation	Dynamic Viscosity (cP)
0.001	4.18	1.3327	0.00001	0.9973	0.8914	0.0007	0.8889
0.002	4.00	1.3326	0.00003	0.9974	0.8930	0.0002	0.8907
0.005	3.77	1.3327	0.00002	0.9978	0.8957	0.0009	0.8937
0.01	3.63				0.8991	0.0005	0.8986
0.02	3.52	1.3333	0.00002	0.9995	0.9053	0.0008	0.9079
0.05	3.23	1.3344	0.00002	1.0029	0.9156	0.0012	0.9151
0.1	3.06	1.3365	0.00001	1.0090	0.9610	0.0002	0.9697
0.2	2.79	1.3405	0.00001	1.0208	1.0299	0.0007	1.0513
0.5	2.38	1.3575	0.00001	1.0540	1.2634	0.0003	1.3316
1	1.77	1.3681	0.00003	1.1098	1.8900	0.0030	2.0976
2	0.48	1.4076	0.00003	1.2096	4.8700	0.0078	5.8907

Table C.2. Density, Kinematic Viscosity and Dynamic Viscosity for Aqueous $BaCl_2 \cdot 6H_2O$.

		Measured Kinematic Viscosity (cS)		
Molarity	Density (g/ml)	Mean	Standard Deviation	Dynamic Viscosity (cP)
0.005	0.9980	0.8913	0.0019	0.8895
0.01	0.9989	0.8927	0.0008	0.8917
0.025	1.0015	0.8952	0.0006	0.8965
0.05	1.0067	0.8954	0.0010	0.9014
0.1	1.0157	0.8947	0.0004	0.9087
0.25	1.0429	0.9056	0.0008	0.9445
0.5	1.0875	0.9199	0.0003	1.0004
0.75	1.1409	0.9406	0.0009	1.0731
1	1.1777	0.9669	0.0007	1.1387
1.2	1.2106	0.9903	0.0005	1.1988

Table C.3. Refractive Index, Density, Kinematic Viscosity and Dynamic Viscosity for Aqueous KBr.

		Kinematic Viscosity (cS)		
Molarity	Density (g/ml)	Mean	Standard Deviation	Dynamic Viscosity (cP)
0.05	1.0015	0.8851	0.0003	0.8864
0.1	1.0056	0.8782	0.0003	0.8831
0.2	1.0142	0.8700	0.0005	0.8823
0.3	1.0228	0.8582	0.0005	0.8775
0.5	1.0397	0.8374	0.0005	0.8706
1	1.0829	0.7929	0.0003	0.8587
2	1.1624	0.7329	0.00054	0.8513
4	1.3222	0.6747	0.0006	0.8921

Table C.4. Refractive Index, Density, Kinematic Viscosity and Dynamic Viscosity for Aqueous KF.

	Refractive Index			Kinematic Viscosity (cS)		
Molarity	Mean	Standard Deviation	Density (g/ml)	Mean	Standard Deviation	Dynamic Viscosity (cP)
0.05	1.3328	0.00001	0.9996	0.8954	0.0006	0.8950
0.1	1.3331	0.00001	1.0021	0.9005	0.0006	0.9024
0.2	1.3337	0.00002	1.0071	0.9094	0.0018	0.9159
0.3	1.3342	0.00002	1.0116	0.9158	0.0013	0.9265
0.5	1.3353	0.00001	1.0202	0.9275	0.0011	0.9462
1	1.3378	0.00002	1.0468	0.9715	0.0028	1.0170
2	1.3410	0.00002	1.0908	1.0527	0.0003	1.1483
5	1.3500	0.00003	1.2140	1.4119	0.0018	1.7140
10	1.3586	0.00001	1.4335	2.5739	0.0034	3.6896

Table C.5. Refractive Index, Density, Kinematic Viscosity and Dynamic Viscosity for Aqueous KSCN.

	Refractive Index			Kinematic Viscosity (cS)		
Molarity	Mean	Standard Deviation	Density (g/ml)	Mean	Standard Deviation	Dynamic Viscosity (cP)
0.05	1.3335	0.00001	0.9996	0.8861	0.0007	0.8857
0.1	1.3344	0.00001	1.0020	0.8831	0.0007	0.8848
0.2	1.3362	0.00003	1.0068	0.8757	0.0003	0.8817
0.3	1.3381	0.00001	1.0115	0.8743	0.0020	0.8844
0.5	1.3415	0.00001	1.0242	0.8554	0.0011	0.8761
1	1.3509	0.00003	1.0455	0.8261	0.0002	0.8637
2	1.3661	0.00002	1.0971	0.7954	0.0008	0.8727
5	1.4117	0.00002	1.2239	0.8589	0.0005	1.0512
8	1.4561	0.00003	1.3406	1.2447	0.0019	1.6688
10				1.9192	0.0016	2.7514

Table C.6. Refractive Index, Density, Kinematic Viscosity and Dynamic Viscosity for Aqueous $Na_4P_2O_7 \cdot 10H_2O$.

	Refractive Index			Kinematic Viscosity (cS)		
Molarity	Mean	Standard Deviation	Density (g/ml)	Mean	Standard Deviation	Dynamic Viscosity (cP)
0.001	1.3325	0.00001	0.9974	0.8940	0.0002	0.8917
0.002	1.3325	0.00001	0.9977	0.8937	0.0007	0.8917
0.005	1.3328	0.00001	0.9985	0.8978	0.0000	0.8965
0.01	1.3330	0.00001	0.9999	0.9025	0.0014	0.9024
0.02	1.3356	0.00002	1.0026	0.9136	0.0006	0.9160
0.05	1.3351	0.00001	1.0103	0.9417	0.0030	0.9514
0.1	1.3375	0.00002	1.0236	0.9853	0.0009	1.0086
0.2	1.3415	0.00003	1.0479	1.0808	0.0006	1.1326

Table C.7. Average Kinematic Viscosity for Four Different Aqueous 1 M $BaCl_2 \cdot 6H_2O$ Solutions.

	Kinematic Viscosity (cP)	
Measurement	Mean	Standard Deviation
1	0.9669	0.00117
2	0.9691	0.00083
3	0.9655	0.00050
4	0.9664	0.00045

VITA

Victoria Susan Stenkamp

Born

June 13, 1964 in Oak Ridge, Tennessee

Education

Ph.D. in Chemical Engineering, 1999: University of Washington, Seattle, WA

M.S. in Environmental Engineering, 1992: University of Washington, Seattle, WA

B.S. in Chemical Engineering, 1986: Washington University, St. Louis, MO

Publications

V.S. Stenkamp and J.C. Berg, "The Effect of Long Tails on Steric Stability and Hydrodynamic Measurements," *Langmuir*, Vol. 13, No. 14, p. 3827, 1997.

V.S. Stenkamp and M.M. Benjamin, "The Effect of an Iron Oxide Coating on Sand Filtration," *The Journal of the American Water Works Association*, August 1994, p. 37- 50.

Co-author on patent #5,310,977 "Configured Microwave Susceptor."